TRANSIENT FREQUENCY CONTROL OPTIONS FOR FUTURE POWER SYSTEMS

by

Ahmed Hassan Yakout

Department of Electronic and Electrical Engineering

August 2010

Thesis submitted in accordance with the requirements of the University of Strathclyde for the degree of Doctor in Philosophy

D E C L A R A T I O N

I hereby declare that this Thesis embodies my own research work and that it is composed by me in the Department of Electronic and Electrical Engineering at the University of Strathclyde. Where appropriate, I have made acknowledgement to the work of others.

Ahmed Yakout

A C K N O W L E D G E M E N T

First of all, the author would like to express all my thanks to GOD for his great help in completing this thesis.

The author would like to express his sincere thanks to his supervisors Prof. Dr. Kwok Lo, Dr. Olimpo Anaya Lara, for their guidance, continuous encouragement and generous help throughout the development of this work.

Acknowledgments are extended to Prof. Dr, Walter Johnstone, chairman of the electronic and electrical department and Prof. Dr. Scott MacGregor, dean of the faculty of engineering.

The author would also like to express his love, gratitude, and appreciation to his parents and beautiful sisters for their endless love, encouragement, patience and prayers during the course of this work and behind

TABLE OF CONTENTS

A B S T R A C T

The frequency of an interconnected power system is controlled through an Automatic Generation Control AGC system, which ensures that the amount of generation is following the load change. However, in the case of extreme contingencies of a cascading failure, the interconnected grid or power system might divide into what so called separated areas or electrical islands. Once this condition is indicated the main AGC is disconnected and the frequency stability and the sustainability of each island becomes a matter of interest for electrical engineers.

This thesis studies different controller design options for frequency instability mitigation. The objective is to investigate different methodologies to ensure the frequency stability of over generated separated areas. Controller design options presented in this thesis are: (i) An island centralized automatic generation tripping controller, (ii) An emergency centralized island AGC and (iii) LQR-based local power plant controllers or auxiliary governors.

The proposed island centralized automatic generation tripping controller assists in sustaining the frequency stability of a separated electrical power exporting areas by reducing the separated area frequency overshoot and minimizing the frequency steady-state deviation. A simple scoring criterion that takes into consideration the dynamic response, restoration time and the economic operation of the generators to be tripped successively is proposed. The amount of generation to be tripped is decided through iterative time domain simulations.

On the other hand, the proposed emergency centralized island AGC is designed using two popular control methodologies, the conventional integral control and the optimal LQR-based control. The two designs are discussed in this thesis and compared. These controllers change the settings of the generating unit speed changer positions. These controllers are found to eliminate the frequency steady-state deviation but have no effect on the first frequency overshoot.

Moreover, LQR-based local power plant controllers (auxiliary governors) are proposed to improve the overspeed controllers of thermal power plants. The designed controller uses the power plant mechanical power and speed as feedback signals. These controllers eliminate the separated area frequency steady-state deviation and contribute in reducing the first frequency overshoot as well.

All the aforementioned techniques have been applied to three different case studies of different generation mix. Time-domain simulations show that LQR-based auxiliary governor does not only remove the steady state frequency error but also improves the first frequency overshoot. In addition to some generation tripping, the frequency response of the three case studies discussed in this thesis is stabilized.

LIST OF ABBREVIATIONS

Acronym	Corresponding Phrase
ACE	Area Control Error
AGC	Automatic Generation Control
BMU	Balancing Mechanism Unit
CCGT	Combined Cycle Gas Turbine
CV	Control Valve
DNO	Distribution Network Operator
E & W	England and Wales
EMS	Energy Management System
FPN	Final Physical Notification
FSIG	Fixed Speed Induction Generator
FTR	Frequency Trend Relay
G	Generator or Generating Station
GB GC	Great Britain Grid Code
GB LFDDS	Great Britain Low Frequency Demand Disconnection Structure
GB SO	Great Britain System Operator
GB SQSS	Great Britain Security and Quality Supply Standard
H	High
HP	High Pressure Turbine
HVDC	High Voltage Direct Current
IP	Intermediate Pressure Turbine
IV	Intercept Valve
IVG	Intercept Valve Gate
IVOB	Intercept Valve Opening Bias

L	Low
LF	Low Frequency
LFDD	Load Frequency Demand Disconnection
LP	Low Pressure Turbine
LQR	Linear Quadratic Regulator
LR	Load Reference
LVG	Low Value Gate
M	Medium
MHC	Mechanical Hydraulic Control
MZT	Minimum Zero Time
NG	National Grid
NGET	National Grid Electric Transmission Ltd.
n/a	not applicable
P	Electric Power or Proportional Controller
PIC	Proportional-Integral Controller
p.u	Per unit
RLC	Resistance Inductance Capacitance
SHETL	Scottish Hydro Electric Transmission Ltd.
SISO	Single Input Single Output
SPT	Scottish Power Transmission Ltd.
SYS	Seven Year Statement
UFLS	Under Frequency Load Shedding
UK	United Kingdom
VL	Very Low

LIST OF SYMBOLS

Symbol	Definition
A	State matrix
$Asys$	System state matrix
B	Input matrix
$Bsys$	System input matrix
C	Output matrix
$Csys$	System output matrix
D	Damping constant or Load frequency dependence
$Dsys$	System load frequency dependence
E_{FD}	Excitation e.m.f
F	Frequency, or Power fraction, Combined rotor and load viscous friction coefficient
F_{HP}	High pressure turbine power fraction
F_{IP}	Intermediate pressure turbine power fraction
F_{LP}	Low pressure turbine power fraction
f	Frequency
f_{ref}	Reference frequency
f_s	System frequency
H	Combined rotor and load inertia constant
J	Objective or cost function, or Combined rotor and load inertia coefficient
K	Gain
K_A	Amplifier gain
K_{AX}	Auxiliary controller gain
K_G	Generator's rotor speed proportional controller gain
K_i	Integral power reference estimator

k	Capacity factor
k_i	Gain of integral controller
k_{icr}	Critical integral gain
L_{C1}	Opening rate limits of CV servo motor
L_{C2}	Closing rate limits of CV servo motor
L_{I1}	Opening rate limits of IV servo motor
L_{I2}	Closing rate limits of IV servo motor
L_m	Magnetizing inductance
L_s, L_r'	Total stator and rotor inductance
M	Inertia constant
M_{eq}	Equivalent inertia constant
P	Electric Power
P_{GVc}	Governor power for coal unit
P_{GVh}	Governor power for hydro unit
P_{GVn}	Governor power for nuclear unit
P_{HPc}	High pressure turbine power for coal unit
P_{HPn}	High pressure turbine power for nuclear unit
P_{IPc}	Intermediate pressure turbine power for coal unit
P_{LPc}	Low pressure turbine power for coal unit
P_{LPn}	Low pressure turbine power for nuclear unit
P_T	Main steam pressure
P_{dc}	Power supplied by HVDC link
P_e	System electrical power or Load
P_h	Hydro unit mechanical power
P_m	Mechanical power
P_{ref}	Reference power setting of generation unit
P_o	Reference power
p	Number of pole pairs

Q	Weight matrix for states
q	State weight
R	Governor droop or Weight matrix for control inputs
R_s, L_{ls}	Stator resistance and leakage inductance
R_r', L_{lr}'	Rotor resistance and leakage inductance
r	Input weighting matrix
S	Speed
S_1	Speed relay output signal
$\dot{S}_1$	Derivative of speed relay output signal
T	Time constant
T_A	Amplifier time constant
T_{CH}	Inlet steam chest time constant
T_E	Exciter time constant
T_e	Electromagnetic torque
T_G	Governor droop time constant
T_m	Shaft mechanical torque
T_R	Reset time
T_{RH}	Reheater time constant
T_{SI}	Intercept valve servo motor time constant
T_{SM}	Control valve servo motor time constant
T_{SR}	Speed relay time constant
T_W	Water time constant
T_{dc}	HVDC link time constant
T_E	Exciter time constant
T_1	Transient droop compensation time constant
t	time
u_{sys}	System power setting or system electrical power

$u_{CONTROL}$	Control input signal
V	Voltage
V'_{dr}, i'_{dr}	d axis rotor voltage and current
V_{ds}, i_{ds}	d axis stator voltage and current
V'_{qr}, i'_{qr}	q axis rotor voltage and current
V_{qs}, i_{qs}	q axis stator voltage and current
V_R	Regulator voltage
V_{ref}	Reference voltage
V_t	Actual voltage
V_1	Auxiliary governor opening bias
x	State variable
$\dot{x}$	Derivative of state variable
x_{sys}	System state variable
$\dot{x}_{sys}$	Derivative of state variable
Y	Output
y_{sys}	System output state variable
θ_r	Electrical rotor angular position
$\varphi_{qs}, \varphi_{ds}$	Stator q and d axis fluxes
$\varphi'_{qr}, \varphi'_{dr}$	Rotor q and d axis fluxes
ω	Speed
ω_m	Angular velocity rotor
ω_r	Rotor speed
ω_{ref}	Reference speed
Σ	Summation
Δ	Parameter change or variation

LIST OF FIGURES

Figure **Page**

List of Tables

CHAPTER 1

INTRODUCTION

1.1 Introduction

This chapter provides introductory information required for understanding the motivation behind the study presented in this thesis. This section provides an outline for this chapter. Section 1.2 gives important terminologies and definitions for Blackouts and describes Blackout causes. Section 1.3 explains the extreme contingency assessment. Finally, Section 1.4, Section 1.5, Section 1.6 and Section 1.7 present the thesis motivation, contribution and organization and associated publications, respectively.

1.2 Blackout Definition and Causes

Thousands of disturbances take place annually in modern power systems. Most of them are eliminated by relay protection devices, other automatic systems and by the actions of dispatching personnel. A small fraction of these disturbances might result in a significant system failure of a cascading nature. If the process of cascading failures continues, the entire system or large parts of it may completely collapse. This is usually referred to as a system Blackout [1-2]. In conclusion, blackout can be defined as [3]:

*"**Blackouts** mean the loss of electricity in a large area for a considerable duration caused by cascading failures but cascading failures does not necessarily cause Blackouts."*

Based on a review study on recent blackouts around the world [3], it was found that a blackout results due to two causes, that is, a primary or triggering cause and a cause of cascading. The triggering cause of blackout is a probabilistic failure, i.e. it could be any disturbance. It could be an unusual primary disturbance, protection device malfunction, failure of automatic emergency control systems, or errors by personnel. This primary cause stresses the network beyond its limits developing secondary causes that lead to cascading failures, and thus blackout. These secondary causes, or causes of cascading failures, can be divided into two categories:

(1) Deterministic Causes: These factors include all causes that are generated from operation constraints or limits which are determined by physical equations of power systems

(2) Probabilistic Causes: Unlike the deterministic factors, probabilistic factors are solely decided by the reliability characteristics of devices.

Table 1-1 summarizes the possible blackout primary causes and causes of cascading [3].

TABLE 1-1 CAUSES OF BLACKOUT [3].

Primary Causes	**Causes of Cascading**	
	Deterministic Factors	**Probabilistic Factors**
1. Primary protective relay failure 2. Line fault 3. High winds causing line failure 4. Line sagged into trees 5. Hidden failure 6. Lightning 7. Phase-to-ground fault 8. Tower causing multiple lines out 9. A sequence of line trappings 10. Etc.	1. Under-frequency 2. Overload 3. Over-current 4. Low voltage 5. Etc.	1. Failure of the tap-changing mechanism 2. Additional lightning 3. Failure of Communication channel 4. Failure of Backup device 5. Operators' unawareness of failures 6. Failure of EMS system 7. Etc.

1.3 Extreme Contingency Assessment

Cascading failures are considered low-probability, high consequence events. After recent blackouts in North America, Europe and Russia [4-23], it becomes clear that the blackout events may happen more frequently. Consequently, the extreme contingency assessment has been recognized [24].

The objective of this assessment is to determine the effects of extreme contingencies on system performance in order to obtain an indication of system strength and to determine the extent of a widespread system disturbance. After analysis and assessment of extreme contingencies, measures are to be used where appropriate to reduce the frequency of occurrence of such

contingencies or to mitigate the consequences that are indicated as a result of simulating for such contingencies [24].

Analysis usually shows that on the advanced stages of cascading failures, uncontrollable system separation may occur. Frequency instability is one of the main problems that accompany uncontrollable system separation. There is a tight limit on frequency that should not be violated; else, power plants will start tripping off by their safe guard protection leading to the separated system blackout.

1.4 Thesis Motivation

The Great Britain System Operator (GBSO) is responsible for the management of the transmission network security and real time balancing of generation with demand. Any imbalance between generation and demand will result in perturbations in the nominal system frequency of 50Hz. GBSO manages the system frequency to defined statutory steady state limits of ±0.5Hz (i.e. 49.5Hz to 50.5Hz) and operational limits of ±0.2 Hz (i.e. 49.8Hz to 50.2Hz). Moreover, the System Frequency could rise to 52Hz or fall to 47Hz in exceptional circumstances. However, if the frequency is above 52 Hz or below 47 Hz independent protective action is permitted to protect generation in the event of danger to safety of plant and/or personnel [25-27].

For separated areas with large generation deficit, frequency declines and generators would trip off, causing the frequency to decline more and more. This condition can be contained by disconnecting some load to ensure that the generation capacity available can cover the remaining connected load. Under Frequency Load Shedding (UFLS) is a hot topic till nowadays [28-29]. Another methodology that might assist in the survival of the aforementioned area, is allocating the proper amount of spinning reserve [30-31].

According to the GB Grid Code, for a large generation deficit in an importing power island following a sudden system split, the National Low Frequency Demand Disconnection (LFDD) scheme is designed to automatically disconnect demand to arrest the incident and prevent a partial shutdown of the power system, where the LFDD scheme is designed to operate and disconnect demand once the frequency drops beyond 48.8 Hz. Figure 1.1 illustrates the frequency control philosophy and frequency stability of the GB power system [25-27, 32].

On the other hand, for the case where the separated area is a power exporting area, once it gets separated from the rest of the grid, the machines in the system overspeed due to the sudden loss of load and the areas mean frequency overshoots to a high frequency value (depending on the areas inertia, control and amount of power interrupted), and then starts to decrease to settle at a

new higher operating point. The challenge is to ensure that the frequency does not reach near to the ceiling value of 52 Hz (for 50 Hz power systems) and avoid frequency swings [25, 33].

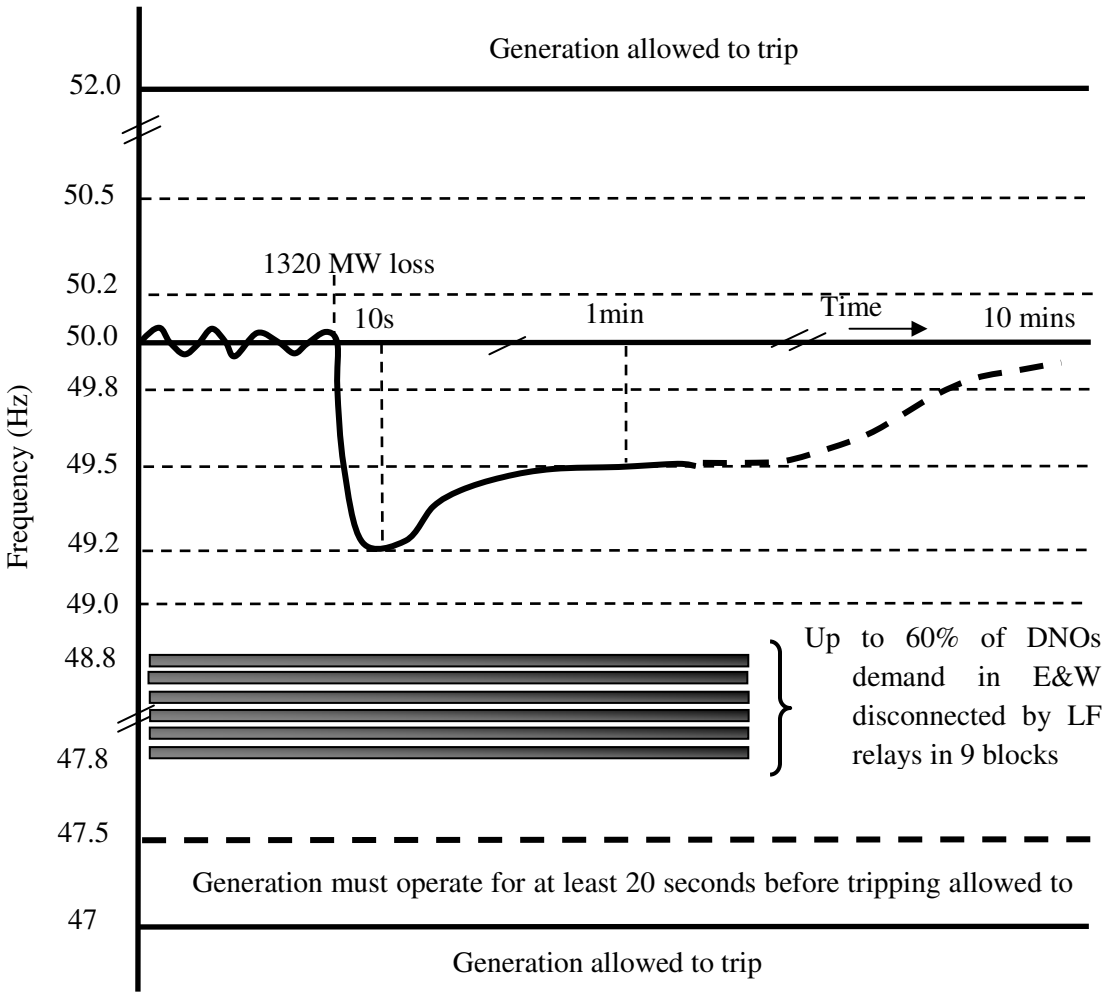

Figure 1.1 The Great Britain frequency control philosophy [32].

There are no clear or published strategies that represent means of avoiding frequency rise in case of generation rich separated areas. Hence, this thesis is devoted to simulate the separation of some generation rich parts of the GB grid and propose means to ensure the frequency stability of such separated areas as a part of an extreme contingency assessment.

Consequently, this thesis studies the frequency stability of generation rich separated areas upon sever upsets in the GB network. Both transient and the steady-state frequency response should be contained within the range where generators can operate safely (the thesis considers the following range: 47Hz-52 Hz). The thesis takes into consideration the following points:

1- Frequency swings are to be avoided.
2- The mean area frequency overshoots should not exceed 52 Hz.

3- Frequency should be restored to its nominal value as fast as possible to help in a swift system restoration [1].

1.5 Thesis Contribution

The main thesis contribution can be summarized as:

1- An island centralized automatic generation tripping controller is proposed to decrease the mechanical power rapidly to assist in sustaining the frequency stability of separated exporting island by reducing the separated area frequency overshoot and minimize the frequency steady state deviation. Moreover, a simple scoring criterion is proposed to arrange the tripped generators in a priority list. This criterion takes into consideration the dynamic response, restoration time and the economic operation of the generators to be tripped successively. The amount of generation to be tripped is decided through iterative time domain simulations.

2- An emergency centralized island AGC is proposed to control the separated area frequency once the area is separated and the main AGC is disconnected. Two popular designs for AGC systems discussed in literature [34-40], the conventional integral control and the optimal LQR-based control, are discussed in this thesis and compared. These controllers change the generating unit speed changer position or power reference settings. These controllers eliminate the frequency steady state deviation but have no effect on the first frequency overshoot.

3- LQR-based local power plant controllers (auxiliary governors) are proposed to improve the overspeed controllers of thermal power plants. Consequently, it assists in sustaining the operation of separated areas with excess generation. The designed controller uses the power plant mechanical power and speed as feedback signals. These controllers eliminate the separated area frequency steady state deviation and contribute in reducing the first frequency overshoot.

4- The effect of high wind energy penetration and the existence of HVDC Links are studied, by applying the different aforementioned methodologies to three different case studies, with different generation mix:

- A case where most of the generation is based on conventional synchronous machines.
- A case with a high penetration level of wind generation, nearly 25%.
- A case where the generation is conventional but with an HVDC Link.

5- The thesis studies the effect of governor rate limiters of the cases under study frequency response. Based on literature, governor rate limiters are assumed to vary from 1 p.u./sec to 0.1 p.u./sec [24, 41-43]. It is important to study the effect of such rate limiters as it increases the governor time delay, depending on the maximum rate limit allowed and the amount of power interrupted. This increase in the governor time delay might affect the frequency response dramatically causing area frequency to swing and be unstable.

1.6 Thesis Organization

This thesis consists of eight chapters and three appendices. Chapter 1 explains the thesis objective and motivation. Furthermore, it describes the thesis organization. Chapter 2 gives introductory background information about the frequency stability problem. It also presents a survey for related work. Chapter 3 introduces the thesis case studies. In addition, a complete case study modelling and analysis is presented. Chapter 4 proposes a centralized generation tripping scheme to improve the frequency response of the thesis case studies. In addition, an emergency island AGC is proposed in Chapter 5. On the other hand, the LQR-based auxiliary governors or local controllers are developed in Chapter 6 to overcome the difficulties that accompany the implementation of an island AGC. Chapter 7 presents the frequency response of the case studies when local controllers are improved and a centralized generation tripping scheme is in action. The conclusions based on the study of the aforementioned controllers are presented in Chapter 8. Finally, the linear quadratic regulator problem, the program flow charts and the linear quadratic regulator gains are given in Appendix A, Appendix B and Appendix C, respectively.

1.7 Associated Publications

Publications associated with this thesis are three conference papers, one IEEE and two IET conference papers. A Journal paper has been submitted for publication and there is one more currently under preparation. These publications are as follows:

1. A.Yakout, O. Anaya- Lara, G. Burt, “Improving the Transient Frequency Response of Islands Using Generation Tripping” The 44th International Universities’ Power Engineering Conference (UPEC), Glasgow, Scotland, 1-4 September 2009.

2. A.Yakout, O. Anaya-Lara, G. Burt “Improving the transient frequency response of unintentional islands via local optimal controllers” The 8th International conference on Advances in Power system Control, operation and Management (APSCOM), Hong Kong, 8-11 Nov., 2009.

3. A.Yakout, O. Anaya-Lara, G. Burt “Improving the transient frequency response of unintentional islands via optimal control” The 13th International Middle East Power System Conference (**MEPCON**'09), Assiut, Egypt, December 20-23, 2009.

4. Journal submitted: A.Yakout, O. Anaya-Lara, G. Burt, K. Lo, “Enhanced Transient Frequency Control of Generation-Rich Separated Areas”, IEEE Transactions on Power Delivery, September 2010.

5. Journal under preparation: A.Yakout, O. Anaya-Lara, G. Burt, K. Lo, “Means for sustaining the frequency stability of generation rich separated areas with high penetration of wind farms in future power systems” Expected for submission: IEEE Transactions on Power Delivery, September 2010.

CHAPTER 2

THE FREQUENCY STABILITY PROBLEM AND EXISTING COUNTERMEASURES

2.1 Introduction

This chapter provides terminology and background required for understanding the frequency stability problem and its main cause. Also, a survey about related work is presented.

Section 2.2 and Section 2.3 introduce the steam turbine construction and the problems associated with the off-nominal frequency operation of steam turbines, respectively. Section 2.4 discuses the main causes of frequency deviation. Section 2.5 states important terminologies and definitions for frequency stability. Section 2.6 enumerates existing frequency instability counteracting methodologies. Section 2.7 illustrates the Great Britain frequency control philosophy. Finally, Section 2.8 summarises this chapter.

2.2 Steam Turbines

All thermal power stations, fossil fuelled or nuclear, mainly consist of:

1- Fossil fuelled furnaces or nuclear reactor (the source of heat).
2- Boilers (the source of superheated steam).
3- Steam Turbines (the source of kinetic energy).
4- Generators (the source of electrical energy).

Steam turbines equipped with each generating unit G usually consist of 2 or more sections connected in series thermally. These sections are known as high pressure turbine HP, intermediate pressure turbine IP and low pressure turbine LP. If all sections are mounted on the same shaft as the generator, the unit is known to have a tandem compound configuration as shown in Figure 2.1. On the other hand, if turbine sections are distributed over two independent shafts, each shaft supplies kinetic energy to a different generator, the unit configuration is called cross compound, see Figure 2.2. Although, the second configuration has two shafts and two generators, it is controlled as one unit [24, 41-43].

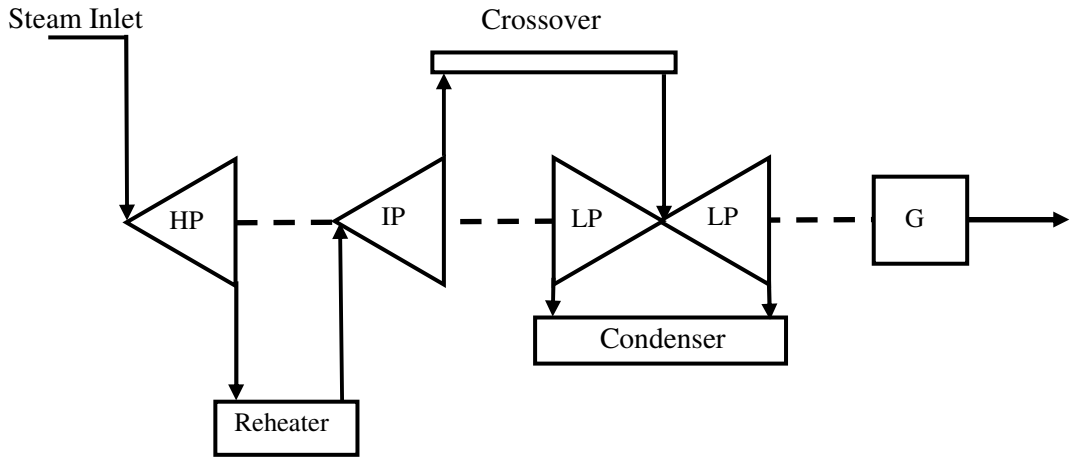

Figure 2.1 Tandem compound steam turbine [24, 41-43].

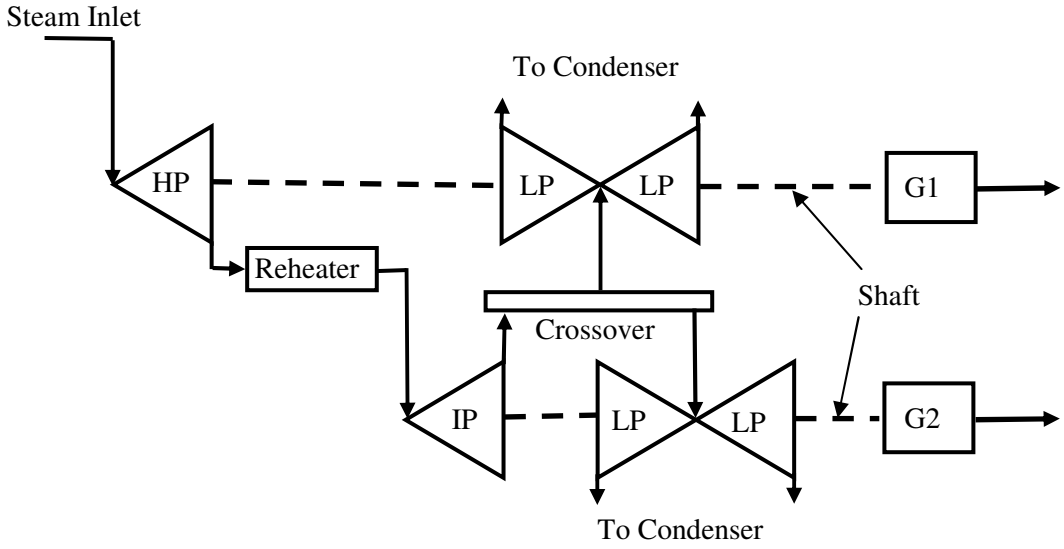

Figure 2.2 Cross compound steam turbine [24, 41-43].

Moreover, each section of the steam turbine has a set of moving blades, called buckets, attached to the rotor. The kinetic energy of the high velocity superheated steam, produced by the boiler, is converted into shaft torque by the buckets. Hence, the shaft on which the turbine is mounted rotates supplying kinetic energy to the generator, mounted on the same shaft [24].

2.3 Off-Nominal Frequency Operation of Steam Power Plants

Problems due to the off frequency operation of steam power plants are discussed in this section. Section 2.3.1 and Section 2.3.2 explain the problems associated with steam turbines and plant auxiliaries, respectively.

2.3.1 Problems Associated With Steam Turbines

Turbines can not tolerate off-frequency operation. Blades are designed so that their vibration modes do not resonate at normal frequency operation. Off-frequency operation of a steam turbine causes the most critical blades, the ones in the last three rows in the LP turbine end and, in some cases, the last row in the IP turbine, to vibrate and resonate. Hence, the possibility of blades failure exists [24].

Figure 2.3 and Figure 2.4 illustrate the relationship between blade failure due to fatigue and off-frequency operation. Below stress level A, the vibration stress amplitude is low enough that no damage results. On the other hand above stress level A, the vibration stress would cause blade damage. The number of vibration cycles that the blade can withstand before failure varies with the stress level. For example, operation at stress level B would produce a failure at 10,000 cycles and a stress level C failure would occur at 1000 cycles. Hence, operation at off-nominal frequencies is time restricted depending on specific blade designs [24].

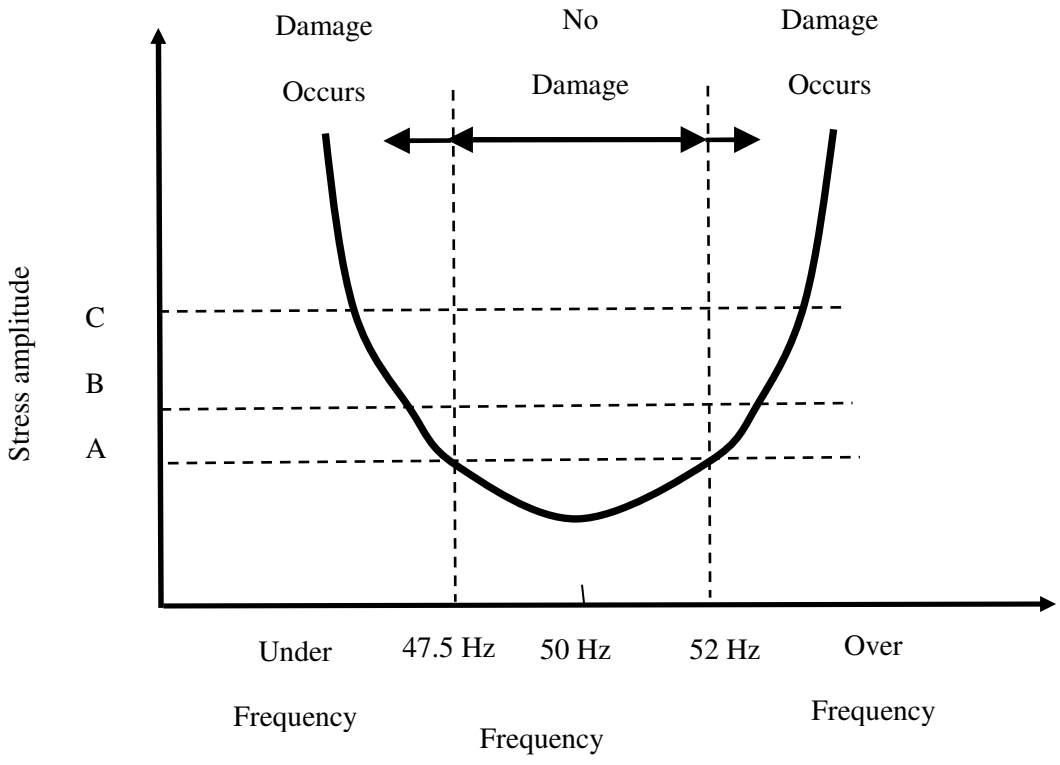

Figure 2.3 Increase in vibration amplitude with off-frequency operation [24].

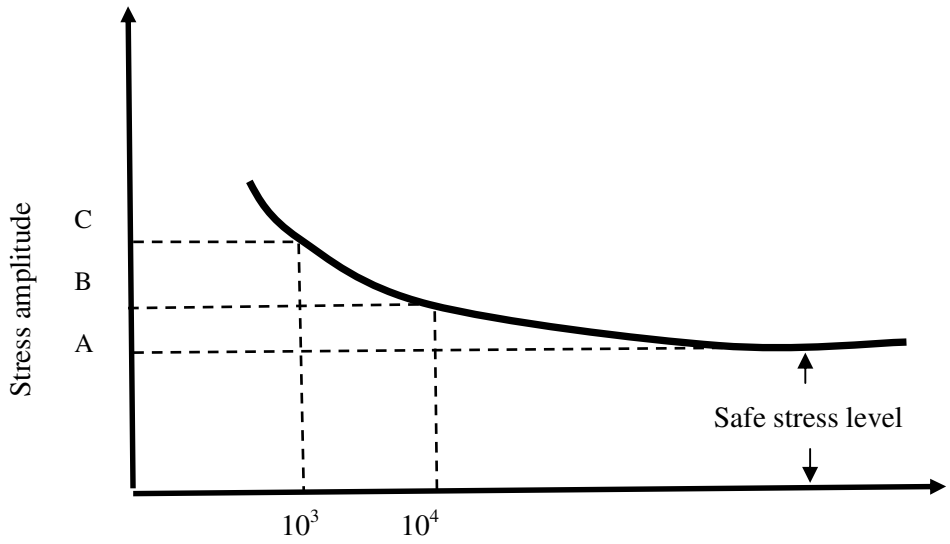

Figure 2.4 Stress versus number of cycles to failures [24].

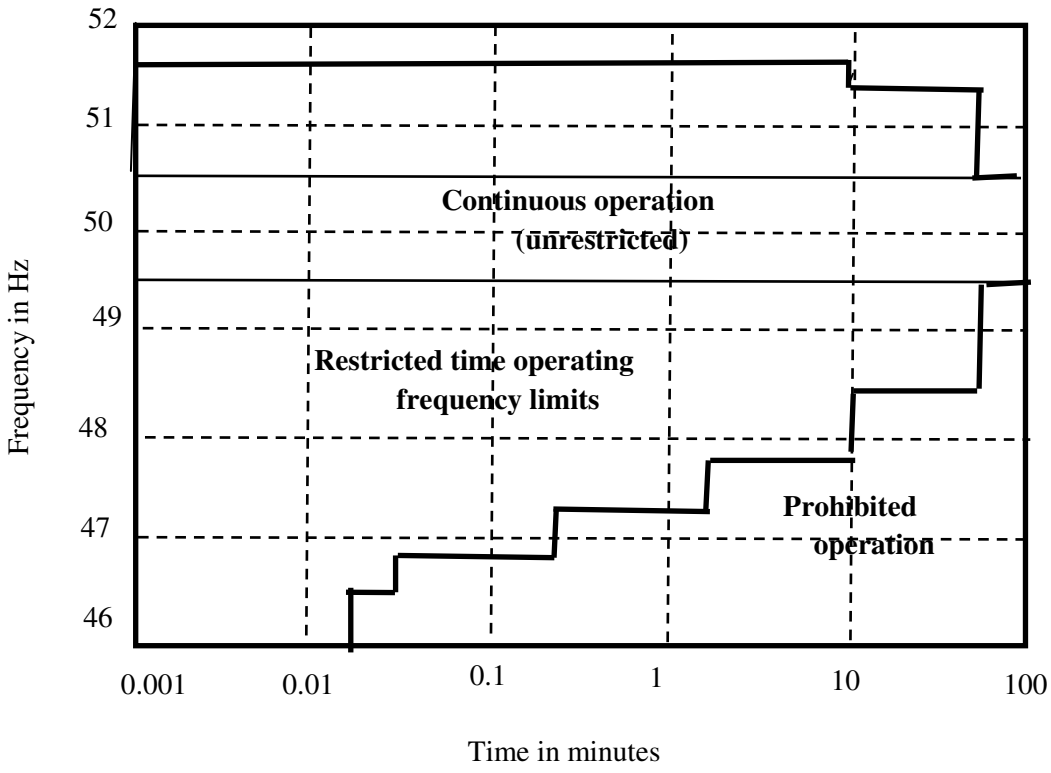

Figure 2.5 Steam turbine partial or full-load operating limitations during abnormal frequency, representing composite worst-case limitations of five manufactures. ANSI/IEEE- 1987 (Adjusted to comply with a 50 Hz system) [24, 44]

Figure 2.5 is a composite representation of steam turbine off nominal frequency limitations of a large sample of turbines built by five different manufacturers, shifted by -10 Hz to represent the case of a 50 Hz system [44]. The figure shows that the sustained operation within the band 49.5

Hz to 50.5 Hz would not have any effect on blade life, while the dotted areas above 50.5 Hz and below 49.5 Hz are areas of restricted time operating frequency limits. Operation outside these areas is not recommended. Hence, protective under and over frequency relays must be provided to trip the generating unit off if the system frequency drops below or rises above certain limits, respectively. This makes the characteristics shown in Figure 2.5 useful for evaluating the requirements for protective relaying schemes. Moreover, the applicable limit for other turbines might be more or less restrictive [24].

2.3.2 Problems Associated with Plant Auxiliaries

At low frequencies the performance of the plant auxiliaries driven by induction motors changes. The plant capability may be severely reduced because of the reduced output of the boiler feeding pumps or fans supplying combustion air. In the case of nuclear power plants, the reactors may overheat due to reduced flow of coolant as the frequency declines [24, 45].

2.4 Causes of Power System Frequency Deviation

In agreement with Newton's second law, the constancy of frequency depends on the ability to maintain equilibrium between generation and load. Interconnected power systems are equipped with Automatic Generation Control (AGC), where the amount of generation is varied continuously to cope with the daily gradual load variations [1, 24, 46 and 47]. However, some sever disturbances or upsets, which are not frequent, cause generation-load imbalances and hence frequency deviations. These upsets can be:

1 A loss of generating stations.
2 A sudden drop of a large load or major load centre.
3 The splitting of an interconnected power system to islands.

2.4.1 Loss of Generating Stations

Unexpected loss of generation stations would cause a generation deficit in the power system. And as the load is more than the remaining generation, the system frequency starts to decline. This decrease in frequency should be contained; else, other generators would start tripping off by their under frequency protection, causing the frequency to decline more and more.

2.4.2 A Sudden Drop of a Major Load Centre

On the other hand, if the power system suffered a sudden drop of a major load centre, the generation becomes more than the remaining connected load. If the generation cannot be decreased quickly to match the connected load, the machines in the system overspeed and the system frequency increases. Similarly, this increase in frequency should be contained; otherwise other generators would start tripping off but this time by their over frequency protection.

2.4.3 Power System Separation

Modern power systems are subjected to tens and hundreds of disturbances annually. Some of these disturbances take the form of cascading failures [2]. These cascading failures might cause the splitting of large interconnected power systems into islands. Some islands suffer frequency overshoots and others suffer frequency undershoots. This problem is illustrated in Figure 2.6.

It is clear from Figure 2.6, that following a system split, Area 1, the power exporting area, would suffer load deficiency and frequency of Area 1 rises, a situation similar to that discussed in Section 2.4.2. On the other hand, Area 2, the importing area suffers generation deficit and the area frequency starts to decrease, a case similar to the case discussed in Section 2.4.1.

Although the power system is in a degraded state (i.e. the interconnected system is split into islands), it is believed that customers are to be served continuously. Following the popular guideline "a successful island is a much better condition than a blackout" [34], it becomes necessary to provide different means to contain the situation in each separated area.

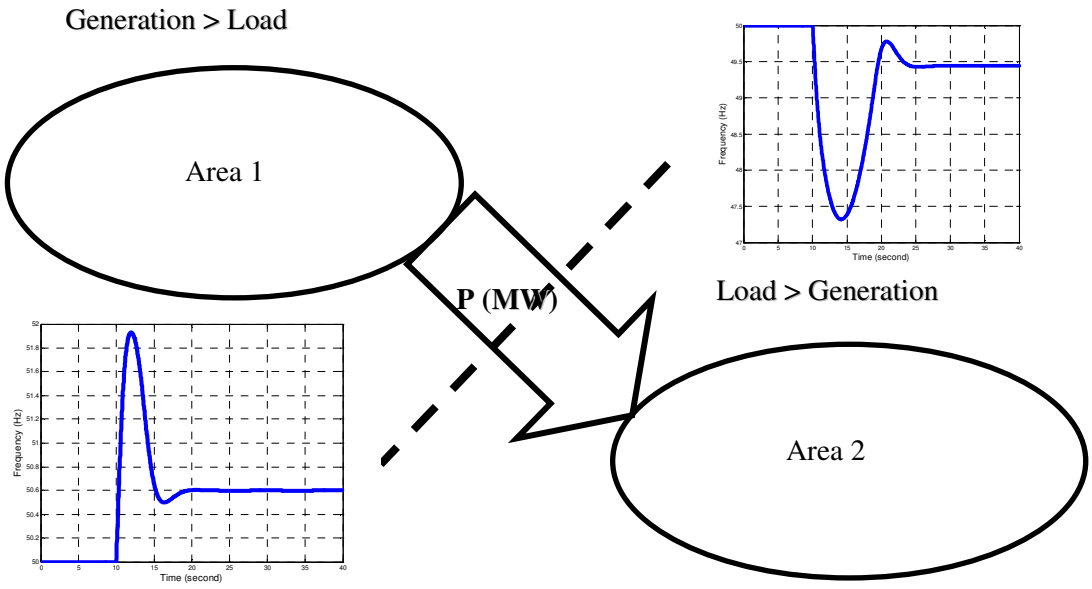

Figure 2.6 Frequency problem associated with the splitting of interconnected power systems.

2.5 Frequency Stability

Due to the adverse consequences that might result from sever frequency deviations, frequency stability was recognized and defined by the IEEE/CIGRE Joint Task Force as:

"*The ability of a power system to maintain steady frequency following a severe system upset resulting in a significant imbalance between generation and load*." [33]

Frequency stability depends on the ability to maintain /restore equilibrium between generation and load, with minimum unintentional loss of load. Instability that may result occurs in the form of sustained frequency swings leading to tripping of generating units and/or loads. One important example discussed by the IEEE/CIGRE Joint Task Force to explain frequency stability is the case of splitting of interconnected large systems into islands. Frequency stability becomes a question of whether or not each island will reach a state of operating equilibrium. During the transition from the pre-separation condition to the post-separation condition, the islands mean frequency should not violate an upper and lower limit. If these limits are violated, the power plants protection would disconnect the plant from the grid, complicating the situation more and increasing the probability of a black out condition [33].

2.6 Frequency Instability Countermeasures

Countermeasures for different frequency problems are presented in this section. Section 2.6.1 enumerates counter measures for negative frequency deviation (i.e. frequency drop). On the other hand, countermeasures for positive frequency deviation (i.e. frequency rise) are presented in Section 2.6.2. Finally, Section 2.6.3 discusses general countermeasures that can work for positive and negative frequency deviations.

2.6.1 Countermeasures for Negative Frequency Deviation

As explained in Section 2.4, negative frequency deviation or frequency drop result from generation deficiency (i.e. load is greater than connected generation). Hence, it becomes necessary to balance the generation and load as fast as possible. One technique is to allocate reserve generation discussed in Section 2.6.1.1. Another, technique, presented in Section 2.6.1.2, is to disconnect some load to regain the balance between generation and load.

2.6.1.1 Spinning Reserve

Spinning reserve is a methodology that assists in limiting the frequency deviation upon unexpected generation loss. It involves running some generation at no load and/or de-loading

other generating units, so that they can pick up any unexpected loss of generation by their governor action. Some research discusses allocating the proper amount of spinning reserve [30, 31].

Although this methodology is considered by utilities, it still has problems due to the prime mover systems limitations, which are summarized as follows [24]:

1- The generation can be increased only to the limits of the available spinning reserve within each affected area. This is a problem in the case of area separation. Some areas might have excessive spinning reserve, other might have none.

2- The load that can be picked up by a thermal unit is limited due to thermal stress in the turbine. Initially, about 10% of turbine rated output can be picked up quickly without causing damage by too rapid heating. This is followed by a slow increase of about 2% per minute.

3- The ability of a boiler to pick up a significant amount of load is limited.

4- The speed governors have a time delay of 3 to 5 seconds.

Consequently, generation reserve available for control of frequency is limited to a fraction of the remaining generation. This means more than the actual calculated reserve is required, which is uneconomical.

2.6.1.2 Load Shedding

Under Frequency Load Shedding (UFLS) is an up-to-date research topic [28, 29]. Load Shedding is considered the first line of defence for the frequency drop problem [24]. It involves disconnecting some load to ensure that the generation capacity available can cover the remaining connected load.

Some load shedding schemes are based on frequency drop, where loads are divided into blocks and are tripped at different frequency levels [24]. This scheme is implemented in Great Britain. Nearly 60% of the GB load, distributed all over England and Scotland, would be tripped before a frequency of 47 Hz is reached (See Section 2.7) [26]. This system has proven to be effective on 27th of May 2008 incident, where about 0.5 GW of load was disconnected to restore the frequency to its statutory limits, upon the unexpected disconnection of two large generating units and some embedded generation [32].

However, a scheme based on frequency drop alone is believed to be acceptable for generation deficiencies up to 25%. For greater generation deficiencies, a scheme which takes into account both frequency drop and rate of change of frequency is recommended to provide increased selectivity and hence preventing unnecessary tripping of load [24]. Ontario Hydro uses such a

relay to trip appropriate amounts of load. The relay is known as Frequency Trend Relay (FTR). Figure 2.7 shows the relays tripping logic, based on a 60 Hz system. The relay sheds up to 50% of the area load [48].

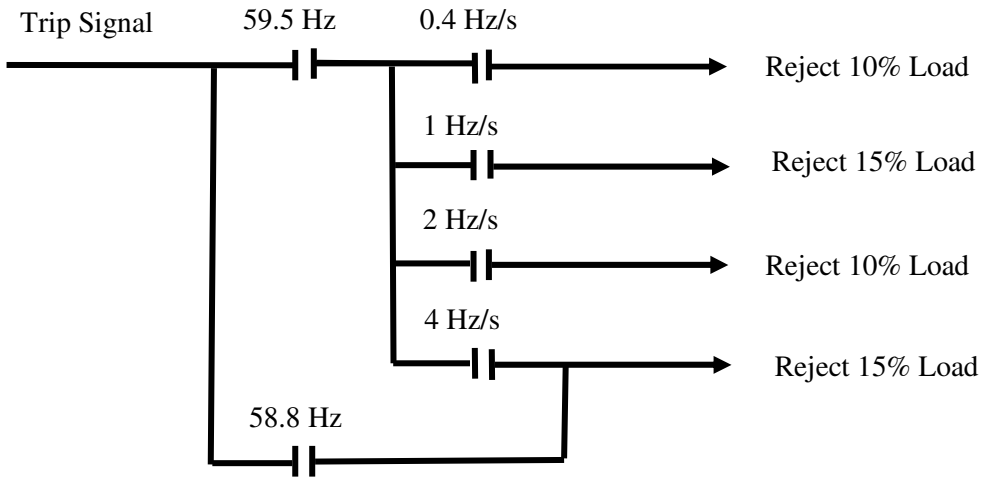

Figure 2.7 Tripping Logic for Frequency Trend Relay [24, 48]

2.6.2 Countermeasures for Positive Frequency Deviation

On the other hand, as explained in Section 2.4, positive frequency deviation or frequency rise result from load loss (i.e. the connected generation is greater than the load). Consequently, it becomes necessary to balance the generation and load as fast as possible. Else, the machines in the system overspeed due to the sudden loss of load and the areas mean frequency overshoots to a high frequency value (depending on the areas inertia, control and amount of power interrupted) and then starts to decrease to settle at a new higher operating point. It becomes important to contain the transient and steady state frequency below a defined limit. If this limit is reached, over frequency protection would trip the generating unit off.

Section 2.6.2.1, Section 2.6.2.2 and Section 2.6.2.3 discuss techniques that improve the generating units governing system response during an overspeed condition.

2.6.2.1 Intercept Valve

For the commonly used reheat type steam turbines, steam enters the HP section through a set of valves, known as the control valves CVs. The HP exhaust steam is then reheated and enters the IP turbine section through another set of valves called intercept valves IVs. The CVs modulate the steam flow through the turbine for load/frequency control during normal operation. On the other hand, in the event of overspeed, the rapid closure of the CVs alone would not be effective because of the large amount of stored steam in the reheater. Therefore, the intercept valve is

used for rapid control of the turbine mechanical power in the event of overspeed due to load rejection. IVs are very effective in this purpose as it is ahead of the reheater and controls the steam flow to the IP and LP turbine sections which generate nearly 70% of the total turbine power [24].

Figure 2.8 shows the block diagram representation of the tandem-compound reheat turbine. The model accounts for the effect of the inlet steam chest, reheater, and control and intercept valves.

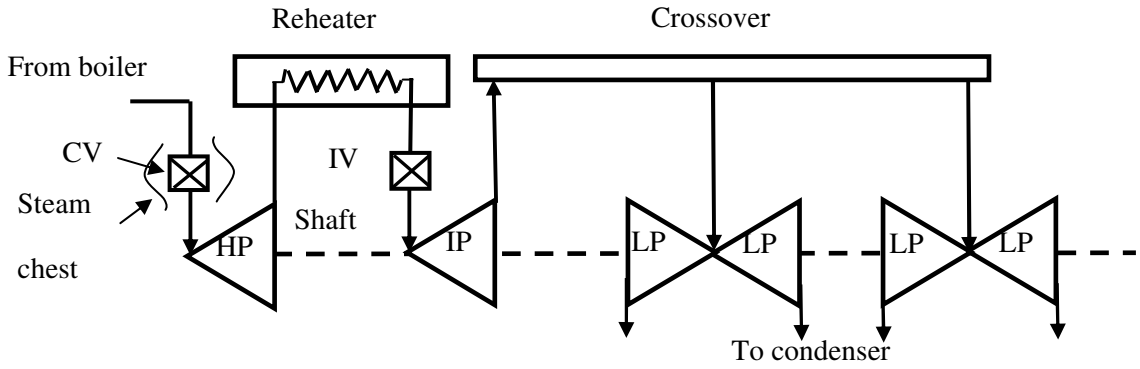

(a) Turbine configuration

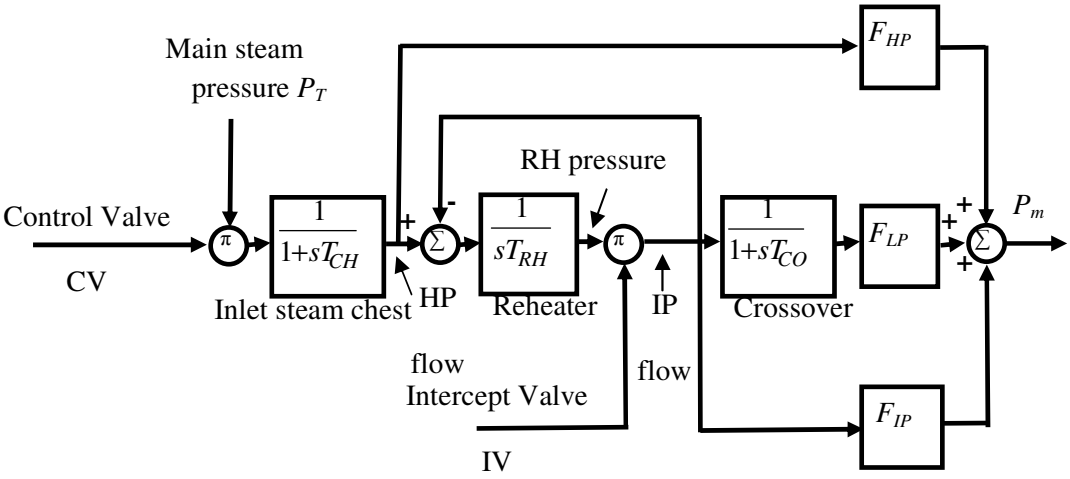

(b) Block diagram representation

Figure 2.8 Single reheat tandem-compound steam turbine model [24]

Where T_{CH} is the inlet steam chest time constant, T_{RH} is the reheater time constant, T_{CO} is the crossover pipe time constant, F_{HP}, F_{IP} and F_{LP} is the high, intermediate and low pressure turbine power fractions respectively, and P_m is the mechanical power.

Moreover, Figure 2.9 shows the functional block diagram of a mechanical-hydraulic control MHC system used for governing a steam turbine. The speed governor output is compared with a

speed/load reference determined by the speed changer position. The resulting error signal is used to control the CVs and the IVs. As mentioned earlier, for normal speed/load control only CVs respond. The IVs are held fully open by an opening bias (IVOB) signal. On overspeed, due to the resulting large speed error signal, the bias is overcome and the IVs are closed rapidly. When the control signal is restored to a value less than the bias, IVs are again fully opened [24].

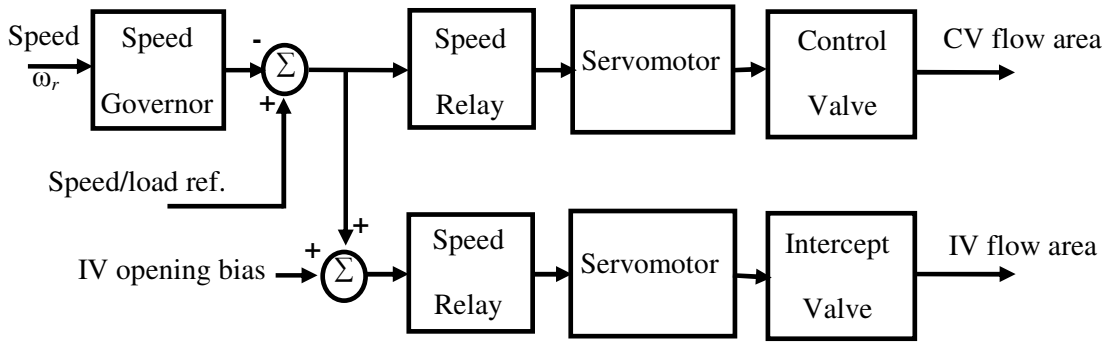

(a) Functional block diagram

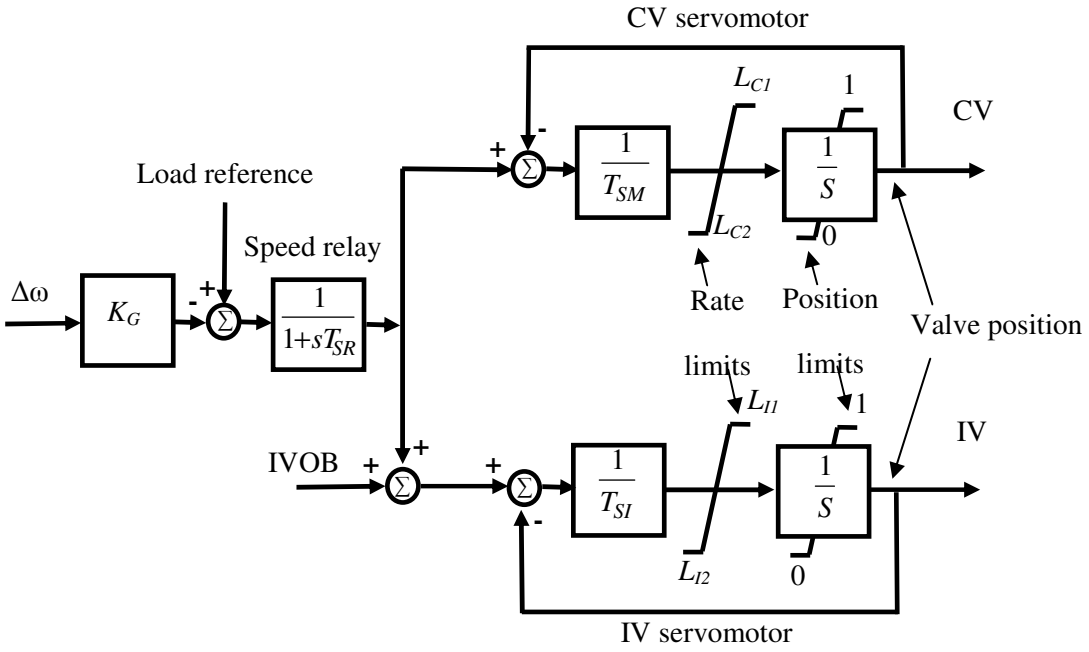

(b) Block diagram representation.

Figure 2.9 Mechanical-hydraulic control (MHC) model [24]

Where T_{SR} is the speed relay time constant, T_{SM} is the control valve servo motor time constant, T_{SI} is the intercept valve servo motor time constant, K_G is the generator's rotor speed proportional controller gain and $\Delta\omega$ is the rotor speed error itself. Moreover, L_{C1}, L_{C2} and L_{I1}, L_{I2} are the opening and closing rate limits of CV and IV servo motors respectively.

Figure 2.10 shows an example of the MHC speed governing system described in references [49] and [50]. The CV position is determined by the speed relay output signal S_1. The IVs respond to the lower of the two signals applied to the low value gate (LVG); these signals are derived from S_1 and its derivative $\dot{S}_1$ (which is proportional to the negative of rotor acceleration). For small speed deviations, the CVs respond to the normal speed/load control command which determines S_1 and the IVs remain fully open due to the opening bias (LVG input is at 1.02). During an overspeed condition, the IVs transiently respond by closing rapidly, driven by the lower of the two signals $\dot{S}_1$ and S_1 which depend on rotor acceleration and speed respectively. The control of IV through signal S_1 has a gain of 2.5 and bias of 1 with K_G =20 (5%droop) and load reference at 100%, the signal S_1 becomes effective in controlling IV when $\Delta\omega \geq 5\%$ and the effective speed control gain is 50 (2% droop) [24, 49].

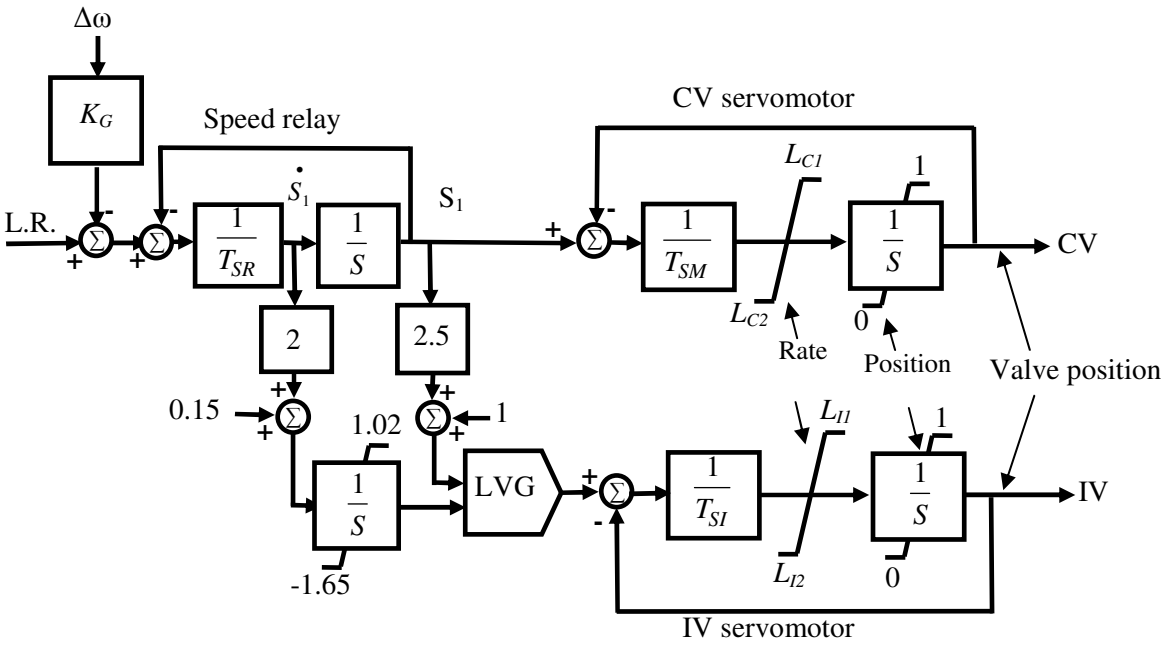

Figure 2.10 An example of the MHC speed governing system IEEE 1990[24, 49].

2.6.2.2 Auxiliary Governor

Figure 2.11 shows the block diagram representation of an MHC speed governing system applicable to one make [51]. The model shown accounts for CV and IV controls and an auxiliary governor for limiting overspeed. Under steady state conditions and during speed deviations, the IVs are kept fully open by the opening bias IVOB, only the CVs provide speed regulation. The auxiliary governor, when speed exceeds its setting V_1 (ranging from 1% to 3% over the rated speed), acts in parallel with the main governor with a gain of K_{AX} so as to effectively increase the gain of the speed control loop by a factor of about 8. This causes the

CVs as well as the IVs to close rapidly and thus limit overspeed. However, studies [51] showed that if the setting of V_1 is not chosen properly; auxiliary governors cause instability of the speed control during system-islanding conditions. The governing system will tend to oscillate. Consequently, all other units in the island will respond to oscillations of the units with auxiliary governors. The overall effect is to cause oscillations of all units. The resulting movements of steam valves or wicket gates continue until the hydraulic systems of the governors run out of oil and cause unit tripping and possibly a blackout of the island.

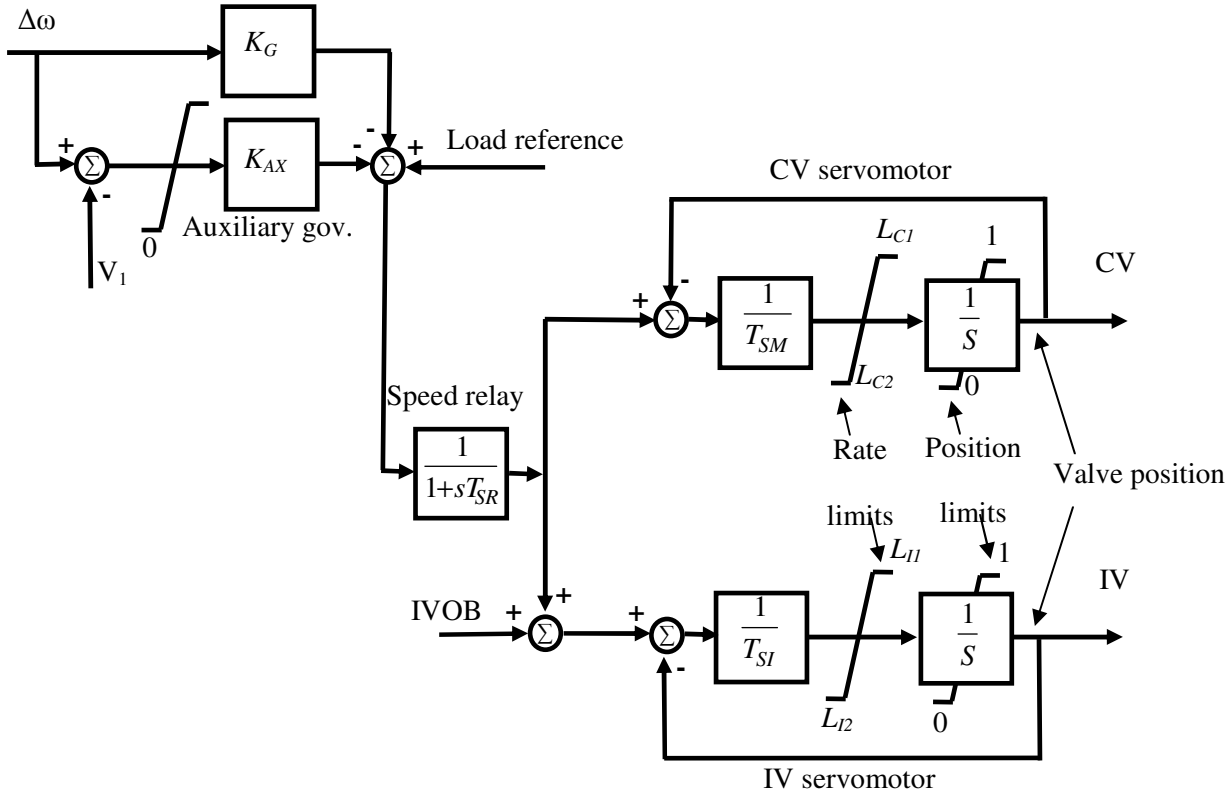

Figure 2.11 Governing system equipped with an auxiliary governor [51].

Where V_1 is the auxiliary governor opening bias and K_{AX} is the auxiliary controller gain.

2.6.2.3 Dynamic Braking

Dynamic braking involves applying shunt resistors to generator terminals to increase the generator output power during transient disturbances and consequently reducing the generator's rotor acceleration. Braking resistors are usually applied to hydraulic generating units; as the sudden shock of switching in of resistors does not have adverse effects on these units. On the other hand, in the case of thermal units, the effect of sudden switching in of braking resistors on the mechanical shaft fatigue life must be examined. Based on such examination, it is sometimes decided that braking resistors are to be switched in three or four steps over a full cycle of the lowest torsional mode [24, 52]. One form of dynamic braking is to apply the resistors for a short

duration of 0.5 second following an occurrence of a fault. Moreover, if the resistors remain connected too long, there is a possibility of instability on the “backswing”. Consequently, the switching time should be based on detailed simulation analyses. [24, 52-54].

2.6.3 Countermeasures for Both Negative and Positive Frequency Deviation

This section discusses a technique that can assist in minimizing the frequency deviations, whether this deviation is positive or negative, known as controlled area separation. Controlled separation is used to prevent the propagation of a certain disturbance throughout the rest of the system. Hence, preventing a sever system break up. Controlled separation is a pre-designed protection scheme that automatically splits the interconnected power system into viable islands that have a reasonably good generation/load balance. As a result, each separated area is more likely to survive. A lot of splitting strategies have been discussed in literature since the early 2000s up till now and some can be applied online while others must be designed in advance offline [55-60].

2.7 The Great Britain Frequency Control Philosophy

National Grid, the Great Britain System Operator (GBSO), is responsible for the management of the transmission network security and real time balancing of generation with demand. Any imbalance between generation input and demand will result in perturbations in the nominal system frequency of 50Hz. National Grid manages the system frequency to defined statutory steady state limits of ±0.5Hz (i.e. 49.5Hz to 50.5Hz) and our Operational limits of ±0.2 Hz (i.e. 49.8Hz to 50.2Hz).

Moreover, the System Frequency could rise to 52Hz or fall to 47Hz in exceptional circumstances. Consequently, design of user's plant and apparatus must enable operation of that plant and apparatus within that range in accordance with the following: (1) 47.5Hz - 52Hz continuous operation is required, (2) 47Hz - 47.5Hz operation for a period of at least 20 seconds.

However, if the frequency is above 52 Hz or below 47 Hz independent protective action is permitted to protect generation in the event of danger to safety of plant and/or personnel. Furthermore, the GB Security and Quality of Supply Standard (GB SQSS) [60] specifies the limits of frequency deviations for secured faults, which include loss of output from a single generating unit, Combined Cycle Gas Turbine Module (CCGT), boiler, nuclear reactor or DC bi-pole lost as a result of an event. These limits are:

(1) For Normal Infeed Loss Risk (1000MW): Maximum frequency deviation should not exceed 0.5Hz.

(2) For Infrequent Infeed Loss Risk (1320MW): Frequency should not deviate outside the range 49.5Hz to 50.5Hz for more than 60 seconds. The largest infrequent infeed loss of 1320MW is derived from the largest possible generation infeed loss on the transmission system that will result from a single event.

Moreover, in the case of infrequent infeed loss risk, National Grid's practice is to ensure that the maximum frequency deviation is limited to 0.8Hz. In addition, National Grid aims to return the frequency to operational limits (49.8Hz to 50.2Hz) within 10 minutes. For a larger generation loss than the Infrequent Infeed Loss Risk or a large generation deficit in an importing power island following a sudden system split, the National Low Frequency Demand Disconnection (LFDD) scheme, described in Table 2-1, is designed to automatically disconnect demand to contain the incident and prevent a total or partial shutdown of the power system. In addition, where the initial frequency is close to the lower operational limit of 49.8 Hz at the time of a 1320MW loss, the lowest planned frequency would be 49Hz. This would still restrict the maximum frequency deviation to 0.8Hz and provide a 0.2Hz margin above the level where the LFDD scheme is designed to operate and disconnect demand.

Table 2-1 Great Britain Low Frequency Demand Disconnection Structure [26]

Frequency (Hz)	**% Demand disconnected for each Network Operator in Transmission Area**		
	National Grid Electricity Transmission Ltd (NGET)	Scottish Power Transmission Ltd (SPT)	Scottish Hydro Electric Transmission Ltd (SHETL)
48.8	5		
48.75	5		
48.7	10		
48.6	7.5		10
48.5	7.5	10	
48.4	7.5	10	10
48.3			
48.2	7.5	10	10
48	5	10	10
47.8	5		
Total % Demand	60	40	40

2.8 Summary

Power system Frequency Deviation results from severe contingencies that lead to large generation–load mismatch. These contingencies can be a sudden loss of generation, a sudden loss of load centre or a sudden loss of a tie line connecting two areas splitting the two areas apart leaving each area with a generation-load mismatch.

For the cases where a part or the whole power system suffers sudden loss of generation, the system frequency will drop. On the other hand if the power system suffers sudden loss of load, the system frequency will rise. Not only that but in some cases where the system is lightly damped or the generators respond slowly, the frequency might suffer unstable swings.

Frequency must not exceed a certain limit or thermal units mechanical system would suffer stresses. Moreover, the system frequency must not decrease than a certain limit, not only would the thermal units mechanical system suffer stresses but also the plant capability may be severely reduced because of the reduced output of boiler feed pumps or fans supplying combustion air in the case of fossil fuelled units and, the reactors may overheat due to reduced flow of coolant in the case of nuclear units.

Consequently, frequency stability has been defined as "*The ability of a power system to maintain steady frequency following a severe system upset resulting in a significant imbalance between generation and load*." [33]

Some Frequency instability has been discussed in literature [30-60]. The first line of defence for frequency drop mitigation would be load shedding, followed by reserve generation planning and allocation. For the case of frequency rise, the machines overspeed controls comes as first line of defence. Another methodology to mitigate the propagation of the effect of a contingency is planned or controlled system splitting were the interconnected power system is divided into viable islands with less generation load mismatch and hence each island frequency is likely to be stable.

Great Britain has a well defined strategy for mitigating frequency drop due to loss of generation or area separation, see Section 2.7. However, there is no clear or published strategy discussing means for avoiding the generation rich separated areas frequency rise. This thesis is devoted to simulate the separation of some generation rich parts of the GB grid described in Chapter 3 and proposes means to ensure the frequency stability of such separated areas in Chapters 4, 5, 6 and 7.

CHAPTER 3

BASE CASE STUDIES MODELING AND ANALYSIS

3.1 Introduction

This chapter presents the modeling and simulation of the base case studies used in this thesis. This section presents an outline of this chapter. Section 3.2 describes the thesis case studies. Section 3.3 discuses the modeling of the various elements of the case studies. Section 3.4 presents the time domain simulation of the thesis case studies. Section 3.5 emphasizes the effect of installing more wind farms in future power systems. Furthermore, the effect of a frequency responsive HVDC link is illustrated in Section 3.6. Finally, Section 3.7 summarizes the chapter.

3.2 Description of Base Case Studies

The case studies discussed in this thesis are based on parts of the GB transmission system. For the purpose of illustrating system performance, studying the transmission capability of critical transmission boundaries and the need for transmission reinforcement and for describing opportunities, the National Grid, the GB transmission system operator, defines 17 critical boundaries that divide the GB grid into 17 study zones. This division is published in an annual report produced by the National Grid called, the Seven Year Statement (SYS) [61].

Two interesting critical boundaries defined by the SYS are the boundaries that separate the Scottish grid and Estuary (south east of GB) from the rest of the UK grid, respectively. These boundaries are operating at their maximum limits and require reinforcements to accommodate higher power levels in the near future [61]. The disconnection of such boundaries at maximum demand condition due to cascading failures would leave Scotland and Estuary areas with excess generation provoking the frequency stability of Scotland and Estuary, respectively. Consequently, this thesis considers three case studies:

1- Case Study based on the Scottish Grid 2009-2010.
2- Case study based on the Scottish Grid 2015-2016.
3- Case study based on Estuary 2009-2010.

The First case study represents the case where most generation are dispatchable frequency responsive thermal units and the power interrupted is less than the local load. The second case study takes into consideration future aspects. It considers the case where more wind is

accommodated to supply future increase of load. Yet, the interrupted power is less than the local load. Finally, the third case study is the case where most generation are dispatchable, frequency responsive, thermal units and the power interrupted is more than the local load. This case study also considers the case where an HVDC link exists.

3.2.1 Case Study 1 (Based on Scotland 2009/2010)

The case study discussed is based on the Scottish grid. Scotland is a generation rich area and exports up to 2.65 GW to England and Wales at system peak load. The Scottish grid is connected to the English Grid through four lines; three 400 kV lines and a 275kV line. The loss of any two lines would cause the overload of the remaining lines. If emergency measures fail to decrease the power transferred across the overloaded lines, all remaining lines would trip, disconnecting Scotland from the rest of the UK grid. Upon disconnection, the Scottish grid might suffer frequency instability.

A network model based on the Scottish network is developed (See Figure 3.1). The 275 and 400 kV transmission system of the south part of the Scottish transmission network is represented in detail while the northern network is neglected. The generic network has seven main power stations that are connected directly to the 275 kV and 400 kV network. Moreover, the rest of the UK grid is represented by one coherent machine and a composite load. Table 3-1 summarizes the data related to the power stations existing in the developed model. These data are obtained from [61]. For the developed model, generation; load and transmitted power are 5.4 GW, 3.5 GW and 1.9 GW respectively.

Table 3-1 Data related to the power stations of case study 1 [61].

Station Location	Plant Type	Plant Size (MW)
G1	Coal	2304
G2	Coal	1152
G3	Nuclear	1210
G4	Nuclear	1200
G5	Hydro	440
G6	Wind	300
G7	Wind	150

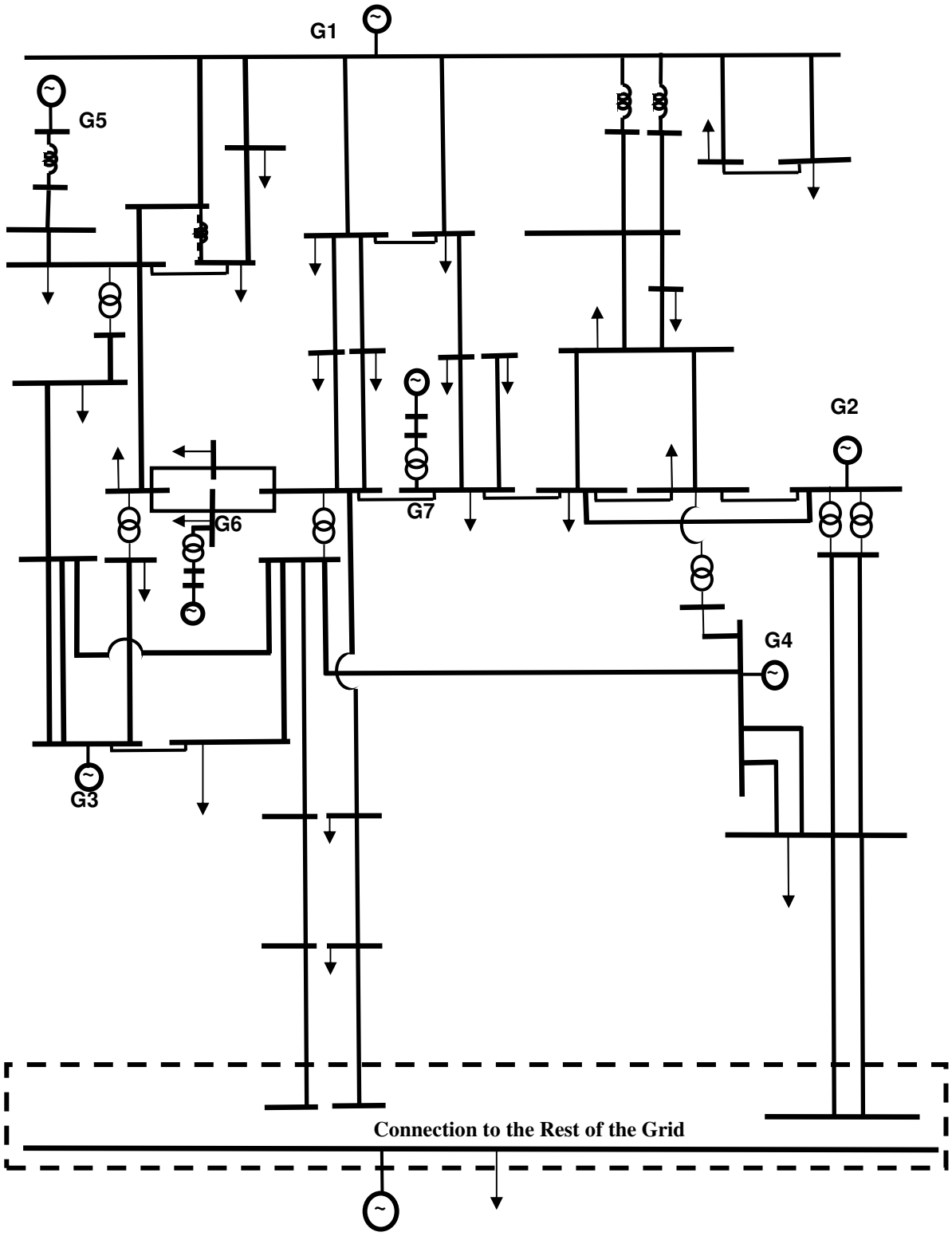

Figure 3.1 Single line diagram of Case Study 1 [61].

3.2.2 Case Study 2 (Based on Scotland 2015/2016)

To achieve the UK target of renewable electricity contribution of 147 TWhr by 2020, some future scenarios were developed [62, 63]. The resulting generation background scenarios, upon which the studies are based, vary the capacity of wind generation to be installed in Scotland from a minimum of 6.6 GW (this is the minimum required to meet the Scottish Government target on top of the existing hydro generation which is assumed to continue to contribute to the target), to 8 GW in a second scenario and a maximum of 11.4 GW by 2020 in a third scenario. For all scenarios and to still achieve the aforementioned total UK renewable electricity contribution of 147 TWhr by 2020, the volume of projected offshore wind farm generation in England and Wales was increased to compensate for any volumes less than 11.4 GW in Scotland [62, 63].

Moreover, all previously mentioned scenarios assume that the minimum amount of 6.6 GW of wind will be installed by 2015. Hence, the expected amount of power to be transferred from Scotland to England would reach 4.5 GW at system peak load. The 275kV line would be upgraded to 400 kV and all four lines would be series compensated to accommodate such increase in the power transferred [62].

It becomes interesting to discuss the stability of the Scottish power system upon disconnection from the rest of the UK grid as more power will be interrupted. Not only is that, but the level of wind farms will also increase. Based on this, the model in Figure 3.1 is upgraded to include extra installed wind farm capacity of about 2.35 GW, see Figure 3.2. Hence, the percentage capacity of each type of generation is updated as shown in Table 3-2. Moreover, the developed model generation; load and transmitted power are 6.5 GW, 3.5 GW and 3 GW respectively. I.e. the increase in generation due to extra wind farms is transmitted to England and Wales, while the Scottish load remains the same as in Case Study 1.

Table 3-2 Power stations % Capacities for case study 1 and case study 2 [61].

Plant Type	**Installed capacity as % of different plant type out of overall installed capacity (2009)**	**Installed capacity as % of different plant type out of overall installed capacity (2015)**
Coal	51.15	38.87
Nuclear	35.67	27.11
Hydro	6.51	2.47
Wind	6.66	31.54

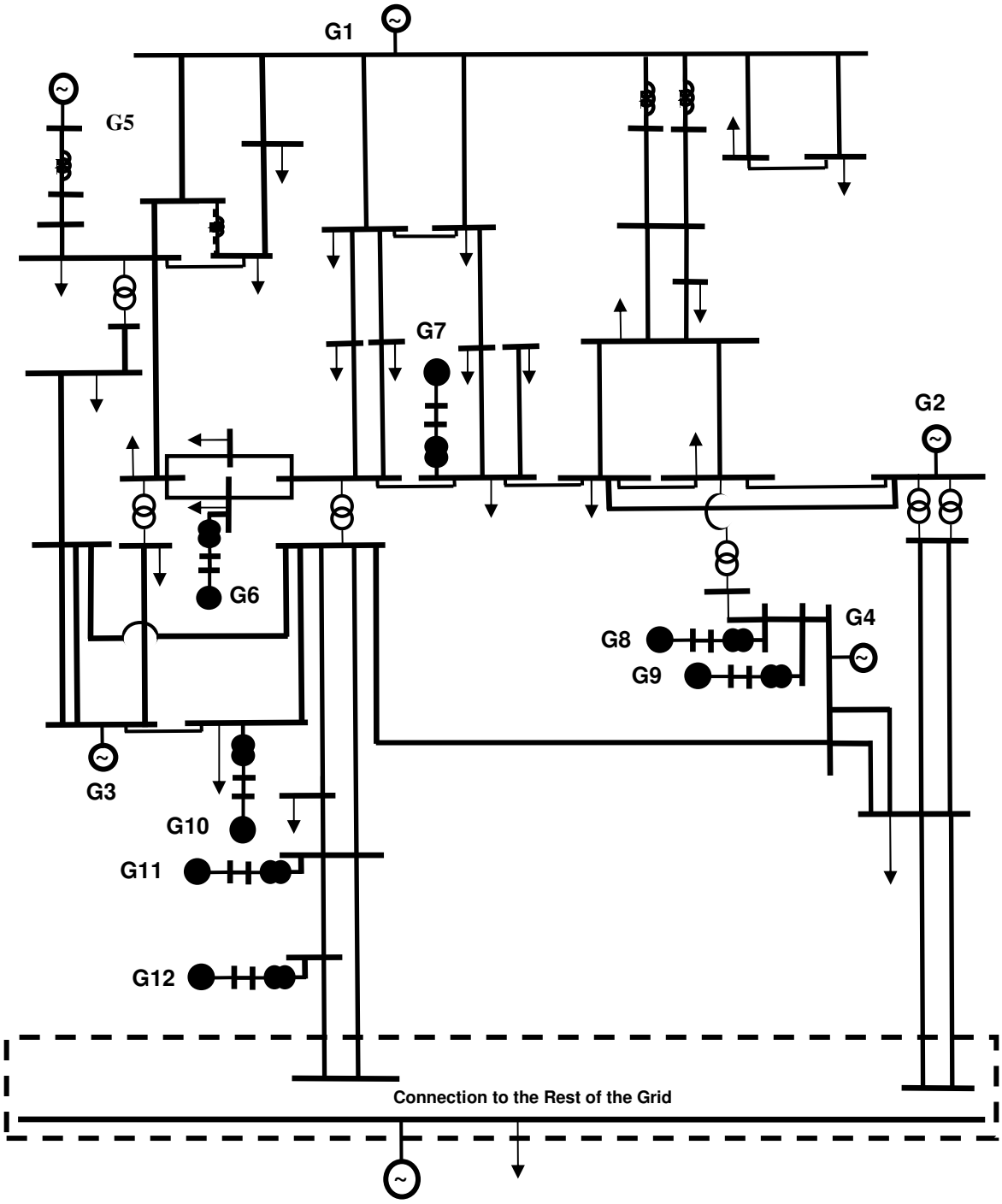

Figure 3.2 Single line diagram of Case Study 2 (dark generators are wind) [61].

3.2.3 Case Study 3 (Based on Thames Estuary 2009/2010)

Thames Estuary is a heavy generating zone, see Figure 3.3. The installed generation capacity of Thames Estuary is 9816 MW while its estimated winter peak demand is only 2180 MW. The actual amount of generation during peak load is estimated as 8255 MW (i.e. this zone delivers about 6075MW to the rest of the UK grid at the time of peak load) [61].

This large amount of energy delivered from the Thames Estuary to the rest of the UK grid at the condition of system peak load, was the main reason to study the frequency stability of this zone in the event of uncontrolled separation from the rest of the UK grid. Another factor that affected this choice is that the Thames Estuary imports power through an HVDC interconnector between UK and France. Consequently, the effect of an HVDC on frequency stability can be investigated. Moreover, the developed model generation; load and transmitted power are 8 GW, 2 GW and 6 GW respectively. Table 3-3 summarizes the data related to the power stations existing in Thames Estuary [61].

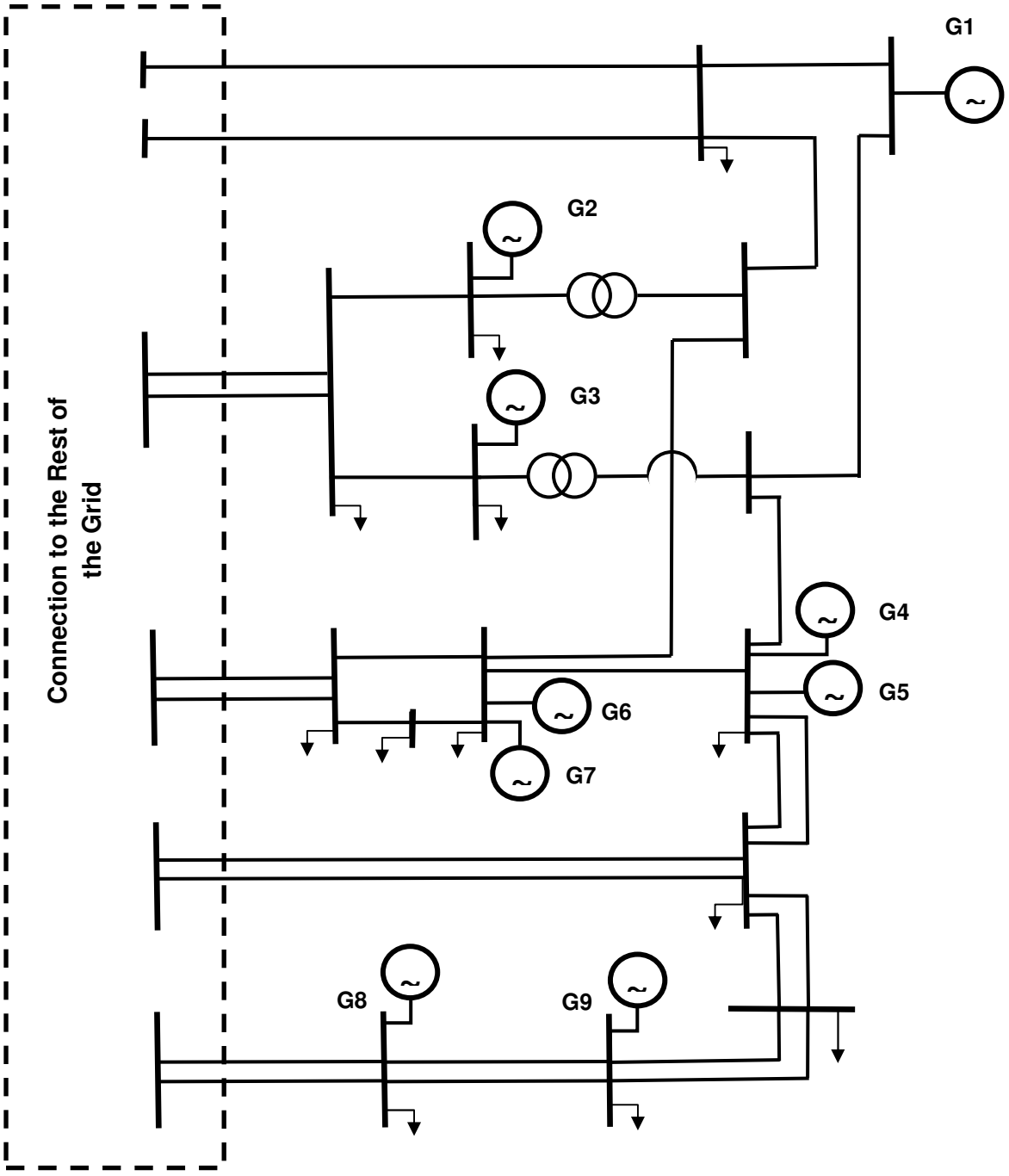

Figure 3.3 Single line diagram of Case Study 3 [61].

Table 3-3 Information related to power stations of case study 3 [61].

Station Code	Plant Type	Plant Size (MW)
G1	CCGT	800
G2	Coal	738
G3	Coal	357
G4	Oil	1355
G5	CCGT	700
G6	CCGT	805
G7	Coal	1966
G8	Nuclear	1081
G9	HVDC	2000

3.3 Modeling Of Network Elements In Case Studies

A generic model for each case study was built using SIM/MATLAB. More details about the models used to represent various elements of the case study models are presented in the following subsections

3.3.1 Conventional Power Stations

Here the details related to the frequency responsive conventional power stations generating units and their controllers are discussed.

3.3.1.1 The Generator Model

Each conventional power station is represented by a single machine generating 80-82% of its capacity. Each of the coal, nuclear and hydro power stations is represented by one coherent synchronous machine equipped with a prime mover.

The electrical part of the synchronous machine is represented by a sixth-order state-space model and the mechanical part by a second-order system, see Appendix A. The model takes into account the dynamics of the stator, field, and damper windings. The equivalent circuit of the model is represented in the rotor reference frame (qd frame) [24, 41-42, 64 and 66-71].

3.3.1.2 The Excitation System Model

For the sake of voltage control, a two time constant excitation system is assumed [24, 64-65]. This excitation system is shown in Figure 3.4.

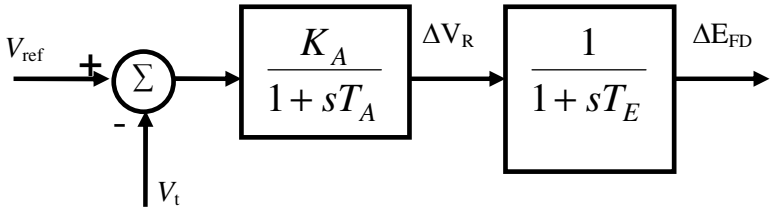

Figure 3.4 A two-time-constant excitation system [64].

Where V_{ref} is the reference voltage, V_t is the actual voltage, K_A is the amplifier gain, T_A is the amplifier time constant, T_E is the exciter time constant, and ΔE_{FD} is the variation of exciter e.m.f.

3.3.1.3 The Turbine Torque and Governor System

Section 3.3.1.3.1 discusses the governor and prime mover models used to represent steam plants. On the other hand, Section 3.3.1.3.2 presents the hydro plant prime mover model.

3.3.1.3.1 Steam Plants (Fossil-Fuelled, Nuclear, and CCGT)

As steam plants are the dominant type of generation in our case studies, more attention has been brought to their modeling. The tandem-compound, single-reheat steam turbine is chosen [24, 64]. The steam turbine has three stages, each modeled by a first-order transfer function. The first stage represents the steam chest with a time constant T_{CH} while the second stage represents the reheater with a time constant T_{RH} and finally the third stage represents the crossover piping and has a time constant T_{CO}. The boiler is not modeled and boiler pressure was assumed to be a constant at 1.0 p.u. Fractions F_{HP}, F_{IP} and F_{LP} are used to distribute the turbine power to the various shaft stages (see Figure 3.5). Furthermore, F_{IP} is set to zero in the case of nuclear units and for simplicity CCGT units are modeled exactly as fossil fueled units.

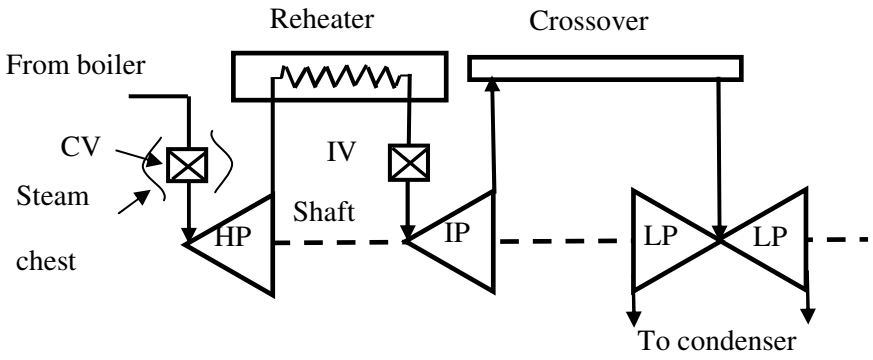

(a) The tandem compound steam turbine configuration.

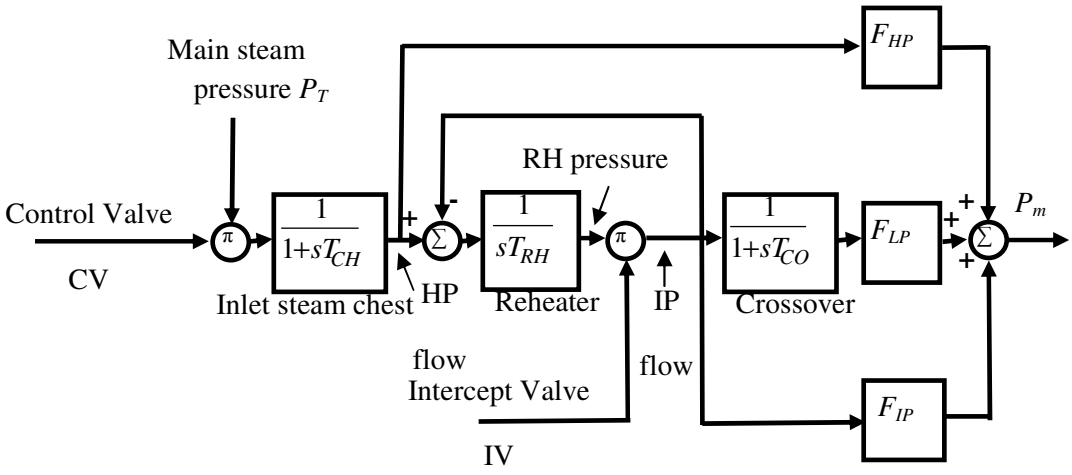

(b) The tandem compound steam turbine transfer function.

Figure 3.5 Case study prime mover models for Steam plants [24].

Moreover, the speed governing system chosen is the mechanical-hydraulic control MHC system used for governing steam turbines [24], see Figure 3.6.

The speed governing system chosen consists of a proportional regulator, a speed relay, and two servomotor systems controlling the control valves CVs and intercept valves IVs, respectively (i.e. overspeed control is modeled as well). As mentioned earlier, for normal speed/load control only CVs respond. The IVs are held fully open by a bias (IV opening bias) signal. On overspeed, due to the resulting large speed error signal, the bias is overcome and the IVs are closed rapidly. When the control signal is restored to a value less than the bias, IVs are again fully opened.

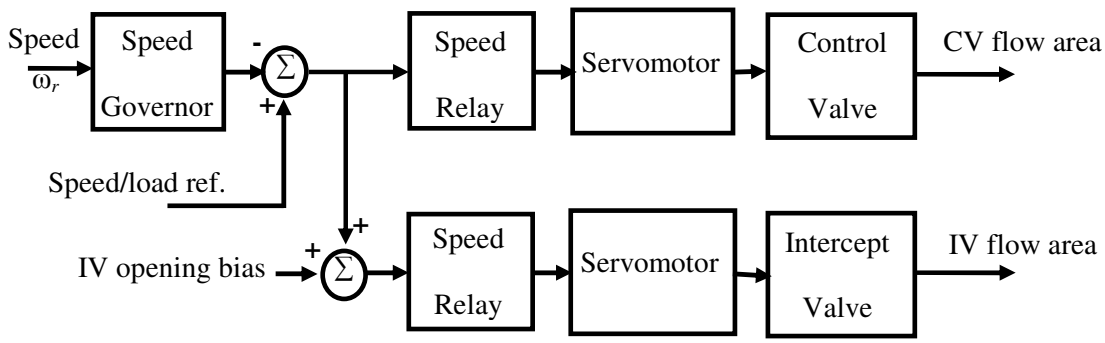

(a) Functional block diagram

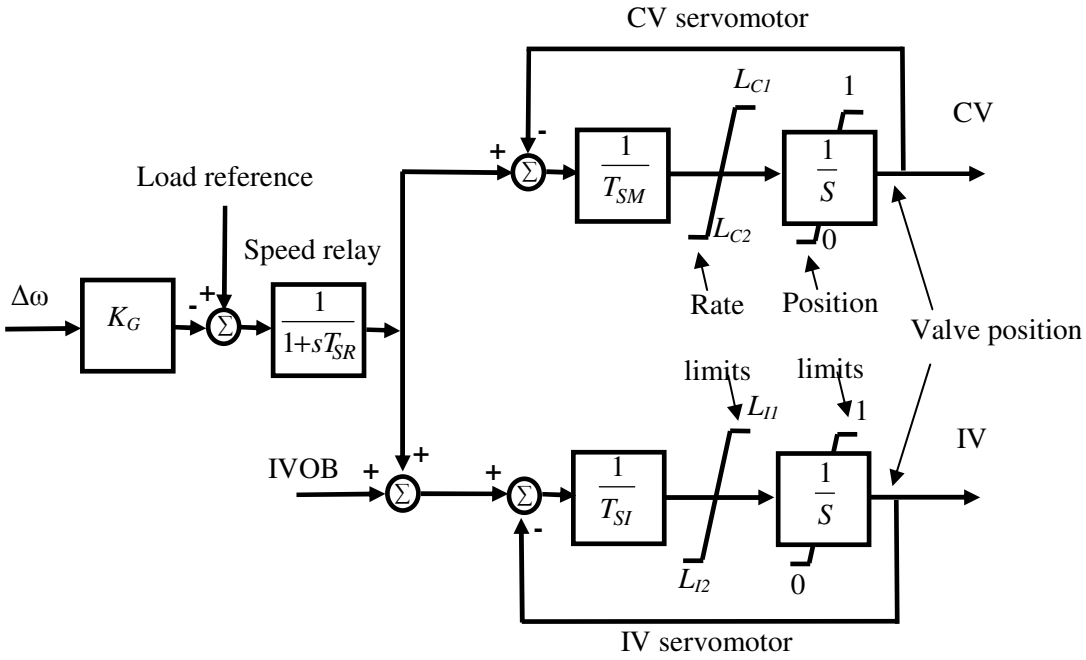

(b) Block diagram representation.

Figure 3.6 Mechanical-hydraulic control (MHC) model.[24]

3.3.1.3.2 Hydro Plants

As hydro generation is minority in our case studies, the governor and prime mover dynamics are presented by the simple block diagram shown in Figure 3.7 [24].

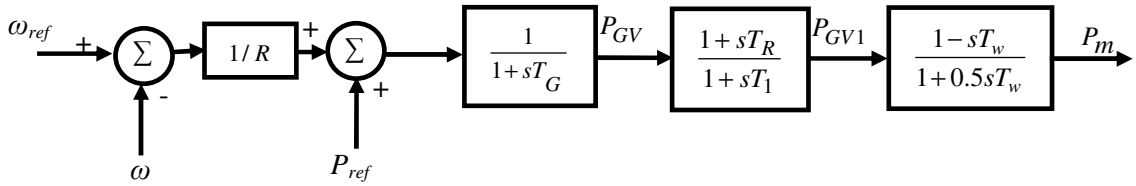

Figure 3.7 Case study prime mover model for hydro plant [24].

Where ω_{ref} is the reference speed, R is the governor droop, T_G is the governor droop time constant, T_R is the rest time, T_1 is transient droop compensation time constant, and T_w is the water time constant.

3.3.2 The Wind Farms Model

The studies presented consider the impact of additional wind generation delivering base load power. The wind generation is provided by wind farms based on Fixed Speed Induction Generators (FSIG). Each wind farm is represented by one coherent induction machine equipped with a steady state wind turbine model. Wind farms are generating 50-60% of their installed capacity. Moreover, capacitive compensation is provided on the generator terminals in order to supply the reactive power demand of the FSIG whilst maintaining the desired voltage profile for the network.

The electrical part of the induction machine is represented by a fourth-order state-space model and the mechanical part by a second-order system. All electrical variables and parameters are referred to the stator. All stator and rotor quantities are in the arbitrary two-axis reference frame (dq frame) [24, 41-42, 64 and 66-73], see Appendix A.

The turbine model is based on the steady-state power characteristics of wind turbines. The stiffness of the drive train is infinite and the friction factor and the inertia of the turbine are combined with the generator coupled to the turbine [72-73].

3.3.3 HVDC Link Model

The HVDC connection in Case Study 3 imports 99.5 % of its capacity [61]. It is represented by a controlled current source with a time constant of 0.5 sec. The HVDC link is operated in a frequency responsive mode. It is equipped with a frequency proportional controller of a 4% droop.

3.3.4 Transmission Line Model

The case study transmission system is represented using distributed parameter lines. The line parameters resistance R, inductance L and capacitance C are obtained from the GB SYS appendices [61].

3.3.5 The Load Model

Loads are represented by a parallel combination of resistive, inductive and capacitive RLC elements. At the specified frequency, the load exhibits constant impedance. The active and reactive powers absorbed by the load are proportional to the square of the applied voltage. Consequently, the case considered here is the worst case scenario where the frequency dependence of the load, D, is zero.

3.4 Time Domain Simulation and Analysis (Base Cases)

Some time responses are presented in this section. The disturbance simulated is the simultaneous opening of all ties connecting the case studies to the rest of the system, the result being an island with generation nearly twice the load. The frequency response of the separated case studies is examined at different governor rate limits. From literature, governor rate limiters can vary from 1 p.u./sec to 0.1 p.u./sec depending on the governor type. It is important to study the effect of such rate limiters as it increases the governor time delay, depending on the maximum rate limit allowed and the amount of power interrupted. This increase in the governor time delay might affect the frequency response dramatically. Consequently, the frequency time response of the thesis case studies is presented for conventional generation with governor rate limits varied from 0.1p.u/sec to 0.9 p.u./sec in increments of 0.1 p.u. Moreover, by default the instant at which all case studies considered in this thesis are disconnected from the rest of the grid is to be 10 seconds from the start of any simulation run presented through the whole thesis. Section 3.4.1, Section 3.4.2 and Section 3.4.3 show the frequency time response of Case Study 1, 2 and 3 respectively.

3.4.1 Case Study 1

Time simulation of the frequency response of Case Study 1 network upon disconnection from the rest of the UK grid is presented in this section. The interrupted power is 28% of the case study installed capacity. This value is chosen to match estimated power flows presented in the GB SYS for winter peak demand. Figure 3.8 shows the frequency response of Case Study 1 upon disconnection from the rest of the grid at different governor maximum rate limits where the overspeed control operating at 52 Hz.

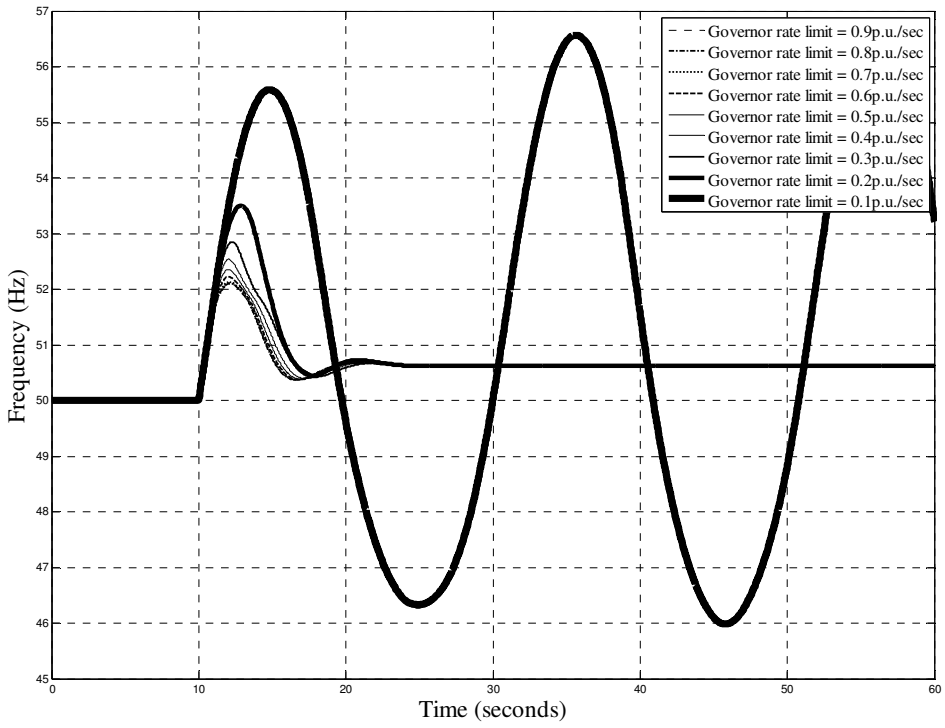

Figure 3.8 Frequency response of Case Study 1 upon disconnection from the rest of the Grid.

Figure 3.8 indicates that the frequency first overshoot exceeds 52 Hz in Case Study 1.Moreover, the frequency response reaches a steady state value that exceeds 50.5 Hz except for the case where the maximum governor rate limit is 0.1 p.u./sec rate, the response shows unstable oscillations.

3.4.2 Case Study 2

Time simulation of the frequency response of Case Study 2 network upon disconnection from the rest of the UK grid is presented in this section. The interrupted power is 38% of the case study installed capacity. This value is chosen to match estimated power flows presented in the GB SYS for winter peak demand. Figure 3.9 shows the frequency response of Case Study 2 upon disconnection from the rest of the grid after 10 seconds, at different governor maximum rate limits where the overspeed control is operating at 52 Hz.

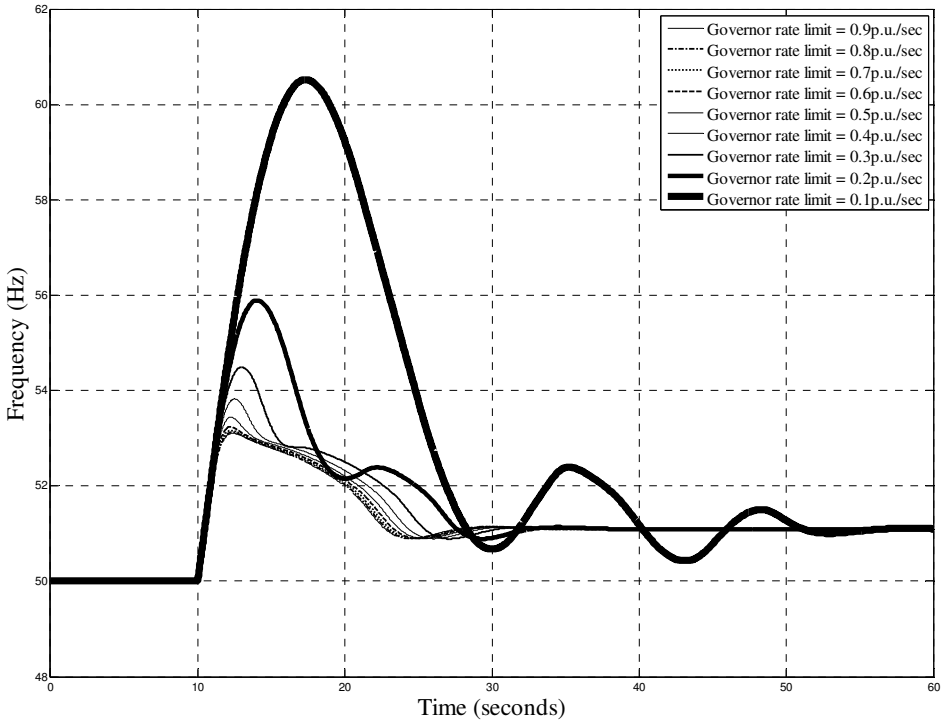

Figure 3.9 Frequency response of Case Study 2 upon disconnection from the rest of the Grid.

As shown in Figure 3.9, the frequency first overshoot exceeds 52 Hz. Moreover, the frequency response shows a stable response and reaches a steady state value that exceeds 51 Hz in all cases. However, the frequency undergoes damped oscillations for the case where the maximum governor rate limit is 0.1p.u./sec

3.4.3 Case Study 3

Time simulation of the frequency response of Case Study 3 network upon disconnection from the rest of the UK grid is presented in this section. The interrupted power is 62 % of the case study installed capacity. This value is chosen to match estimated power flows presented in the GB SYS for winter peak demand. Figure 3.10 shows the frequency response of Case Study 3 upon disconnection from the rest of the grid after 10 seconds at different governor maximum rate limits where the overspeed control is operating at 52 Hz.

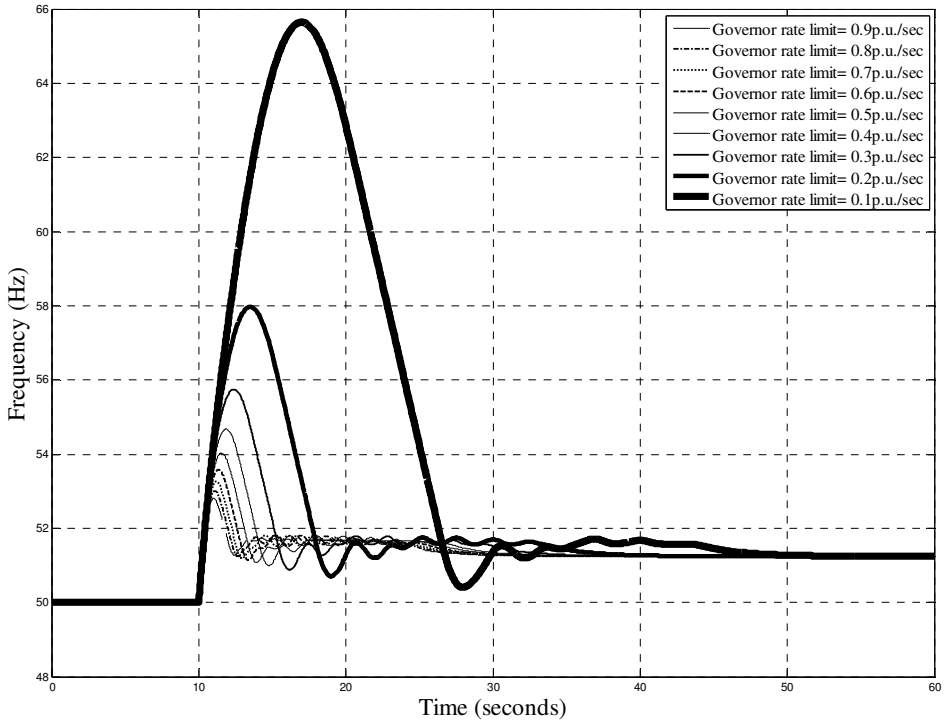

Figure 3.10 Frequency response of Case Study 3 upon disconnection from the rest of the Grid.

From Figure 3.10, the frequency first overshoot exceeds 52 Hz; the frequency response shows a stable response and reaches a steady state value that exceeds 51 Hz in all cases.

3.5 Effect of Increased Wind Energy Penetration

This section compares the frequency response of Case Study 1, where wind generation is still developing to Case Study 2 where more wind generation would have been installed. Two scenarios for Case Study 2 are simulated. Scenario 1 where the interrupted power is 38% of the installed capacity (i.e. any increase in generation due to newly installed wind farms is to be transmitted to England and Wales and the load in Case Study 2 remains the same as the load in Case Study 1). Moreover, Case Study 2 is modified to simulate Scenario 2. Scenario 2 considers an increase in the local load of case study 2. This lessens the interrupted power to 28% of the installed capacity, matching the p.u. conditions of Case Study 1. Figure 3.11 shows the frequency response of Case Study 1 and Case Study 2 upon disconnection from the rest of the grid at different governor maximum rate limits where the following three cases are compared in each subplot: (a) Case Study 1, (b) Case Study 2, and (c) Case Study 2 Modified.

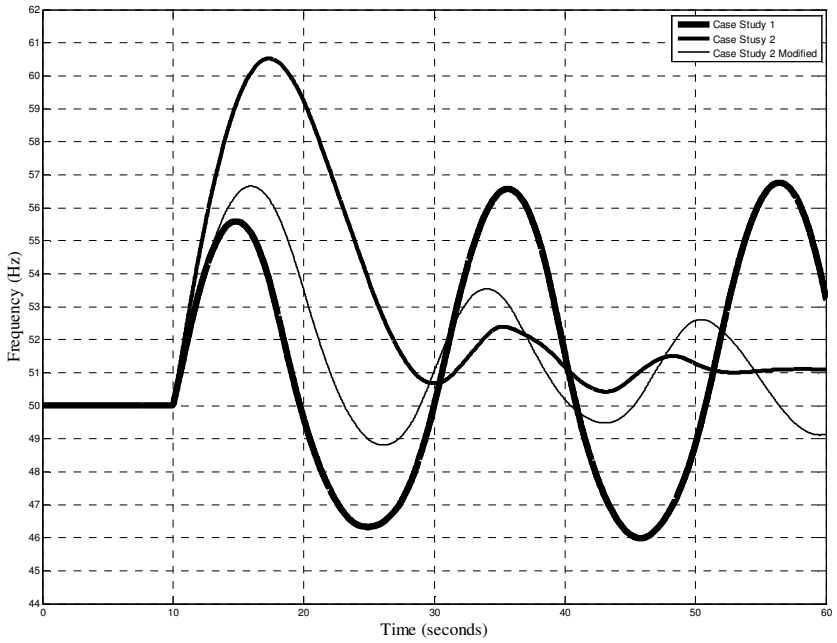

(a) Maximum governor rate limit= 0.1 p.u./sec

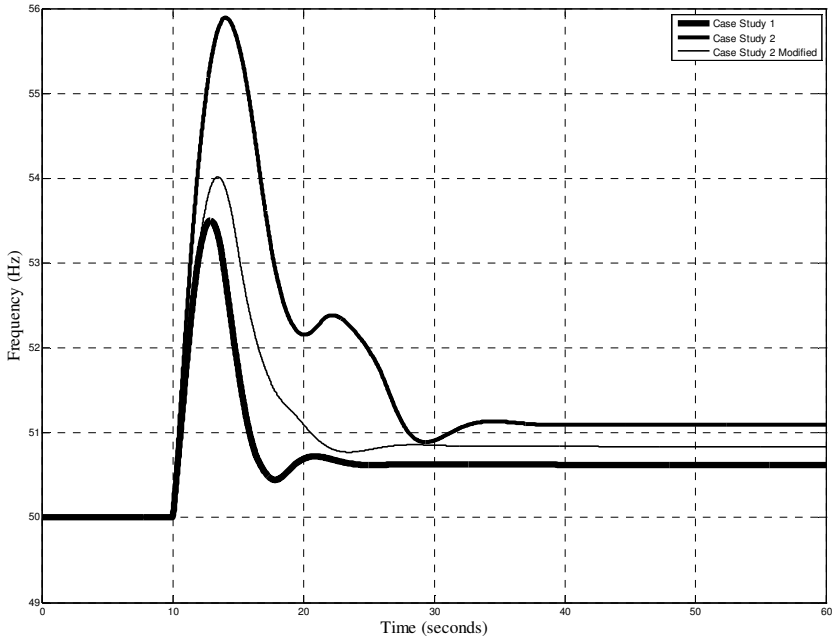

(b)Maximum governor rate limit= 0.2 p.u./sec

Figure 3.11 Frequency responses of Case Study 1 and Case Study 2 upon disconnection from the rest of the Grid.

Comparing Case Study 2 to Case Study 1, see Figure 3.11, it can be concluded that over generated separated areas with high proportions of wind generation would suffer higher

frequency first overshoot, and higher steady state frequency values upon disconnection. However, in case of very slow governor response, specifically governors with maximum rate limit of 0.1 p.u./sec, increasing the proportion of frequency non-responsive wind generation has assessed in stabilizing the frequency response and damping the low frequency oscillations.

3.6 Performance with HVDC Link

This section investigates the effect of the current HVDC link in Case Study 3 on the frequency response of the case study upon separation from the rest of the grid. In order to provide a base line, against which HVDC influence on network frequency response can be judged, the case where the power is provided only by conventional synchronous generation is also considered. Moreover, the HVDC link is assumed to be frequency responsive with no limitations on the rate of change of power. Figure 3.12 shows the frequency response of Case Study 3 upon disconnection from the rest of the grid at Maximum governor rate limit= 0.2 p.u./sec, where the following three cases are compared in each subplot:(a)All generators are conventional,(b)A unidirectional HVDC link exists,(c) An HVDC link that allows power reversal exists.

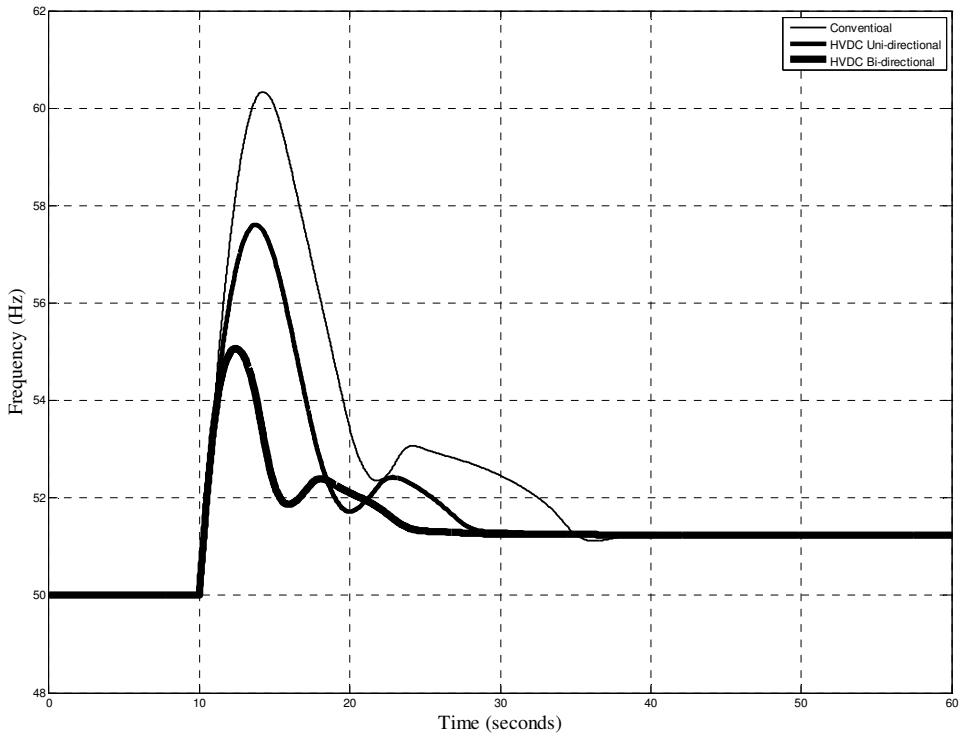

Figure 3.12 Frequency response of Case Study 3 with and without HVDC Link upon disconnection from the rest of the Grid.

The investigation of the effect of the existence of an HVDC connection in Case Study 3 has lead to the conclusion that the frequency first overshoot is decreased. Not only that, but allowing the

power reversal operation of the HVDC connection would improve the frequency response and decrease the frequency first overshoot more and more, see Figure 3.12 .

3.7 Conclusions

Dependent on the assumptions made in the modelling, the studies conducted on the generic network model (with generic parameters employed, see Appendix B) indicate that the frequency first overshoot exceeds 52 Hz in all Case Studies. Moreover, the frequency response of all three case studies reaches a steady-state value that exceeds 50.5 Hz except for Case Study 1, where the maximum governor rate limit is 0.1 p.u./sec, the response shows unstable oscillations.

These results lead to the understanding that, the higher the proportions of wind generation, as in Case Study 2, or the existence of a fast acting HVDC connection in the separated over generated area, as in Case Study 3, assess in stabilizing the frequency response and damping the low frequency oscillations in the case of very slow governor response, specifically governors with maximum rate limit of 0.1 p.u./sec.

But as results show that the frequency response overshoots to values higher than the generating unit's over frequency protection relay settings of 52 Hz, the following chapters will discuss possible methodologies to improve the frequency response (transient and steady state response) of separated generation rich areas resulted due to sever disturbance, specifically the thesis three base case studies.

CHAPTER 4

AUTOMATIC GENERATION TRIPPING

4.1 Introduction

Selective tripping of generating units at appropriate locations is recognised to reduce power transferred over critical transmission interferences. Before the 1970s, this practice was confined to hydro units only. With time, this practice has gradually been extended to thermal units to solve sever stability problems. Moreover, special facilities are to be provided, else the rejected unit goes through a standard shut down and start up cycle, consequently, full power may not be available for several hours. To overcome this situation, many utilities design thermal units so that, after tripping, units continue to run, supplying unit auxiliaries. This permits the units to be resynchronized to the system and restored to full load in about 15 to 30 minutes [74].

The scheme used for detection of system conditions requiring unit tripping is often an extension of trip circuits from various remote and local line protections. If the faulted line is restored within minutes, the rejected units are brought back online quickly. Since generating units can be tripped rapidly, this is a very effective means of improving transient stability. An automatic operating generation tripping scheme would decrease the mechanical power rapidly in an over generated island to reduce the area frequency overshoot and minimize the frequency steady state error.

This chapter discusses the possibility of designing a centralized island automatic generation tripping controller. The challenge now is in estimating the amount of generation needed to be tripped and a criterion to arrange the tripped generators in a priority list.

This section provides introductory information and presents this chapter outline. Section 4.2 develops a simple scoring mechanism to select which power station has priority to be tripped. Time domain simulations for the thesis case studies considering generation tripping is presented in Section 4.3. Finally, Section 4.4 summarizes this chapter.

4.2 Selective Tripping

This section ranks generators taking into consideration the dynamic response of different units (i.e. is the unit frequency responsive or not?), the ability of the area to be restored quickly and the most economic operation.

4.2.1 Dynamic Response

Here generators are ranked according to their response to variations. It is important not to trip the stations that could change its output quickly to reach an equilibrium state as fast as possible and ensure a low overshoot. The HVDC is ranked H, high, as it can change from zero to maximum capacity in only 2-5 seconds if no rate limiters are applied while all other stations are ranked as M, medium, as they respond slowly due to the turbines and machines inertia. And finally, wind is considered as L low as the wind generation is assumed to be less frequency responsive within this thesis study.

4.2.2 Minimum Zero Time

The Minimum Zero Time (MZT) is one of the dynamic parameters defined for each generating unit. It is the minimum time that a unit which has been exporting must operate at zero before returning to export. It becomes interesting to take this information into consideration to ensure fast system restoration. Table 4-1 shows MZT for different types of generation [75].

Table 4-1 Minimum Zero Time [75]

Fuel Type	MZT (min)
Nuclear	999
Wind	n/a (expected to be very small)
Gas	300-360
Coal	240-999
France (HVDC Link)	n/a (expected to be very small)
Pumped storage (Hydro)	30
Oil	240-360

Based on the values given in Table 4-1, generators are ranked as H, M, L or VL. H means that such generator has a high minimum time and will take a long time to be restored. Hence should be the last to be tripped as in the case of nuclear and some coal power stations. Moreover, M and L mean medium and low minimum zero time. Generators with MZT of 300 or 360 are considered medium and generators of 240 MZT are considered Low. This is the case of oil, coal and CCGT power stations. Finally, HVDC and wind is ranked as very low VL, as they can be restored faster than the aforementioned types of generating units.

4.2.3 Economic Rank

In Great Britain, the electricity market is an open market, where bilateral contracts are formed between generation and demand since March 2001. The aim of this was to overcome some shortcomings in the old 'pool' based model. For example it will increase transparency of the market, encourage demand side participation and lower prices for customers. It becomes the system operator task to ensure that (a) total generation matches demand, (b) constrains of the system are respected and (c) there is an adequate backup to cover failures.

All of this is achieved through the balancing mechanism tool, where Balancing Mechanism Units (BMUs) submit its Final Physical Notification (FPN) 3.5 hours before the real time operation. The FPN is simply a notification of a market participant's energy profile throughout a settlement period. Together with an FPN it also submits a set of Bid- offers pairs that enable the National Grid to alter the output from the BMUs. Offers show the willingness of the generator to increase its generation. However bids show the willingness of the unit to decrease the generation [76].

So it is the bid price that is taken into consideration to discuss generation tripping. Power stations with negative bids show unwillingness to be tripped and would mean that the GB system operator has to pay the power station owner. On the other hand, power stations with positive bid values show the willingness to decrease its output and would mean that the power station owner is willing to pay the system operator money which is balanced by the fuel savings.

Table 4-2 shows the average prices experienced over 2005-2007 across the broad operation of the Balancing Mechanism ('BM'), by class of plant [62].

Power stations with negative bid values are given the notation H which means very expensive to change and not to be tripped if possible. On the other hand, power stations with positive Bids are given the notation L which means that the output of such generators can be lowered at a low price and hence would be advised to be tripped first if required.

Table 4-2 Average Bid Prices [62]

Fuel Type	Bid Price (£/MWh)
Nuclear	-100
Wind	-50
Gas	10
Coal	15
France (HVDC Link)	20
Pumped storage (Hydro)	75
Oil	100

4.2.4 Case Studies Priority to Trip Lists

Based on the ranking given for each power station, the power stations are numbered in an ascending order indicating which one has the priority to be tripped first. The generating unit dynamic or transient rank is considered first, where slow or non frequency responsive units have the priority to be tripped than fast frequency responsive generating units. If generating units match in their dynamic response rank, then the second step is to consider the MZT rank of such different units, where units that can be recovered faster have the priority to be tripped to assist in a fast restoration process. If still generating units match in both the dynamic and MZT rank, the average bid price is considered. If all previous mentioned ranks match, the priority to be tripped is given to the generating unit with smallest size to avoid excess unnecessary generation tripping. Table 4-3, Table 4-4 and Table 4-5 present the thesis case studies power stations ranked and arranged according to the above successively scoring criteria.

Table 4-3 Case Study 1 power station ranks and priority to be tripped

Station Number	G1	G2	G3	G4	G5	G6	G7
Station Type	C	C	N	N	H	W	W
Dynamic Response	M	M	M	M	M	L	L
Minimum Zero Time	M	M	H	H	M	L	L
Economic Rank	L	L	H	H	L	H	H
Priority to be Tripped	5	4	6	5	3	2	1

Table 4-4 Case Study 2 power station ranks and priority to be tripped

Station Number	G1	G2	G3	G4	G5	G6	G7	G8	G9	G10	G11	G12
Station Type	C	C	N	N	H	W	W	W	W	W	W	W
Dynamic Response	M	M	M	M	M	L	L	L	L	L	L	L
MZT	M	M	H	H	M	L	L	L	L	L	L	L
Economic Rank	L	L	H	H	L	H	H	H	H	H	H	H
Priority to be Tripped	10	9	12	11	8	4	2	1	3	7	6	5

Table 4-5 Case Study 3 power station ranks and priority to be tripped

Station Number	G1	G2	G3	G4	G5	G6	G7	G8	G9
Station Type	CCGT	C	C	Oil	CCGT	CCGT	C	N	DC
Dynamic Response	M	M	M	M	M	M	M	M	H
Minimum Zero Time	M	M	M	M	M	M	M	H	L
Economic Rank	L	L	L	L	L	L	L	H	L
Priority to be Tripped	6	3	2	1	5	7	4	8	9

4.3 Generation Tripping Simulation

After ordering the generators in the previous section, comes the second question which is how much power stations are to be tripped. This can be decided via time domain simulations, tripping different amount of plants and observing the frequency overshoot just after disconnection. Moreover, generation tripping should always ensure that the un-tripped generation capacity still exceeds the load level; else frequency would start to decline and loads will start to be shed if a load shedding scheme exists within this separated area if not generators in that separated area would trip off by their low frequency protection leading to an area blackout.

The disturbance simulated is the simultaneous opening of all ties connecting the case studies to the rest of the system. The frequency response of the separated case studies is examined at different governor rate limits and with different amounts of generation tripped once the separation takes place and the frequency exceeds the statutory limit of 50.5 Hz. As mentioned in Chapter 3, the frequency time response of the thesis case studies is presented for conventional generation with governor rate limits varied from 0.1 p.u./sec to 0.9 p.u./sec in increment of 0.1 p.u.

4.3.1 Case Study 1

Time simulation of the frequency response of Case Study 1 network upon disconnection from the rest of the UK grid is presented in this section with different amounts of generation tripped taking the priority list into consideration. Figure 4.1 shows the frequency response of Case Study 1 upon disconnection from the rest of the grid at different governor maximum rate limits where the following five cases are compared in each subplot: (a) no generation tripped, (b) 1 wind farm tripped, (c) 2 wind farms tripped. (d) 2 wind farms and 1 hydro plant tripped and (e) 2 wind farms, 1 hydro plant and 1 coal-fired plant tripped.

Time domain simulation shows that at most 4 power stations are to be tripped to ensure that the frequency first overshoot is below 52 Hz. Moreover, time domain simulation shows that the more generators tripped the more the steady state frequency decreases to be within the frequency statutory values. Figure 4.1 and Table 4-6 show that for generators with a governor rate limit higher than 0.6 p.u./sec , tripping 2 wind farms is sufficient to contain the first frequency overshoot below the 52 Hz. If the generators governor rate limit is 0.4 or 0.5 p.u./sec , an extra hydro power station is to be tripped. Finally, for the case of generators with governor rate limiters between 0.3 and 0.1 p.u./sec, the whole 4 power stations, 2 wind farms, 1 hydro plant and 1 coal fired, are required to be tripped to contain the separated area frequency first overshoot below 52 Hz. However, for the case of governor rate limiters of 0.1 p.u. /sec the frequency swings and shoots to frequency levels higher than the 52 Hz on the second swing.

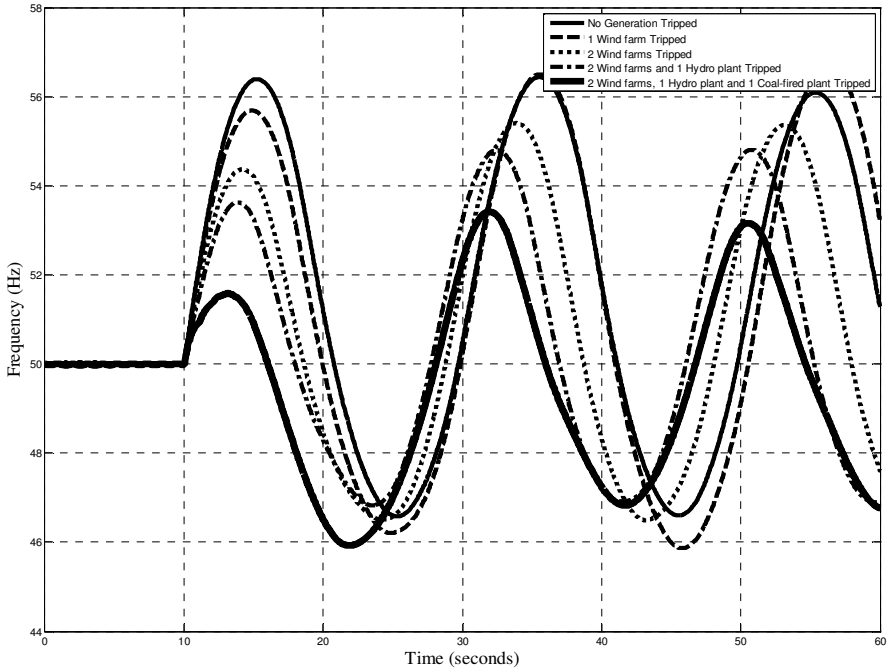

(a) Maximum governor rate limit= 0.1 p.u./sec.

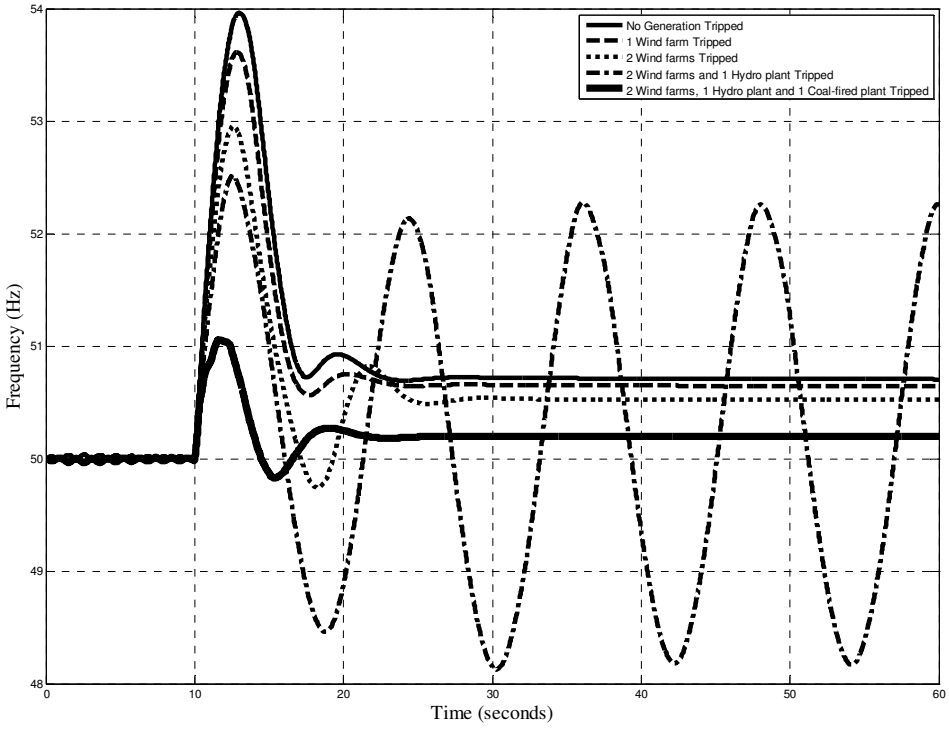

(b) Maximum governor rate limit= 0.2 p.u./sec.

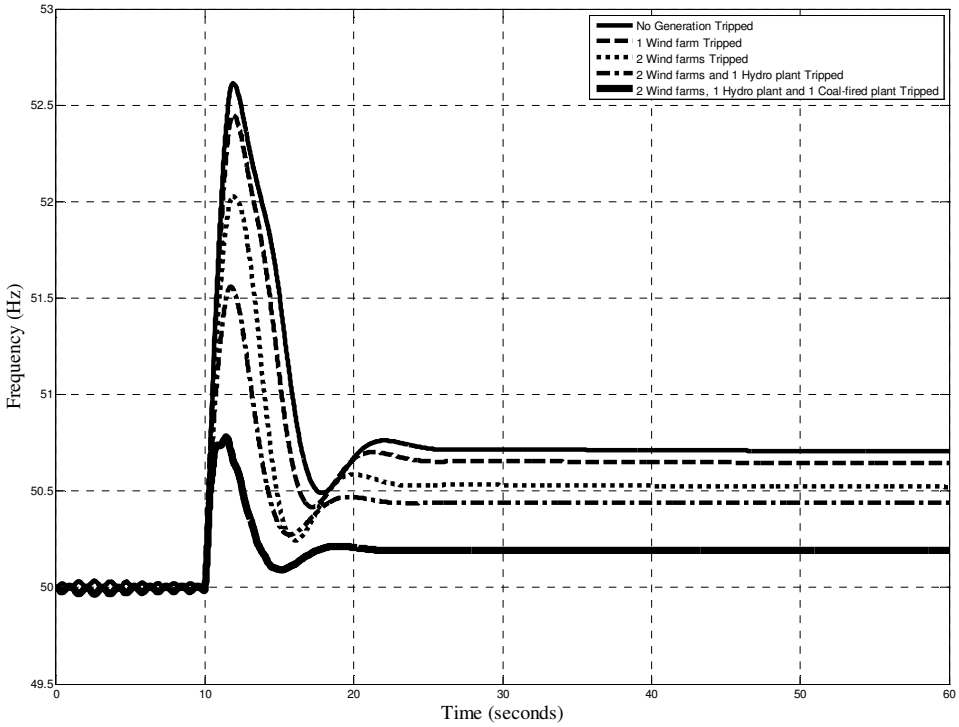

(c) Maximum governor rate limit= 0.5 p.u./sec.

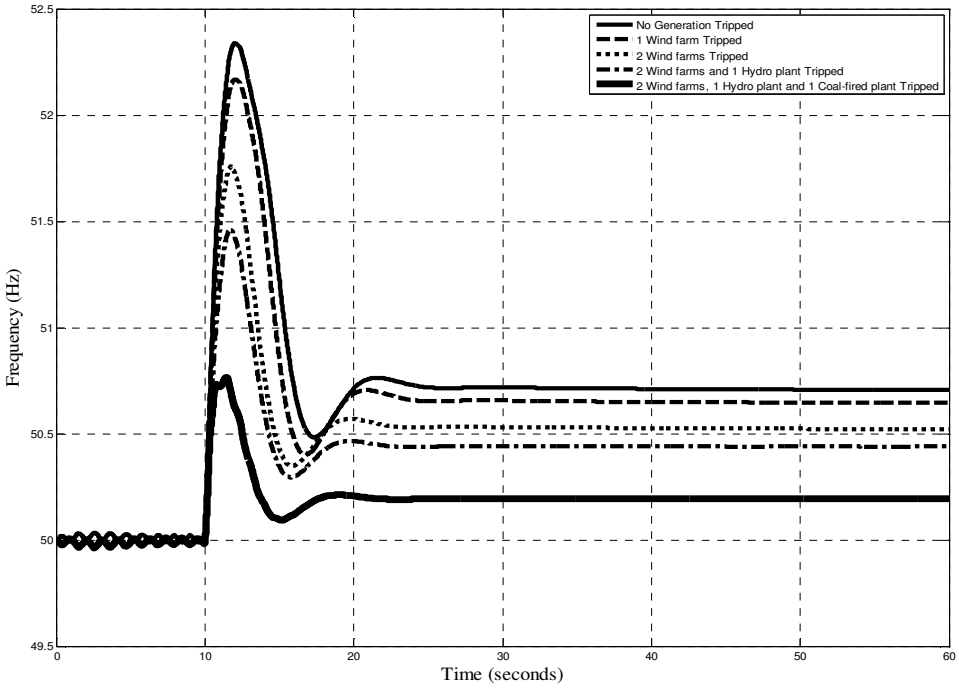

(d) Maximum governor rate limit= 0.9 p.u./sec

Figure 4.1 Frequency response of Case Study 1 upon disconnection from the rest of the Grid.

An interesting result that would need further investigation and discussion is Figure 4.1 (b). It can be noticed that when the two wind farms and one hydro plant are tripped (plot 4), the area frequency first overshoot is damped but the frequency swings unstably in opposition to the rest of the plots existing in the same figure. This can be explained by two reasons:

1- Reason one: The change in generation mix as all the remaining connected generation is pure thermal units. This explains why the considered plot differs from the case where wind and hydro still exists (previous plots).

2- Reason two: The more generation that is required to be lessened plus the low rate limits of the governor servomotor (0.2 p.u. /sec). This causes the governor to have a long time response than the case of tripping an extra thermal unit and the generation to be lessened is less (the following plot). (I.e. according to calculation the amount of generation needed to be lessened for the plot considered is equal to 0.22 p.u. and so it will take the governor servomotor 0.22/(governor rate limit of 0.2)=1.1 sec to apply this change. However, for the last plot in Figure 4.1(b) the amount of generation required to be lessened is 0.076 p.u. experiencing a shorter delay of 0.076/0.2 =0.38 sec and hence a quick stable response). This effect can be cleared by applying an eigenvalue analysis showing the effect of slow governor responses on the system frequency stability. This will be discussed in more details in Section 5.3.1.

Table 4-6 Specifications of the frequency time response of Case Study 1 at different generation tripping levels.

Generation Tripped	No Generation Tripped		1 Wind Farm Tripped		2 Wind Farms Tripped		2Wind Farms + 1 Hydro plant Tripped		2 Wind Farms + 1 Hydro plant + 1 Coal fired Station Tripped	
Governor rate limits (p.u./sec)	$F_{overshoot}$ (Hz)	$F_{steady\text{-}state}$ (Hz)	$F_{overshoot}$ (Hz)	$F_{steady\text{-}state}$ (Hz)	$F_{overshoot}$ (Hz)	$F_{steady\text{-}state}$ (Hz)	$F_{overshoot}$ (Hz)	$F_{steady\text{-}state}$ (Hz)	$F_{overshoot}$ (Hz)	$F_{steady\text{-}state}$ (Hz)
0.1	56.36	n/a	55.64	n/a	54.36	n/a	53.45	n/a	**51.49**	n/a
0.2	54.00	50.69	53.62	50.65	52.92	50.54	52.46	n/a	**51.08**	**50.23**
0.3	53.20	50.70	52.90	50.64	52.50	50.53	52.10	50.43	**50.90**	**50.20**
0.4	52.82	50.70	52.61	50.65	52.23	50.52	**51.76**	**50.43**	**50.82**	**50.20**
0.5	52.64	50.70	52.45	50.64	52.02	50.52	**51.59**	**50.43**	**50.80**	**50.19**
0.6	52.50	50.71	52.31	50.65	**51.85**	50.53	**51.46**	**50.44**	**50.75**	**50.19**
0.7	52.42	50.71	52.23	50.65	**51.77**	50.53	**51.44**	**50.43**	**50.79**	**50.19**
0.8	52.35	50.71	52.15	50.65	**51.76**	50.52	**51.44**	**50.44**	**50.77**	**50.19**
0.9	52.32	50.71	52.15	50.64	**51.75**	50.52	**51.44**	**50.44**	**50.77**	**50.19**

Where n/a means not available. I.e. the frequency time response swings unstably and doesn't reach a steady state value.

4.3.2 Case Study 2

Time simulation of the frequency response of Case Study 2 network upon disconnection from the rest of the UK grid is presented in this section. The interrupted power is 38% of the case study installed capacity. Figure 4.2 shows the frequency response of Case Study 2 upon disconnection from the rest of the grid at different governor maximum rate limits where the following five cases are compared in each subplot: (a) no generation tripped, (b) 60% of wind farms tripped, (c) all wind farms tripped (d) all wind farms and 1 hydro plant tripped and (e) all wind farms, 1 hydro plant and 1 coal-fired plant tripped.

Figure 4.2 and Table 4-7 show that for generators with a governor rate limit higher than 0.6 p.u./sec, tripping all wind farms is sufficient to contain the first frequency overshoot below the 52 Hz and contain the steady-state frequency value within the statutory limits. If the generators governor rate limit is 0.5 or 0.6 p.u./sec, an extra hydro power station is to be tripped. Finally, for the case of generators with governor rate limiters of 0.3 or 0.4 p.u./sec, all wind farms, 1 hydro plant and 1 coal fired, are required to be tripped to contain the separated area frequency first overshoot below 52 Hz. However, for the case of governor rate limiters of 0.2 p.u./sec the frequency undershoots to a value just below the 49 Hz, hence under frequency load shedding should be adjusted to operate at a frequency of 48.5 Hz or below. Finally, for the case of governor rate limiters of 0.1 p.u./sec the frequency swings and overshoots to frequency levels higher than the 52 Hz .

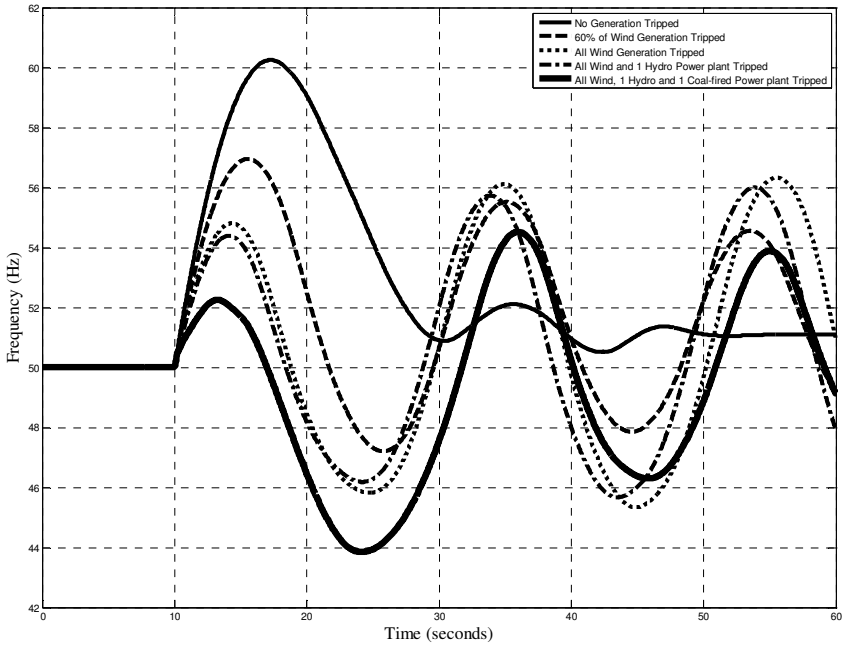

(a) Maximum governor rate limit= 0.1 p.u./sec.

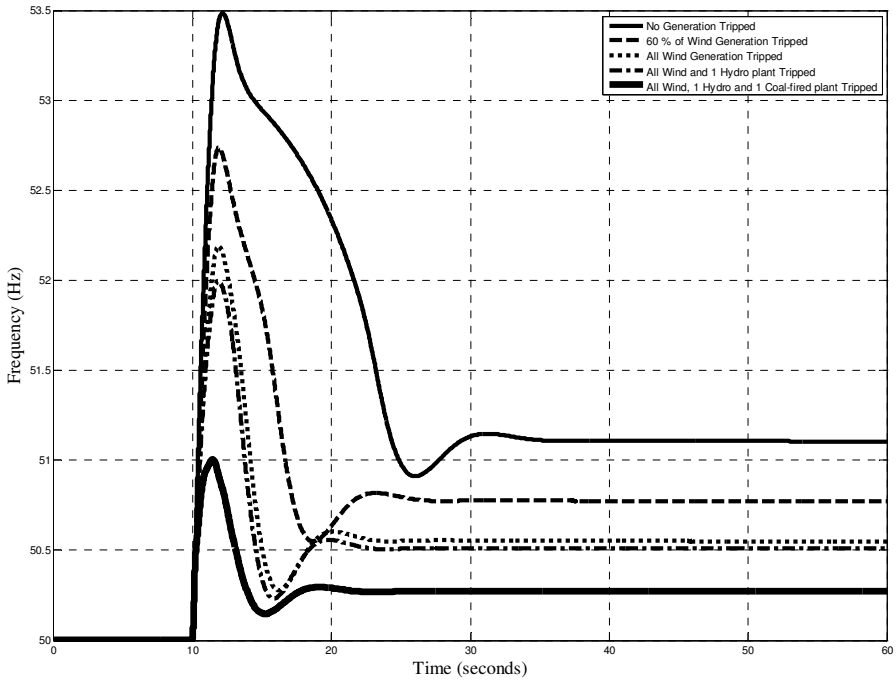

(e) Maximum governor rate limit= 0.5 p.u./sec.

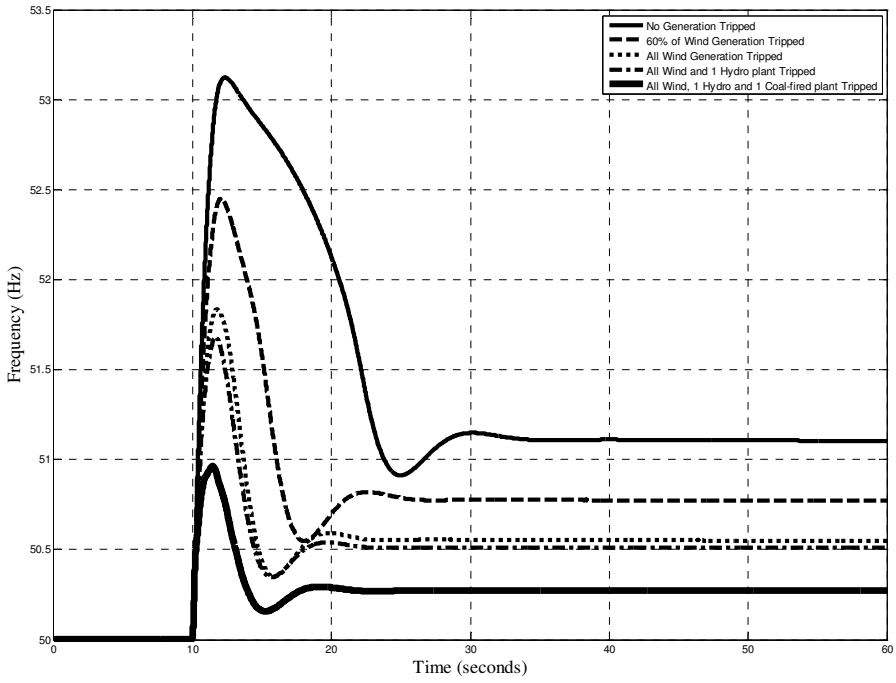

(h) Maximum governor rate limit= 0.9 p.u./sec.

Figure 4.2 Frequency response of Case Study 2 upon disconnection from the rest of the Grid.

Table 4-7 The specifications of the frequency time response of Case Study 2 at different generation tripping levels.

Generation Tripped	No Generation Tripped		60% of Wind Generation Tripped		All Wind Farms Tripped		All Wind Farms+1 Hydro plant Tripped		All Wind Farms + 1 Hydro plant +1 Coal fired Station	
Governor rate limits (p.u./sec)	$F_{overshoot}$ (Hz)	$F_{steady-state}$ (Hz)	$F_{overshoot}$ (Hz)	$F_{steady-state}$ (Hz)	$F_{overshoot}$ (Hz)	$F_{steady-state}$ (Hz)	$F_{overshoot}$ (Hz)	$F_{steady-state}$ (Hz)	$F_{overshoot}$ (Hz)	$F_{steady-state}$ (Hz)
0.1	60.38	51.10	57.00	n/a	54.75	n/a	54.31	n/a	52.30	n/a
0.2	56.00	51.10	54.25	50.75	53.20	50.52	52.90	50.79	**51.55**	**50.25**
0.3	54.57	51.12	53.40	50.75	52.63	50.53	52.47	50.77	**51.27**	**50.28**
0.4	53.85	51.12	53.00	50.76	52.38	50.54	52.22	50.50	**51.13**	**50.25**
0.5	53.50	51.11	52.73	50.77	52.18	50.55	52.00	50.50	**51.00**	**50.27**
0.6	53.29	51.10	52.64	50.77	52.04	50.55	**51.81**	**50.50**	**51.00**	**50.27**
0.7	53.18	51.11	52.55	50.77	**51.91**	50.55	**51.70**	**50.50**	**51.00**	**50.27**
0.8	53.16	51.11	52.50	50.76	**51.82**	50.55	**51.68**	**50.50**	**51.00**	**50.27**
0.9	53.14	51.10	52.45	50.77	**51.84**	50.55	**51.68**	**50.50**	**50.95**	**50.27**

Where n/a means not available. I.e. the frequency time response swings unstably and doesn't reach a steady state value.

4.3.3 Case Study 3

Time simulation of the frequency response of Case Study 3 network upon disconnection from the rest of the UK grid is presented in this section. The interrupted power is 62 % of the case study installed capacity. Figure 4.3 shows the frequency response of Case Study 3 upon disconnection from the rest of the grid at different governor maximum rate limits where the following six cases are compared in each subplot: (a) no generation tripped, (b) 1 oil-fired plant tripped, (c) 1 oil-fired plant and 1 coal-fired plant tripped (d) 1 oil-fired plant and 2 coal-fired plant tripped, (e) 1 oil-fired plant and 3 coal-fired plant tripped and (f) 1 oil-fired plant, 3 coal-fired plant and 1 CCGT plant tripped.

Time domain simulation shows that at most 5 power stations are to be tripped to ensure that the frequency first overshoot is below 52 Hz. Moreover, time domain simulation shows that the more generators tripped the more the steady state frequency decreases to be within the frequency statutory values. Figure 4.3 and Table 4-8 show that for generators with a governor rate limit higher than 0.7 p.u./sec , tripping 4 generators, 1 oil-fired and 3 coal-fired is sufficient to contain the first frequency overshoot below the 52 Hz. If the generators governor rate limit is lower than 0.7 p.u./sec , an extra CCGT power station is to be tripped. The advantage of the existence of an HVDC link in this case study appears in preventing frequency swings in the case where generators have low governor rate limiters.

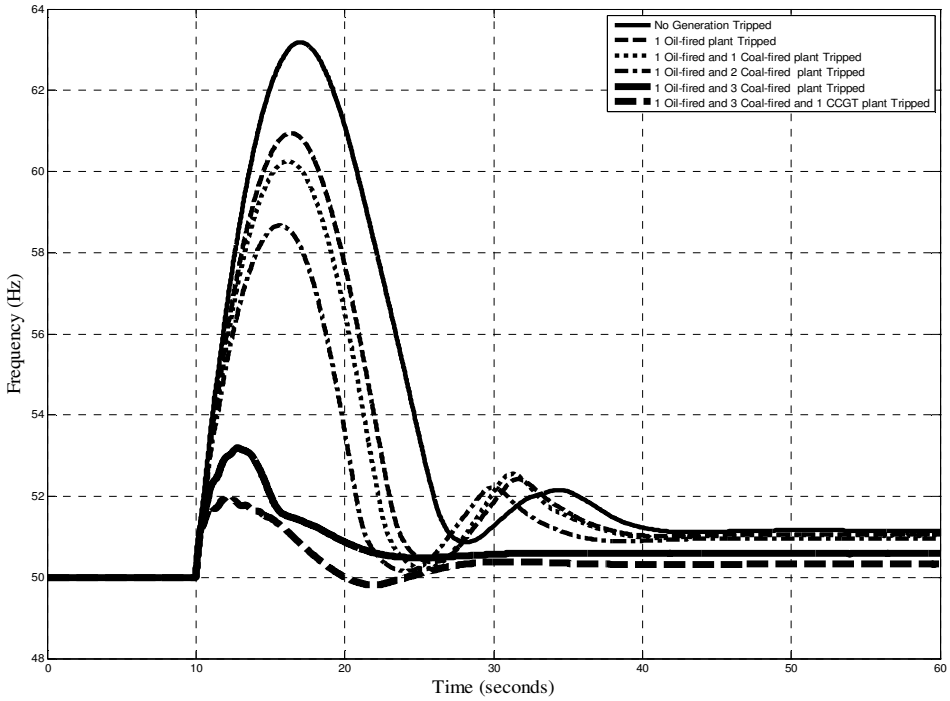

(a) Maximum governor rate limit= 0.1 p.u./sec.

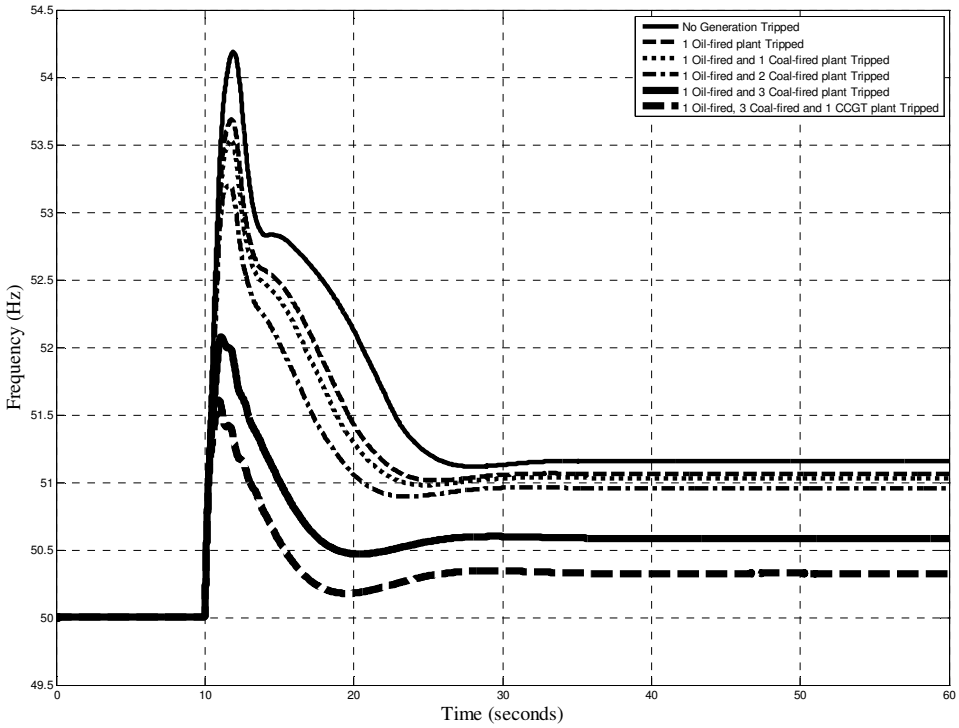

(b) Maximum governor rate limit= 0.6 p.u./sec.

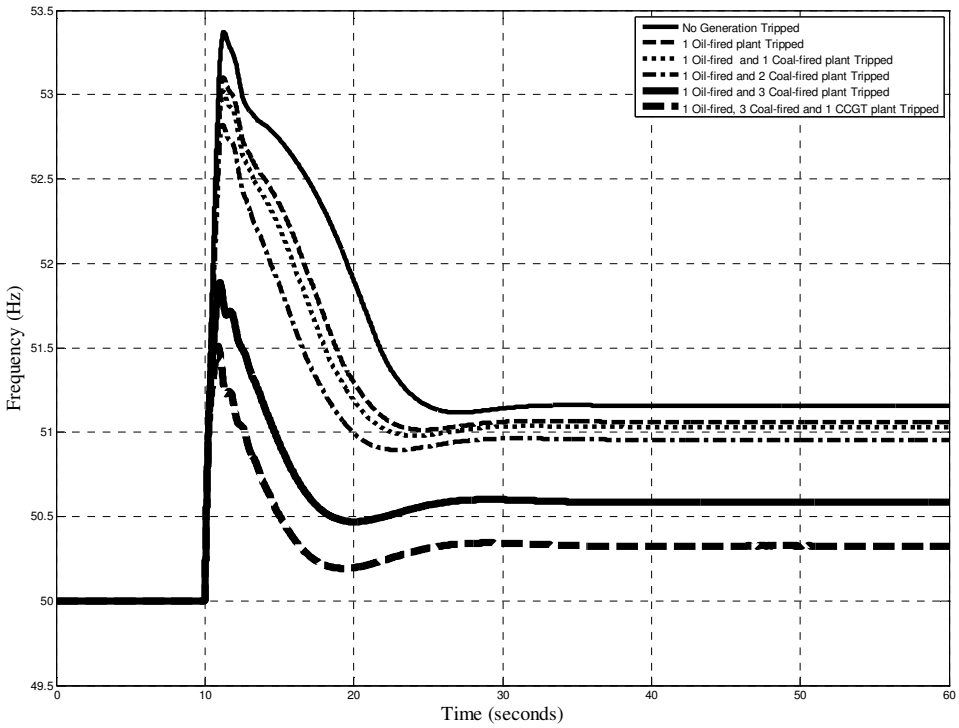

(d) Maximum governor rate limit= 0.9 p.u./sec.

Figure 4.3 Frequency response of Case Study 3 upon disconnection from the rest of the Grid.

Table 4-8 The specifications of the frequency time response of Case Study 3 at different generation tripping levels.

Generation Tripped	No Generation Tripped		1 Oil Fired Plant Tripped		1 Oil Fired Plant +1Coal Fired Plant Tripped		1 Oil Fired Plant + 2 Coal Fired Plant Tripped		1 Oil Fired Plant + 3 Coal Fired Plant Tripped		1 Oil Fired Plant +3 Coal Fired Plant + 1CCGT Plant Tripped	
Governor rate limits (p.u./sec)	$F_{overshoot}$ (Hz)	$F_{steady\text{-}state}$ (Hz)	$F_{overshoot}$ (Hz)	$F_{steady\text{-}state}$ (Hz)	$F_{overshoot}$ (Hz)	$F_{steady\text{-}state}$ (Hz)	$F_{overshoot}$ (Hz)	$F_{steady\text{-}state}$ (Hz)	$F_{overshoot}$ (Hz)	$F_{steady\text{-}state}$ (Hz)	$F_{overshoot}$ (Hz)	$F_{steady\text{-}state}$ (Hz)
0.1	63.26	51.20	61.00	51.05	60.80	50.95	58.60	50.80	53.20	50.54	**52.00**	**50.32**
0.2	57.45	51.24	56.33	51.00	56.00	50.95	55.17	50.90	52.59	50.56	**51.78**	**50.28**
0.3	55.60	51.18	54.82	51.05	54.55	51.00	54.10	50.95	52.32	50.59	**51.70**	**50.32**
0.4	54.73	51.15	54.15	51.04	53.95	51.00	53.51	50.93	52.15	50.58	**51.62**	**50.31**
0.5	54.19	51.16	53.70	51.06	53.50	51.02	53.20	50.95	52.08	50.60	**51.61**	**50.31**
0.6	53.83	51.15	53.41	51.06	53.24	51.03	53.03	50.97	52.04	50.59	**51.56**	**50.35**
0.7	53.61	51.16	53.25	51.08	53.12	51.03	52.90	50.95	52.00	50.59	**51.56**	**50.32**
0.8	53.44	51.16	53.20	51.06	53.06	51.03	52.87	50.95	**51.92**	50.58	**51.55**	**50.33**
0.9	53.37	51.16	53.11	51.06	53.00	51.03	52.82	50.97	**51.87**	50.58	**51.50**	**50.32**

4.4 Conclusions

Inter-tripping is an effective method to sustain the frequency stability of a generation rich area upon uncontrolled separation from the rest of the grid. It provides a fast mean for matching generation with load. Hence, it reduces the frequency first over shoot to be less than the value at which generators are tripped by its protection. An effective selective tripping pattern is introduced. This pattern uses an effective station priority list based on generation dynamic response, generation minimum zero time and bid prices to select the proper amount of generation to be tripped. Although, the transient response of the separated area is improved, still there is a problem with the steady state value. The steady state frequency level does not return to its nominal value. More means have to be provided.

For the sake of fairness, it must be stated that generation tripping fails to stabilize the frequency in the case where the separated area contains only slow conventional generation equipped with governors of low rate limiter operating at high load levels. Although the first overshoot is minimized to be below the 52 Hz, but the frequency stability is lost by the second swing.

Not only that, but generation tripping has its own complications. In a bilateral environment like the UK system, generation tripping involves compensations fees paid by the operator to the tripped generator owner. This compensation does not only cover the price of the amount of power that should have been delivered by the unit but also it covers a price for the mechanical stresses suffered by the tripped generating unit as these stresses affect the generating unit life time. Consequently, not all generating stations owners agree to be involved in an operator controlled generation tripping process.

As a result, it becomes necessary to look for other methodologies that would assist in improving the frequency response of over generated separated areas. This is to either eliminate the need of controlled generation tripping or to at least minimize the amount of generation to be tripped. The following chapters will discuss the possibility of improving the frequency response (transient and steady state response) of separated generation rich areas, resulted due to sever disturbance, through methodologies other than generation tripping.

CHAPTER 5

ISLAND AUTOMATIC GENERATION CONTROL

5.1 Introduction

It has been shown in Chapter 4, that generation tripping is an effective method of improving the frequency response of over generated areas upon separation from the rest of the system. Although it does not restore the area frequency to the nominal value, 50 Hz in our case studies, but yet it damps the first frequency overshoot to be below 52 Hz and hence prevents uncontrolled generation tripping, which might lead to complications and a blackout condition.

On the other hand, generation tripping has its own complications. In a bilateral environment like the UK system, generation tripping involves compensations fees paid by the operator to the tripped generator owner. This compensation does not only cover the price of the amount of power that should have been delivered by the unit but also it covers a price for the mechanical stresses suffered by the tripped generating unit as these stresses affect the generating unit's life time. Consequently, not all generating stations owners agree to be involved in an operator controlled generation tripping process.

As a result, it becomes necessary to look for other methodologies that would assist in improving the frequency response of over generated separated areas. This is to either eliminate the need of controlled generation tripping or to at least minimize the amount of generation to be tripped. This chapter discusses the possibility of improving the frequency response (transient and steady-state response) of separated generation rich areas, resulted due to sever disturbance, via an Island AGC.

During extreme contingencies or emergency case that might lead to area separation, the main system AGC is disconnected. This is to avoid any improper corrective action that might complicate the situation more. For example, if a system is split into two areas area 1 and area 2 a corrective action for area 1 might be applied through generation control of some units in area 2. Consequently, the problem in area 1 is not resolved and the situation in area 2 might get more complicated [1, 24].

While the system is operating in a degraded construction (i.e. split into electrical islands), it becomes the operator challenge to restore the frequency in every area to the nominal value and reconnect the islands to regain the unified system.

An island AGC, implemented for Virginia tech system, has been suggested for the purpose of automatically operating surviving, identified by operators, separated areas. The main contribution of such controller is the ability to restore the frequency of the chosen area to its nominal frequency automatically while the operator focuses on the rest of the power system.[34] Moreover, the contribution of this island AGC towards improving the transient response and hence assisting the survival of the separated area was not discussed.

Consequently, this chapter proposes a pre-designed Island AGC ready to control the generation of areas once these areas is separated from the system and the main AGC is disconnected. Two popular designs for AGC systems discussed in the literature [1, 24 and 34-40] are the conventional integral control and the optimal LQR-based control. This chapter discusses and compares both designs.

This section presents an introductory information and outline for this chapter. Section 5.2 discusses AGC Analysis methodologies. Section 5.3 proposes a conventional-based Island AGC. An LQR-based Island AGC is proposed in Section 5.4. Finally, the chapter is concluded in Section 5.5.

5.2 AGC Analysis

This Section discusses the modelling of a power system in preparation to design an AGC. Section 5.2.1 discusses the development of an equivalent system model used to represent the thesis case studies for the purpose of AGC design and analysis. This is followed by presenting the aforementioned equivalent model in the state space format and applying an eigenvalue analysis in Section 5.2.2

5.2.1 Equivalent System

In the analysis of AGCs, the target is the study of the collective performance of all generators in the system. The inter-machine oscillations and transmission system performance are therefore not considered. The coherent response of all generators to changes in system load is assumed. Hence, all generators are represented by an equivalent generator [24]. The equivalent generator has an inertia constant M_{eq} equal to the sum of the inertia constants of all the generating units and is driven by the combined mechanical outputs of the individual turbines as illustrated in

Figure 5.1. The speed of the equivalent generator represents the system frequency and in per unit the two are equal. *D* is the frequency load dependence constant and is assumed to be zero.

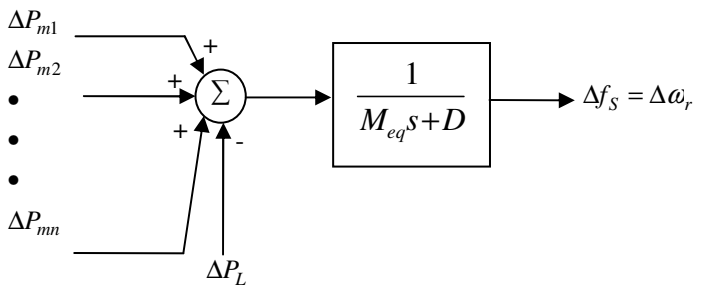

Figure 5.1 The equivalent generator model [24].

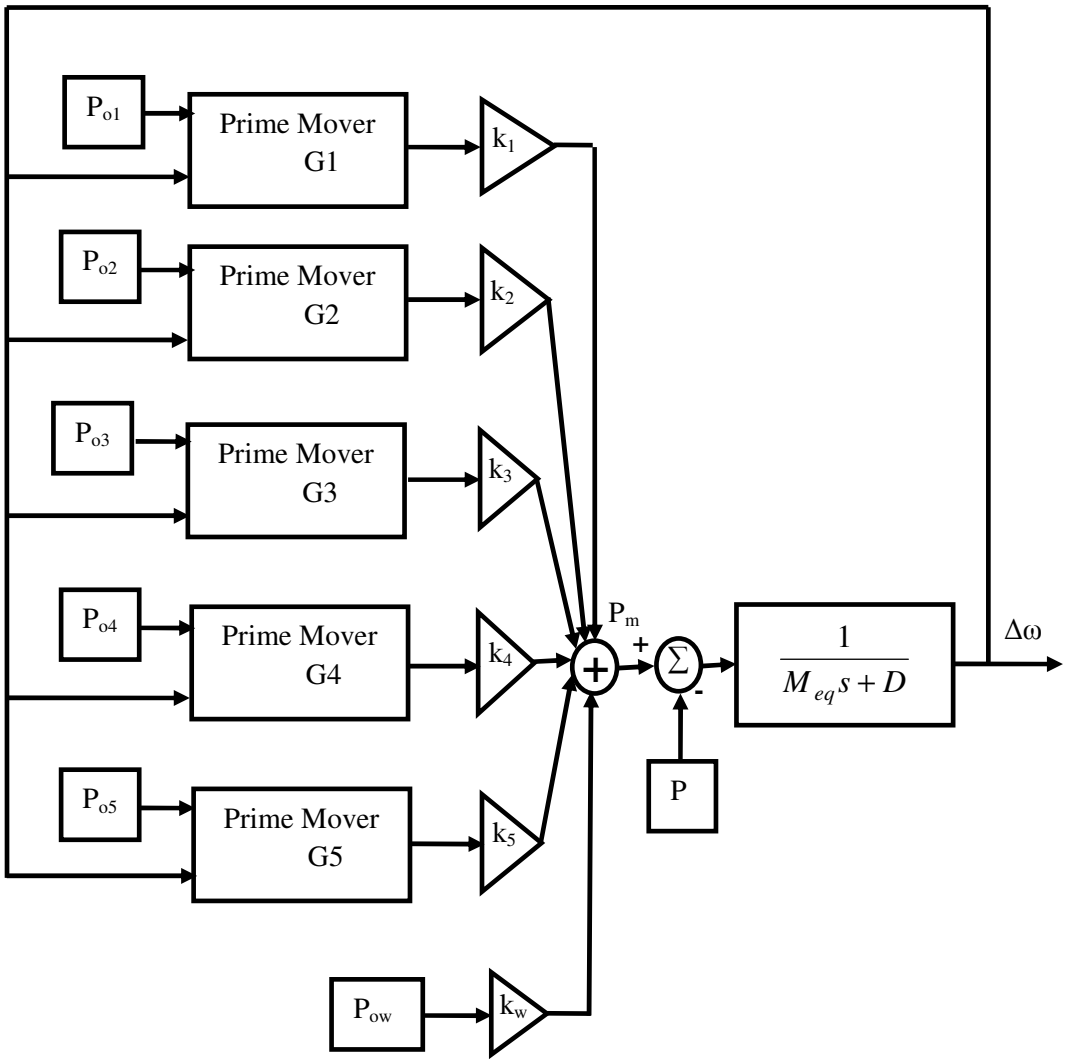

Figure 5.2 Equivalent models of Case Study 1 and Case Study 2.

Hence, Case Study 1 and Case Study 2 can represented as in Figure 5.2. The equivalent system has five prime movers presenting the five frequency responsive power stations. Power stations G1, G2 are presented by a fossil-fuel unit prime mover. While G3, G4 are presented by the

nuclear unit prime mover, see Figure 5.4. G5 is a hydro station and is presented as shown in Figure 5.5. Finally, the rest of the non responsive power station, wind farms, are aggregated and presented as a constant value. The only difference between Case Study 1 and Case Study 2 is the value of the k constants shown in Figure 5.2, where k represents the ratio of the installed capacity of each generator to the total area installed capacity. Following the same principle, the equivalent system presenting Case Study 3 would be as in Figure 5.3, where G1 to G7 are represented by fossil fuel prime movers, G8 by a nuclear prime mover and finally G9 prime mover is as in Figure 5.6 to model an HVDC link.

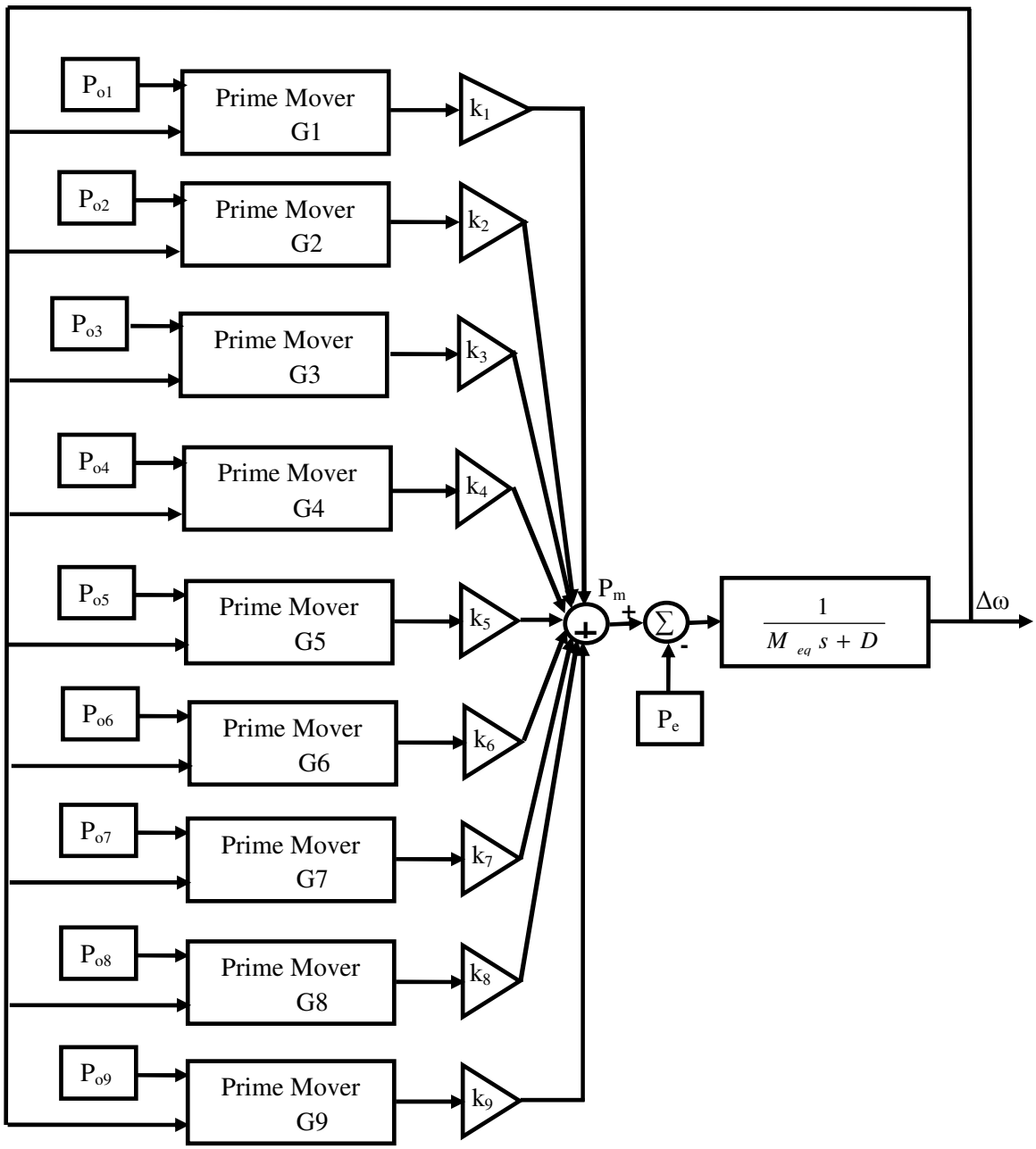

Figure 5.3 Equivalent model of Case Study 3

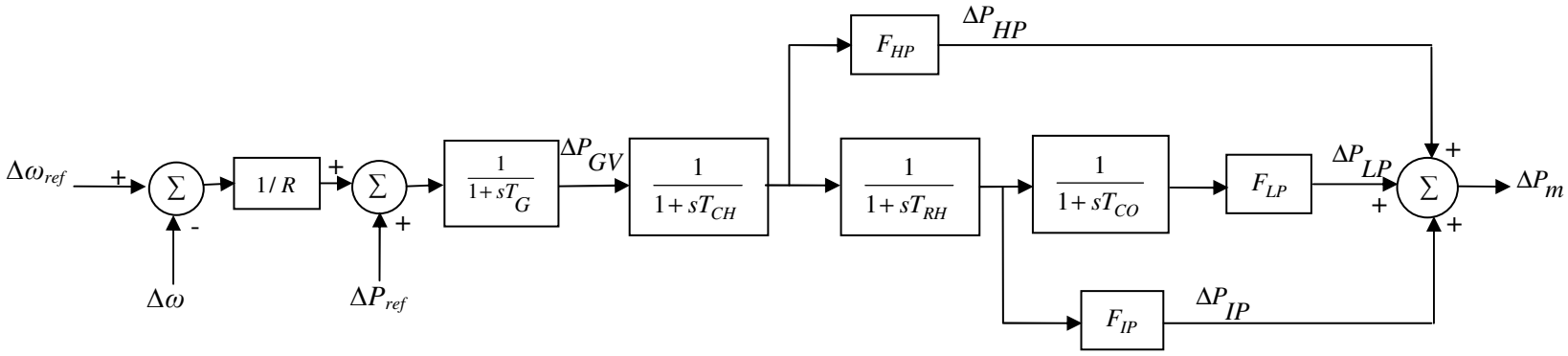

(a)

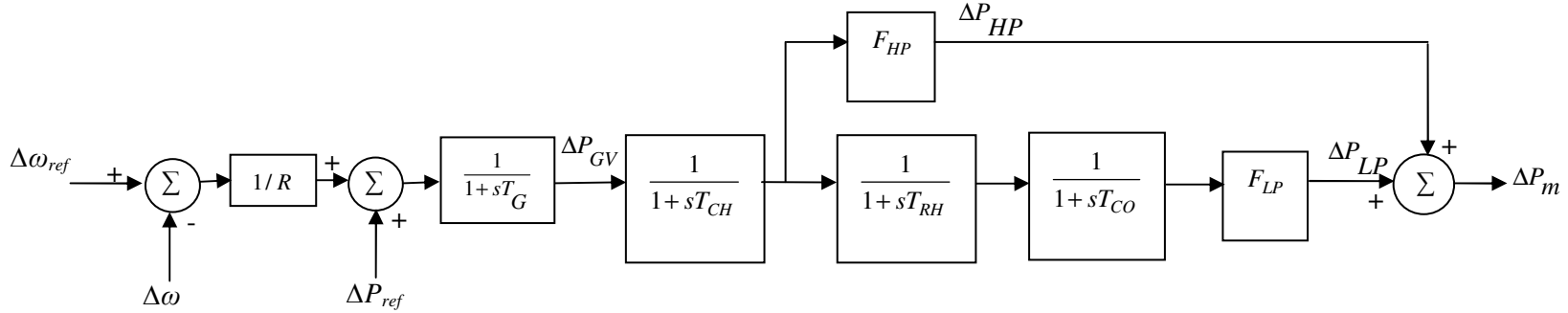

(b)

Figure 5.4 Case study linearized prime mover models for (a) Fossil-fuelled plants (b) Nuclear plants. [24]

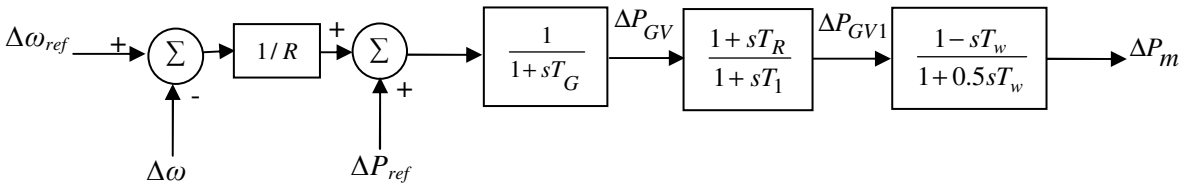

Figure 5.5 Case study linearized prime mover models for Hydro [24].

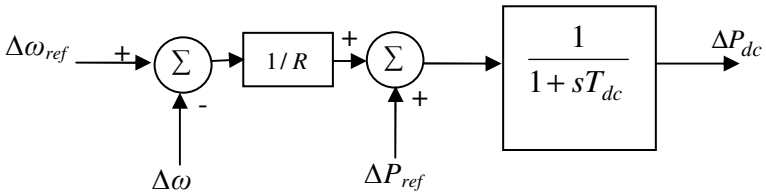

Figure 5.6 Case study linearized prime mover models for dc link.

Where T_{dc} is HVDC link time constant and P_{dc} is the power supplied by HVDC link. Moreover, Figure 5.7 shows some time domain simulation comparing the frequency response of the detailed model to the equivalent model for Case Study 1 at different governor rate limiters. This is to justify the validity of using this equivalent model in the frequency control studies.

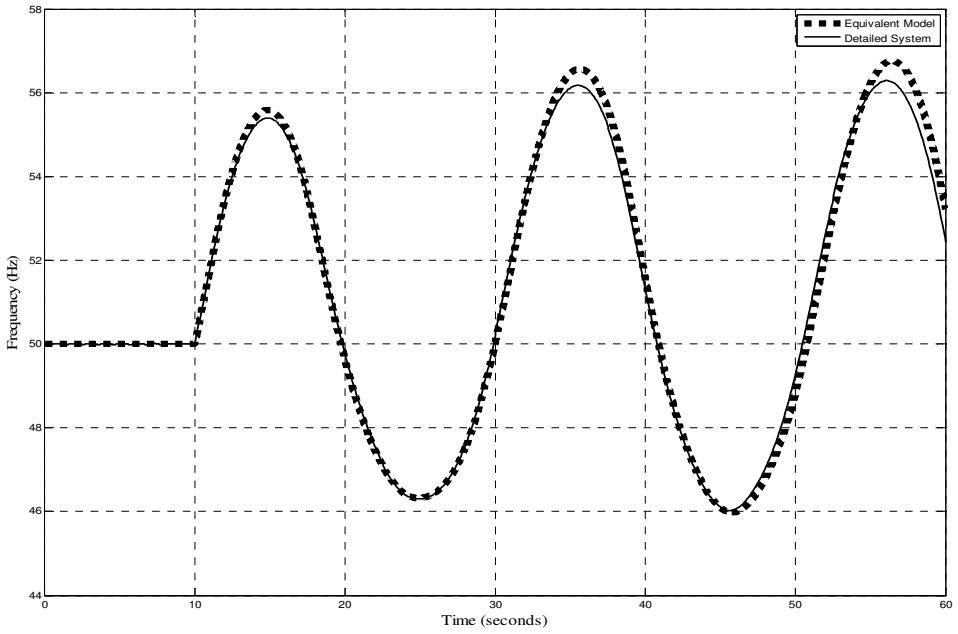

(a) Maximum governor rate limit= 0.1 p.u./sec

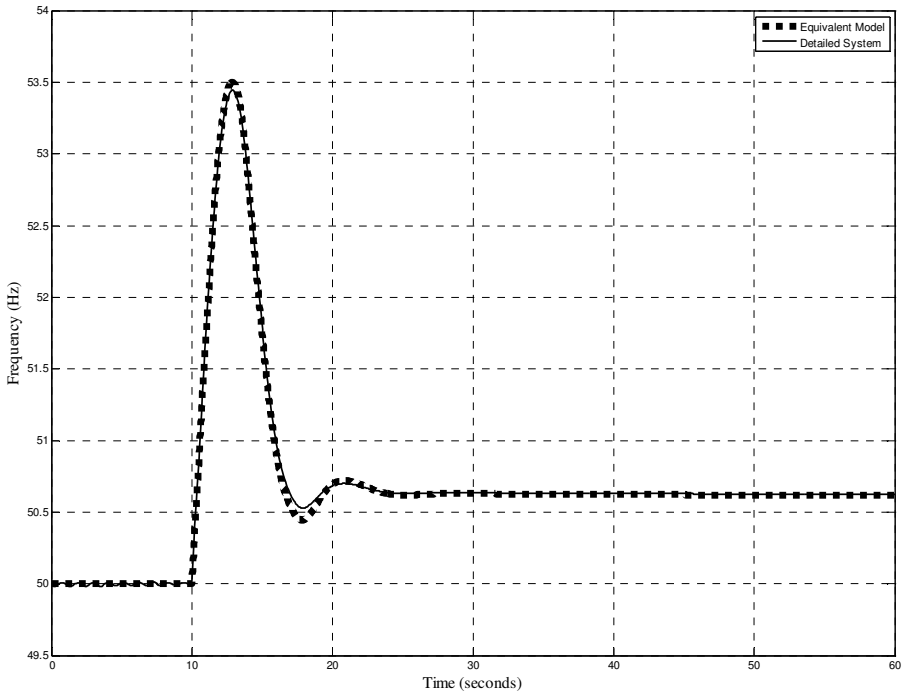

(b) Maximum governor rate limit= 0.2 p.u./sec.

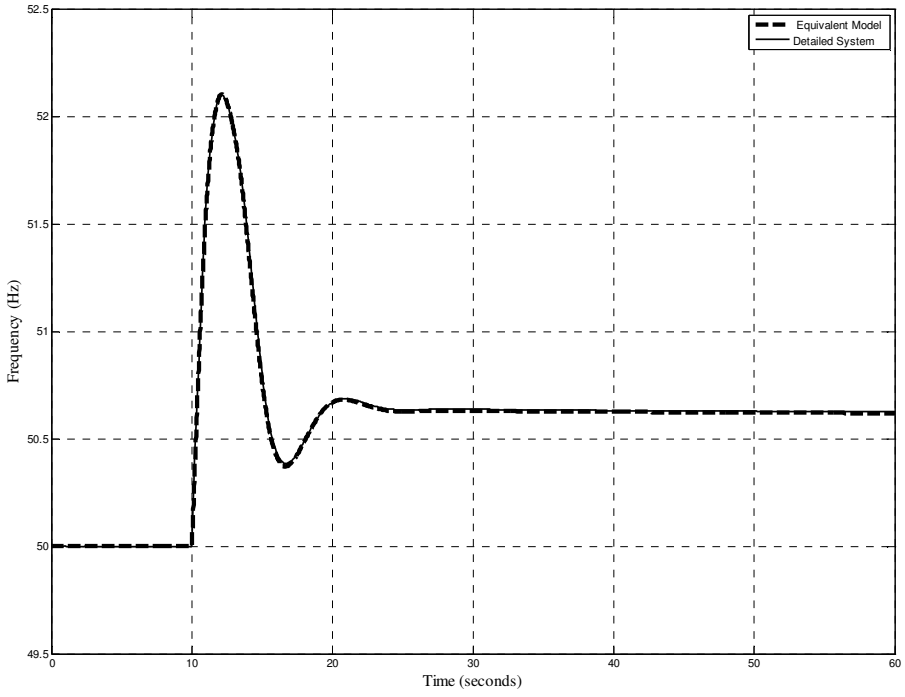

(c) Maximum governor rate limit= 0.9 p.u./sec

Figure 5.7 Frequency of Case Study 1(Detailed Network Model versus Equivalent Model).

5.2.2 Case Studies State Space Representation And Eigen Value Analysis

In this section the equations describing the case studies equivalent models discussed in Section 5.2.1 are written in the following format [24, 72 and 77-84]:

$$\dot{\boldsymbol{x}}_{sys} = \boldsymbol{A}_{sys}\boldsymbol{x}_{sys} + \boldsymbol{B}_{sys}\boldsymbol{u}_{sys}$$

$$\boldsymbol{y}_{sys} = \boldsymbol{C}_{sys}\boldsymbol{x}_{sys} + \boldsymbol{D}_{sys}\boldsymbol{u}_{sys} \tag{5.1}$$

Where $\boldsymbol{x}_{sys}$ is the system state variable vector whose components are as:

(a) P_{GVc}, P_{HPc}, P_{IPc}, P_{LPc} for every fossil-fuelled power station.
(b) P_{GVn}, P_{HnP}, P_{LPn},: for every nuclear power station
(c) P_{GVh},P_{GVh1}, P_h, for every hydro power station
(d) P_{dc} for every dc link.
(e) ω. Only one variable to represent the area frequency in p.u.

Where all state variables are in p.u. and are defined as follows,

P_{GVc} is the Governor power for coal unit,

P_{GVh} is the Governor power for hydro unit,

P_{GVn} is the Governor power for nuclear unit,

P_{HPc} is the High pressure turbine power for coal unit,

P_{HPn} is the High pressure turbine power for nuclear unit,

P_{IPc} is the Intermediate pressure turbine power for coal unit,

P_{LPc} is the Low pressure turbine power for coal unit,

P_{LPn} is the Low pressure turbine power for nuclear unit,

P_{dc} is the Power supplied by HVDC link and

ω is the area frequency or the average speed of area machines.

Moreover, $\boldsymbol{y}_{sys}$ is the system output which is the area frequency ω. And finally $\boldsymbol{u}_{sys}$ the system inputs are

(a) P_{ref} the power reference settings of generation units.
(b) P_e , the system electrical power or load.

Hence considering Case Study 1 or Case Study 2, the system order would be 18, 4 variables per fossil fuelled power station x 2 fossil fuelled power stations + 3 variables per nuclear power station x 2 nuclear power stations + 3 variables per nuclear power station x 1 hydro power stations + 1 speed variable. And the state space matrices would be as follows

$$A_{CaseStudy1,CaseStudy2} = \begin{bmatrix} A_{G1} & 0 & 0 & 0 & 0 & A_{G1}{}^{a} \\ 0 & A_{G2} & 0 & 0 & 0 & A_{G2}{}^{a} \\ 0 & 0 & A_{G3} & 0 & 0 & A_{G3}{}^{a} \\ 0 & 0 & 0 & A_{G4} & 0 & A_{G4}{}^{a} \\ 0 & 0 & 0 & 0 & A_{G5} & A_{G5}{}^{a} \\ A_{G1}{}^{b} & A_{G2}{}^{b} & A_{G3}{}^{b} & A_{G4}{}^{b} & A_{G5}{}^{b} & -D/M \end{bmatrix},$$

$$B_{CaseStudy1,CaseStudy2} = \begin{bmatrix} B_{G1} & 0 \\ B_{G2} & 0 \\ B_{G3} & 0 \\ B_{G4} & 0 \\ B_{G5} & 0 \\ 0 & -1/M_{eq} \end{bmatrix},$$

$$C_{CaseStudy1,CaseStudy2} = [0 \quad 0 \quad 0 \quad 0 \quad 0 \quad 0 \quad 0 \quad 0 \quad 0 \quad 0 \quad 0 \quad 0 \quad 0 \quad 0 \quad 0 \quad 0 \quad 0 \quad 1],$$

$$\text{and } D_{CaseStudy1,CaseStudy2} = [0 \quad 0] \tag{5.2}$$

Where

$$\boldsymbol{A_{G1} = A_{G2} = A_{Fossil}}, \boldsymbol{A_{G3} = A_{G4} = A_{Nuclear}} \text{ and } \boldsymbol{A_{G5} = A_{Hydro}}$$

$$\boldsymbol{A_{G1}{}^{a} = A_{G2}{}^{a} = A_{Fossil}{}^{a}}, \boldsymbol{A_{G3}{}^{a} = A_{G4}{}^{a} = A_{Nuclear}{}^{a}} \text{ and } \boldsymbol{A_{G5}{}^{a} = A_{Hydro}{}^{a}}$$

$$\boldsymbol{A_{G1}{}^{b} = A_{G2}{}^{b} = A_{Fossil}{}^{b}}, \boldsymbol{A_{G3}{}^{b} = A_{G4}{}^{b} = A_{Nuclear}{}^{b}} \text{ and } \boldsymbol{A_{G5}{}^{b} = A_{Hydro}{}^{b}}$$

$$\boldsymbol{B_{G1} = B_{G2} = B_{Fossil}}, \boldsymbol{B_{G3} = B_{G4} = B_{Nuclear}} \text{ and } \boldsymbol{B_{G5} = B_{Hydro}} \tag{5.3}$$

And

$$A_{Fossil} = \begin{bmatrix} -1/T_G & 0 & 0 & 0 \\ F_{HP}/T_{CH} & -1/T_{CH} & 0 & 0 \\ 0 & F_{IP}/F_{HP}T_{RH} & -1/T_{RH} & 0 \\ 0 & 0 & F_{LP}/F_{IP}T_{CO} & -1/T_{CO} \end{bmatrix},$$

$$A_{Fossil}{}^{a} = \begin{bmatrix} -1/RT_G \\ 0 \\ 0 \\ 0 \end{bmatrix}, A_{Fossil}{}^{b} = \begin{bmatrix} 0 & k/M & k/M & k/M \end{bmatrix}, B_{Fossil} = \begin{bmatrix} 1/T_G \\ 0 \\ 0 \\ 0 \end{bmatrix},$$

$$A_{Nuclear} = \begin{bmatrix} -1/T_G & 0 & 0 \\ F_{HP}/T_{CH} & -1/T_{CH} & 0 \\ 0 & F_{LP}/F_{HP}(T_{RH}+T_{CO}) & -1/(T_{RH}+T_{CO}) \end{bmatrix},$$

$$A_{Nuclear}{}^{a} = \begin{bmatrix} -1/RT_G \\ 0 \\ 0 \end{bmatrix}, A_{Nuclear}{}^{b} = \begin{bmatrix} 0 & k/M & k/M \end{bmatrix}, B_{Nuclear} = \begin{bmatrix} 1/T_G \\ 0 \\ 0 \end{bmatrix},$$

$$A_{Hydro} = \begin{bmatrix} -1/T_G & 0 & 0 \\ 1/T_1 - T_R/T_1T_G & -1/T_1 & 0 \\ -2\left(1/T_1 - T_R/T_1T_G\right) & 2/T_w + 2/T_1 & -2/T_w \end{bmatrix},$$

$$A_{Hydro}{}^{a} = \begin{bmatrix} -1/RT_G \\ -T_R/T_1RT_G \\ 2T_R/T_1RT_G \end{bmatrix}, A_{Hydro}{}^{b} = \begin{bmatrix} 0 & 0 & k/M \end{bmatrix}, B_{Hydro} = \begin{bmatrix} 1/T_G \\ T_R/T_1T_G \\ -2T_R/T_1T_G \end{bmatrix} \quad (5.4)$$

Following the same principle, the state space matrix representing Case Study 3 would be of order 33. 4 variables per fossil fuelled power station x 7 fossil power stations + 3 variables per nuclear power station x 1 nuclear power stations + 1 variable per dc link x 1 dc link + 1 speed variable. And the State space matrices would be as follows

$$
A_{CaseStudy3} = \begin{bmatrix}
A_{G1} & 0 & 0 & 0 & 0 & 0 & 0 & 0 & 0 & A_{G1}{}^{a} \\
0 & A_{G2} & 0 & 0 & 0 & 0 & 0 & 0 & 0 & A_{G2}{}^{a} \\
0 & 0 & A_{G3} & 0 & 0 & 0 & 0 & 0 & 0 & A_{G3}{}^{a} \\
0 & 0 & 0 & A_{G4} & 0 & 0 & 0 & 0 & 0 & A_{G4}{}^{a} \\
0 & 0 & 0 & 0 & A_{G5} & 0 & 0 & 0 & 0 & A_{G5}{}^{a} \\
0 & 0 & 0 & 0 & 0 & A_{G6} & 0 & 0 & 0 & A_{G6}{}^{a} \\
0 & 0 & 0 & 0 & 0 & 0 & A_{G7} & 0 & 0 & A_{G7}{}^{a} \\
0 & 0 & 0 & 0 & 0 & 0 & 0 & A_{G8} & 0 & A_{G8}{}^{a} \\
0 & 0 & 0 & 0 & 0 & 0 & 0 & 0 & A_{G9} & A_{G9}{}^{a} \\
A_{G1}{}^{b} & A_{G2}{}^{b} & A_{G3}{}^{b} & A_{G4}{}^{b} & A_{G5}{}^{b} & A_{G6}{}^{b} & A_{G7}{}^{b} & A_{G8}{}^{b} & A_{G9}{}^{b} & -D/M
\end{bmatrix}
$$

$$
B_{CaseStudy3} = \begin{bmatrix}
B_{G1} & 0 \\
B_{G2} & 0 \\
B_{G3} & 0 \\
B_{G4} & 0 \\
B_{G5} & 0 \\
B_{G6} & 0 \\
B_{G7} & 0 \\
B_{G8} & 0 \\
B_{G9} & 0 \\
0 & -1/M
\end{bmatrix},
$$

$C_{CaseStudy3}$ = [0 0 0 0 0 0 0 0 0 0 0 0 0 0 0 0 0 0 0 0 0 0 0 0 0 0 0 0 0 0 0 0 1];

$$\text{and } D_{CaseStudy3} = \begin{bmatrix} 0 & 0 \end{bmatrix} \tag{5.5}$$

Where,

$$\boldsymbol{A_{G1} = A_{G2} = A_{G3} = A_{G4} = A_{G5} = A_{G6} = A_{G7} = A_{Fossil}},\ \boldsymbol{A_{G8} = A_{Nuclear}}\ \textit{and}\ \boldsymbol{A_{G9} = A_{dc}}$$

$$\boldsymbol{A_{G1}{}^{a} = A_{G2}{}^{a} = A_{G3}{}^{a} = A_{G4}{}^{a} = A_{G5}{}^{a} = A_{G6}{}^{a} = A_{G7}{}^{a} = A_{Fossil}{}^{a}},\ \boldsymbol{A_{G8}{}^{a} = A_{Nuclear}{}^{a}}\ \textit{and}\ \boldsymbol{A_{G9}{}^{a} = A_{dc}{}^{a}}$$

$$\boldsymbol{A_{G1}{}^{b} = A_{G2}{}^{b} = A_{G3}{}^{b} = A_{G4}{}^{b} = A_{G5}{}^{b} = A_{G6}{}^{b} = A_{G7}{}^{b} = A_{Fossil}{}^{b}},\ \boldsymbol{A_{G8}{}^{b} = A_{Nuclear}{}^{b}}\ \textit{and}\ \boldsymbol{A_{G9}{}^{b} = A_{dc}{}^{b}}$$

$$\boldsymbol{B_{G1} = B_{G2} = B_{G3} = B_{G4} = B_{G5} = B_{G6} = B_{G7} = A_{Fossil}},\ \boldsymbol{B_{G8} = A_{Nuclear}}\ \textit{and}\ \boldsymbol{B_{G9} = A_{dc}} \tag{5.6}$$

And

$$A_{dc} = \left[-1/T_{dc}\right], A_{dc}{}^{a} = \left[-1/RT_{dc}\right], A_{dc}{}^{b} = \left[k_{dc}/M\right], B_{dc} = \left[1/T_{dc}\right] \tag{5.7}$$

During the development of the state space models, all nonlinearities were neglected, including the governor rate limiter. Now that the state space model is built, and the system data is applied, the eigenvalues are calculated for each Case Study. Case Study 1 and Case Study 2 have 18 eigenvalues, while Case Study 3 has 33 eigenvalues. The rough system frequency response can be predicted through the eigenvalues. If a positive eigenvalue exists, an unstable response is predicted. On the other hand the response is stable if all system eigenvalues are of negative value. Moreover, the eigenvalues that have very small negative values, near to zero, are known as the dominant eigenvalues. These dominant eigenvalues are the most important eigenvalues as a small change of any of the systems parameters might lead to shift these dominant eigenvalues from the small negative value to positive values and hence an instability case. If the dominant eigenvalues are complex numbers, the response is expected to be an oscillatory response [24, 72 and 77-84].

Table 5-1 shows the dominant oscillatory system eigenvalues for all three case studies. Case study 3 has more negative dominant eigenvalues, hence a more stable system, illustrating the damping effect of the existence of an HVDC link.

Table 5-1 Dominant Eigenvalues of Case Study 1, Case Study 2 and Case Study 3

Case Study 1	Case Study 2	Case Study 3
-0.4949 + 0.7598i	**-0.3773 + 0.5881i**	**-0.9081 + 1.3282i**
-0.4949 - 0.7598i	**-0.3773 - 0.5881i**	**-0.9081 - 1.3282i**

5.3 Integral Control Based Island AGC

The integral AGC has always been the conventional AGC. The output of the integral AGC is the change in reference power setting of units, operating on the AGC, required to eliminate by what is known as Area Control Error (ACE). This error usually consists of a linear combination of tie-line errors and frequency error. Here in this section the design of an integral AGC is considered. And since the main concern is improving the frequency response of the thesis case studies, the ACE will be nothing except the frequency deviation. Consequently, the controller's construction is the simple construction shown in Figure 5.8 [1 and 46-47]. The main design parameter would be choosing the proper integral gain ki. A study of the governor time delay effect on system performance is discussed in Section 5.3.1. This is followed by discussing the integral controller design approach.

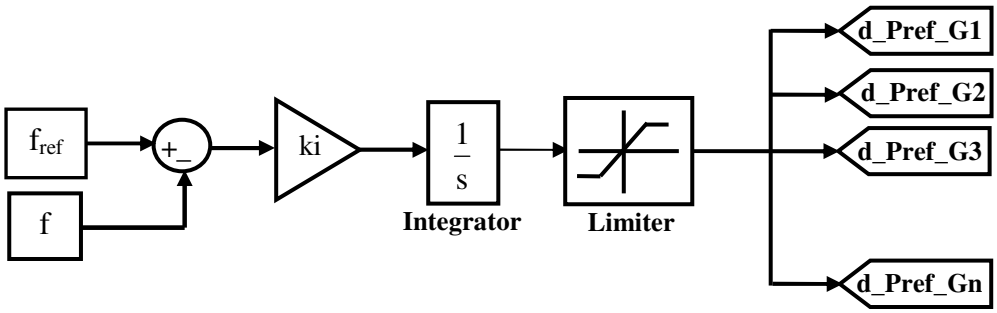

Figure 5.8 Integral based AGC construction [1 and 46-47].

5.3.1 Governor Time Delay Effect on System Performance

As discussed earlier in Chapter 3, the effect of an existing governor rate limiter is to increase the governor time delay. This can be studied by increasing the governor time constant in simulation studies. Here, the effect of increasing the governor time delay constant on system performance is studied. This is through plotting the dominant eigenvalues of the thesis case studies at different governor time constants, specifically 0.2 (no rate limiter case), 1, 2, 3, 5 and 10 seconds. See Figure 5.9. Based on Figure 5.9, it can be seen clearly that if the rate limiter equipped with the governor causes the governor to respond with a 2 sec time constant, Case Study 1, frequency would oscillate and go unstable. On the other hand, Case Study 2 would lose its stability if equipped to what is equivalent to a 3 sec time constant governor. And finally, the frequency response of Case Study 3 is always stable due to the presence of a fast acting, frequency responsive HVDC link.

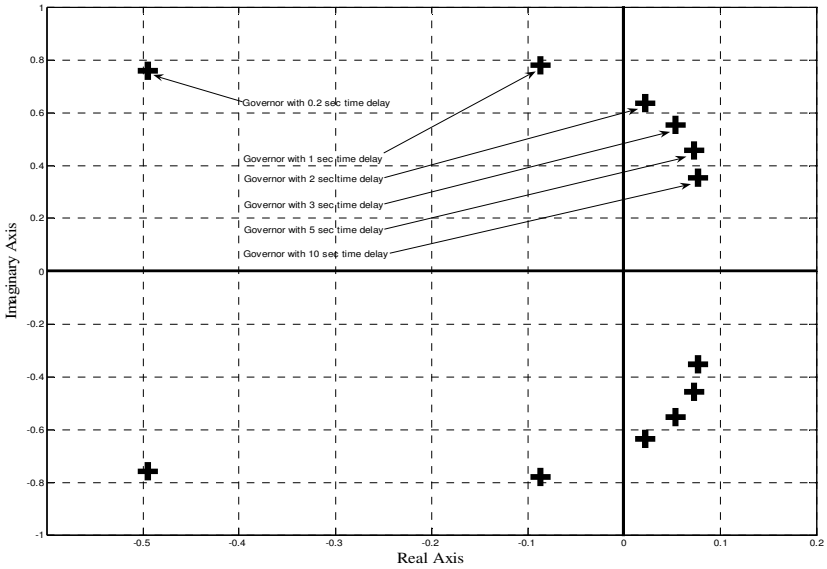

(a)Case Study 1

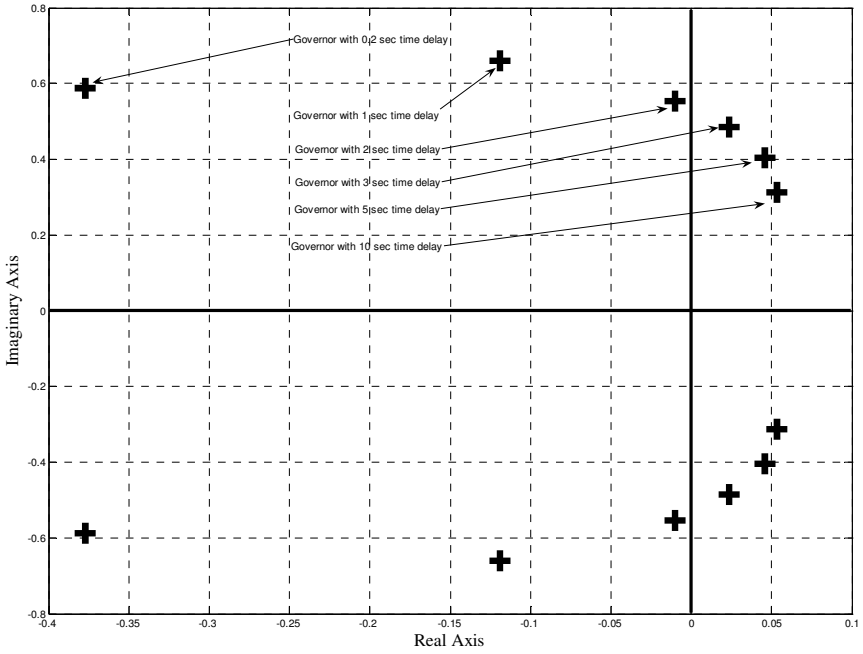

(b) Case Study 2.

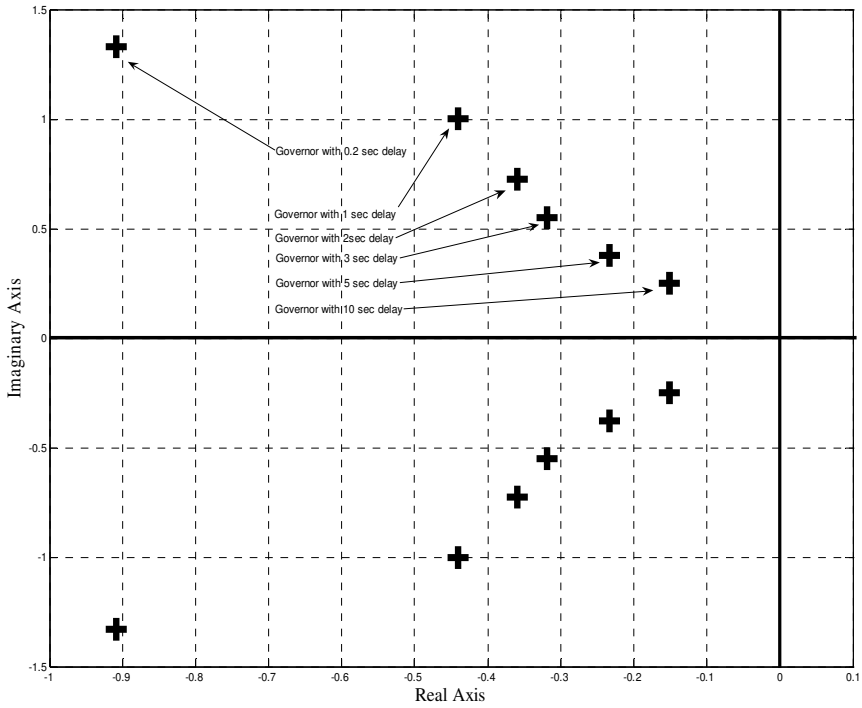

(c) Case Study 3.

Figure 5.9 Dominant Eigen value with Governor Time delay.

5.3.2 Controller Design Approach

The design considers all generating units speed changer settings as one input. Hence, the case studies are considered as a Single Input Single Output (SISO) problem [77-79]. The only system output is area frequency and the only input is the reference settings of the units operating on the AGC. All units other than wind are considered to be operating on the AGC. The controller design approach is as follows:

1- Obtain the case study SISO transfer function.
2- Plot the root locus showing the pole place movements with change of integral controller gain, at different governor time constants.
3- Find ki_{cr}, the critical integral gain where the dominant poles change from a negative value to a positive value, for every plot.
4- Set ki to $ki_{cr}/2$ to obtain good response, Ziegler-Nicholas method [77].

It must be noted that the near ki is from ki_{cr}, the more oscillatory the system becomes. However the first overshoot will be strongly damped. On the other hand a very small ki would lead to a slow over damped response but the first overshoot will not be affected.

5.3.3 Case Studies Results

The root locus results and time domain simulation for Case Study 1, Case Study 2 and Case Study 3 is presented and discussed in Section 5.3.3.1, Section 5.3.3.2 and Section 5.3.3.3 respectively.

5.3.3.1 Case Study 1

The root locus plot for Case Study 1 at different governor time constants is presented in this section. Some plots, specifically at governor time constants of 0.2,1 and 10 seconds, are presented in Figure 5.10. ki_{cr} was found to be equal to 20 and 2.5 for the case of 0.2 and 1 second governor time constant respectively. Moreover, if the governor time constant is more than 1 sec, the dominant poles would be of positive along its whole trajectory, see Figure 5.10(c). I.e. ki_{cr} does not exist or no ki exists to stabilize such case.

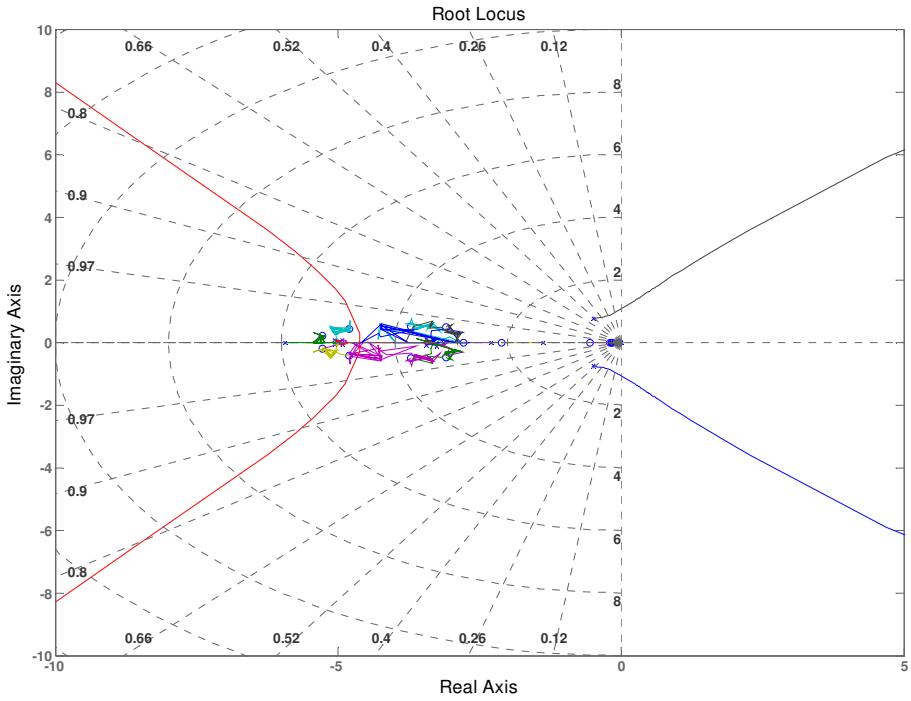

(a) Governor with a 0.2 sec time constant.

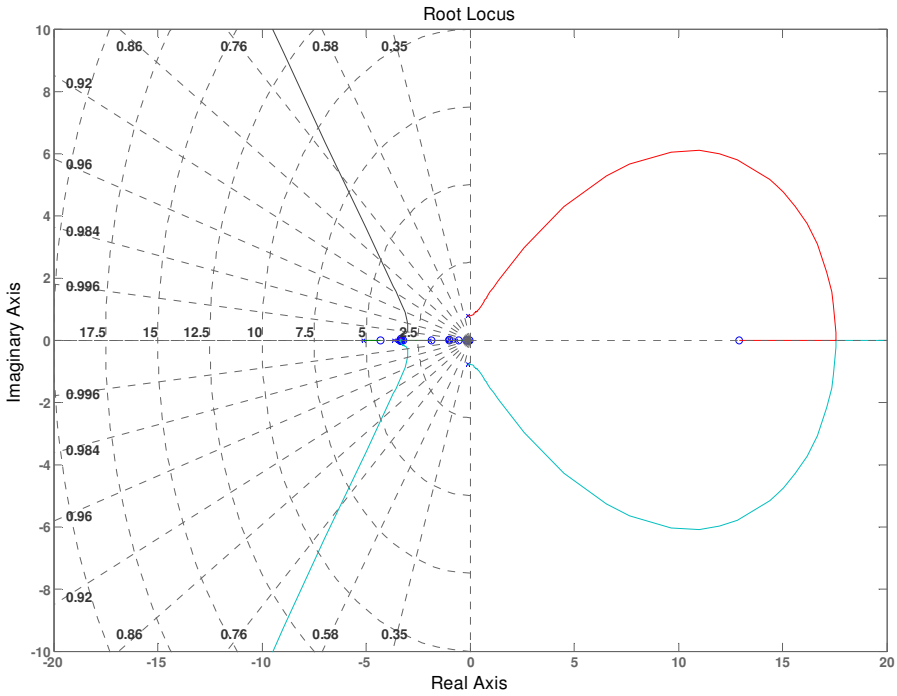

(b) Governor with a 1 sec time constant.

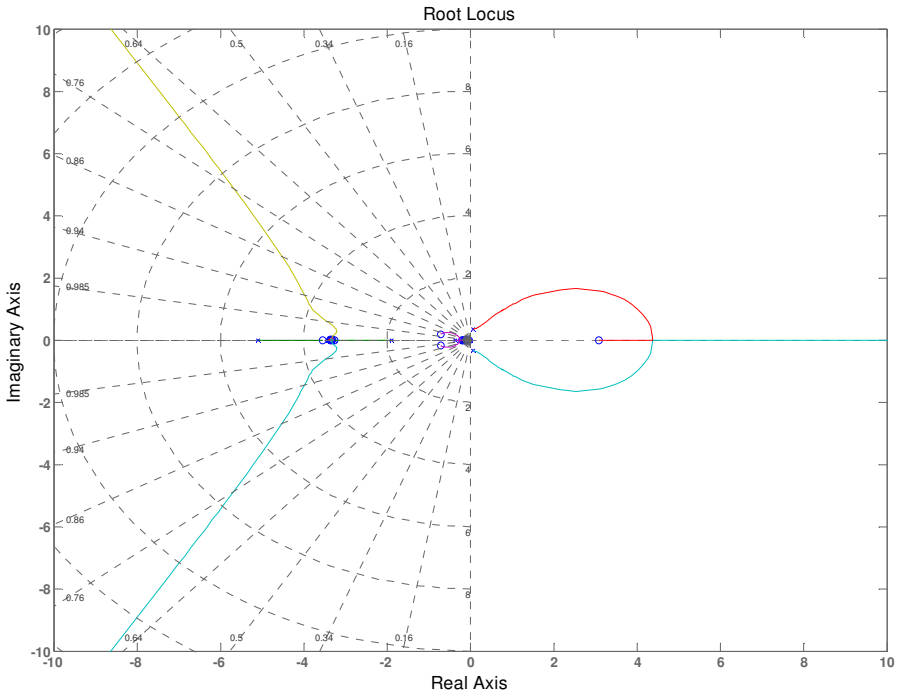

(c) Governor with a 10 sec time constant.

Figure 5.10 Root locus plots for Case Study 1.

Moreover, Figure 5.11 shows some time domain simulations of the frequency response of Case Study 1 network upon disconnection from the rest of the grid at different governor maximum rate limits where the following five cases are compared in each subplot:

(a) Without Island AGC.

(b) With Integral Island AGC whose ki_{cr}=20.

(c) With Integral Island AGC whose ki=20/2=10.

(d) With Integral Island AGC whose ki_{cr}=2.5.

(e) With Integral Island AGC whose ki=2.5/2=1.25.

From Figure 5.11, it can be seen that Case Study 1 equipped with a ki of 10 AGC losses stability if the maximum governor rate limit is less than 0.4 p.u./sec. On the other hand Case study 1 equipped with a ki of 1.25 AGC losses stability if the maximum governor rate limit is less than 0.1 p.u./sec. For all stable cases, although the first frequency overshoot is not affected but the steady state frequency error is eliminated, i.e. the frequency always settles at its nominal value.

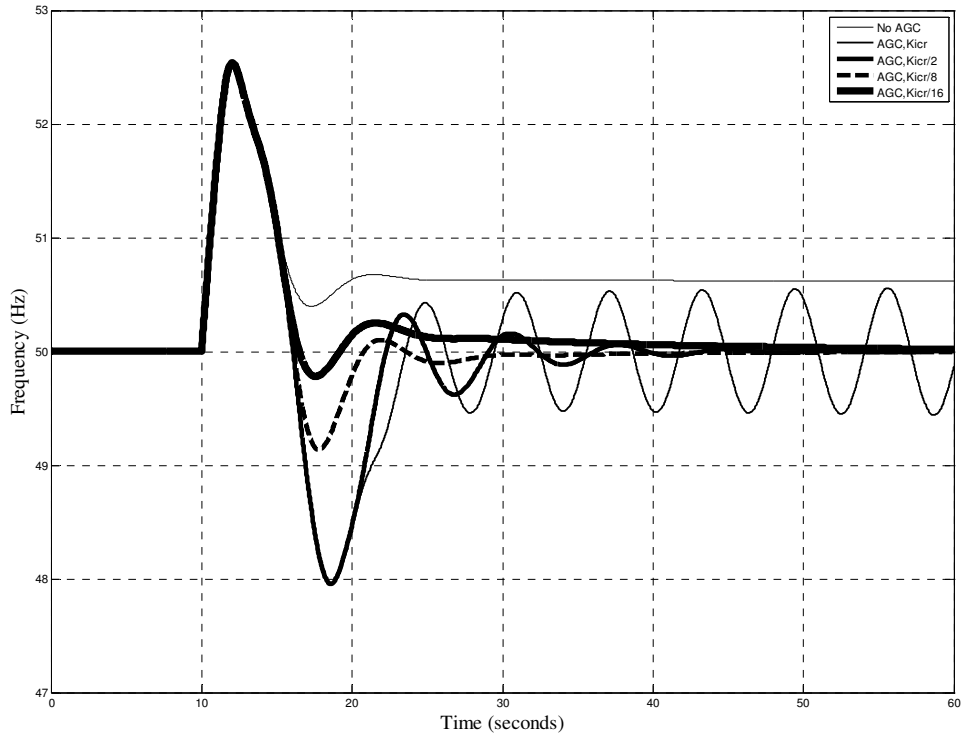

(a) Maximum governor rate limit= 0.9 p.u./sec.

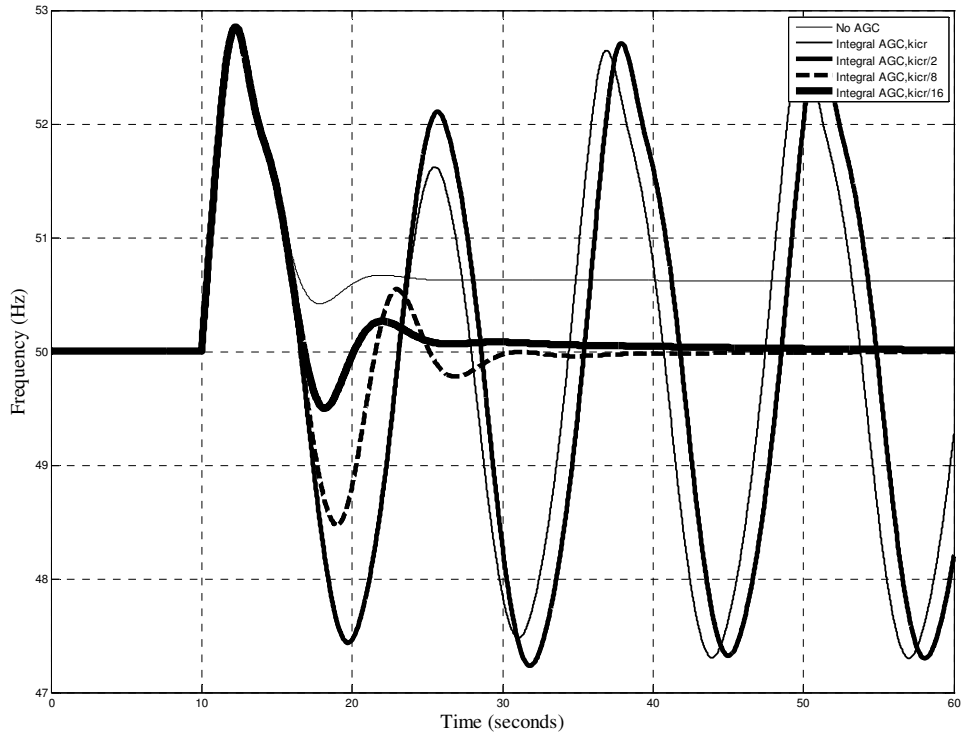

(b) Maximum governor rate limit= 0.3 p.u./sec.

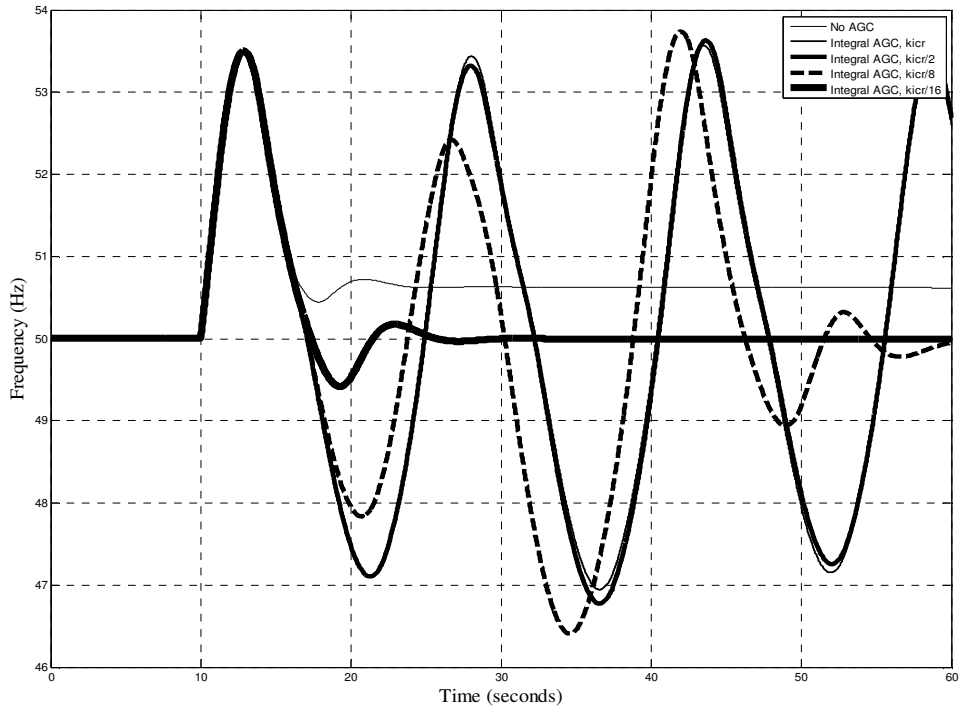

(c) Maximum governor rate limit= 0.2 p.u./sec.

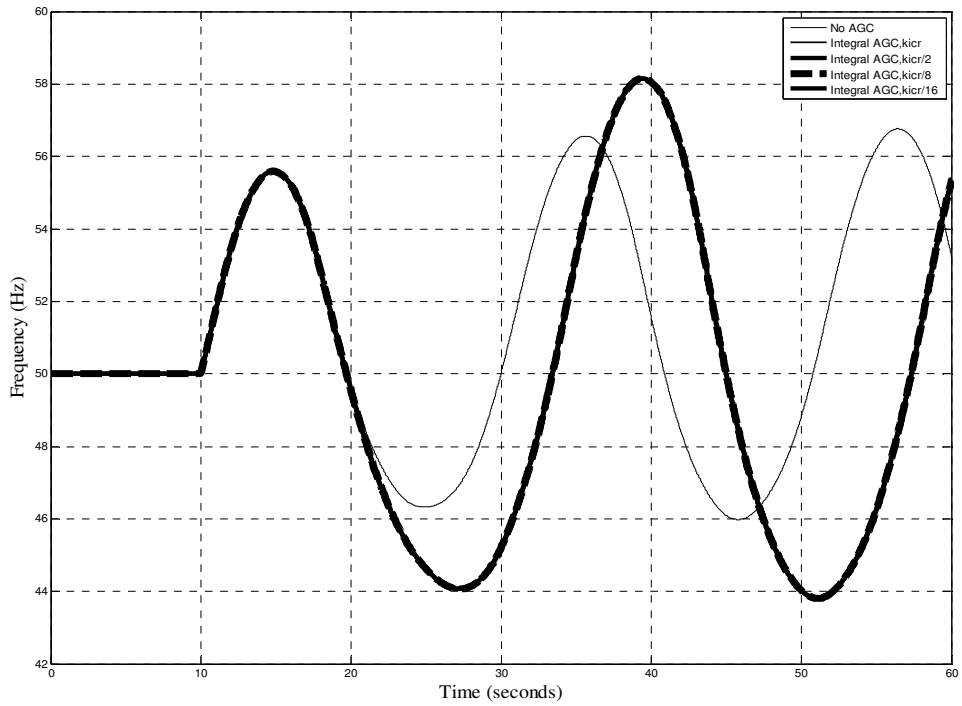

(d) Maximum governor rate limit= 0.1 p.u./sec.

Figure 5.11 Frequency response of Case Study 1 with conventional AGC.

5.3.3.2 Case Study 2

Similarly, the root locus plot against ki is plot for Case Study 2 at different governor time constants. Some plots, specifically at governor time constants of 0.2, 2 and 10 seconds, are presented in Figure 5.12 ki_{cr} was found to be equal to 20 and 5 for the case of 0.2 and 2 second governor time constant respectively. Moreover, if the governor time constant is more than 2 sec, the dominant poles would be of positive along its whole trajectory, see Figure 5.12(c). I.e. ki_{cr} does not exist or no ki exists to stabilize such case.

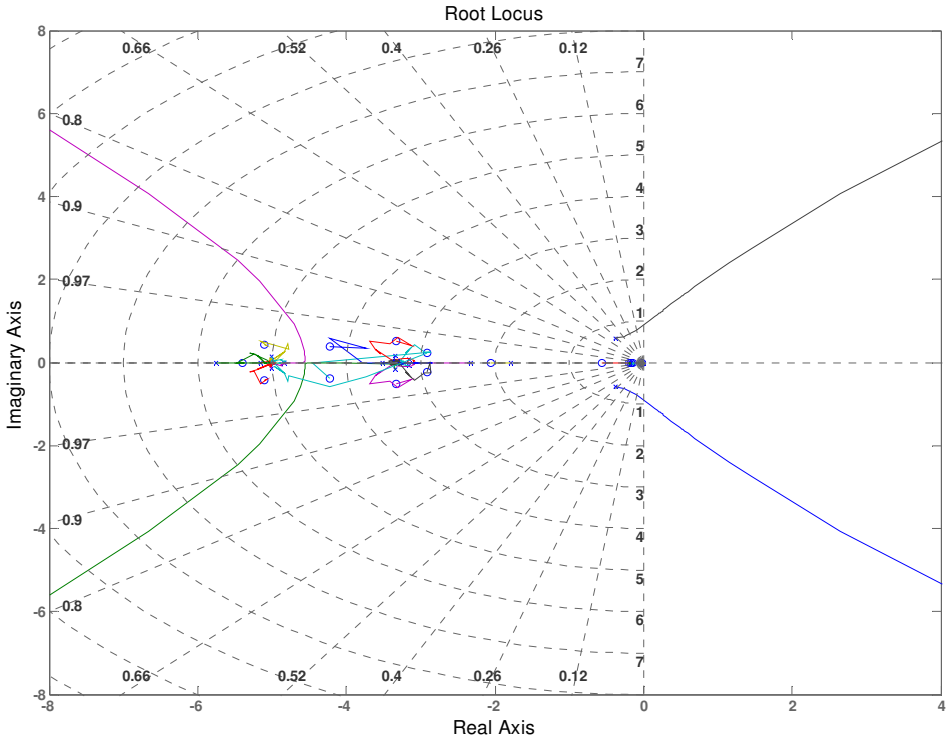

(a) Governor with a 0.2 sec time constant.

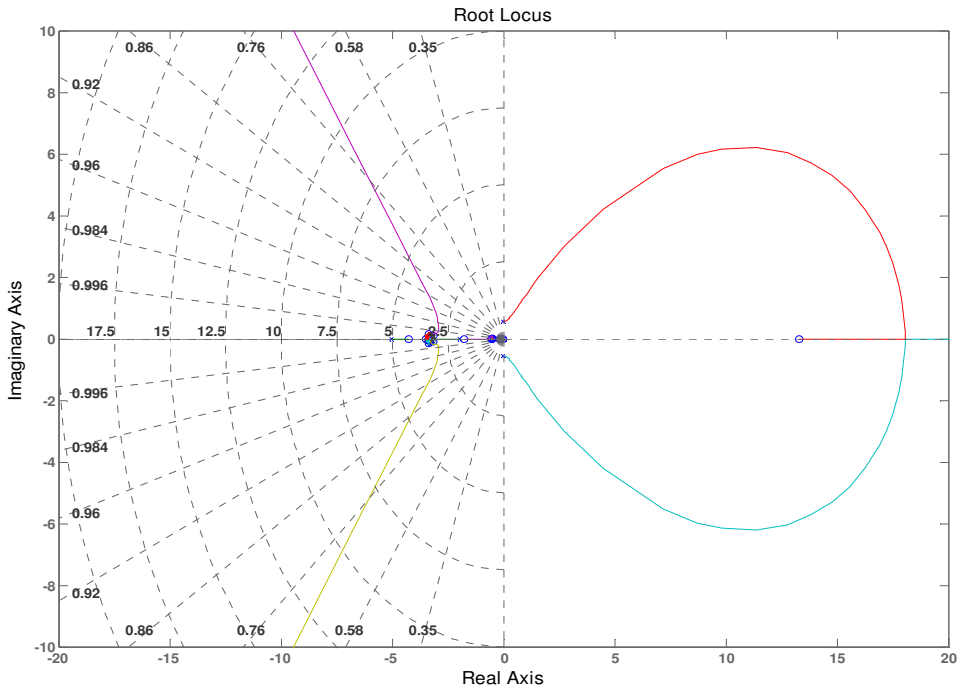

(b) Governor with a 2 sec time constant.

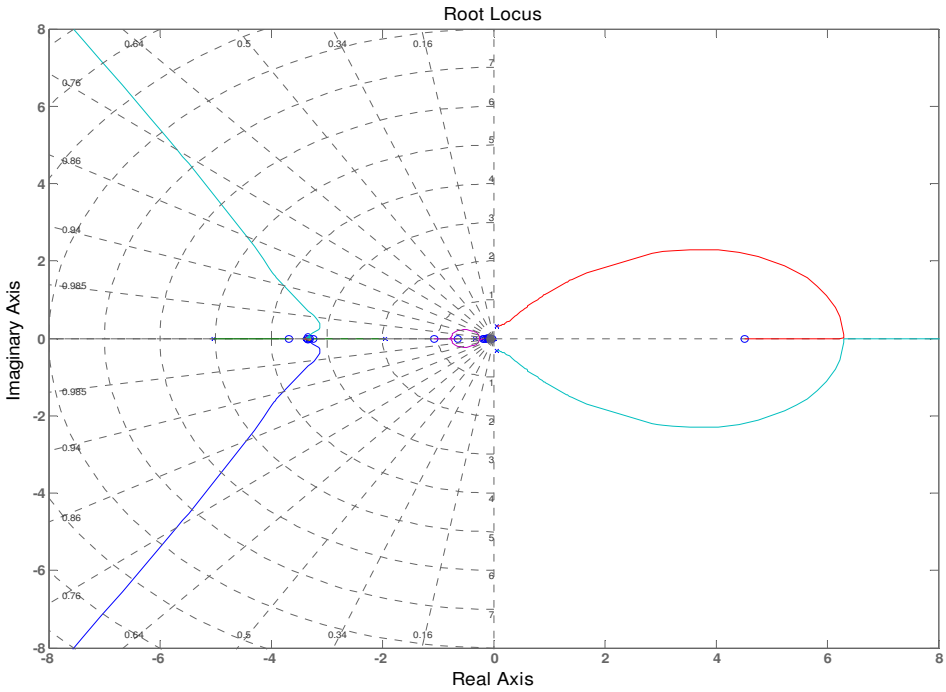

(c) Governor with a 10 sec time constant.

Figure 5.12 Case Study 2 root locus plots.

Moreover, Figure 5.13 shows some time domain simulation of the frequency response of Case Study 2 network upon disconnection from the rest of the grid at different governor maximum rate limits where the following five cases are compared in each subplot:

(a) Without Island AGC.

(b) With Integral Island AGC whose ki=20/2=10.

(c)With Integral Island AGC whose ki=25/2=2.5.

From Figure 5.13, it can be seen that Case Study 2 never loses stability except for the case where ki= 10 and maximum rate limit of 0.1 p.u./sec. This means for all cases the governor time constant does not exceed 2 seconds. Furthermore, the frequency always settles at its nominal value. The time it takes to reach this nominal frequency value depends on the maximum value of the governor limiter rate.

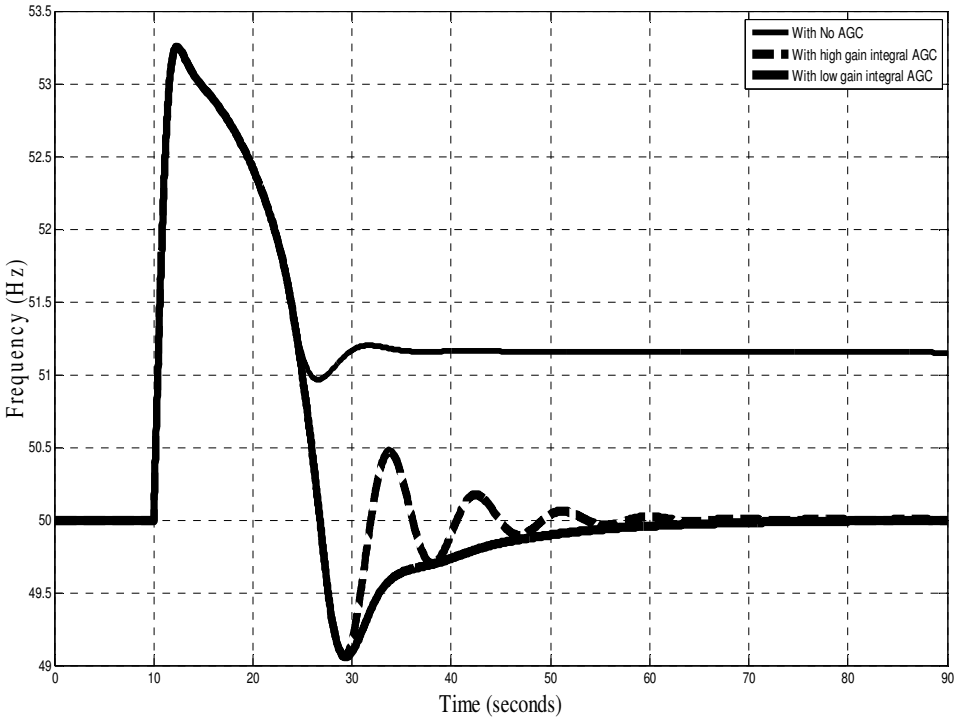

(a) Maximum limiter rate is 0.9 p.u./sec.

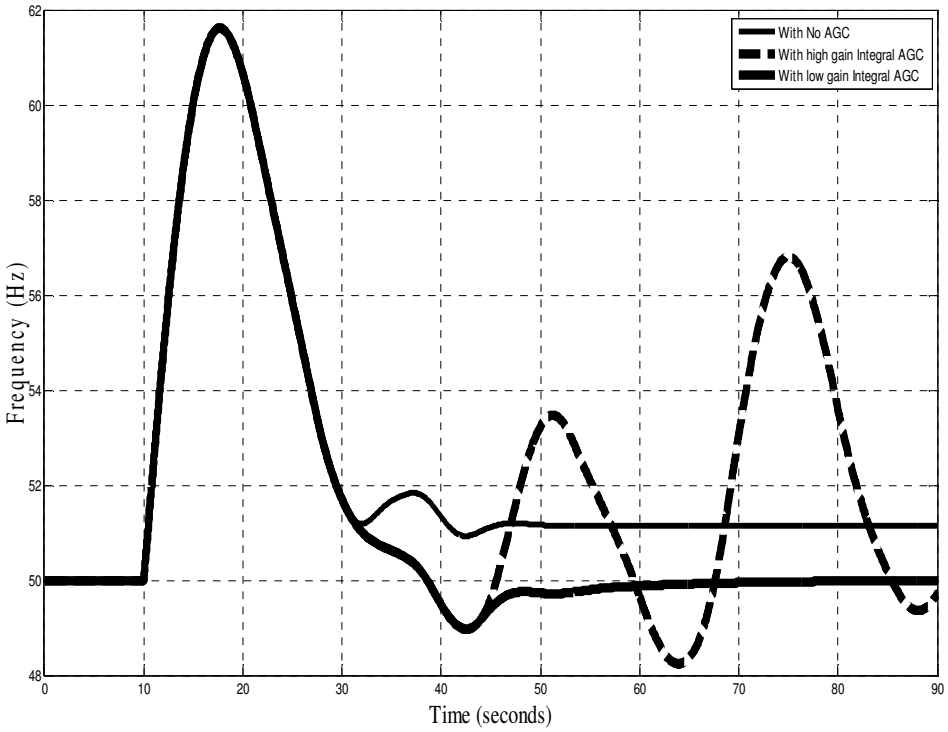

(b) Maximum limiter rate is 0.1 p.u./sec

Figure 5.13 Frequency response of Case Study 1 with conventional AGC.

5.3.3.3 Case Study 3

Similarly, the root locus plot for Case Study 3 is shown in Figure 5.14 kicr was found to be equal to 50. Moreover, Figure 5.15 shows some time domain simulation of the frequency response of Case Study 3 network upon disconnection from the rest of the grid at different governor maximum rate limits where the following five cases are compared in each subplot: (a) Without Island AGC. (b) With Integral Island AGC whose ki=50/2=25.

From Figure 5.15, it can be seen that Case Study 3 never loses stability. Furthermore, the frequency always settles at its nominal value. The time it takes to reach this nominal frequency value depends on the maximum value of the governor limiter rate.

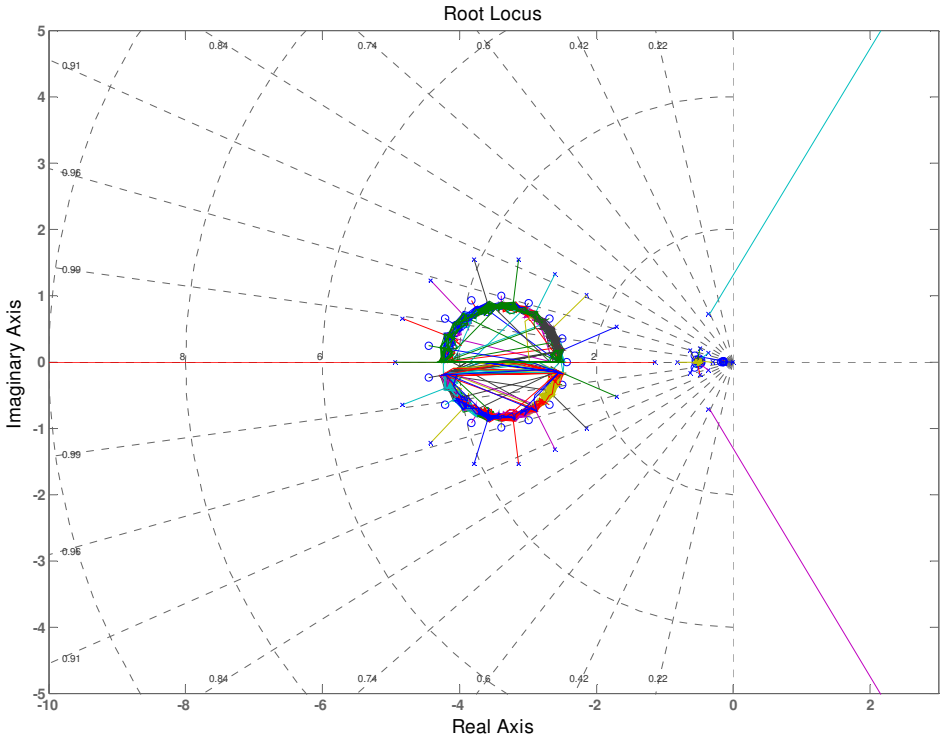

Figure 5.14 Case Study 3 root locus plot.

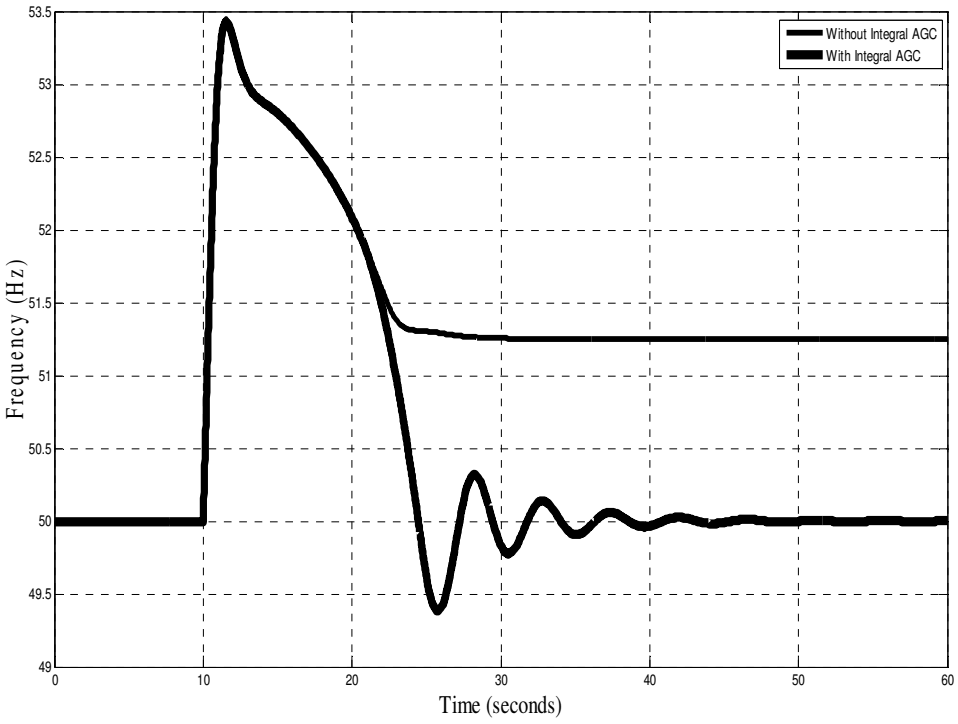

(a) Maximum limiter rate is 0.9 p.u./sec.

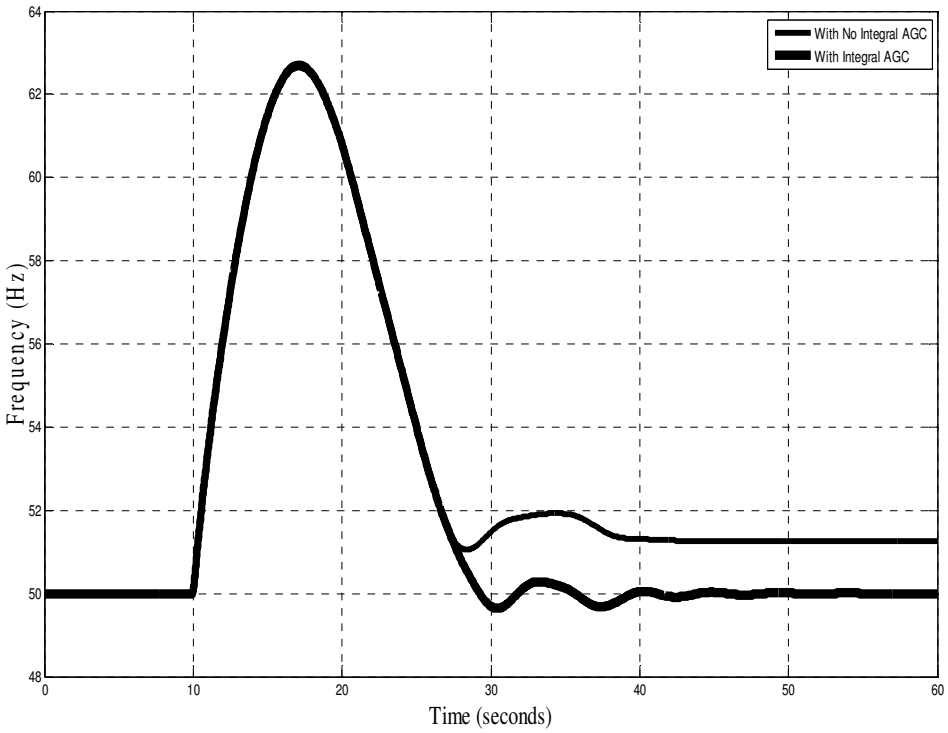

(b) Maximum limiter rate is 0.1 p.u./sec.

Figure 5.15 Frequency response of Case Study 3 with conventional AGC.

5.4 LQR-Based Island AGC

The linear quadratic control developed in late 1960's. It uses the system state space representation and not the transfer function representation. It is an optimal control technique because it involves minimizing an objective function or a performance index which is usually an integral function of the system states and control inputs [77-80].

Although the literature discusses other control techniques than the LQR methodology for AGC systems design such as predictive control, H_∞ control and etc., the LQR was chosen for the emergency island AGC application discussed in this section for its well known advantages. It provides a powerful controller design methodology that is applicable to both single and multiple input systems. It also leads to linear control laws (i.e. proportional controllers) that are easy to implement and analyze. This technique has proved to provide good results, better than the conventional controllers, in the area of designing AGCs. Papers discussing this kind of control age from the 1970's, 1980's [35-36] to study the two area systems where each area was represented by one machine to the 2000's to study more complicated power systems [37] and to include the deregulated market environment [38-40]. Another advantage of this technique is the flexibility of its objective function, which can always be modified to include more constraints and different variables.

This section designs an LQR-based Island AGC that operates once the main AGC is disconnected as the system goes islanded and the area machines overspeed. A background related to the LQR problem is discussed in Section 5.4.1. Section 5.4.2 discusses the design approach, while Section 5.4.3 presents the design results when applied to the linearized model. And finally the case studies time domain simulation is presented in Section 5.4.4

5.4.1 The Output LQR Problem

The LQR problem discussed here is the special case, where the outputs instead of the states are weighted. It considers the linear system and the quadratic objective function or cost function:

$$\dot{\boldsymbol{x}} = \boldsymbol{Ax} + \boldsymbol{Bu}$$
$$\boldsymbol{y} = \boldsymbol{Cx}$$

$$J = \frac{1}{2}\int_0^T \left(y'Qy + u'Ru\right)dt \tag{5.8}$$

The problem is to minimize J with respect to the control input u. Generally, Q and R represent respective weights on different states and control channels. This makes Q and R the main design parameters. These parameters are chosen, in general, through several design iterations to obtain a stable optimal system with "good" response. For a meaningful optimization problem, Q must be symmetric positive semi definite (written as $Q \geq 0$) and R must be symmetric definite ($R > 0$) [77-81]. Moreover, solving such problem is exactly the same as solving the state LQR problem, see Appendix C. The only difference is that Q is to be replaced $\overline{Q}$.

Where $$\overline{\boldsymbol{Q}} = \boldsymbol{C'QC} \tag{5.9}$$

If the system is scalar (i.e. first order), the cost function becomes

$$J = \frac{1}{2}\int_0^T qy^2 + ru^2 dt \tag{5.10}$$

If r is very large relative to q, the control energy is penalized very heavily. This means smaller motors, actuators, and amplifier gains are needed to implement the control law. Like wise, if q is much larger than r, the state is penalized heavily, resulting in a much more damped system [77-81]. Moreover, it is worth mentioning that this control problem results in a full state feedback regulator (i.e. $\boldsymbol{u=-kx}$).

5.4.2 The Output LQR Application And Design Approach

The control design process starts with identifying the state variables of the system studied which are as follows:

(a) P_{GVc}, P_{HPc}, P_{IPc}, P_{LPc} for every existing fossil-fueled power station.
(b) P_{GVn}, P_{HPn}, P_{LPn},: for every existing nuclear power station
(c) P_{GVh},P_{GVh1}, P_h, for every existing hydro power station
(d) P_{dc} for every existing dc link.
(e) ω. only one variable to represent the area frequency

The next step is to obtain the dynamic equations representing the system. Rearrange them in the state space or ABCD format. As the main objective is to improve the frequency response of the separated system, the output is chosen to be only the average area speed ω which is the average area frequency in p.u.. Moreover, the controller designed will produce only one common control signal for all dispatchable units

$$J = \frac{1}{2}\int_0^T q\Delta\omega^2 + r\Delta P_{ref}{}^2 dt \tag{5.11}$$

Where, P_{ref} represents the speed governor speed changer or load reference setting point and

$$\Delta P_{ref} = \Delta P_{refc} = \Delta P_{refn} = \Delta P_{refh} \tag{5.12}$$

Following the process of calculating the *A, B and C* system matrices, the controller design approach is as shown in Appendix B. This can be summarized as follows

1- Calculate *A, B, C*, and *D* matrices for a certain case study.
2- Apply LQR technique, assuming *q = 1, r = 1*.
3- Increase q in order to obtain a more damped system till the system frequency response starts to oscillate.

Actually, increasing the speed weighting leads to higher gains and hence, resulting in a much damped system. However, the system might lose stability if such gains reach very high values due to saturation problems and controller limiters. As mentioned previously the controller is full state feedback controller. As an example, the controller construction for Case Study 1 and Case Study 2 is shown in Figure5.16. Here in this case we have 18 states to define the system.

Moreover, it is clear from Figure 5.16 that the designed LQR needs two reference values, one for speed and the other for power. The speed reference value is set to 1 p.u. However, the power reference value can be set to the initial operating power or the electrical output power, or it may even be estimated through a speed integral control as shown in Figure 5.17. The choice of the power reference value is investigated in this study.

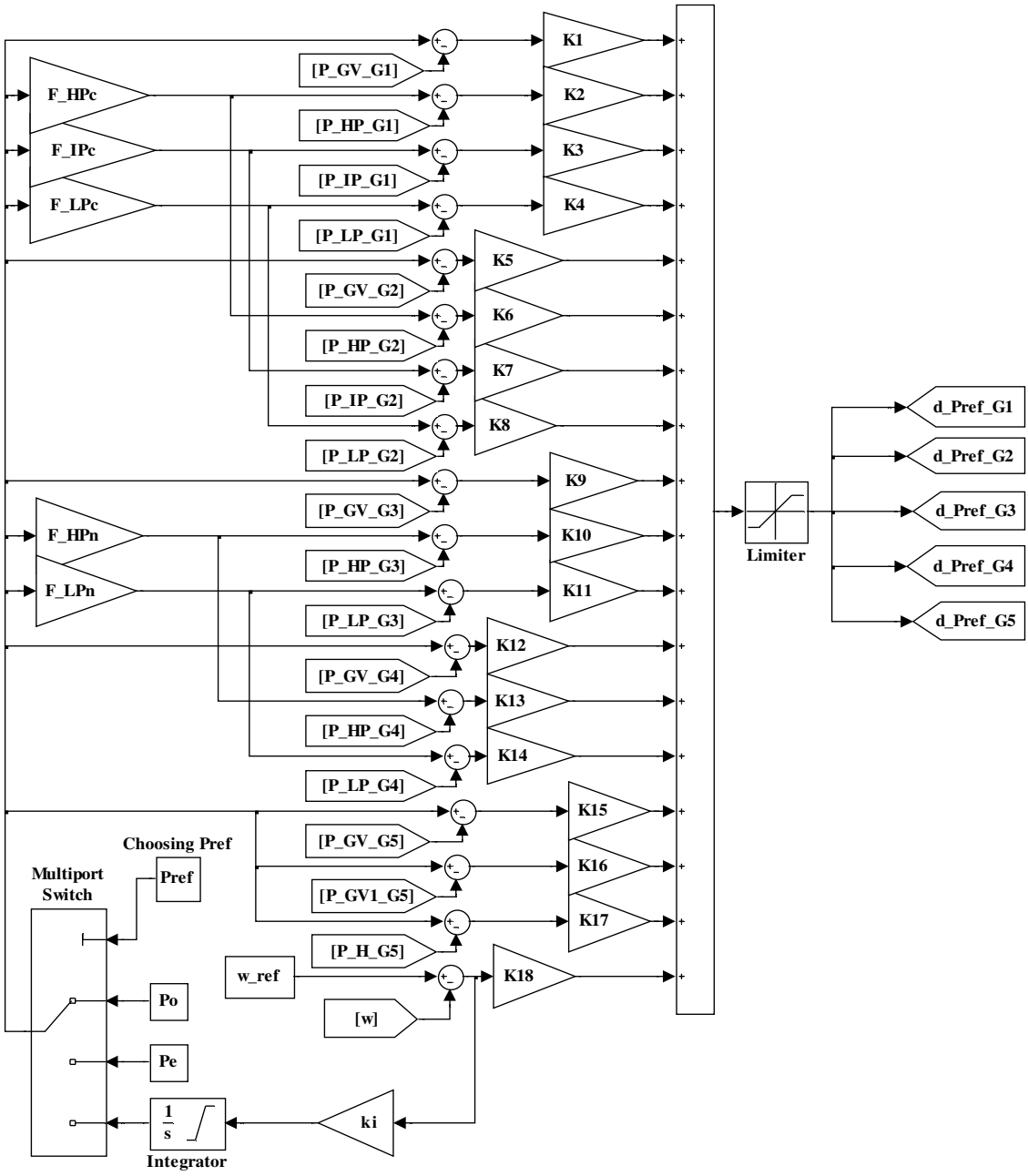

Figure 5.16 The controller construction.

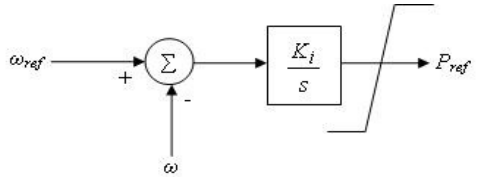

Figure 5.17 Integral Controller to estimate the required reference power value to be used in the LQR.

5.4.3 Linear System Results

The effect of increasing the speed weighting on the dominant eigenvalues of Case Study 1, Case Study 2 and Case Study 3 is presented in Figure 5.18. The designed LQR gains at different weightings for Case Study 1, Case Study 2 and Case Study 3 are presented in Appendix C. Moreover, the frequency time response Case Study 1, Case Study 2 and Case Study 3 is simulated. The LQR controller is applied once the speed exceeds 1% of the nominal rating after the load disturbance has taken place. Figure 5.19 and Figure 5.20 show the frequency response at different speed weightings for a controller whose reference power is set to the initial power and electrical output power, respectively. Moreover, Figure 5.21, Figure 5.22, and Figure 5.23 present the frequency response at different speed weightings for a controller whose power reference is estimated through an integral speed controller with an integral gain equal to 1, 10 and 100, respectively.

Based on the results presented, it can be seen that increasing the weighting of the speed during the LQR design would result in high gains and hence improved transient response. The more the speed weight is increased the more the steady- state error is minimized.

An LQR whose power reference value is set to the pre load loss value would damp the first speed overshoot but would not eliminate the steady state error (Figure 5.19). On the other hand, if the new load value or the electrical machine power output is used to set the power reference of the LQR, the frequency first overshoot would be damped but the steady state error will be eliminated only if very high gain values are used (Figure 5.20).

Another proposed method is to estimate the power reference of the LQR through an integral controller whose input signal is the speed deviation. Caution must be observed in choosing the integral gain as low integral gains would result in a slow response (Figure 5.21). Moreover, very high integral gains would lead to instability (Figure 5.23). Choosing a moderate integral gain and using high proportional gains for the LQR would damp the first speed overshoot and eliminate the steady state error is rapidly (Figure 5.22). Although this seems the best performance, caution must be considered as the frequency undershoots before reaching the nominal value and might provoke the under frequency load disconnection system if drops below 48.5-49 Hz.

Moreover, at high gains (gains designed at speed weighting above 1e9, some oscillations appear due to the saturation problems that accompany the use of very high gains. Hence, the gains of the LQR designed at the speed weighting of 1e6 and a power reference integral estimator of Ki =1-5 are picked to be applied to the non-linear case studies in the following

section, Section 5.4.4 where the overspeed control and governor rate limiters are taken into consideration.

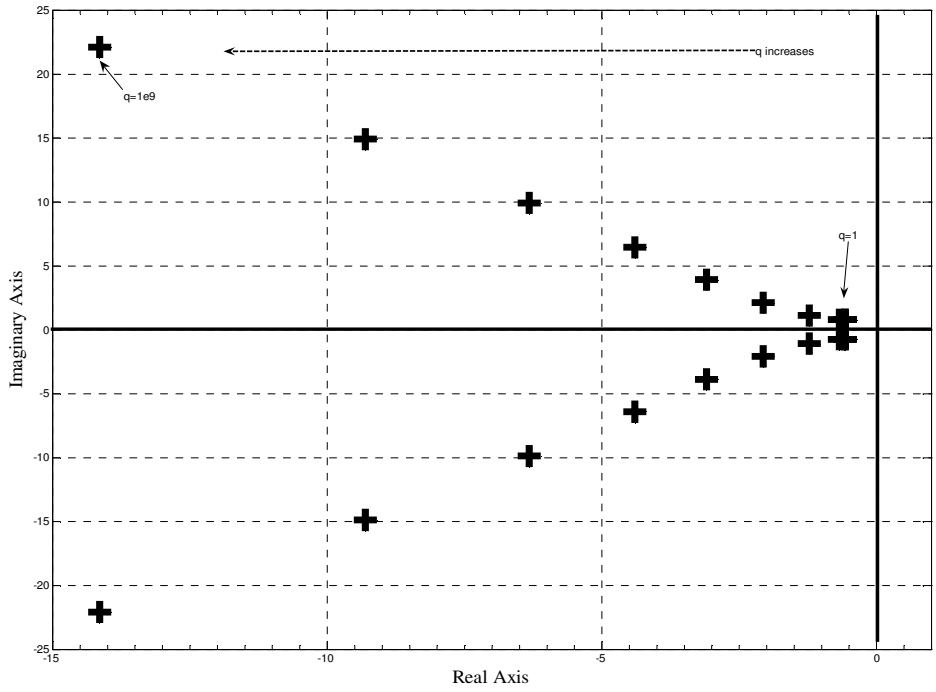

(a) Case Study 1

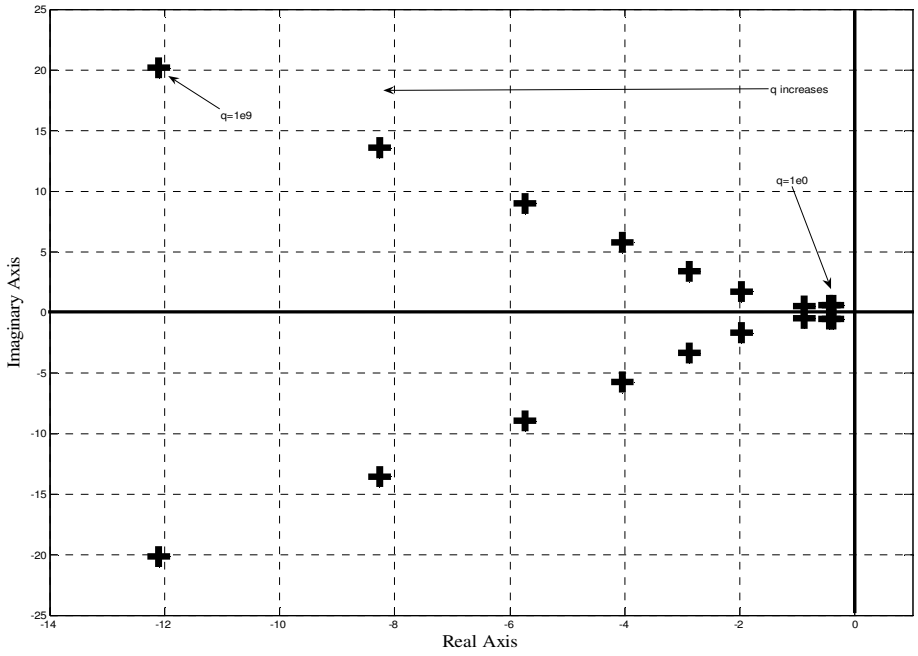

(b) Case Study 2

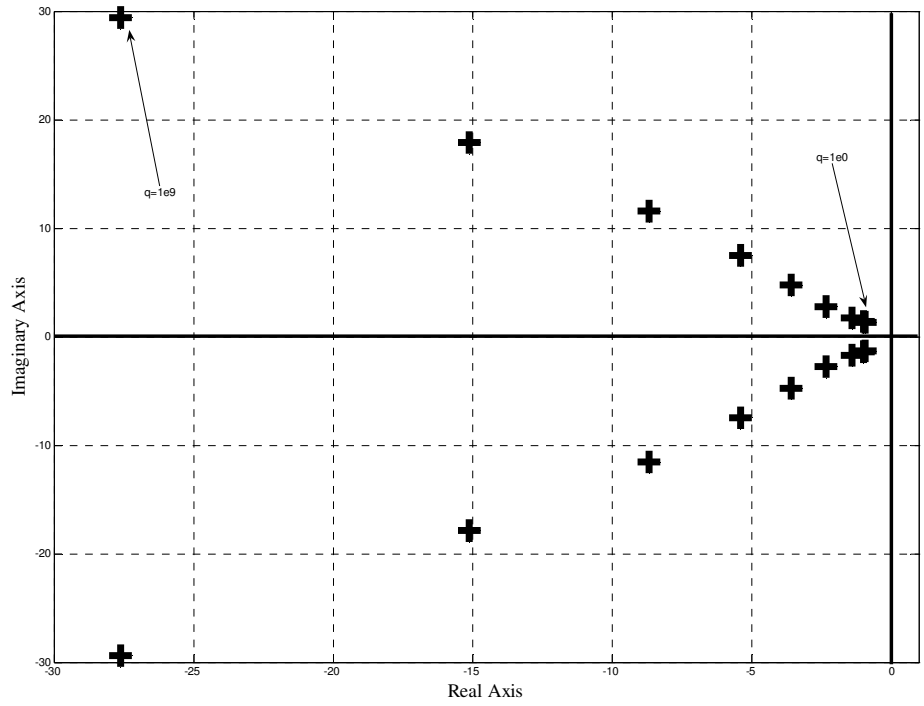

(c) Case Study 3

Figure 5.18 Effect of increasing the speed weightings on case studies dominant poles.

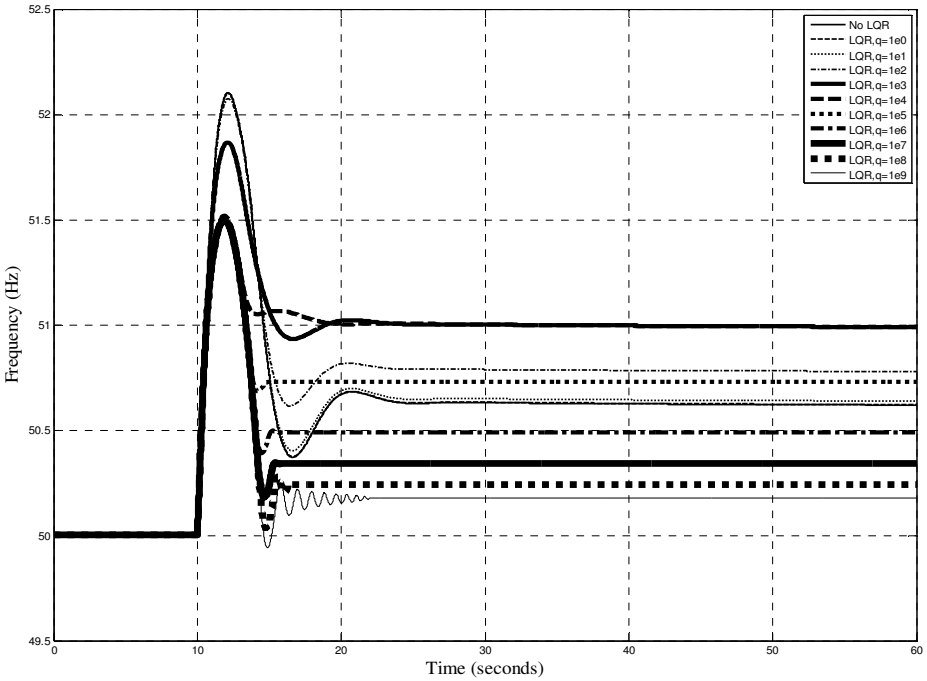

(a) Case Study 1

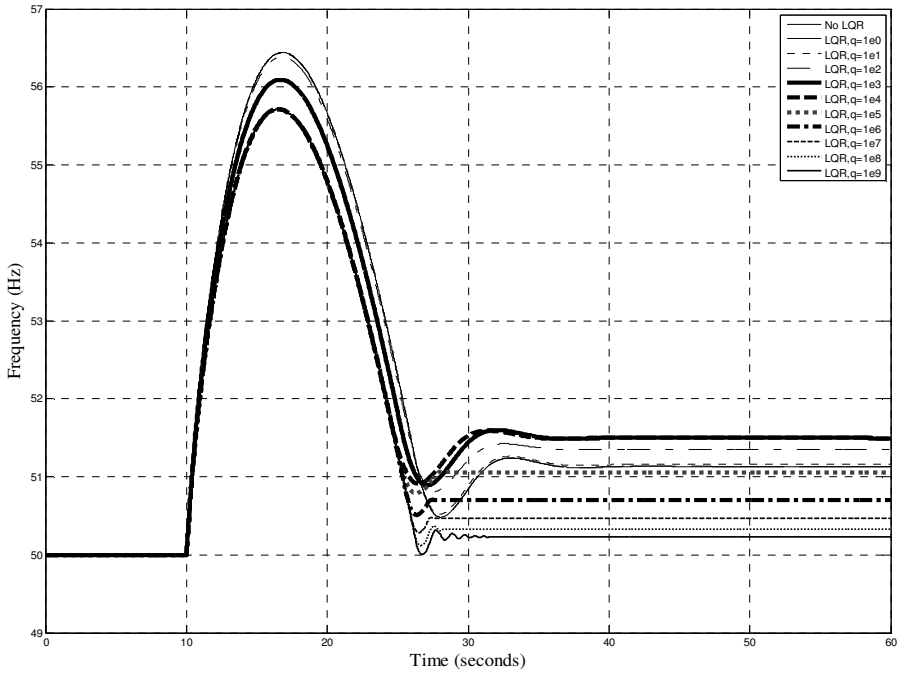

(b) Case Study 2

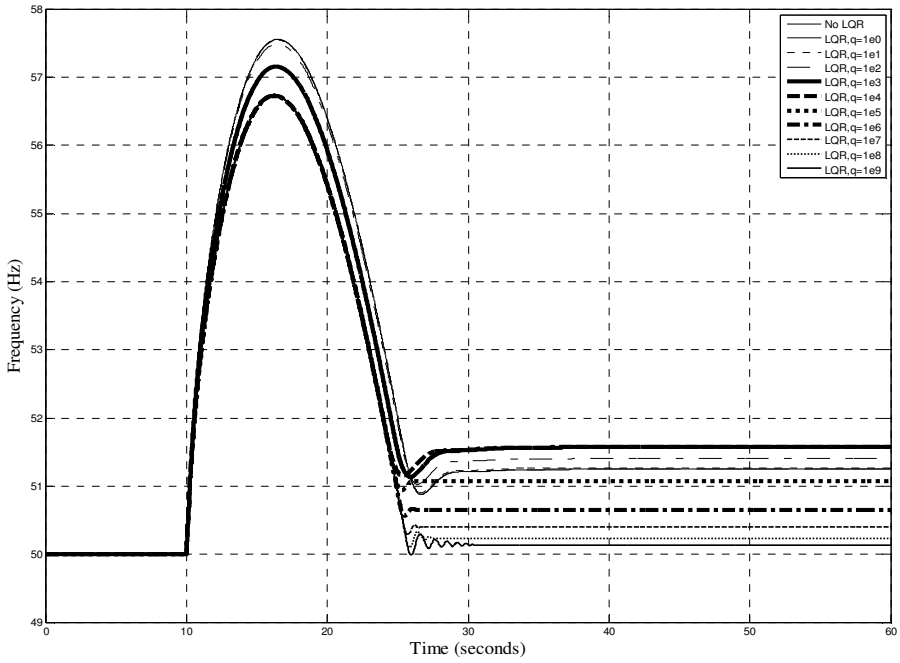

(c) Case Study 3

Figure 5.19 Frequency responses with LQR-based AGC and reference power set to the initial loading value

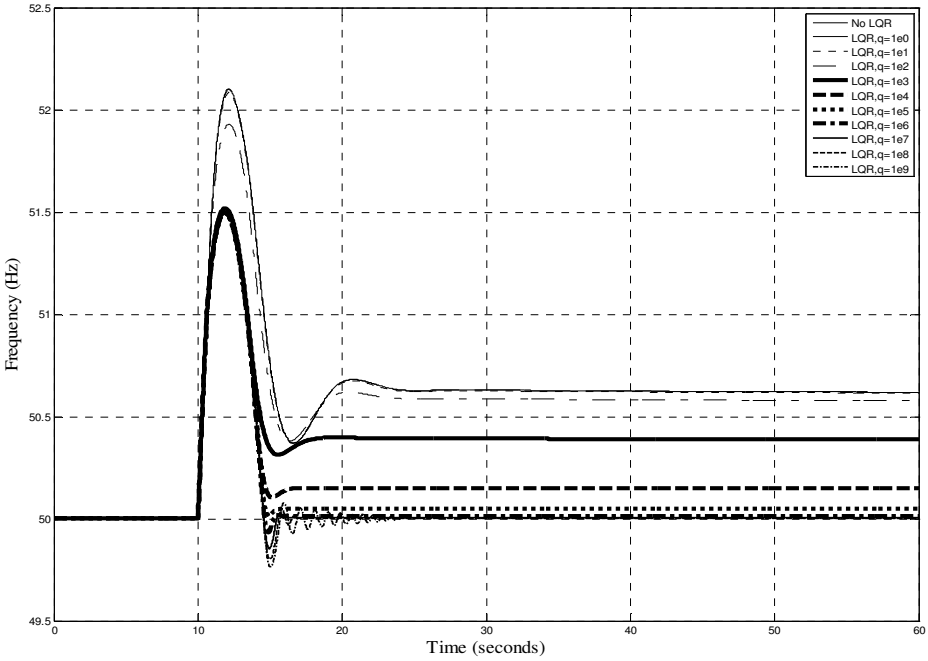

(a) Case Study 1.

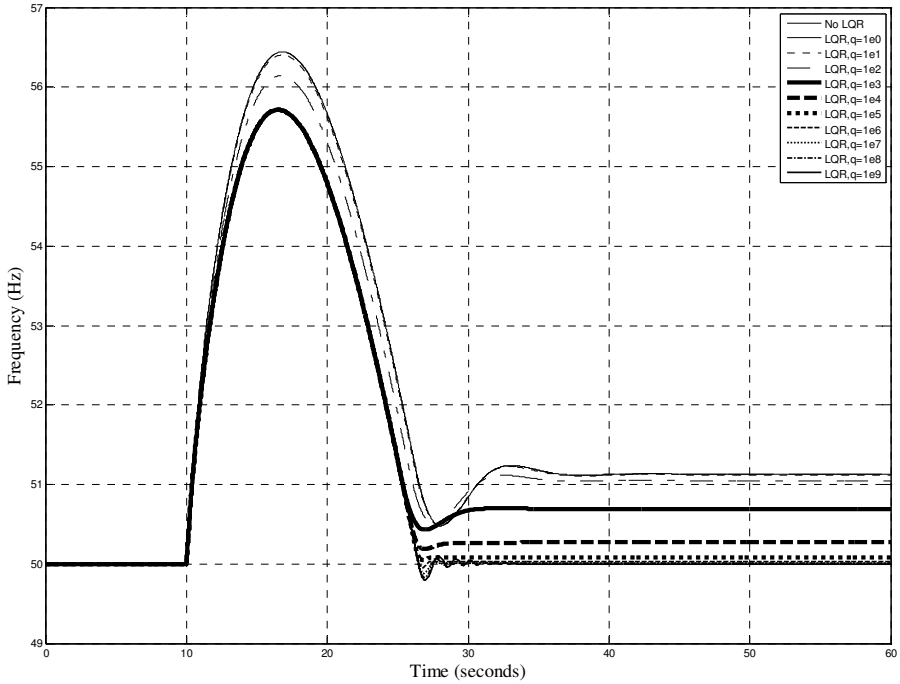

(b) Case Study 2.

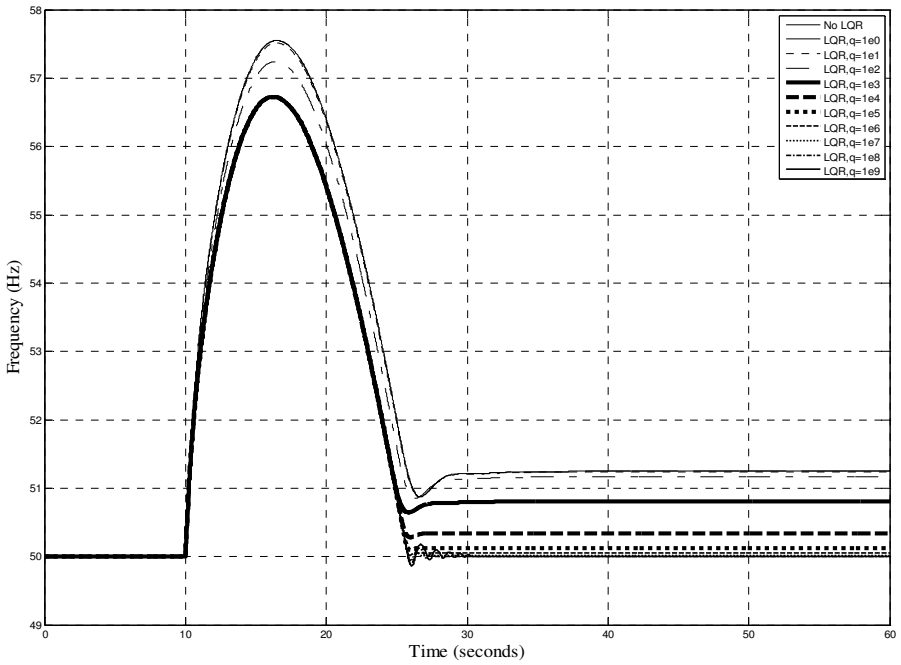

(c) Case Study 3

Figure 5.20 Frequency responses with LQR-based AGC and reference power set to the electric machine output power.

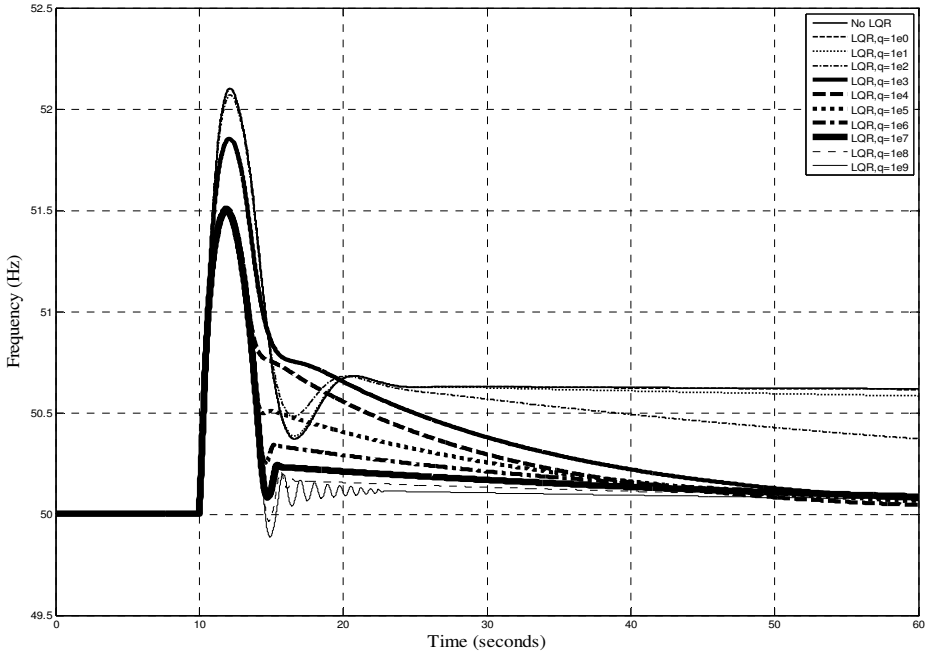

(a) Case Study 1.

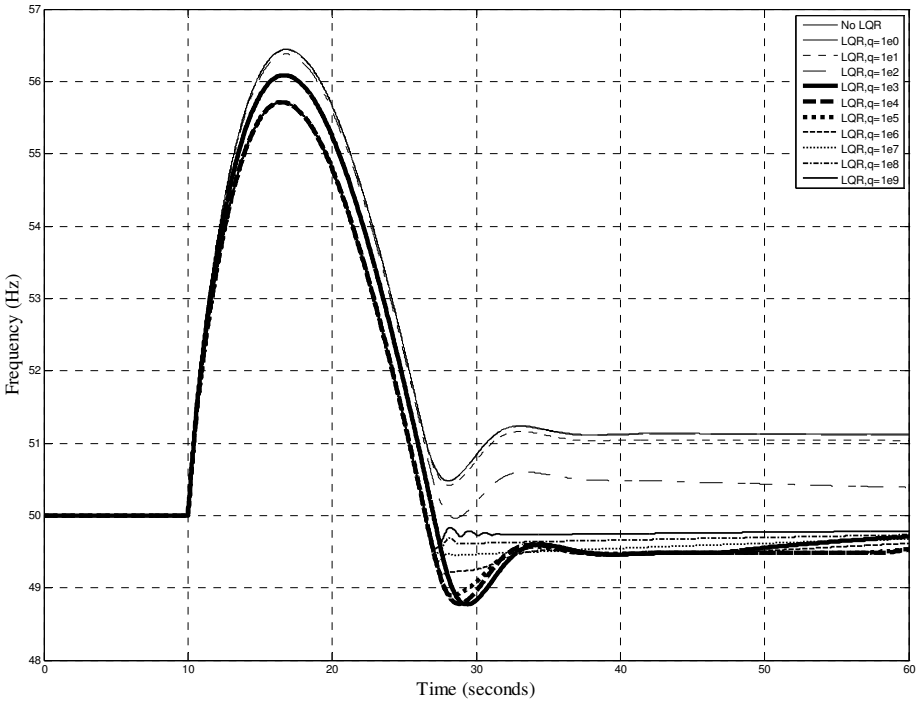

(b) Case Study 2

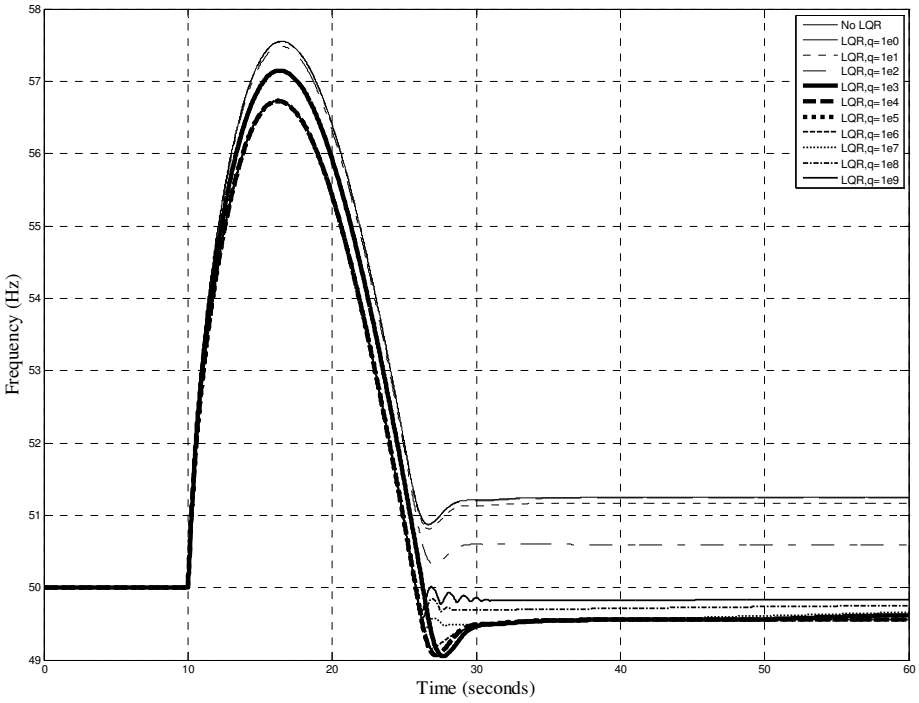

(c) Case Study 3

Figure 5.21 Frequency responses with LQR-based AGC and integral power reference estimator of Ki=1.

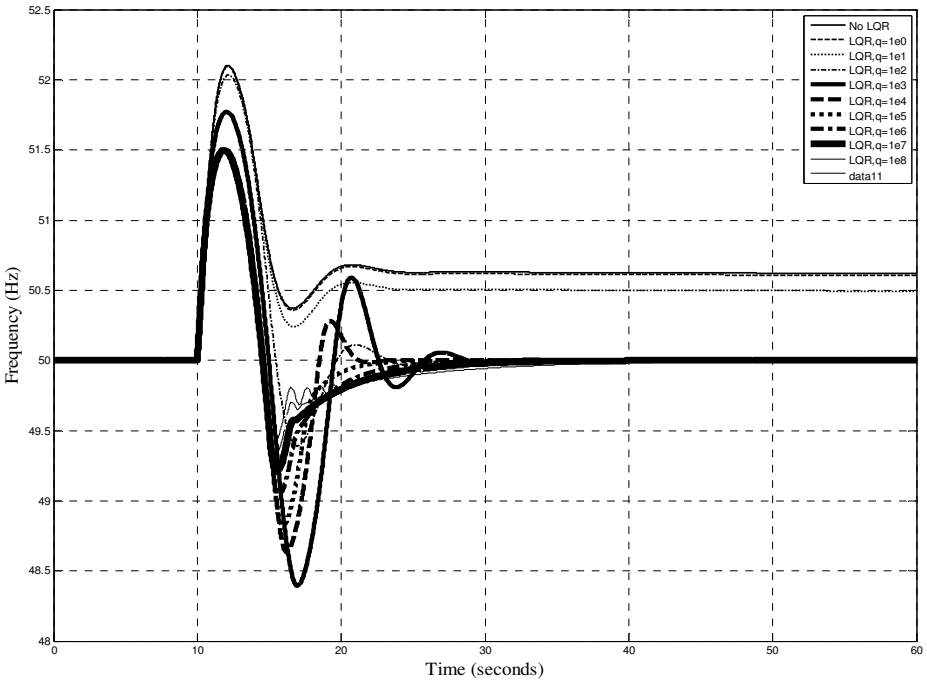

(a) Case Study 1.

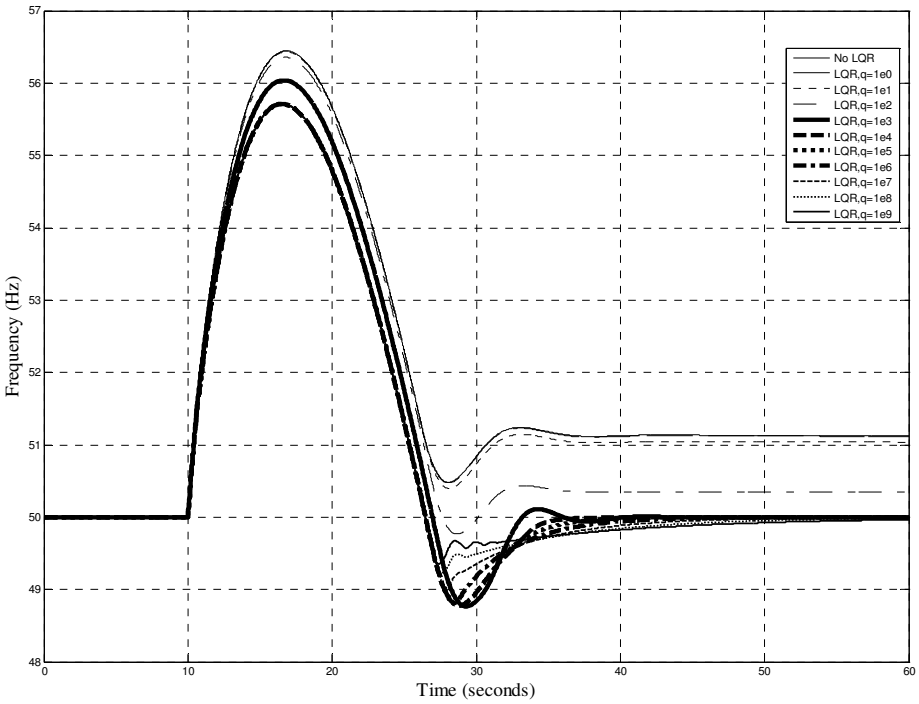

(b) Case Study 2

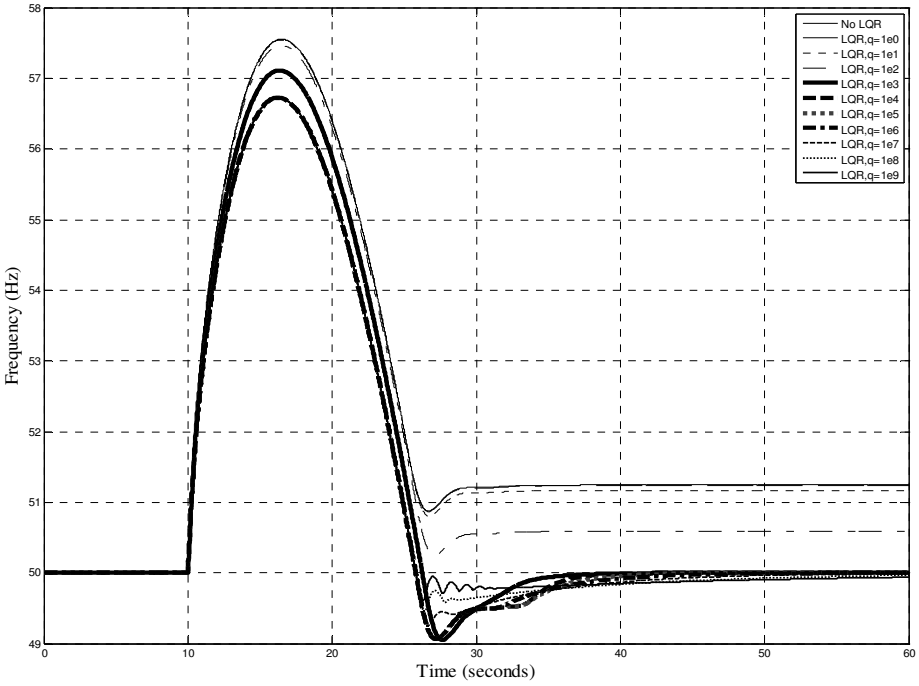

(c) Case Study 3.

Figure 5.22 Frequency responses with LQR-based AGC and integral power reference estimator of Ki=10.

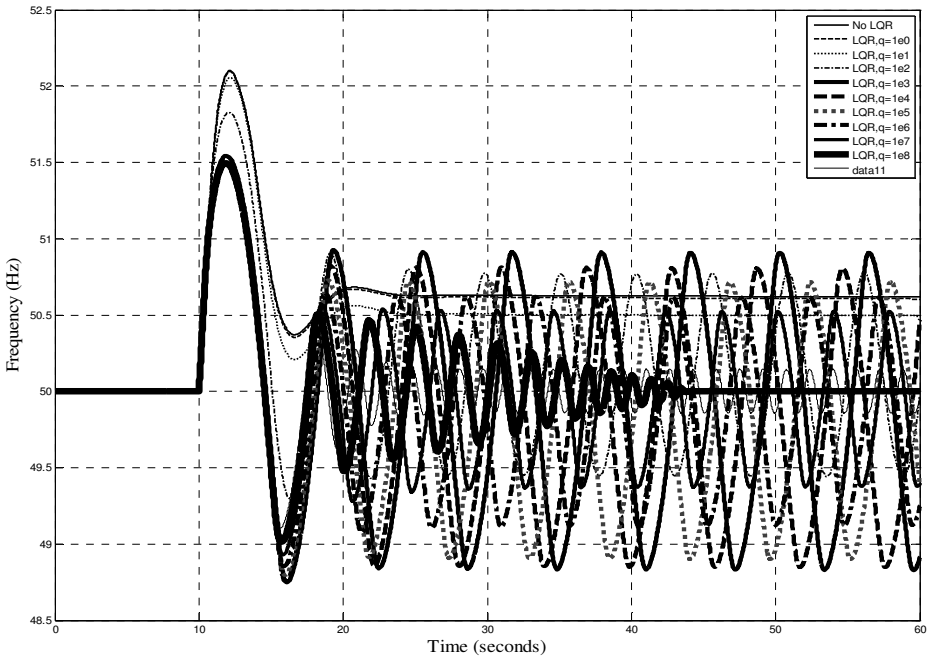

(a) Case Study 1.

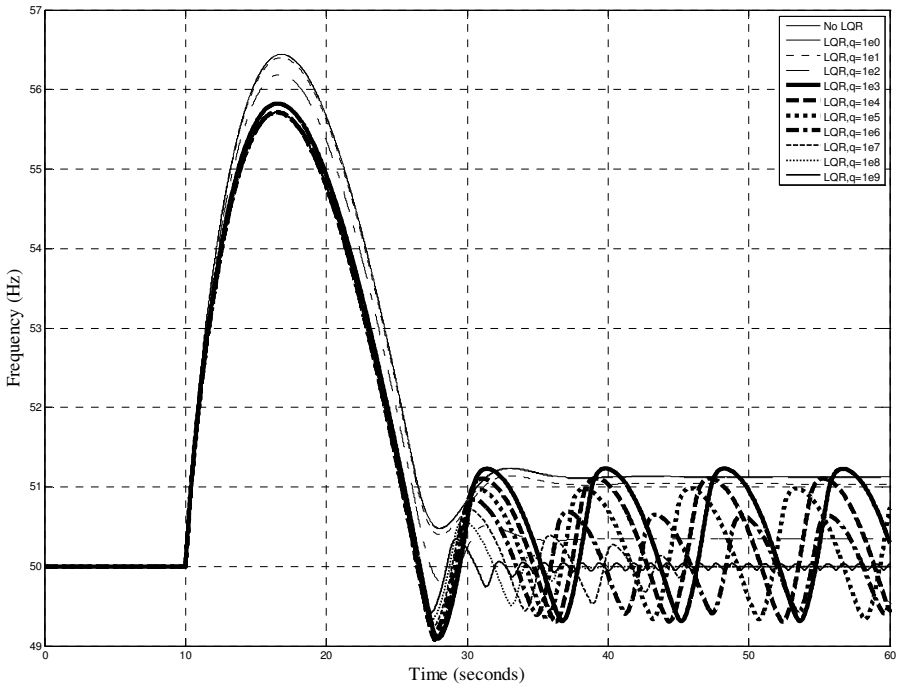

(b) Case Study 2.

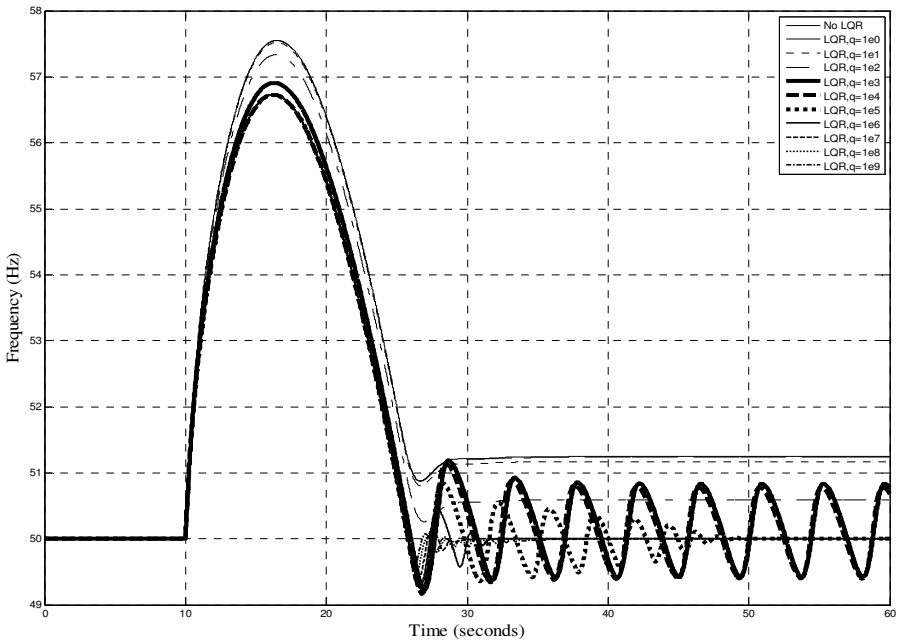

(c) Case Study 3.

Figure 5.23 Frequency responses with LQR-based AGC and integral power reference estimator of Ki=100.

5.4.4 Case Studies Time Domain Simulation

Some time responses are presented in this section. The disturbance simulated is the simultaneous opening of all ties connecting the case studies to the rest of the system. The frequency response of the separated case studies is examined with and without an LQR – based Island AGC at different governor rate limits.

Time simulation of the frequency response of Case Study 1 network upon disconnection from the rest of the UK grid is presented in this section. The interrupted power is 28% of the case study installed capacity. This value is chosen to match estimated power flows presented in the GB SYS for winter peak demand. Figure 5.24 shows the frequency response of Case Study 1 upon disconnection from the rest of the grid at different governor maximum rate limits where the following two cases are compared in each subplot: (a) Without AGC.(b) With LQR-based AGC.

Based on the results presented, the frequency first overshoot is not affected. However, the frequency response reaches the nominal steady state value of 50 Hz except for the case where the maximum governor rate limit is 0.1 p.u./sec rate , the response shows unstable oscillations.

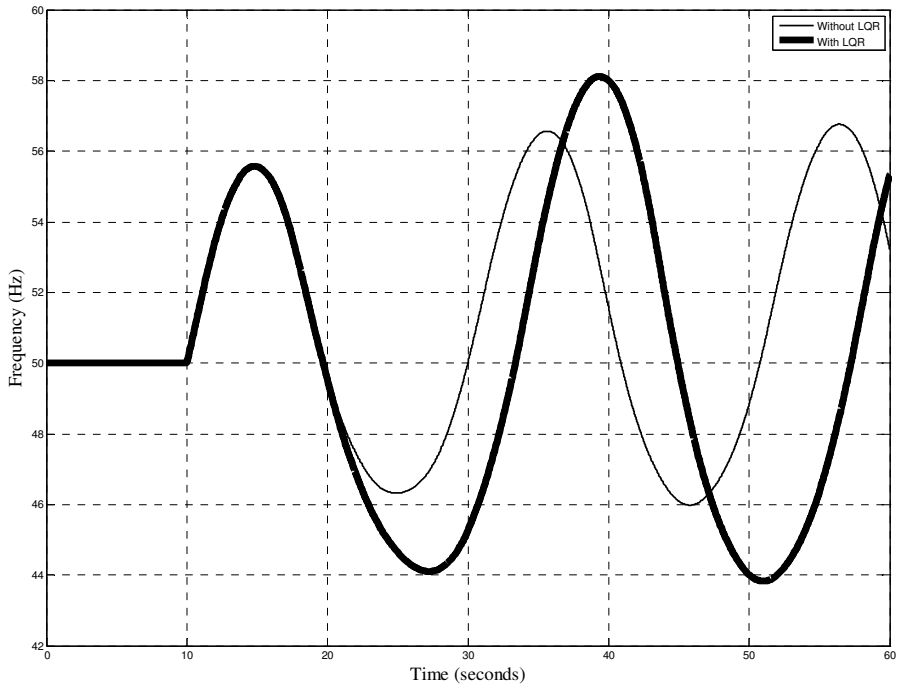

(a) Maximum governor rate limit= 0.1 p.u./sec.

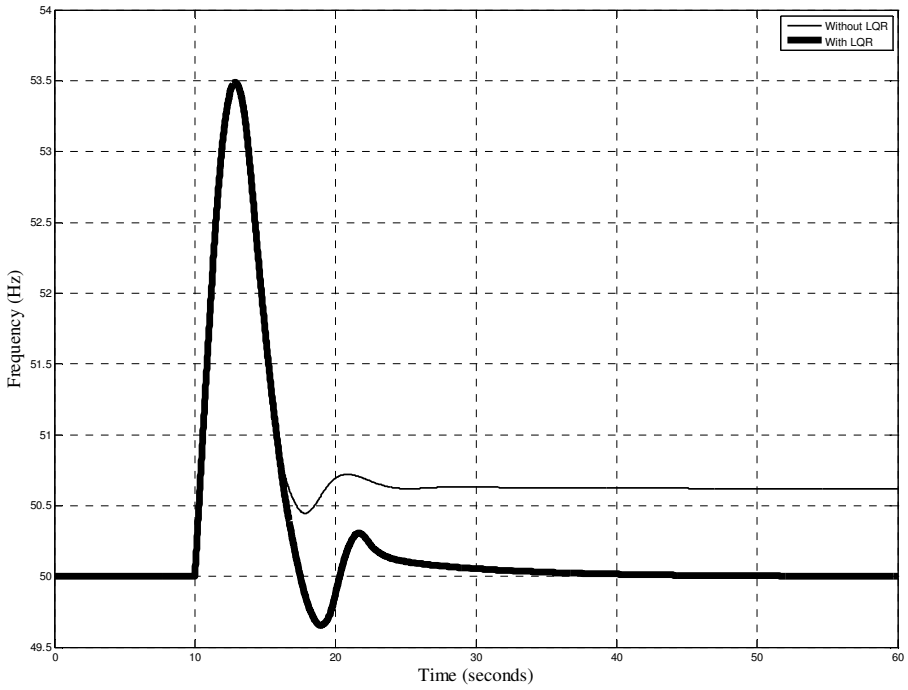

(b) Maximum governor rate limit= 0.2 p.u./sec.

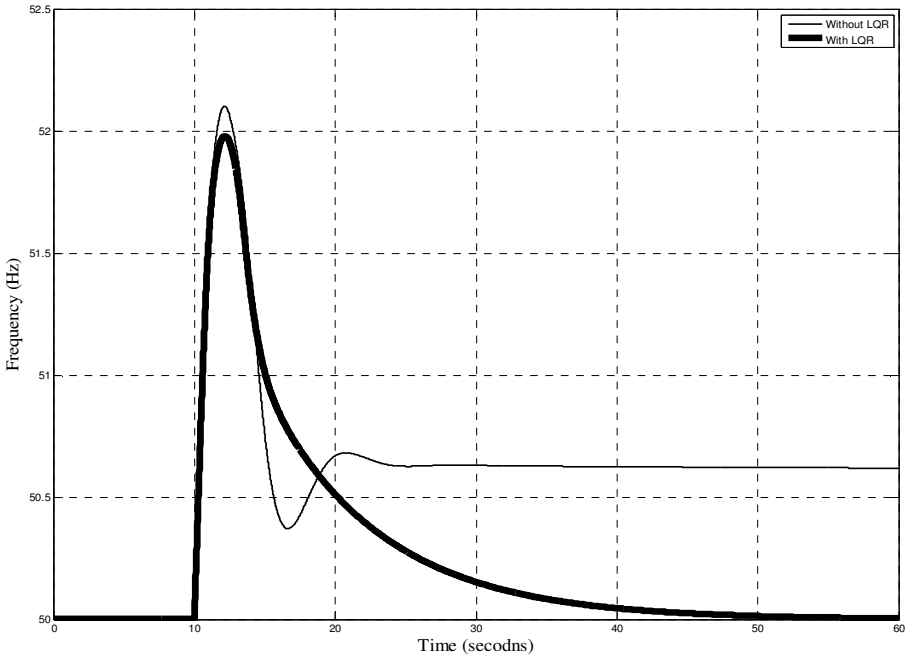

(c) Maximum governor rate limit= 0.9 p.u./sec.

Figure 5.24 Frequency response of Case Study 1 upon disconnection from the rest of the Grid.

5.4.4.1 Case Study 2

Time simulation of the frequency response of Case Study 2 network upon disconnection from the rest of the UK grid is presented in this section. The interrupted power is 38% of the case study installed capacity. This value is chosen to match estimated power flows presented in the GB SYS for winter peak demand. Figure 5.25 shows the frequency response of Case Study 2 upon disconnection from the rest of the grid at different governor maximum rate limits where the following four cases are compared in each subplot: (a) Without AGC.(b) With LQR-based AGC. Based on the results presented, the frequency first overshoot is not affected. However, the frequency response reaches the nominal steady state value of 50 Hz for all cases

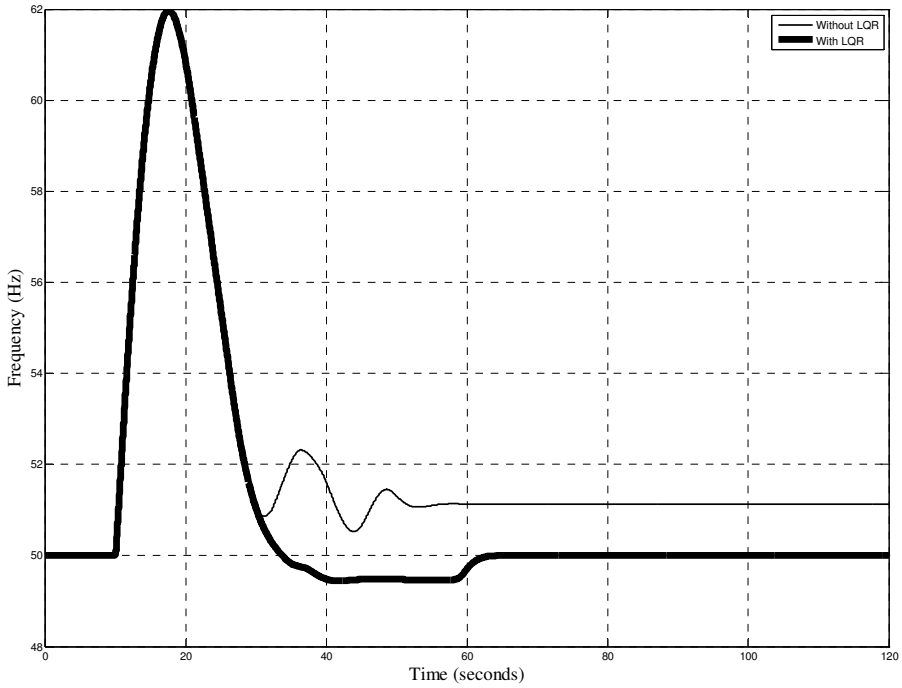

(a) Maximum governor rate limit= 0.1 p.u./sec.

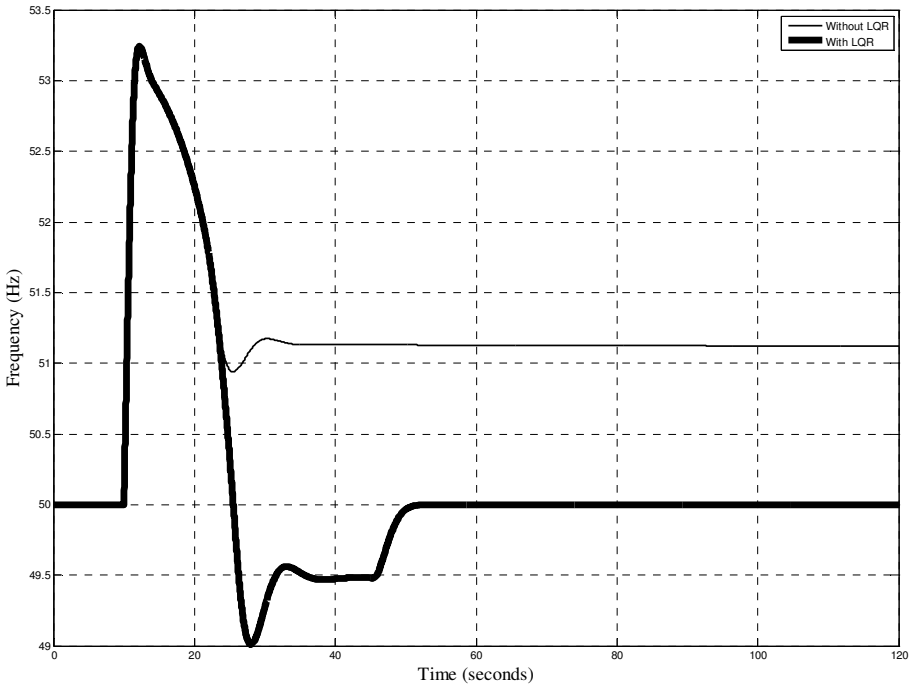

(b) Maximum governor rate limit= 0.9 p.u./sec.

Figure 5.25 Frequency response of Case Study 2 upon disconnection from the rest of the Grid.

5.4.4.2 Case Study 3

Time simulation of the frequency response of Case Study 3 network upon disconnection from the rest of the UK grid is presented in this section. The interrupted power is 62 % of the case study installed capacity. This value is chosen to match estimated power flows presented in the GB SYS for winter peak demand. Figure 5.26 shows the frequency response of Case Study 3 upon disconnection from the rest of the grid at different governor maximum rate limits where the following four cases are compared in each subplot: (a) Without AGC.(b) With LQR-based AGC. Based on the results presented, the frequency first overshoot is not affected. However, the frequency response reaches the nominal steady state value of 50 Hz for all cases equipped with the Island AGC.

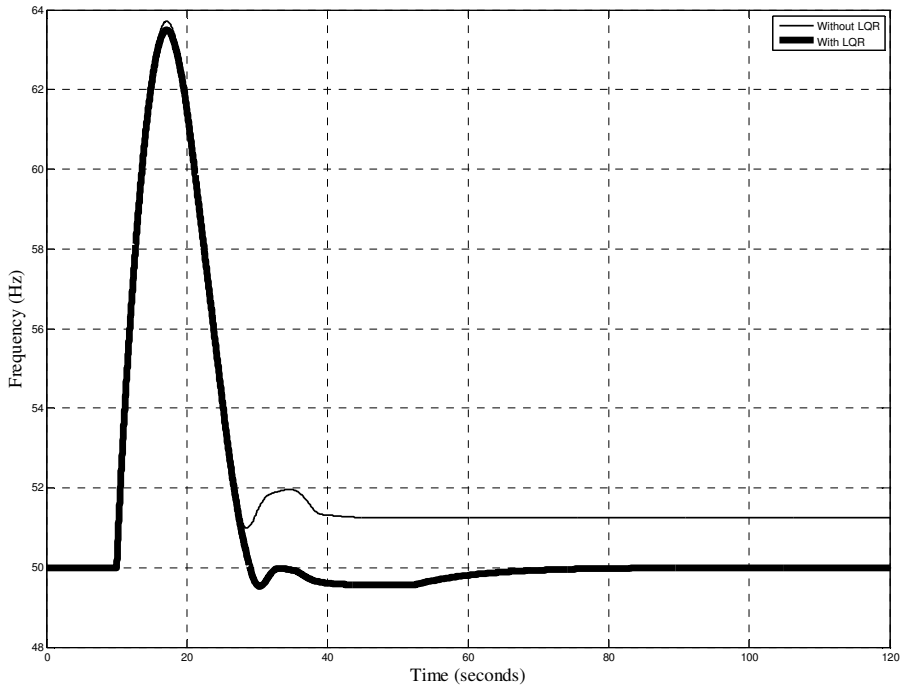

(a) Maximum governor rate limit= 0.1 p.u./sec.

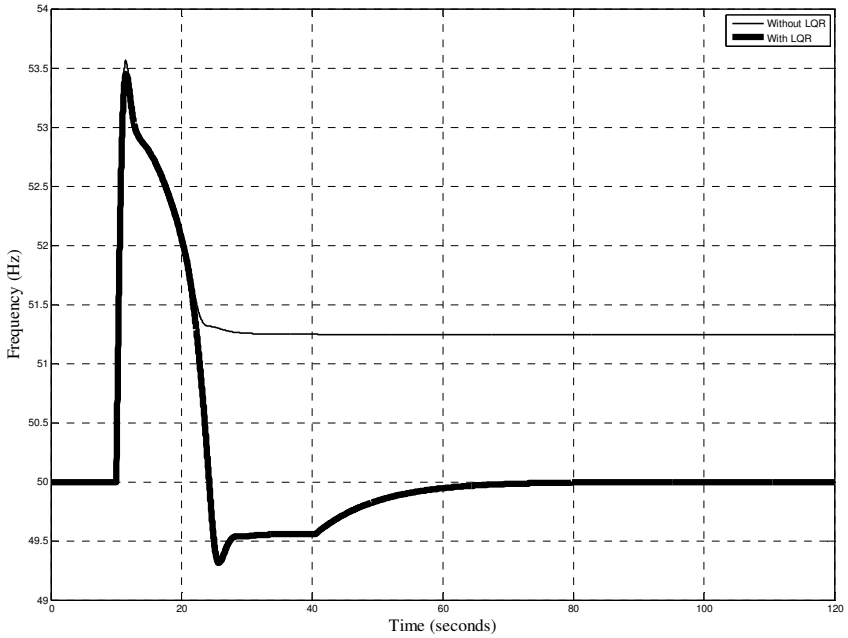

(b) Maximum governor rate limit= 0.9 p.u./sec.

Figure 5.26 Frequency response of Case Study 3 upon disconnection from the rest of the Grid.

5.5 Conclusions

The proposed Island AGCs assists in improving the frequency response. Two Island AGCs designs have been discussed in this chapter. The first design is the conventional design, an integral controller based design, while the second design is the LQR design methodology. The conventional design has proven to have a poor contribution in improving the frequency response of separated areas. It only eliminates the frequency steady state error and does not assist in damping the first frequency overshoot. This is because having an integral controller with high gain leads to an unstable frequency oscillatory response problem. Moreover, in some case studies where the units are equipped with very slow governors, an integral controller capable of restoring the system frequency stability might cease to exist.

On the other hand, the LQR-based Island AGC allows the ability of increasing the proportional speed gains to high values while stabilizing the system through feedback from the rest of the state variables. Hence, the first frequency overshoot is damped. This was observed while studying the linearized model. However, once the nonlinearities were modeled, the overspeed control damped the first overshoot more and over shadowed the damping effect of the proposed AGC. Moreover, as the LQR-based AGC is equipped with an integral controller that estimates the reference power value, the main contribution of this proposed AGC appears in its ability to eliminate the frequency steady state error rapidly for areas whose units have governors with slow response. Consequently, a better response than the integral controller based AGC is achieved. Not only that but the AGC controller has shown robustness, as one design is sufficient to operate stably over a different range of governor rate limits (0.1-0.9 p.u./sec).

The only drawback of this methodology is that its results in a full-state feedback controller, which makes some engineers believe that this controller would not be practical as all states are not always measurable. Based on this fact, the next chapter will discuss the possibility of gaining the advantages accompanying the proposed LQR and still overcome the difficulties accompanying the measuring of all states. This will be discussed through proposing local LQR-based controllers other than a Central LQR- based AGC.

CHAPTER 6

LOCAL OPTIMAL CONTROLLERS

6.1 Introduction

This chapter uses the optimal control, specifically the Linear Quadratic Regulator (LQR) methodology, to design a new local power plant controller capable of improving the frequency response of thermal power plants. Consequently, it assists in sustaining the operation of separated areas with excess generation. The designed controller uses the power plant mechanical power and speed as feedback signals.

This section provides an outline for this chapter. Section 6.2 introduces the idea of an existing mechanical hydraulic governing system equipped with an auxiliary governor. The disadvantages of the make discussed in Section 6.2, will be overcome by proposing an LQR–based auxiliary in Section 6.3. Section 6.4 presents the thesis case studies time domain simulation, comparing the frequency response of the case studies for the cases where the thermal units are equipped once with no auxiliary governor, once with a proportional auxiliary governor and finally with the proposed LQR-based auxiliary governor .This chapter is then summarized and concluded in Section 6.5.

6.2 Auxiliary Governor

Over speed controllers are local controllers that are used to ensure that the speed of the turbine does not exceed 120% of its rated speed upon disconnection from the grid. This control uses the intercept valves to enhance the transient performance of the unit speed. It has the effect of doubling the governor gain once the speed exceeds 104-105% of its rated speed.

Moreover, some research discussed the improvement of the overspeed controllers by installing auxiliary governors that operate in parallel with the original governor. Figure 6.1

shows the block diagram representation of a mechanical hydraulic speed governing system applicable to one make [24]. The model shown accounts for CV and IV controls and an auxiliary governor for limiting overspeed. Under-steady state conditions and during speed deviations, the IVs are kept fully open by the opening bias IVOB, only the CVs provide speed regulation. The auxiliary governor, when speed exceeds its setting V1 (ranging from 1% to 3over the rated speed), acts in parallel with the main governor so as to effectively increase the gain of the speed control loop by a factor of about 8. This causes the CVs as well as the IVs to close rapidly and thus limit overspeed [24, 51].

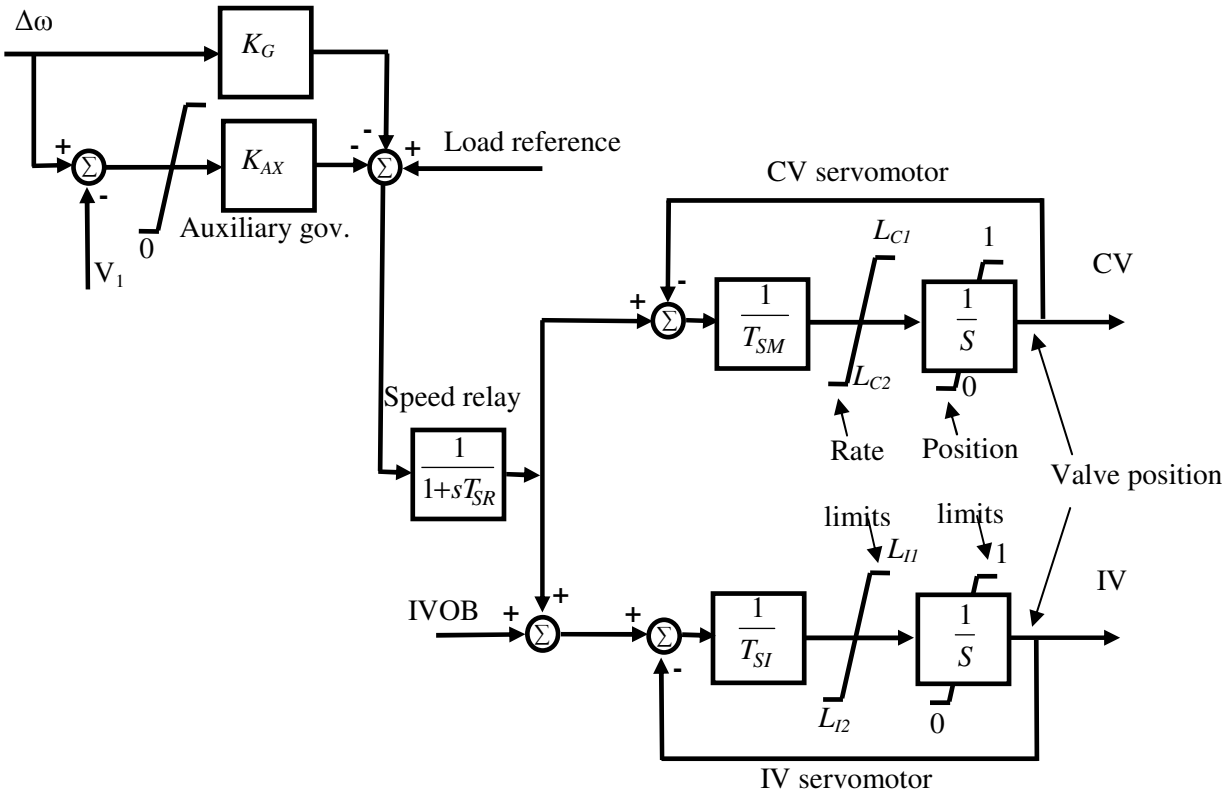

Figure 6.1 Governing system equipped with an auxiliary governor [24, 51].

However, studies [51] showed that if the setting V_1 is not chosen properly; auxiliary governors cause instability of the speed control during system-islanding conditions. The governing system will tend to oscillate. Consequently, all other units in the island will respond to oscillations of the units with auxiliary governors. The overall effect is to cause oscillations of all units. The resulting movements of steam valves continue until the hydraulic systems of the governors run out of oil and cause unit tripping and possibly a blackout of the island.

6.3 The Proposed LQR-Based Auxiliary Governor

This section designs an LQR-based auxiliary governor that operates in parallel with the original governing system once the system goes islanded and the area machines overspeed.

6.3.1 The Design Approach

Similarly as Chapter 5, the LQR problem discussed here is the special case, where the outputs instead of the states are weighted. However**,** the aforementioned controller design methodology is applied to each thermal power station at a time (i.e. designed controllers are local controllers). This study focuses on thermal power stations as most of the existing generation in the case studies discussed is fossil-fuelled or nuclear.

The control design process starts with identifying the state variables of each generating unit. For example, in the case of coal power units, the dynamics of the system can be well determined through the following states: P_{GV}, P_{HP}, P_{IP}, P_{LP} and ω. The next step is to obtain the linearized model representing the thermal system prime mover, see Figure 6.2. The overspeed control and the governor rate limiters are neglected for simplicity.

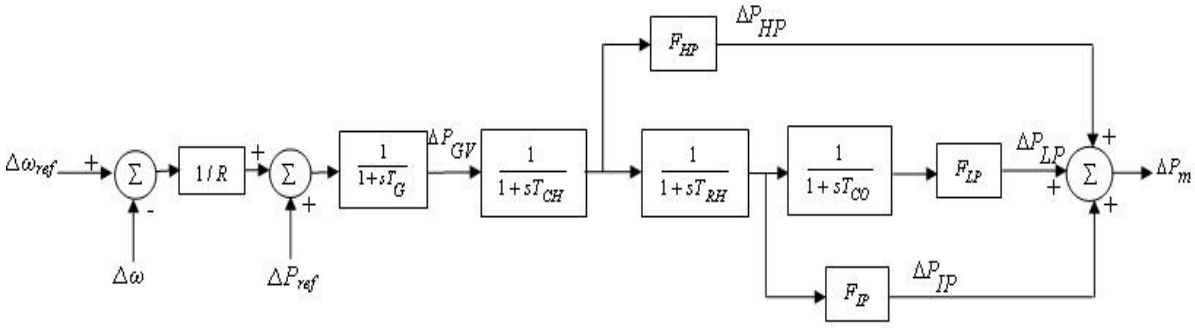

Figure 6.2 Linearized prime mover model for Coal plants.

The dynamic equations are then arranged in the state space format shown in 6.1.

$$\begin{bmatrix} \Delta\dot{P}_{GV} \\ \Delta\dot{P}_{HP} \\ \Delta\dot{P}_{IP} \\ \Delta\dot{P}_{LP} \\ \Delta\dot{\omega} \end{bmatrix} = \begin{bmatrix} -1/T_G & 0 & 0 & 0 & -1/RT_G \\ F_{HP}/T_{CH} & -1/T_{CH} & 0 & 0 & 0 \\ 0 & F_{IP}/F_{HP}T_{RH} & -1/T_{RH} & 0 & 0 \\ 0 & 0 & F_{LP}/F_{IP}T_{co} & -1/T_{co} & 0 \\ 0 & 1/M & 1/M & 1/M & 0 \end{bmatrix} \begin{bmatrix} \Delta P_{GV} \\ \Delta P_{HP} \\ \Delta P_{IP} \\ \Delta P_{LP} \\ \Delta\omega \end{bmatrix} + \begin{bmatrix} 1/T_G & 0 \\ 0 & 0 \\ 0 & 0 \\ 0 & 0 \\ 0 & -1/M \end{bmatrix} \begin{bmatrix} \Delta P_{ref} \\ \Delta P_L \end{bmatrix}$$

$$[\Delta\omega] = [0 \quad 0 \quad 0 \quad 0 \quad 1] \begin{bmatrix} \Delta P_{GV} \\ \Delta P_{HP} \\ \Delta P_{IP} \\ \Delta P_{LP} \\ \Delta\omega \end{bmatrix} \quad \ldots\ldots\ldots\ldots\ldots\ldots\ldots \quad (6.1)$$

As the main objective is to improve the frequency response of the power plants the system output is chosen to be only the machine speed ω. Hence, the objective function becomes

$$J = \frac{1}{2}\int_0^T q\Delta\omega^2 + r\Delta P_{ref}{}^2 dt \quad (6.2)$$

Where, P_{ref} represents the speed governor speed changer or load reference setting point.

Following the process of calculating the *A, B and C* system matrices, a very simple procedure was applied where the input weighting factor was set to 1 while the speed weighing is increased till stability is lost. Actually, increasing the speed weighting leads to higher gains and hence, resulting in a much damped system. However, the system might lose stability if such gains reach very high values. It is worth mentioning that the design stops at a weighting of 1e8 as a weighting of 1e9, would start to cause stability problems. The controller construction is shown in Figure 6.3 where the control signal takes the form $u_{\text{control}} = K_1 \Delta P_{GV} + K_2 \Delta P_{HP} + K_3 \Delta P_{IP} + K_4 \Delta P_{LP} + K_5 \Delta \omega$

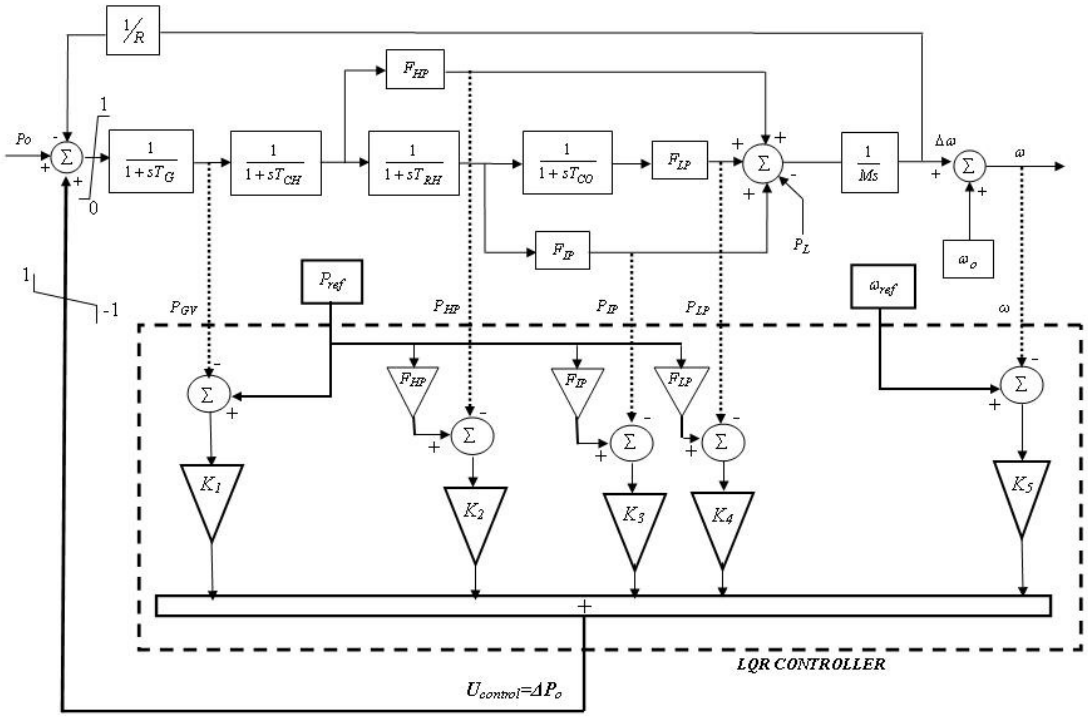

Figure 6.3 The Proposed Controller.

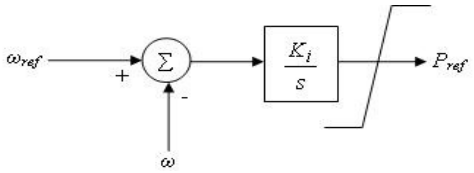

Figure 6.4 Integral Controller to estimate the required reference power value to be used in the LQR

Moreover, it is clear from Figure 6.3 that the designed LQR needs two reference values, one for speed and the other for power. The speed reference value is set to 1 p.u. However, the power reference value can be set to the initial operating power or the electrical output power or it may even be estimated through a speed integral control as shown in Figure 6.4. The choice of the power reference value is also investigated in this study.

The procedure followed for designing the controller for the coal power plant is repeated for the nuclear power plants. The only difference is that the LQR control signal does not contain a ΔP_{IP} component. Finally, the designed controllers are applied to each thermal power station and the separation of the Scottish grid is simulated.

6.3.2 Linear System Results

The frequency (scaled speed) time response of the coal machine to a loss of load of about 28%, 38% and 62% of the generator capacity is simulated. These load loss values correspond to the transmitted power loss experienced by Case Study 1, 2 and 3 respectively. The LQR controller is to be applied once the speed exceeds 1% of the nominal rating after the load disturbance has taken place. Figure 6.5 and Figure 6.6 show the frequency response at different speed weightings for a controller whose reference power is set to the initial power and electrical output power, respectively. Moreover, Figure 6.7, Figure 6.8, and Figure 6.9 present the frequency response at different speed weightings for a controller whose power reference is estimated through an integral speed controller with an integral gain equal to 1, 10 and 100, respectively. Moreover, Figure 6.10 shows the frequency response of the machine if the power feedbacks are disconnected

Based on the results presented, it can be seen that increasing the weighting of the speed during the LQR design would result in high gains and hence improved transient response. The more the speed weight is increased the more the steady- state error is minimized.

An LQR whose power reference value is set to the pre load loss value would damp the first speed overshoot but would not eliminate the steady state error (Figure 6.5). On the other hand, if the new load value or the electrical machine power output is used to set the power reference of the LQR, the frequency first overshoot would be damped but the steady state error will be eliminated only if very high gain values are used (Figure 6.6).

Another proposed method is to estimate the power reference of the LQR through an integral controller whose input signal is the speed deviation. Caution must be observed in choosing the integral gain as low integral gains would result in a slow response (Figure 6.7). Moreover, very high integral gains would lead to instability (Figure 6.9). Choosing a moderate integral gain and using high proportional gains for the LQR would lead damp the first speed overshoot and eliminate the steady state error rapidly (Figure 6.8). Although this seems the best performance, caution must be considered as the frequency undershoots before reaching the nominal value and might provoke the under frequency load disconnection system if frequency drops below 48.5-49 Hz.

Furthermore, it is worth knowing that the LQR proposes very high speed gains to improve the transient frequency response and uses other feedback signals from the rest of the states (i.e. power measurements) to stabilize the system. So the disconnection of any of the power feedback signals would lead to system instability (Figure 6.10). Hence, it is more suitable to

use the proposed controller in emergency conditions. Moreover, protection must be provided to disconnect the proposed controller if any of the feedback signals is lost.

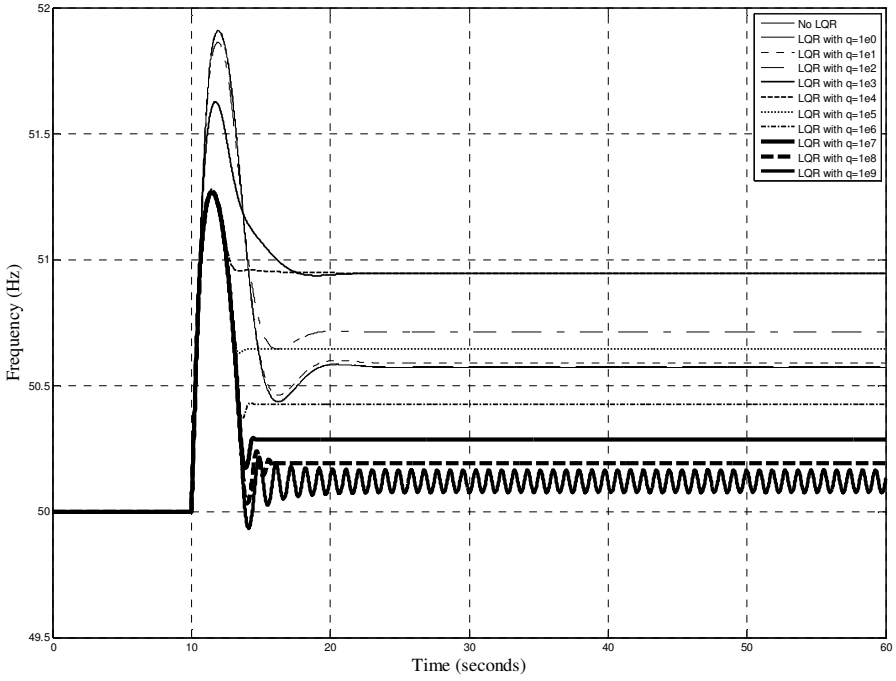

(a) Interrupted Power =0.28 p.u.

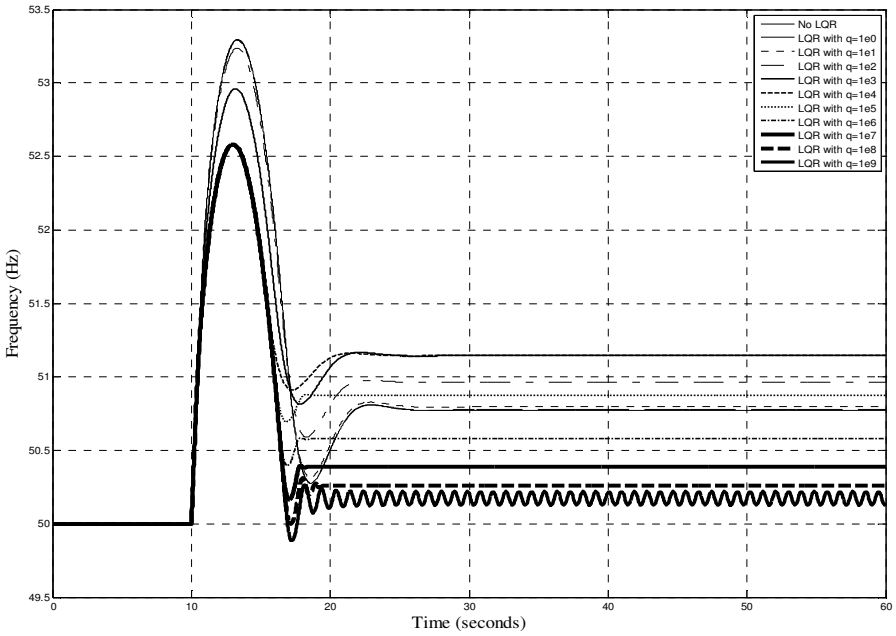

(b) Interrupted Power =0.38 p.u.

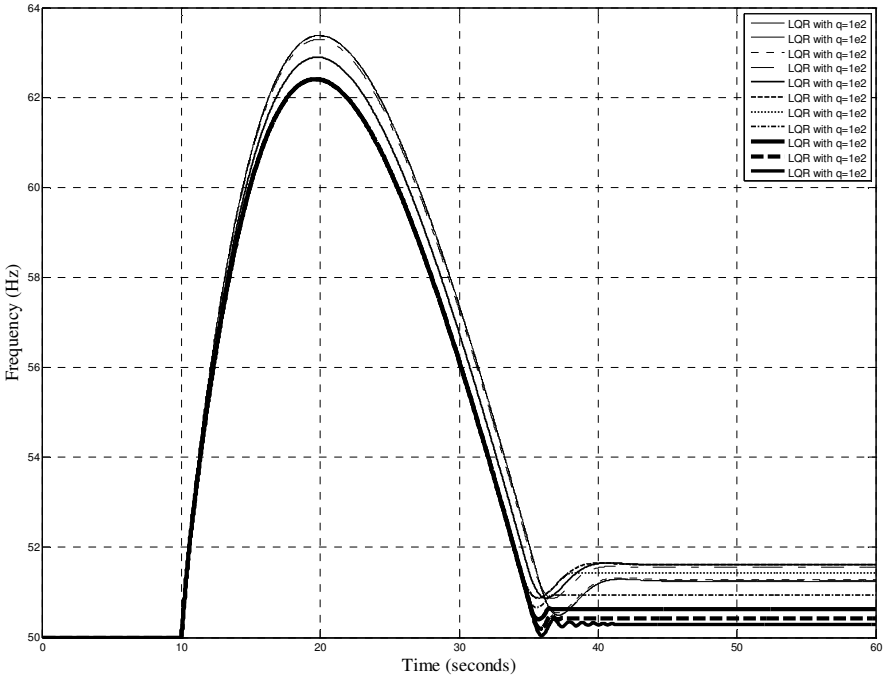

(c)Interrupted Power =0.62 p.u.

Figure 6.5 Thermal plant frequency response upon load loss with LQR and reference power set to the initial loading value

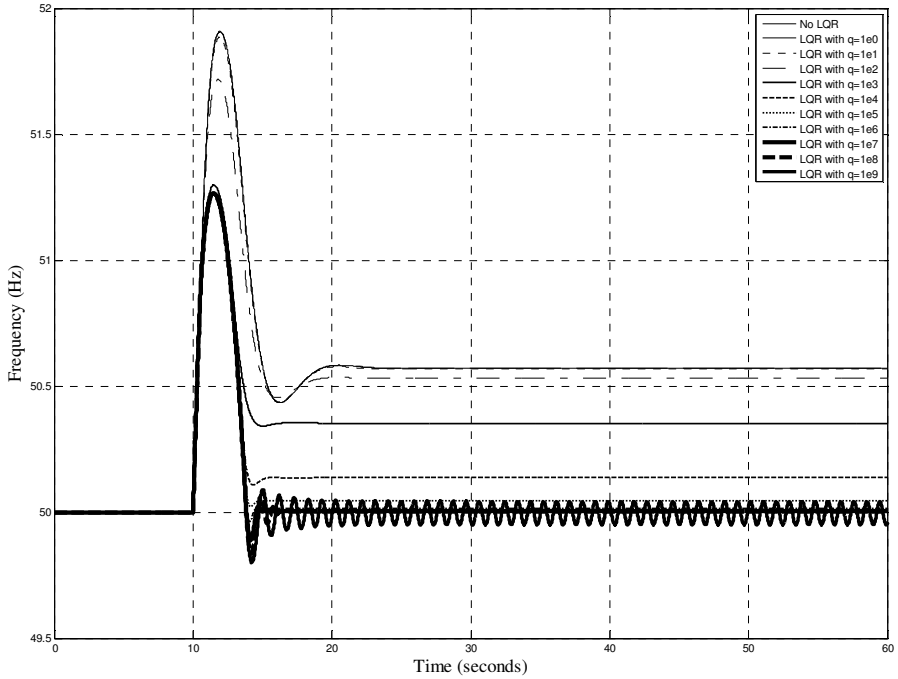

(a) Interrupted Power =0.28 p.u.

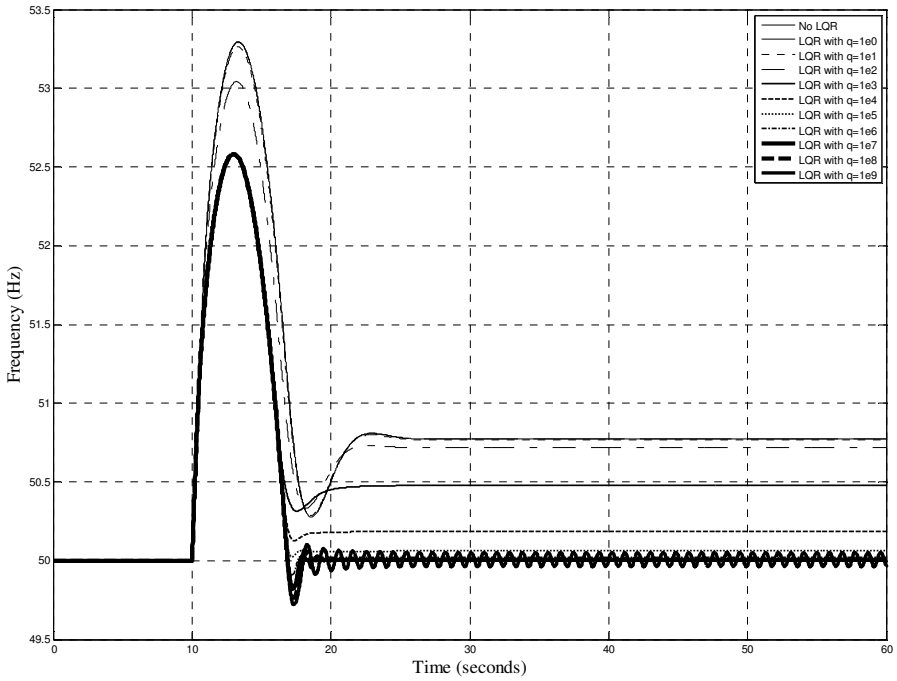

(b) Interrupted Power =0.38 p.u.

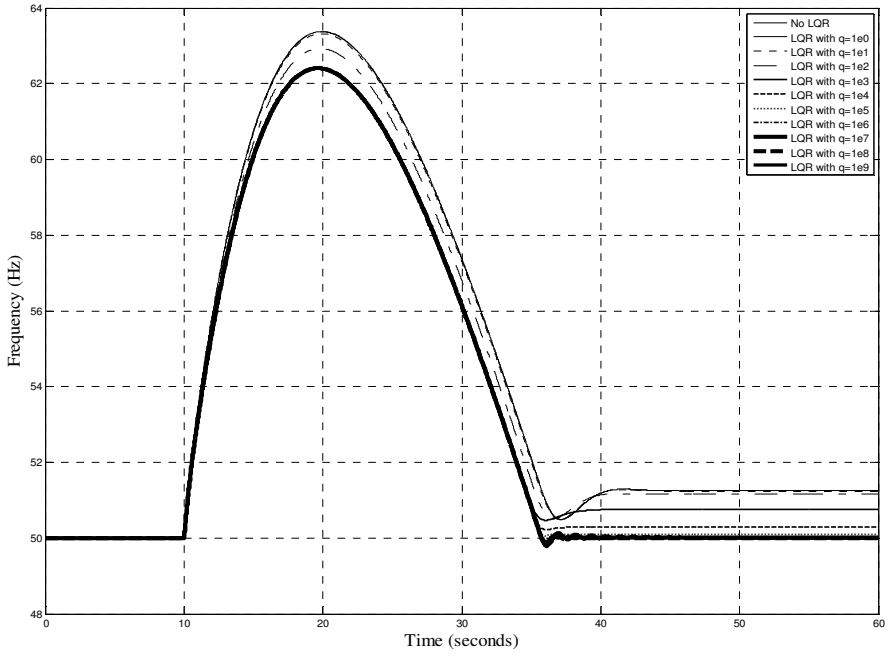

(c) Interrupted Power =0.62 p.u.

Figure 6.6 Thermal plant frequency response upon load loss with LQR and reference power set to the electric machine output power.

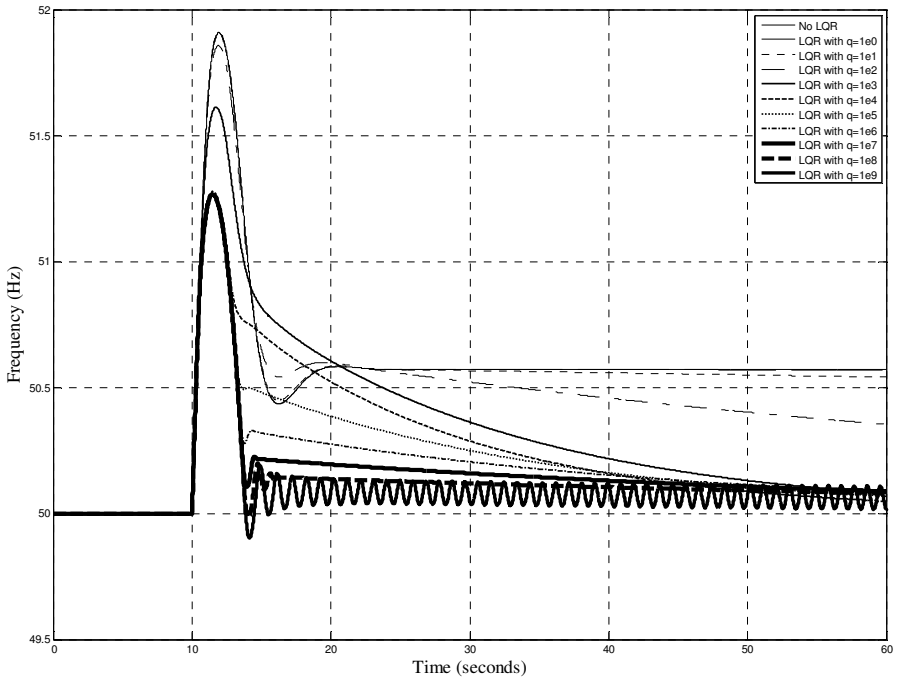

(a) Interrupted Power =0.28 p.u.

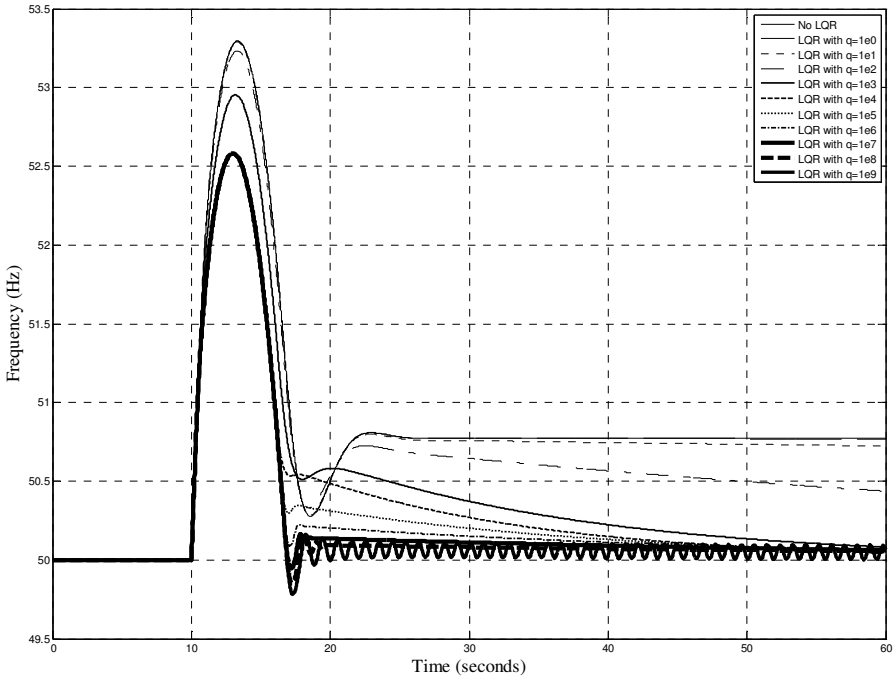

(b) Interrupted Power =0.38 p.u.

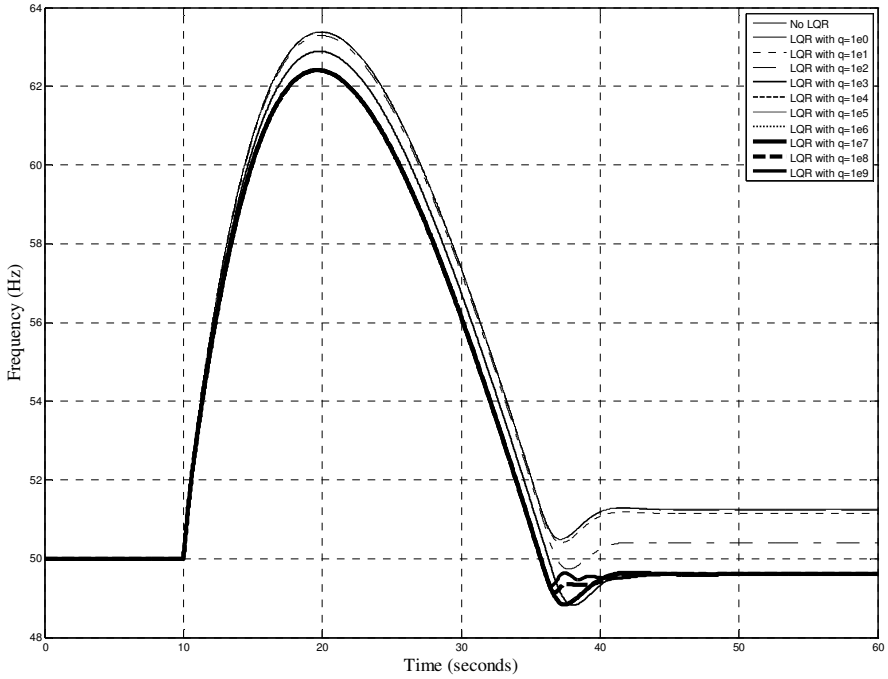

(c) Interrupted Power =0.62 p.u.

Figure 6.7 Thermal plant frequency response upon load loss with LQR and integral control Ki=1.

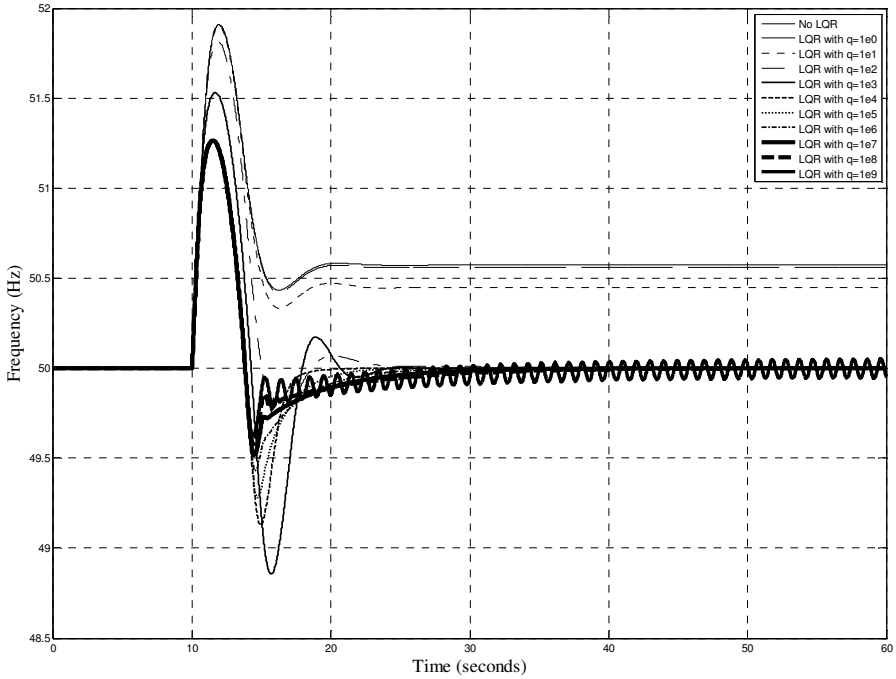

(a) Interrupted Power =0.28 p.u.

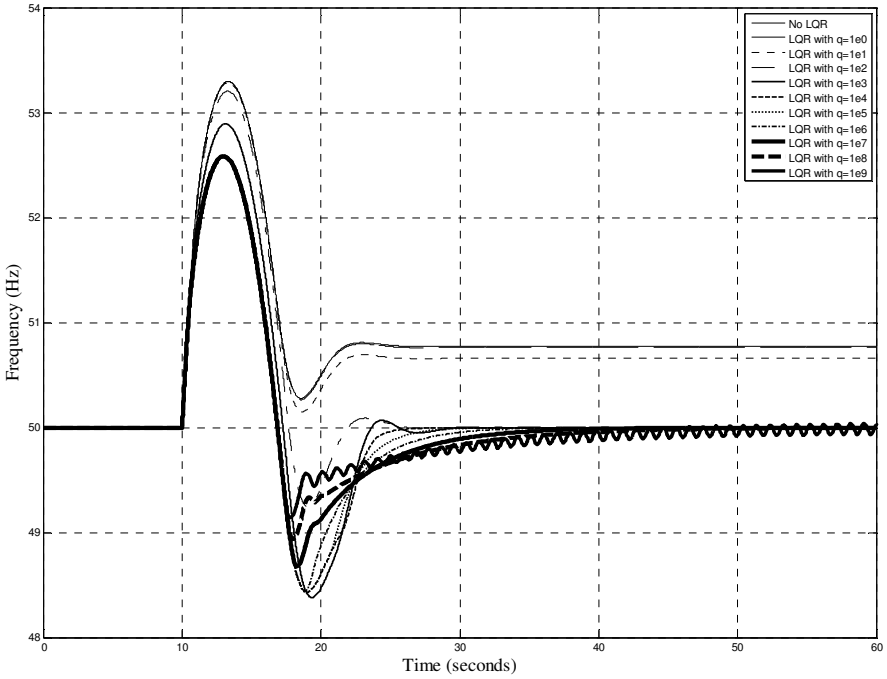

(b) Interrupted Power =0.38 p.u.

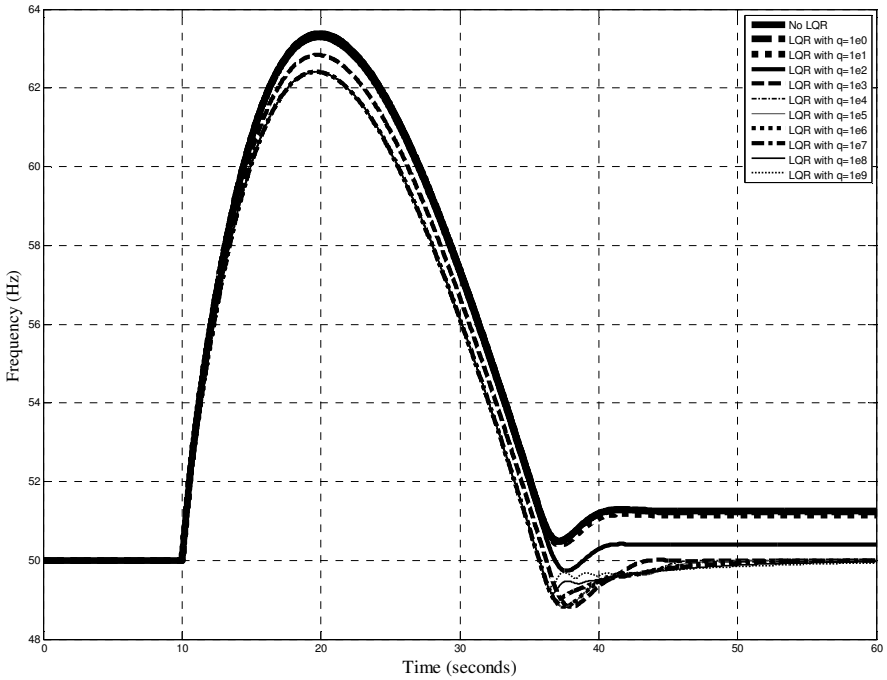

(c) Interrupted Power =0.62 p.u.

Figure 6.8 Thermal plant frequency response upon load loss with LQR and integral control Ki=10.

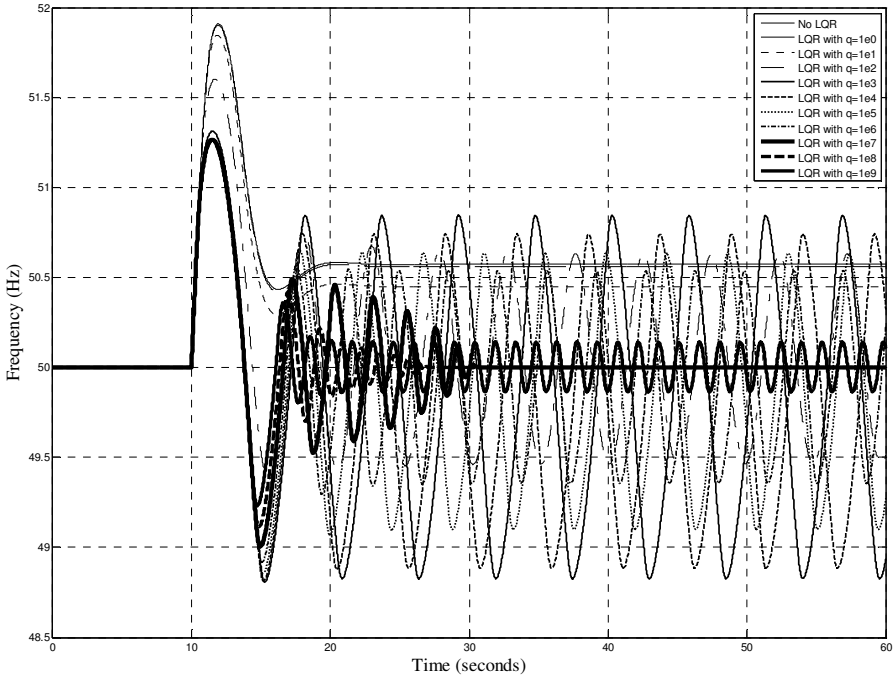

(a) Interrupted Power =0.28 p.u.

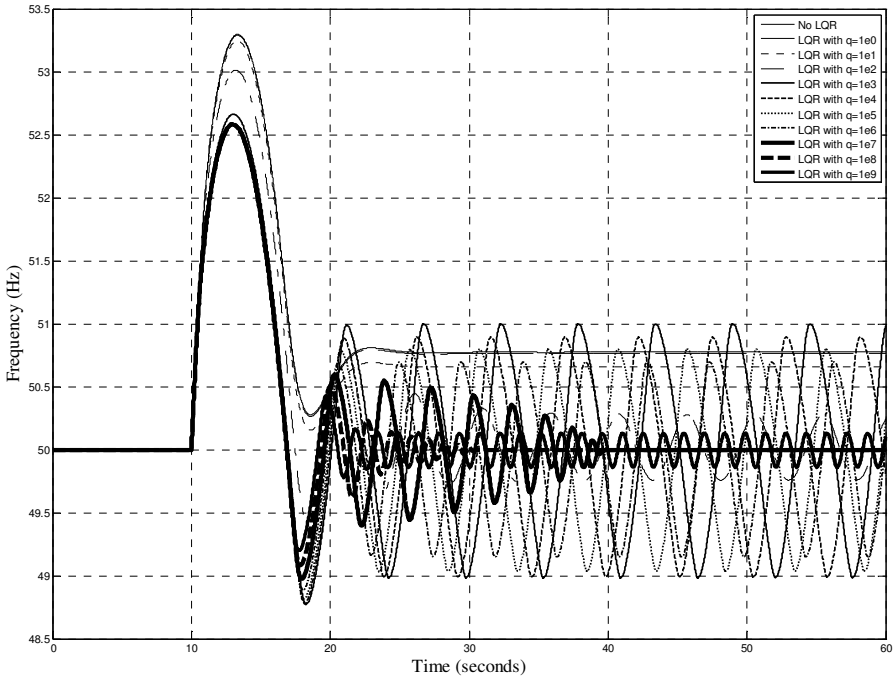

(b) Interrupted Power =0.38 p.u.

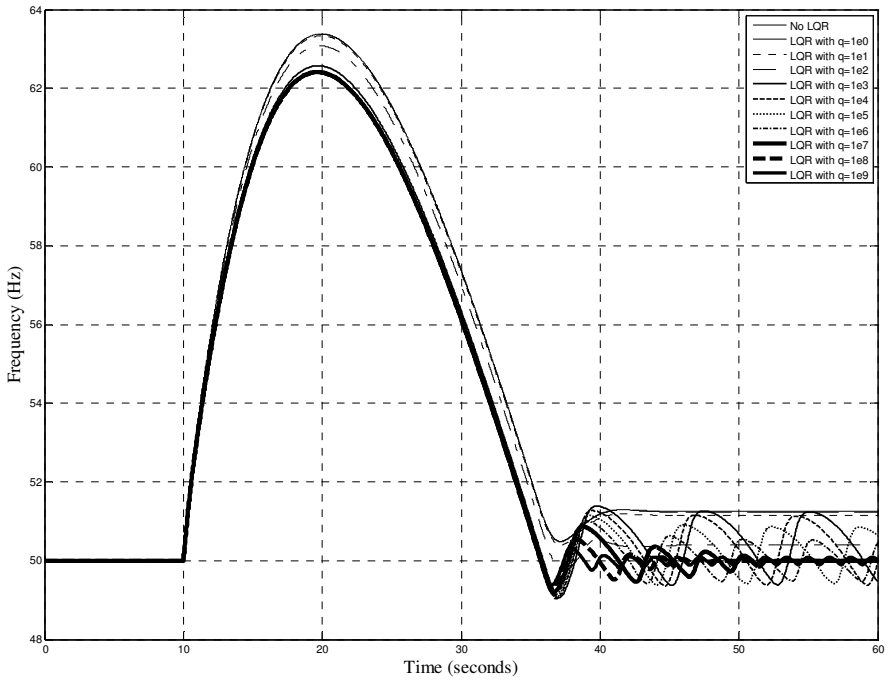

(c) Interrupted Power =0.62 p.u.

Figure 6.9 Thermal plant frequency response upon load loss with LQR and integral control Ki=100.

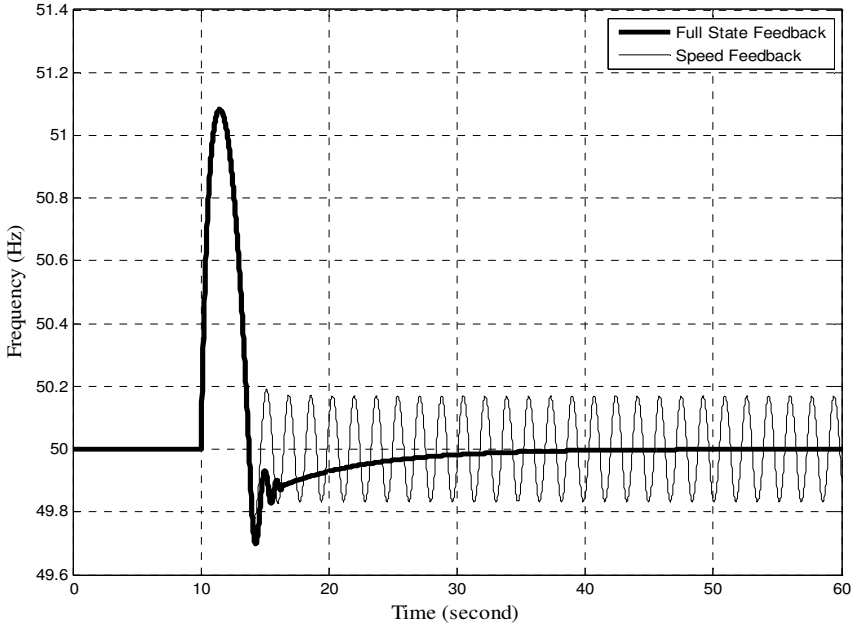

Figure 6.10 Thermal plant frequency response upon load loss with a full state feedback LQR and with only speed feedback.

6.4 Case Studies Time Domain Simulations

Some time responses are presented in this section. The disturbance simulated is the simultaneous opening of all ties connecting the case studies to the rest of the system, the result being an island with generation nearly twice the load. The frequency response of the separated case studies is examined with different auxiliary governor designs and at different governor rate limits.

6.4.1 Case Study 1

Time simulation of the frequency response of Case Study 1 network upon disconnection from the rest of the UK grid is presented in this section. The interrupted power is 28% of the case study installed capacity. This value is chosen to match estimated power flows presented in the GB SYS for winter peak demand. Figure 6.11 shows the frequency response of Case Study 1 upon disconnection from the rest of the grid at different governor maximum rate limits where the following four cases are compared in each subplot:

(a) Thermal units with no auxiliary governor.

(b) Thermal units with proportional auxiliary governors operating at 50.5 Hz.

(c) Thermal units with proportional auxiliary governors operating at 51 Hz.

(d) Thermal units with equipped with the proposed LQR-based auxiliary governor.

Based on the results presented, the frequency first overshoot exceeds 52 Hz, unless the proposed auxiliary governor is adjusted to operate at 50.5 Hz and the governor maximum rate limit exceeds 0.3 p.u./sec. Moreover, the frequency response reaches the nominal steady state value of 50 Hz except for the case where the maximum governor rate limit is 0.1 p.u./sec rate, the response shows unstable oscillations. Furthermore, it can be seen clearly that oscillatory problem that accompanies the use of proportional auxiliary governors is eliminated without compromising the reduction of the first frequency overshoot.

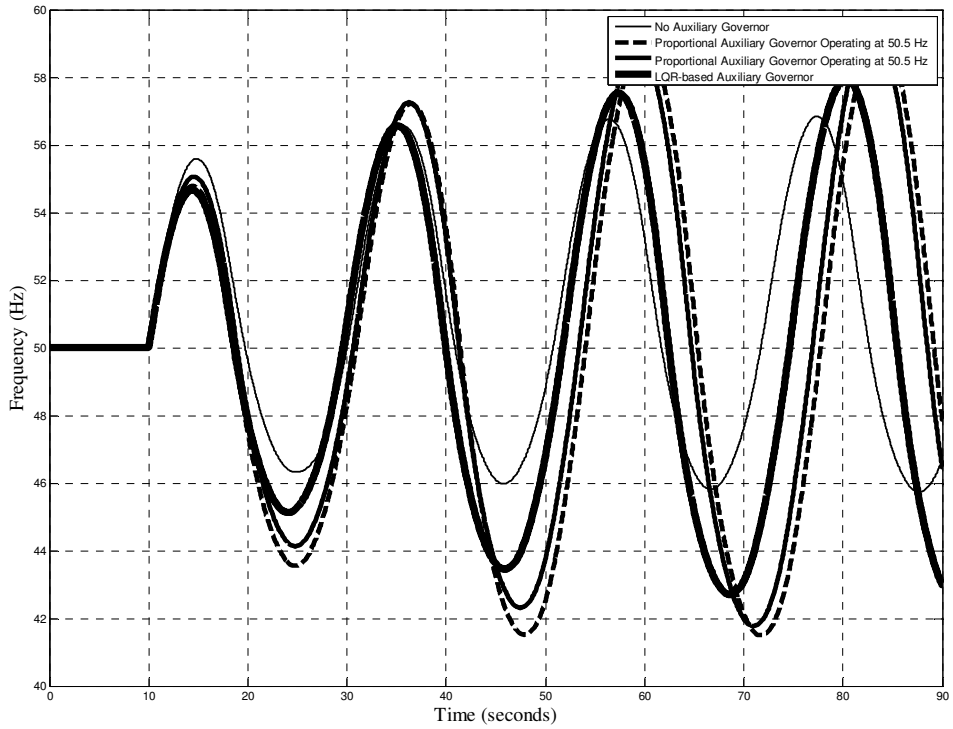

(a) Maximum governor rate limit= 0.1 p.u./sec.

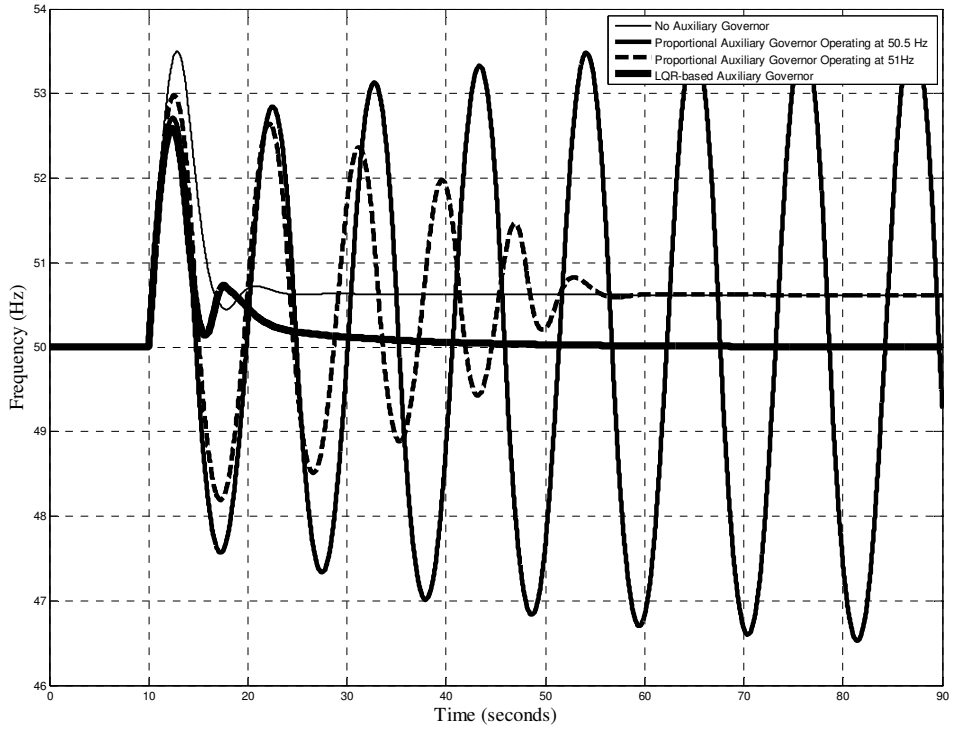

(b) Maximum governor rate limit= 0.2 p.u./sec.

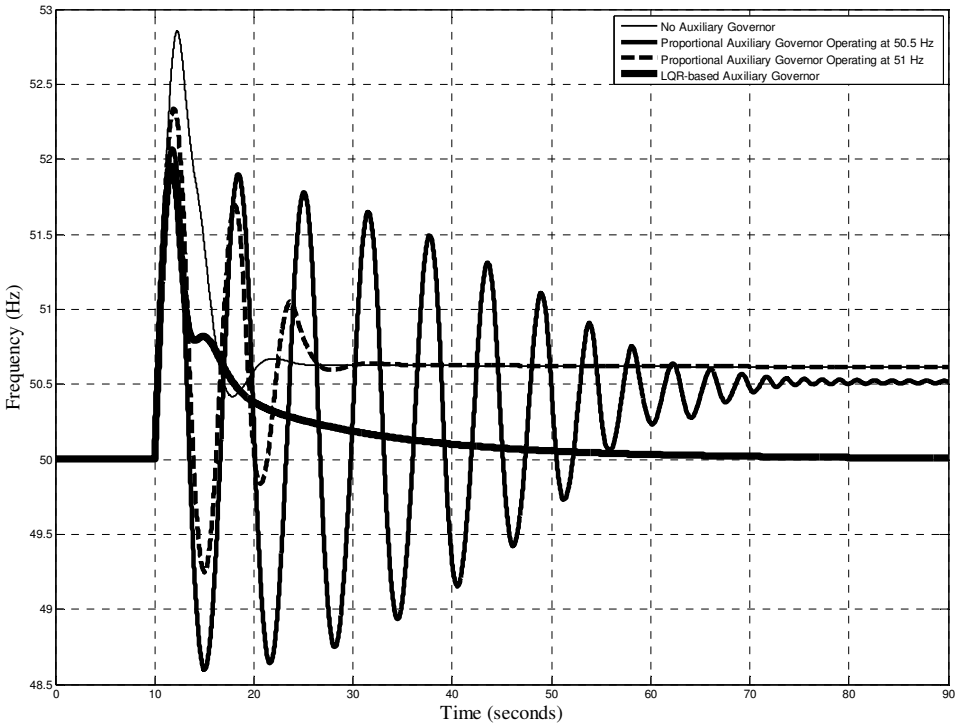

(c) Maximum governor rate limit= 0.3 p.u./sec.

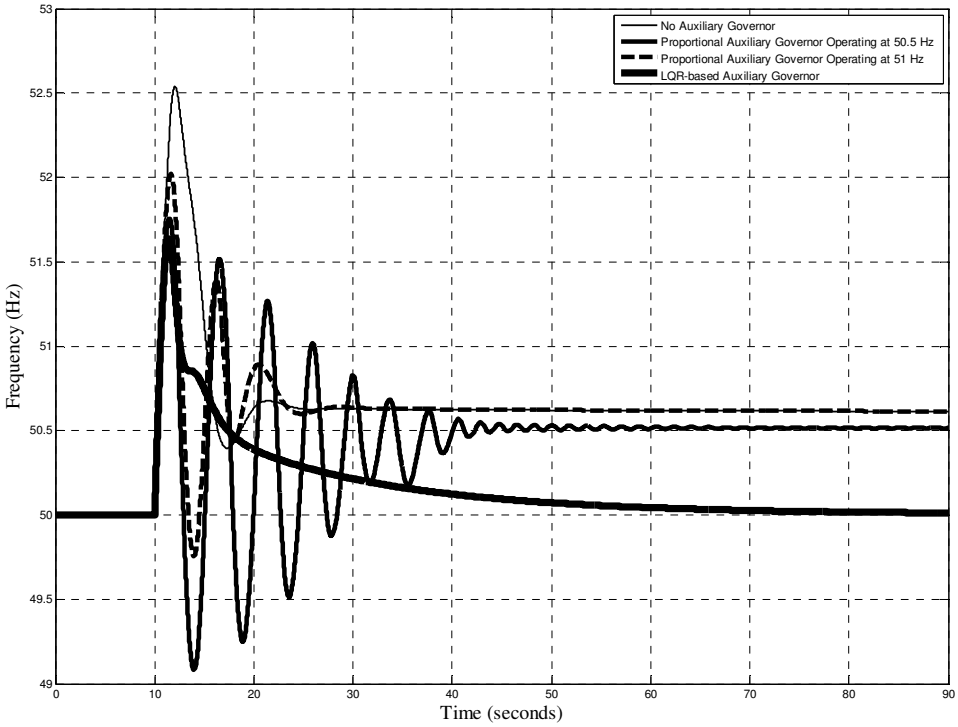

(d) Maximum governor rate limit= 0.4 p.u./sec.

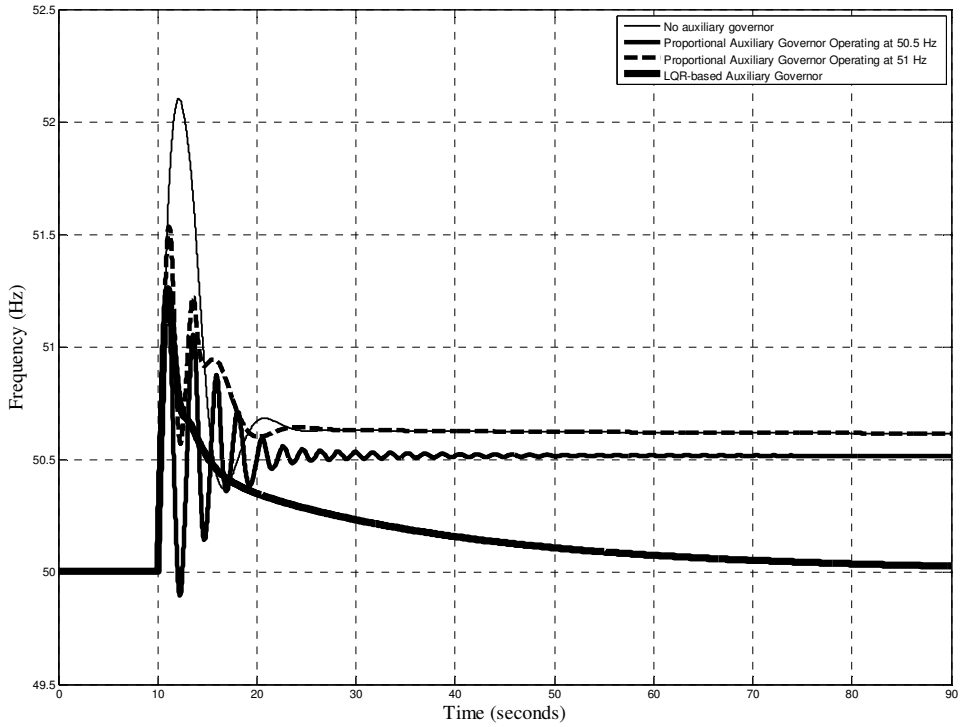

(e) Maximum governor rate limit= 0.9 p.u./sec.

Figure 6.11 Frequency response of Case Study 1 upon disconnection from the rest of the Grid.

6.4.2 Case Study 2

Time simulation of the frequency response of Case Study 2 network upon disconnection from the rest of the UK grid is presented in this section. The interrupted power is 38% of the case study installed capacity. This value is chosen to match estimated power flows presented in the GB SYS for winter peak demand. Figure 6.12 shows the frequency response of Case Study 2 upon disconnection from the rest of the grid at different governor maximum rate limits where the following four cases are compared in each subplot:

(a) Thermal units with no auxiliary governor.

(b) Thermal units with proportional auxiliary governors operating at 50.5 Hz.

(c) Thermal units with proportional auxiliary governors operating at 51.5 Hz.

(d) Thermal units with the proposed LQR-based auxiliary governor.

Based on the results presented, the frequency first overshoot exceeds 52 Hz unless the proposed auxiliary controllers are adjusted to operate at 50.5 Hz and the governor maximum

rate limit exceeds 0.8 p.u./sec. Moreover, the frequency response shows a stable response and reaches the nominal steady state value of 50 Hz in all cases. Finally, it can be seen clearly that the problem of frequency oscillations that accompanies the use of proportional auxiliary governors is solved without compromising the reduction of the first frequency overshoot.

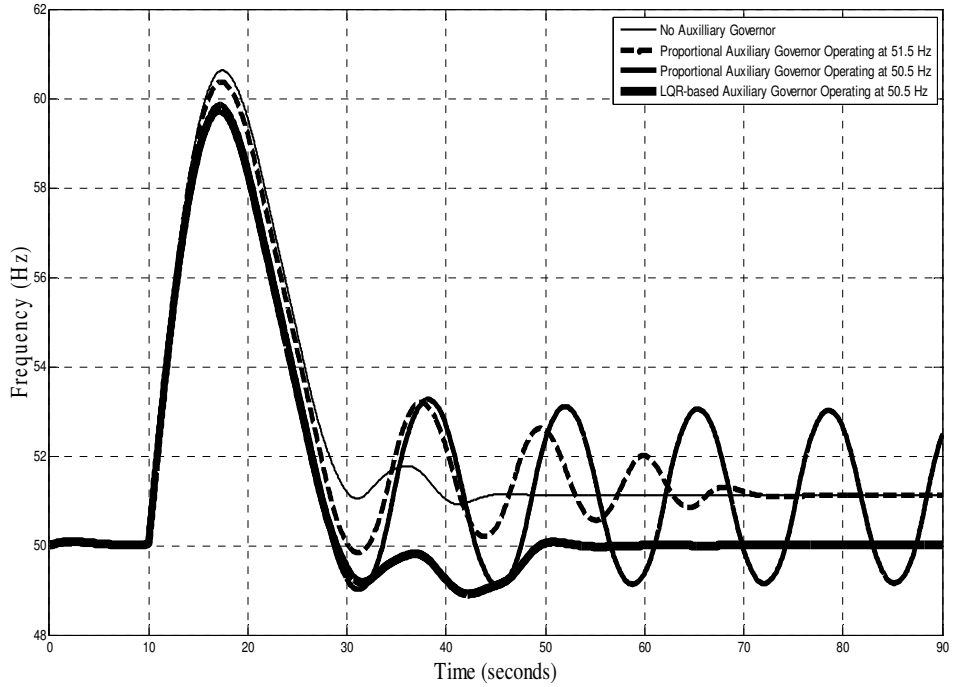

(a) Maximum governor rate limit= 0.1 p.u./sec.

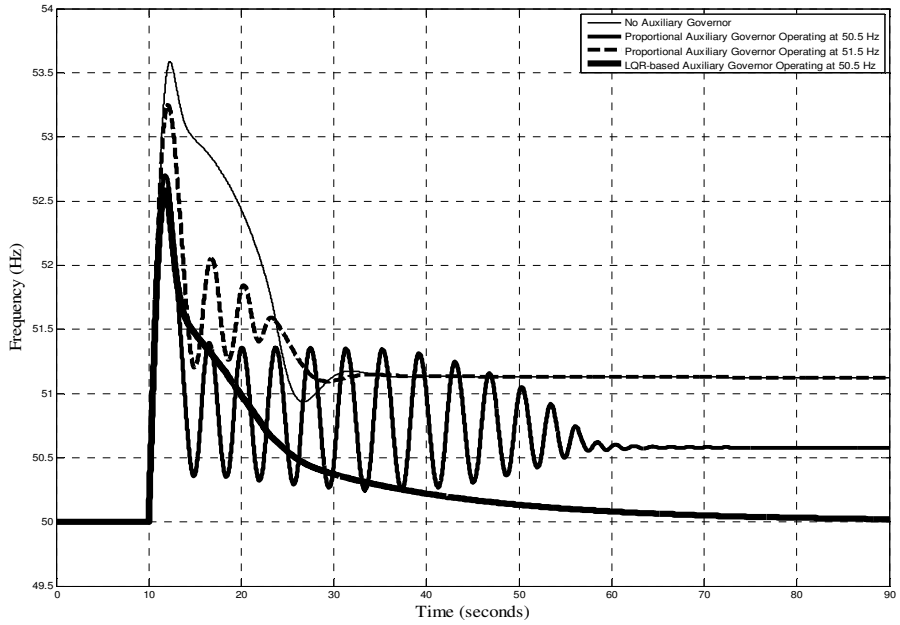

(b) Maximum governor rate limit= 0.5 p.u./sec.

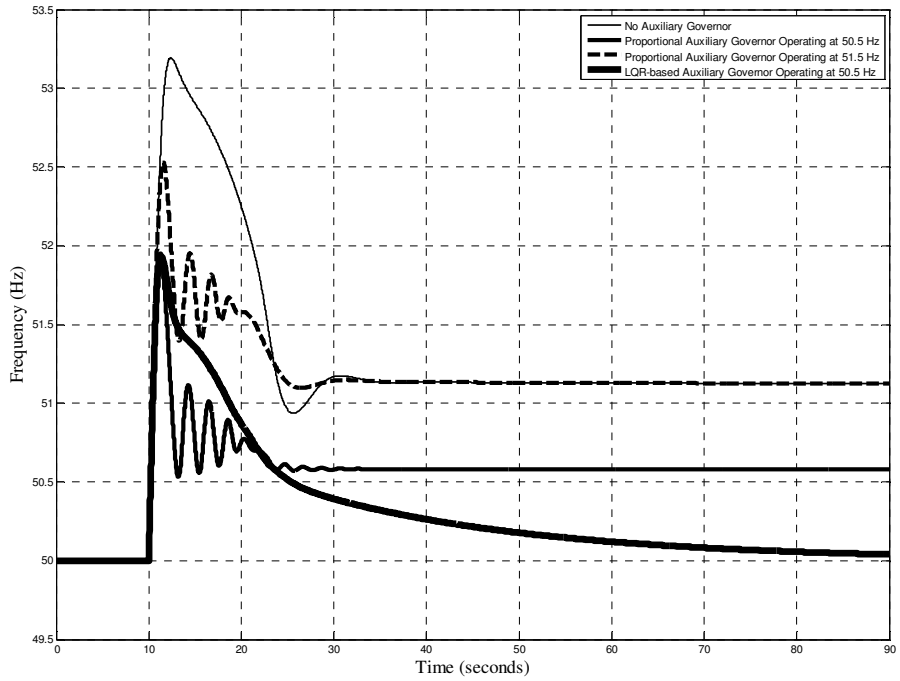

(c) Maximum governor rate limit= 0.9 p.u./sec.

Figure 6.12 Frequency response of Case Study 2 upon disconnection from the rest of the Grid.

6.4.3 Case Study 3

Time simulation of the frequency response of Case Study 3 network upon disconnection from the rest of the UK grid is presented in this section. The interrupted power is 62 % of the case study installed capacity. This value is chosen to match estimated power flows presented in the GB SYS for winter peak demand. Figure 6.13 shows the frequency response of Case Study 3 upon disconnection from the rest of the grid at different governor maximum rate limits where the following four cases are compared in each subplot:

(a) Thermal units with no auxiliary governor.

(b) Thermal units with proportional auxiliary governors operating at 50.5 Hz.

(c) Thermal units with the proposed LQR-based auxiliary governor.

Based on the results presented, the frequency first overshoot always exceeds 52 Hz and the frequency response shows a stable response and reaches the nominal steady state value of 50 Hz in all cases where the proposed auxiliary governor is used.

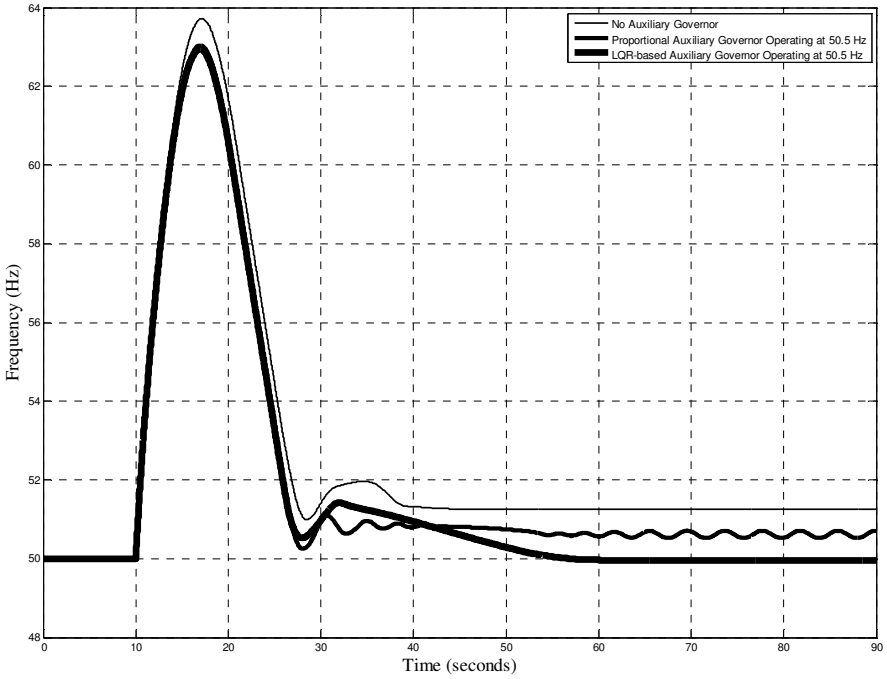

(a) Maximum governor rate limit= 0.1 p.u./sec.

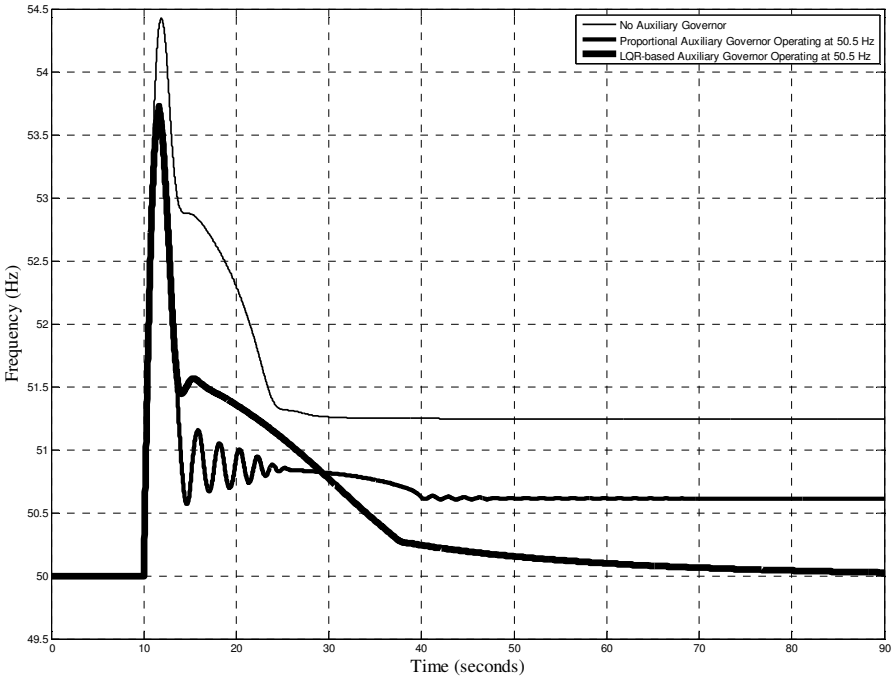

(b) Maximum governor rate limit= 0.5 p.u./sec.

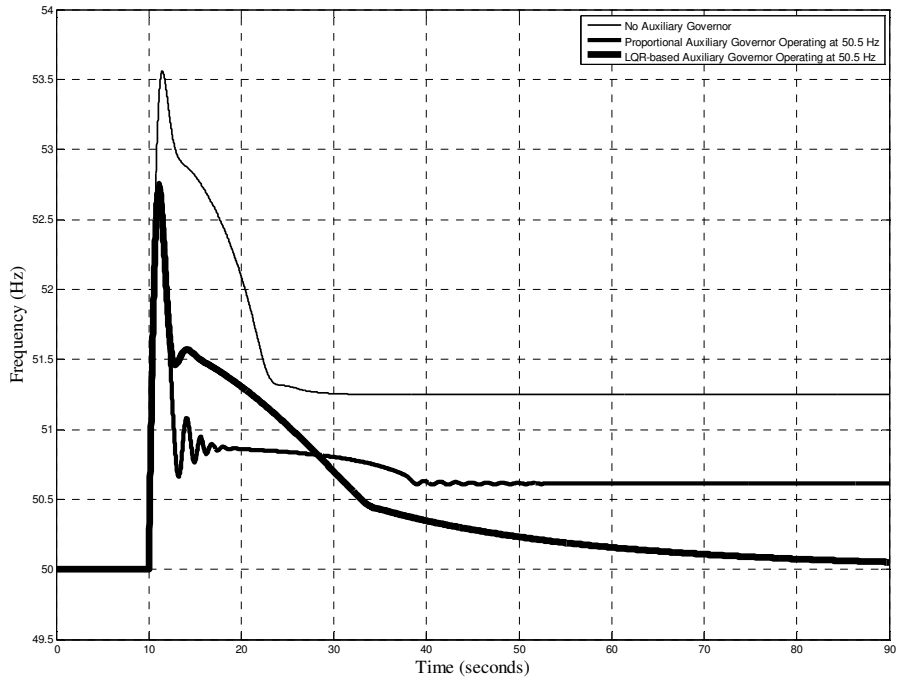

(c) Maximum governor rate limit= 0.9 p.u./sec.

Figure 6.13 Frequency response of Case Study 3 upon disconnection from the rest of the Grid.

6.5 Conclusions

The proposed local optimal controller assists in damping the first frequency overshoot. The optimal control allows the ability of increasing the proportional speed gains to high values while stabilizing the system through feedback from the rest of the state variables. The integral controller designed to estimate the reference power value for the LQR designed has proven good response. Not only is the first overshoot is damped but the steady state error is also removed. Consequently, the separated area would be ready at any moment to be reconnected back to the grid, making the interconnected system restoration process a lot quicker. Although the frequency might still be above 52 Hz in most cases, the proposed auxiliary governors contribute in improving the overall area response and hence minimizing the amount of generation required to be tripped. Finally, the problem frequency oscillatory response that accompanies the use of proportional auxiliary governors is solved without compromising the reduction of the first frequency overshoot.

CHAPTER 7

GENERATION TRIPPING AND LOCAL OPTIMAL CONTROLLERS

7.1 Introduction

This chapter discusses the simultaneous application of the two aforementioned techniques discussed in Chapter 4 and Chapter 6 to the case studies discussed. It re-estimates the amount of generation needed to be tripped, while applying the LQR-based auxiliary governor.

This section provides introductory information and presents this chapter outline. Section 7.2 presents the generation tripping simulation after adding the LQR –based auxiliary governor to the thermal units. Finally, Section 7.3 summarizes this chapter.

7.2 Generation Tripping Simulation

Similar to Section 4.3, using the order of generators in Table 4-3, Table 4-4 and Table 4-5 for Case Study1, 2 and 3 respectively , how much power stations are to be tripped is decided through running time domain simulations, tripping different amount of plants and observing the frequency overshoot just after disconnection. However, this time the generators are equipped with the proposed LQR-based auxiliary governor.

Similarly, the disturbance simulated is the simultaneous opening of all ties connecting the case studies to the rest of the system. The frequency response of the separated case studies is examined at different governor rate limits and with different amounts of generation tripped once the separation takes place and the frequency exceeds the statutory limit of 50.5 Hz. As mentioned in Chapter 3, the frequency time response of the thesis case studies is presented for conventional generation with governor rate limits varied from 0.1p.u/sec to 0.9 p.u./sec in increment of 0.1 p.u..

7.2.1 Case Study 1

Time simulation of the frequency response of Case Study 1 network upon disconnection from the rest of the UK grid is presented in this section with different amounts of generation tripped taking the priority list into consideration. Figure 7.1 shows the frequency response of Case Study 1 upon disconnection from the rest of the grid at different governor maximum rate limits where the following five cases are compared in each subplot: (a) no generation tripped, (b) 1 wind farm tripped, (c) 2 wind farms tripped, (d) 2 wind farms and 1 hydro plant tripped and (e) 2 wind farms, 1 hydro plant and 1 coal-fired plant tripped.

Time domain simulation shows that for generators with a governor rate limit higher than 0.3 p.u./sec , there is no need to trip any generation to contain the first frequency overshoot below the 52 Hz. If the generators governor rate limit is 0.3 p.u./sec , 2 wind farms need to be tripped. An extra hydro power station is to be tripped for the case of generators with governor rate limiter of 0.2 p.u./sec. Finally, for the case of generators with governor rate limiters of 0.1 p.u./sec, 4 power stations, 2 wind farms, 1 hydro plant and 1 coal fired, are required to be tripped to contain the separated area frequency first overshoot below 52 Hz. Moreover, for all cases the frequency returns to its nominal value, see Figure 7.1. Table 7-1 compares the amount of generation needed to be tripped before applying the LQR-based auxiliary governors to the thermal power plants and after.

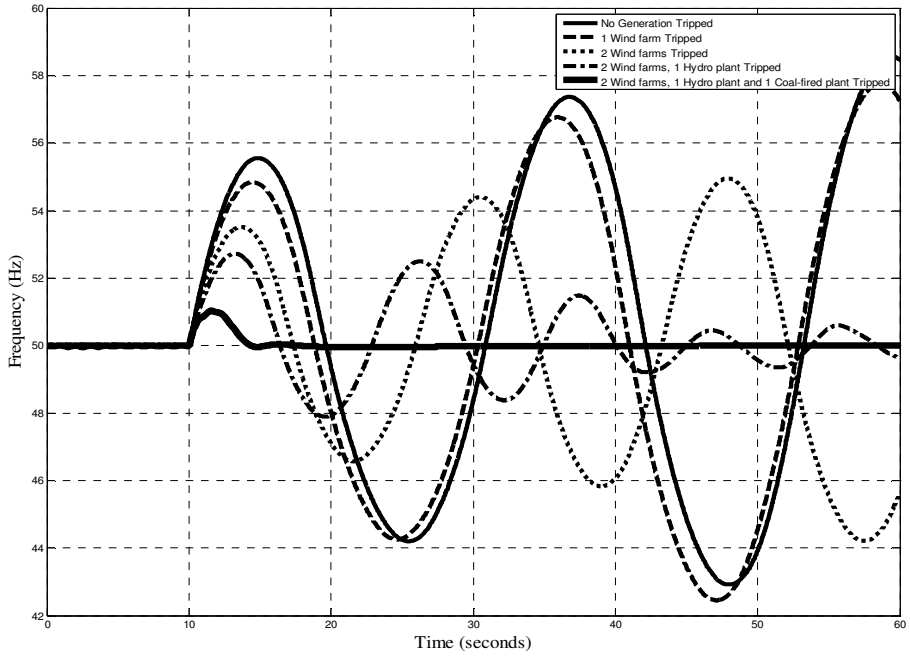

(a) Maximum governor rate limit= 0.1 p.u./sec.

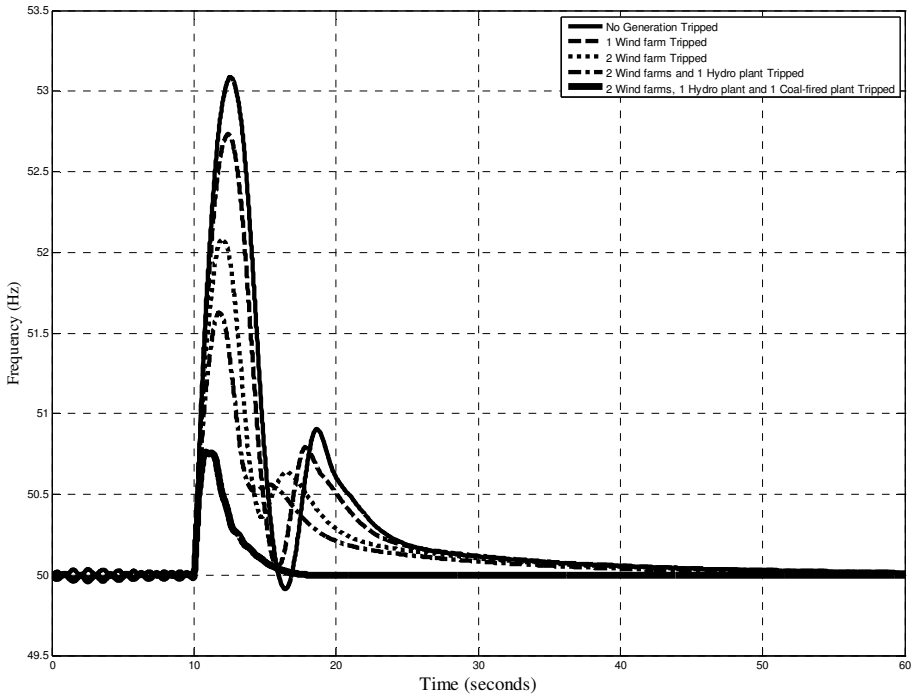

(b) Maximum governor rate limit= 0.2 p.u./sec.

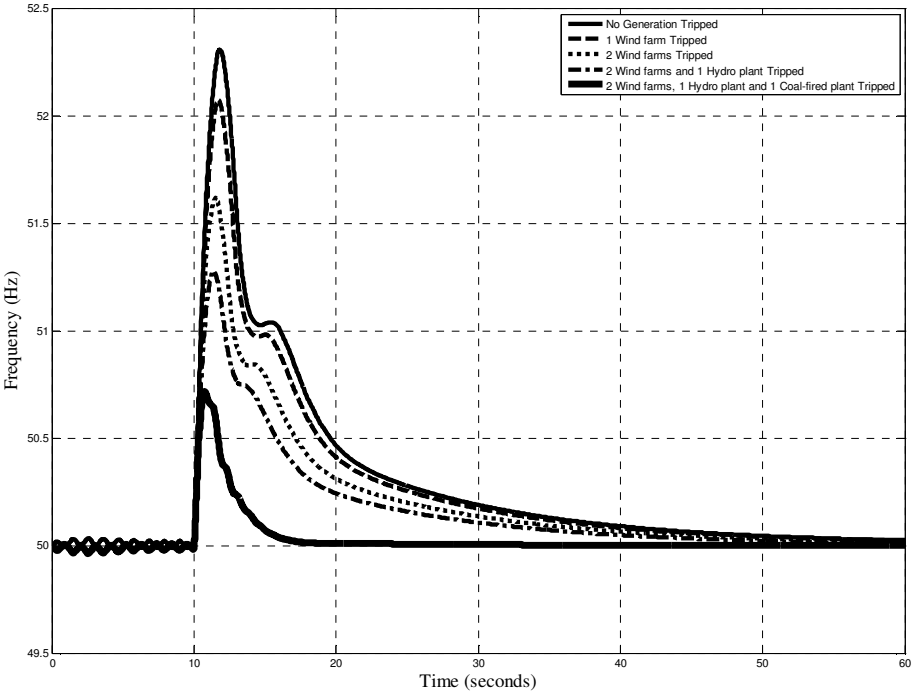

(c) Maximum governor rate limit= 0.3 p.u./sec.

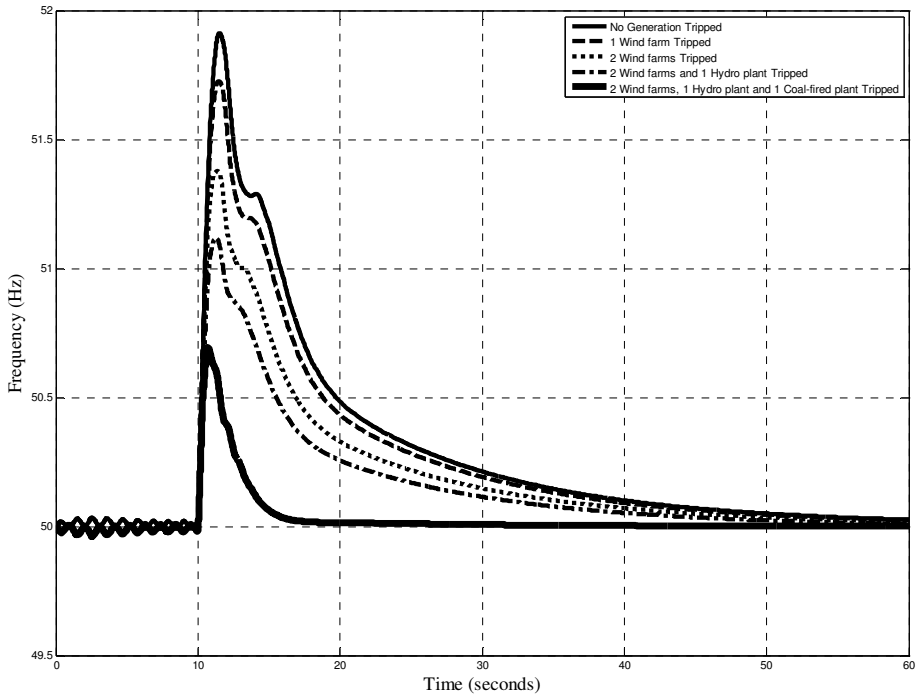

(d) Maximum governor rate limit= 0.4 p.u./sec.

Figure 7.1 Frequency response of Case Study 1 upon disconnection from the rest of the Grid.

Table 7-1 Generation required to be tripped with and without LQR-based auxiliary governors for Case Study 1

Governor rate limit	**Generation Tripped without LQR-based auxiliary governor**	**Generation Tripped with LQR-based auxiliary governor**
0.1 p.u. /sec	4 plants and still not enough	4 plants
0.2 p.u. /sec	4 plants	3 plants
0.3 p.u. /sec	4 plants	2 plants
0.4 p.u. /sec	3 plants	No Need
0.5 p.u. /sec	3 plants	No Need
0.6 p.u. /sec	2 plants	No Need
0.7 p.u. /sec	2 plants	No Need
0.8 p.u. /sec	2 plants	No Need
0.9 p.u. /sec	2 plants	No Need

7.2.2 Case Study 2

Time simulation of the frequency response of Case Study 2 network upon disconnection from the rest of the UK grid is presented in this section. The interrupted power is 38% of the case study installed capacity. Figure 7.2 shows the frequency response of Case Study 2 upon disconnection from the rest of the grid at different governor maximum rate limits where the following five cases are compared in each subplot: (a) no generation tripped, (b) 60% of wind farms tripped, (c) all wind farms tripped (d) all wind farms and 1 hydro plant tripped and (e) all wind farms, 1 hydro plant and 1 coal-fired plant tripped.

Figure 7.2 shows that for generators with a governor rate limit higher than 0.4 p.u./sec , tripping 60% of wind farms is sufficient to contain the first frequency overshoot below the 52 Hz. If the generators governor rate limit is 0.3 or 0.4 p.u./sec , all wind farms are to be tripped. Finally, for the case of generators with governor rate limiters of 0.1 or 0.2 p.u./sec, all wind farms, 1 hydro plant and 1 coal fired, are required to be tripped to contain the separated area frequency first overshoot below 52 Hz. Moreover, for all cases of governor rate limiters, the frequency reaches its nominal value. Table 7-2 compares the amount of generation needed to be tripped before applying the LQR-based auxiliary governors to the thermal power plants and after.

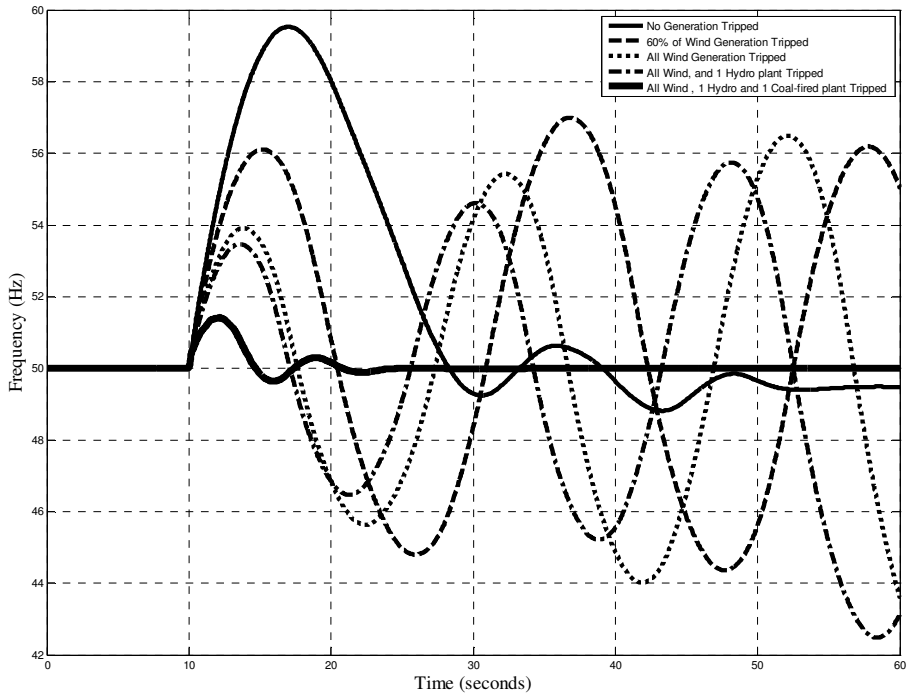

(a) Maximum governor rate limit= 0.1 p.u./sec.

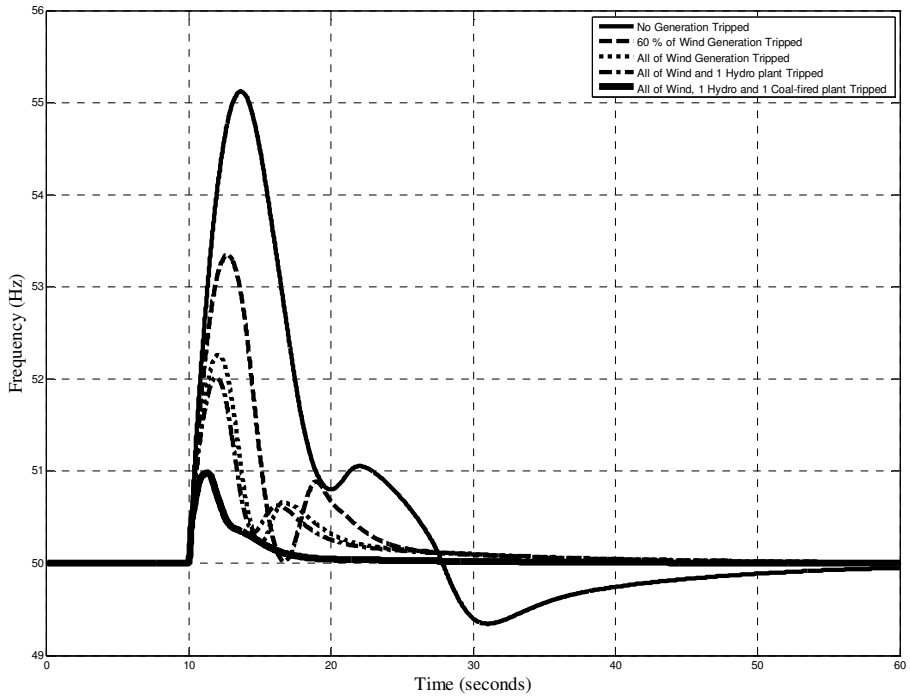

(b) Maximum governor rate limit= 0.2 p.u./sec.

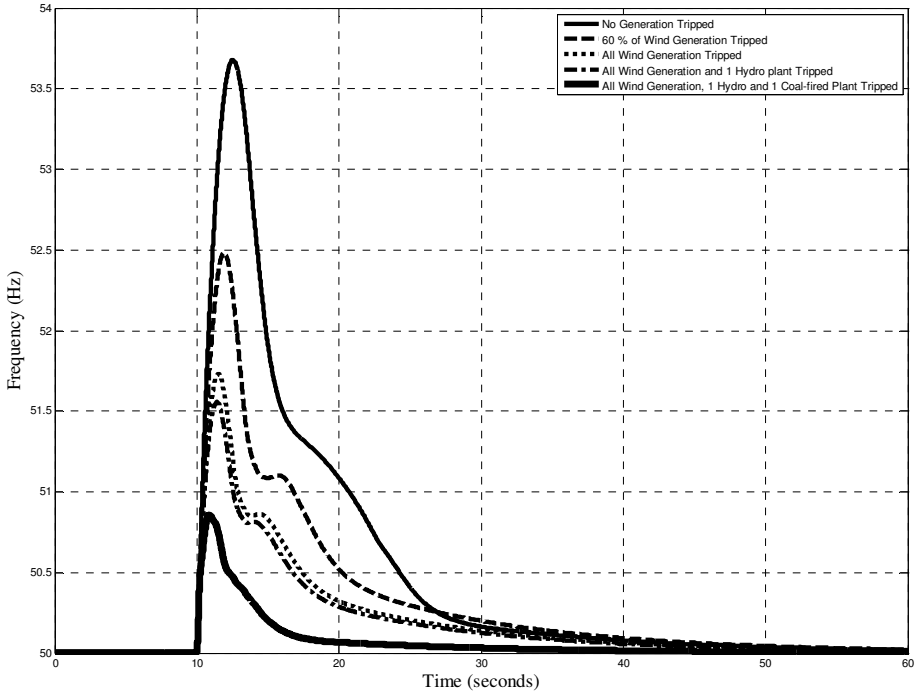

(c) Maximum governor rate limit= 0.3 p.u./sec.

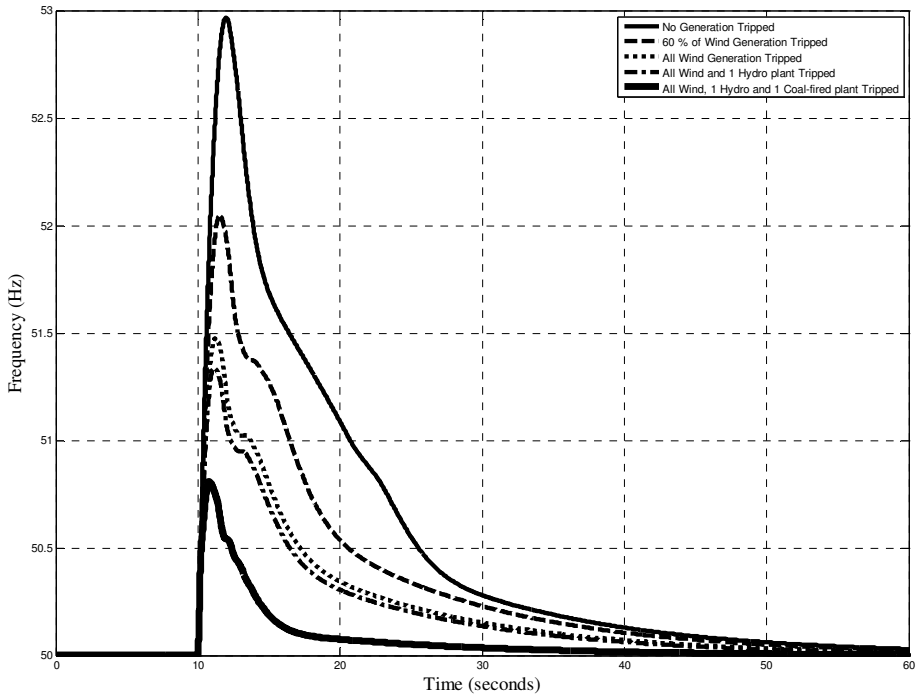

(d) Maximum governor rate limit= 0.4 p.u./sec.

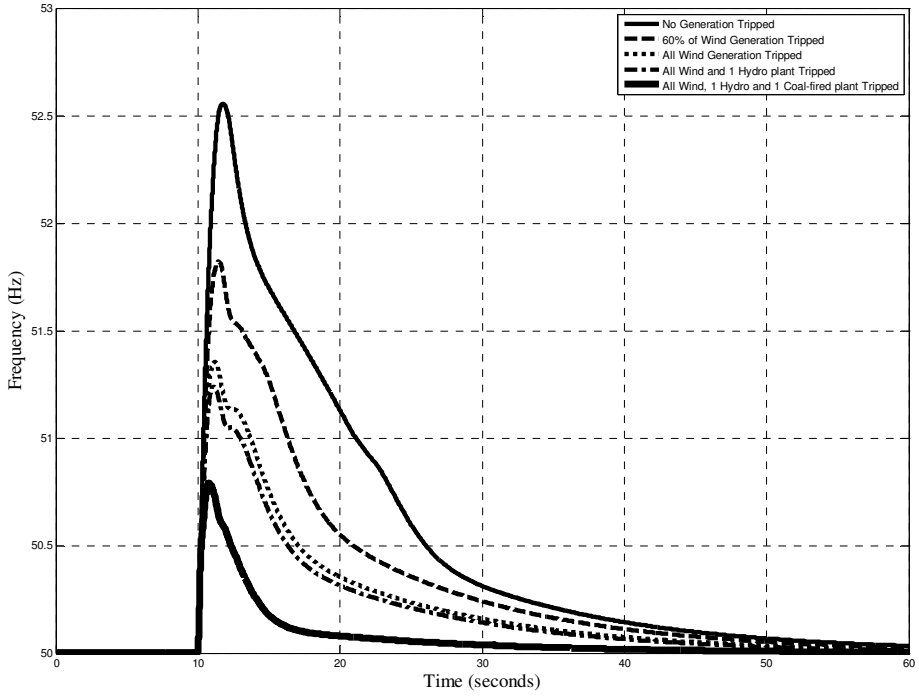

(e) Maximum governor rate limit= 0.5 p.u./sec.

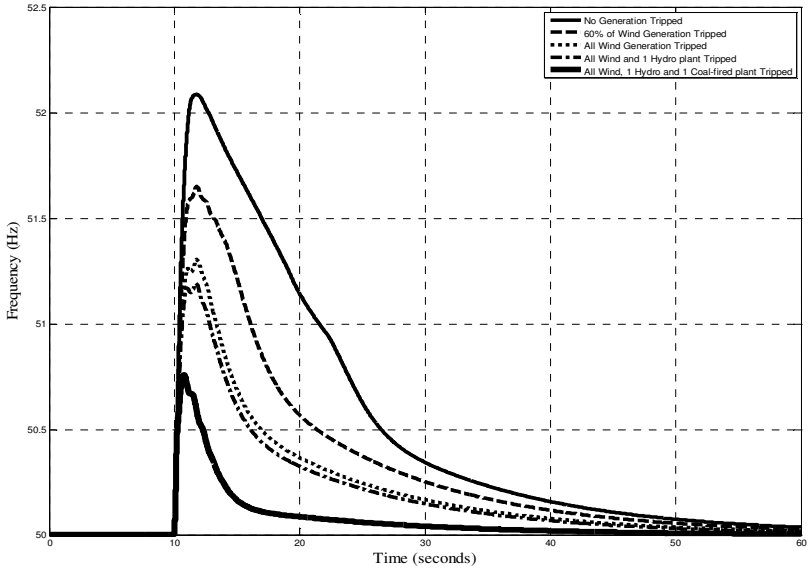

(i) Maximum governor rate limit= 0.9 p.u./sec.

Figure 7.2 Frequency response of Case Study 2 upon disconnection from the rest of the Grid.

Table 7-2 Generation Required to be tripped with and without LQR-based auxiliary governors for Case Study 2.

Governor rate limit	**Generation Tripped without LQR-based auxiliary governor**	**Generation Tripped with LQR-based auxiliary governor**
0.1 p.u. /sec	All Wind Farms,1Hydro,1 Coal fired And Still unstable	All Wind Farms, 1Hydro,1 Coal fired
0.2 p.u. /sec	All Wind Farms,1Hydro,1 Coal fired And Still unstable	All Wind Farms, 1Hydro, 1 Coal fired
0.3 p.u. /sec	All Wind Farms,1 Hydro,1 Coal fired	All Wind Farms
0.4 p.u. /sec	All Wind Farms, 1Hydro, 1 Coal fired	All Wind Farms
0.5 p.u. /sec	All Wind Farms+1Hydro	60% of Wind Farms
0.6 p.u. /sec	All Wind Farms+1Hydro	60% of Wind Farms
0.7 p.u. /sec	All Wind Farms	60% of Wind Farms
0.8 p.u. /sec	All Wind Farms	60% of Wind Farms
0.9 p.u. /sec	All Wind Farms	60% of Wind Farms

7.2.3 Case Study 3

Time simulation of the frequency response of Case Study 3 network upon disconnection from the rest of the UK grid is presented in this section. The interrupted power is 62 % of the case study installed capacity. Figure 7.3 shows the frequency response of Case Study 3 upon disconnection from the rest of the grid at different governor maximum rate limits where the following six cases are compared in each subplot: (a) no generation tripped, (b) 1 oil-fired plant tripped, (c) 1 oil-fired plant and 1 coal-fired plant tripped (d) 1 oil-fired plant and 2 coal-fired plant tripped, (e) 1 oil-fired plant and 3 coal-fired plant tripped and (f) 1 oil-fired plant, 3 coal-fired plant and 1 CCGT plant tripped.

Time domain simulation shows that at most 5 power stations are to be tripped to ensure that the frequency first overshoot is below 52 Hz. Moreover, time domain simulation shows that the steady state frequency reaches its nominal value of 50 Hz in all cases, see Figure 7.3. For generators with a governor rate limit higher than 0.2 p.u./sec , tripping 4 generators, 1 oil-fired and 3 coal-fired is sufficient to contain the first frequency overshoot below the 52 Hz. If the generators governor rate limit is 0.2 or 0.1 p.u./sec , an extra CCGT power station is to be tripped. The improvement of the frequency response due to the existence of an HVDC link in this case study dominates the improvement due to the LQR-based auxiliary governor, where generation required to be tripped is less by only 1 plant for the case where generators have governor rate limits from 0.3 to 0.6 p.u./sec, see Table 7-3.

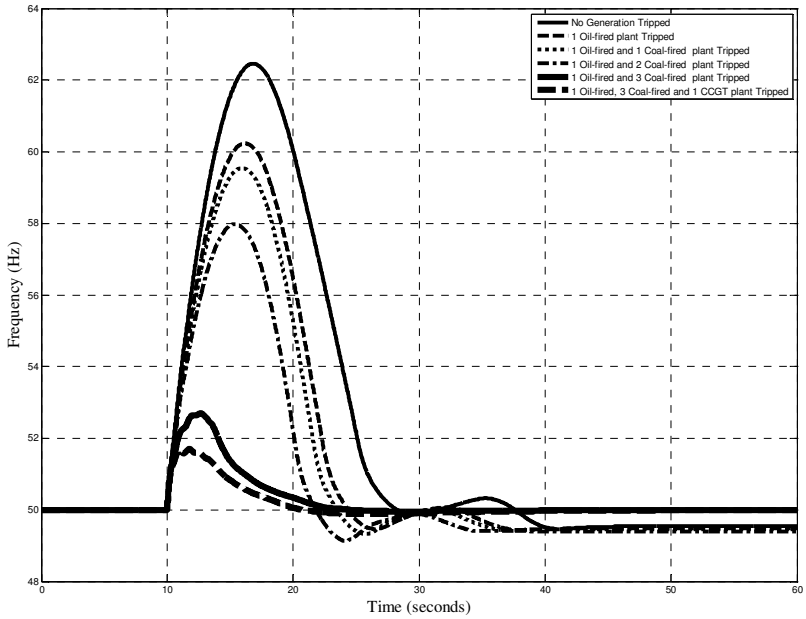

(a) Maximum governor rate limit= 0.1 p.u./sec.

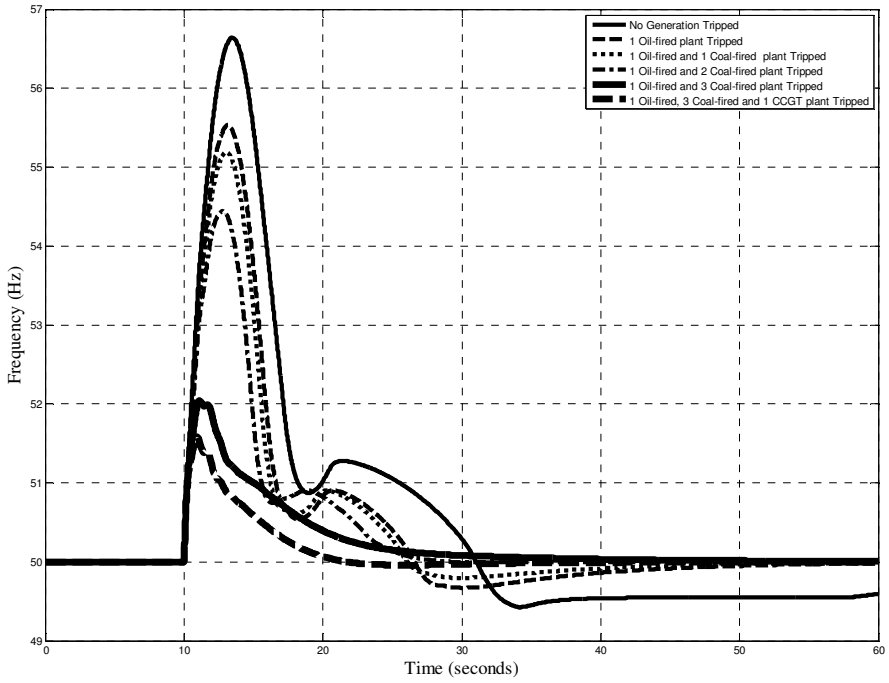

(b) Maximum governor rate limit= 0.2 p.u./sec.

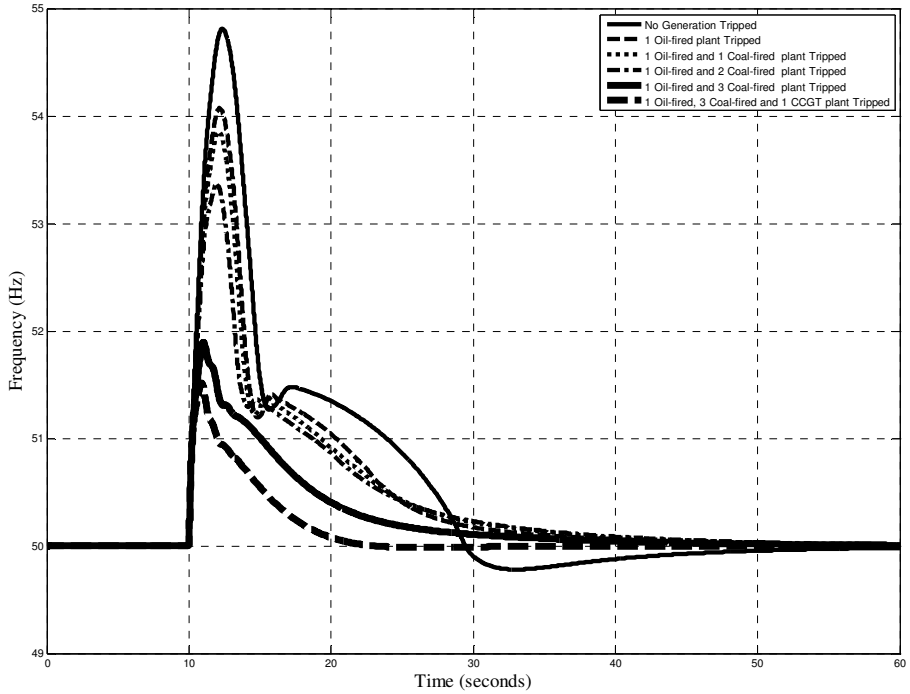

(c) Maximum governor rate limit= 0.3 p.u./sec.

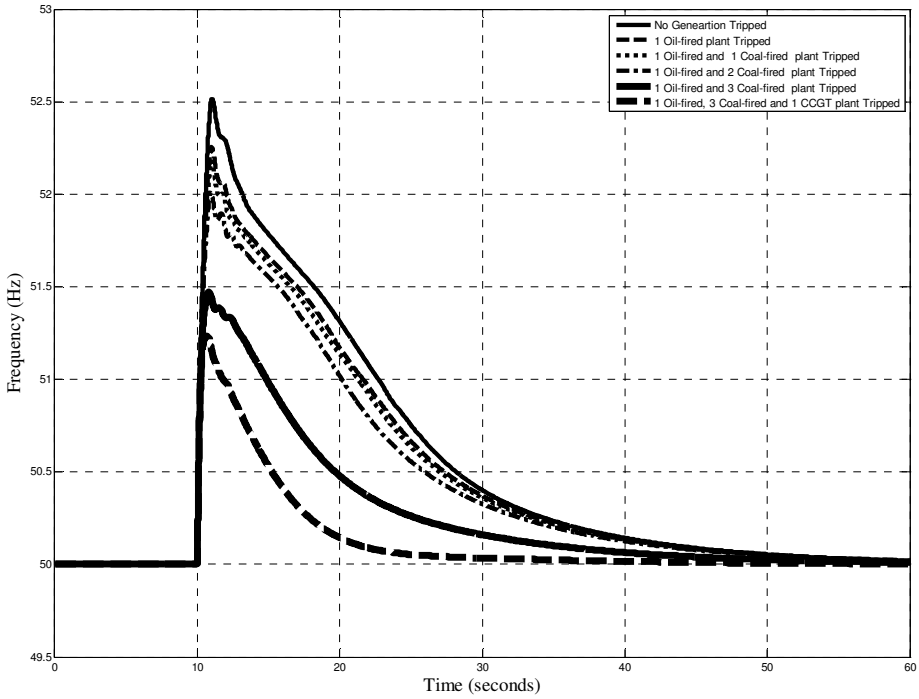

(d) Maximum governor rate limit= 0.9 p.u./sec.

Figure 7.3 Frequency response of Case Study 3 upon disconnection from the rest of the Grid.

Table 7-3 Generation Required to be tripped with and without LQR-based auxiliary governors for Case Study 3.

Governor rate limit	**Generation Tripped without LQR-based auxiliary governor**	**Generation Tripped with LQR-based auxiliary governor**
0.1 p.u. /sec	5 plants	5 plants
0.2 p.u. /sec	5 plants	5 plants
0.3 p.u. /sec	5 plants	4 plants
0.4 p.u. /sec	5 plants	4 plants
0.5 p.u. /sec	5 plants	4 plants
0.6 p.u. /sec	5 plants	4 plants
0.7 p.u. /sec	4 plants	4 plants
0.8 p.u. /sec	4 plants	4 plants
0.9 p.u. /sec	4 plants	4 plants

7.3 Conclusions

LQR–based governors assisst in improving the frequency response of generation rich separated areas. Consequently , the amount of generation needed to be tripped to minimize the frequency first overshoot is less than the case where the LQR-based governors do not exist. Not only that , but the steady state frequency value settles at the nominal value of 50 Hz. Moroever , for the case of rate limiters with low values, the frequency response suffers no unstable swings anymore.

CHAPTER 8

CONCLUSIONS AND RECOMMENDATIONS

8.1 Conclusions

Based on the results obtained during this work, the following conclusions are drawn:

1. Generation tripping is an effective method to sustain the transient frequency stability of a generation rich separated areas. It provides a fast means for matching generation with load. Hence, it reduces the frequency overshoot to be less than the value which triggers generators overspeed protection. A selective tripping pattern is introduced. This pattern uses a station priority list based on generation dynamics, minimum zero time and bid prices, to select the proper amount of generation to be tripped for all thesis case studies is found to be effective.

2. Although Generation Tripping is a fast solution for improving the frequency response of separated areas, it has some disadvantages. It costs the operator compensations to the tripped power station owners. Tripping is accompanied with mechanical stresses that affects the generating unit life time. Hence, Generation tripping should be minimized and other solutions have to be proposed. Moreover, generation tripping might not eliminate unstable frequency swings if the considered area machines are equipped with very slow response governors. Finally, generation tripping does not eliminate the frequency steady-state deviation completely and more methodologies need to be introduced to help in restoring any area frequency back to its nominal value.

3. One solution is the use of an island AGC. Both proposed island AGCs, integral control-based and LQR-based, are found incapable of damping the first frequency overshoot, but they eliminate the frequency steady-state error.

4. Introducing both methodologies discussed in 1 and 3 simultaneously, seem to be a good solution to restore the frequency to its nominal value. However, it saves the operator no money. Based on this, another methodology must be introduced to enhance the transient response as well.

5. LQR-based local overspeed controllers or simply LQR-based auxiliary governors for thermal units are proposed. These controllers were found to assist in enhancing the frequency transient response by damping the frequency first overshoot. This LQR control allows the ability of increasing the proportional speed gain to high values while stabilizing the system through feedback from the rest of the state variables (i.e. mechanical power components). Moreover, an integral controller is designed to estimate the reference power value for the LQR designed and hence eliminate the frequency-steady state error as well.

6. As the LQR-based overspeed controllers, show better response than the centralized controller, the island AGC. They improve the frequency response (transient and steady-state) upon interconnected system splitting. So choosing the decentralized technique participates in lessening the amount of generation required to be tripped and hence saving the operator some compensation fees. Moreover, the author thinks that local controllers would be the best as it seems to be the best practical solution to accompany the generation tripping technique discussed in 1. Furthermore, local controllers will contribute in improving the frequency stability of the separated area whether this separation was controlled or uncontrolled.

7. Furthermore, if the separated area has high wind penetration, the author thinks that starting with tripping the wind farms would be the best solution as wind farms output are assumed not to be sensitive to grid frequency during this study. Moreover, wind farms can be easily restored and hence tripping them first would make the overall system restoration faster.

8. Finally, HVDC Links assist in stabilizing the frequency response of generation rich separated areas especially if power reversal is allowed across the links. HVDC links

operate rapidly to damp any unstable frequency swings that might result in the case of power stations having units with slow governor responses.

8.2 Recommendations

The following points are recommended for further work in improving the frequency response of generation rich separated areas:

1. This work could be revisited after conducting industry, to use real life dynamic governor representations and use actual governor rate limits and constraints, to discuss the practicality and robustness of the Island AGC and the local overspeed controllers.

2. Studying the possibility of estimating the different state variables discussed during this thesis.

3. Mixing the nowadays research that focuses on building wind turbine controllers capable of providing support to the grid frequency with the study of separated areas with high penetration of wind generation.

4. Applying LQR to micro grids and distribution systems, where generation delays are less significant than the case of main thermal power stations. Consequently, designed LQR controllers would show more robustness and more promising frequency response improvements in case of islanded micro grids.

REFERENCES

[1] Wood, A. J., Wollenberg, B.F., Power Generation, Operation And Control , second edition, John Wiley & Sons, INC., New York, 1996, Ch.11, pp. 452.

[2] Makarov, Y.V., Reshetov, V.I., Stroev, A., Voropai, I., Blackout Prevention in the United States, Europe, and Russia, Proceedings of the IEEE Volume 93, Issue 11, Nov. 2005 Page(s):1942 – 1955

[3] Gou, Bei; Zheng, Hui; Wu, Weibiao; Yu, Xingbin ; Probability Distribution of Power System Blackouts; Power Engineering Society General Meeting, 2007. IEEE 24-28 June 2007 Page(s):1 – 8

[4] Zin, A.A.M.; Karim, S.P.A.;The Application of Fault Signature Analysis in Tenaga Nasional Berhad Malaysia Power Delivery, IEEE Transactions on Volume 22, Issue 4, Oct. 2007 Page(s):2047 – 2056

[5] Chunyan Li,; Yuanzhang Sun,; Xiangyi Chen,;Analysis of the blackout in Europe on November 4, 2006 Power Engineering Conference, 2007. IPEC 2007. International 3-6 Dec. 2007 Page(s):939 – 944

[6] Xiangyi Chen,; Changhong Deng,; Yunping Chen,; Chunyan Li,;Blackout prevention: Anatomy of the blackout in Europe Power Engineering Conference, 2007. IPEC 2007. International 3-6 Dec. 2007 Page(s):928 – 932

[7] Bialek, Janusz W.;Why has it happened again? Comparison between the UCTE blackout in 2006 and the blackouts of 2003 Power Tech, 2007 IEEE Lausanne 1-5 July 2007 Page(s):51 – 56

[8] Chunyan Li; Yuanzhang Sun; Xiangyi Chen; Recommendations to improve power system security: Lessons learned from the europe blackout on November 4 Universities Power Engineering Conference, 2007. UPEC 2007. 42nd International 4-6 Sept. 2007 Page(s):529 – 533

[9] PSERC report," Resources for Understanding the Moscow Blackout of 2005".

[10] Wikipedia article, "2005 Moscow power blackout"

[11] Vournas, C.D.; Nikolaidis, V.C.; Tassoulis, A.;Experience from the Athens blackout of July 12, 2004 Power Tech, 2005 IEEE Russia27-30 June 2005 Page(s):1 – 7

[12] Vournas, C.D.; Nikolaidis, V.C.; Tassoulis, A.A.; Postmortem analysis and data validation in the wake of the 2004 Athens blackoutPower Systems, IEEE Transactions onVolume 21, Issue 3, Aug. 2006 Page(s):1331 – 1339

[13] Corsi, S.; Sabelli, C.;General blackout in Italy Sunday September 28, 2003, h. 03:28:00, Power Engineering Society General Meeting, 2004. IEEE 6-10 June 2004 Page(s):1691 - 1702 Vol.2

[14] Berizzi, A.; The Italian 2003 blackout; Power Engineering Society General Meeting, 2004. IEEE, 6-10 June 2004 Page(s):1673 - 1679 Vol.2

[15] Sforna, M.; Delfanti, M.;Overview of the events and causes of the 2003 Italian blackout, Power Systems Conference and Exposition, 2006. PSCE '06. 2006 IEEE PES, Oct. 29 2006-Nov. 1 2006 Page(s):301 – 308

[16] Preliminary report, "The black-out in southern Sweden and eastern Denmark, 23 September, 2003"

[17] Wikipedia article, "2003 southern Malaysia blackout".

[18] Tracing the London Blackout Power Engineer, Power Engineering Journal, volume 17, Issue 5, Oct.-Nov. 2003, page(s):8 – 9.

[19] Makarov, Y.V.; Reshetov, V.I.; Stroev, V.A.; Voropai, N.I.; Blackouts in North America and Europe: Analysis and generalization Power Tech, 2005 IEEE Russia 27-30 June 2005, Page(s):1 – 7

[20] Wikipedia article, "2003 London blackout"

[21] Final Report on the August 14, 2003 Blackout in the United States and Canada: Causes and Recommendations, U.S. – Canada Power System Outage Task Force, April 5, 2004.

[22] Technical Analysis of the August 14, 2003, Blackout: What Happened, Why, and What Did We Learn? Report to the NERC Board of Trustees by the NERC Steering Group, NERC, July 13, 2004

[23] Andersson, G.; Donalek, P.; Farmer, R.; Hatziargyriou, N.; Kamwa, I.; Kundur, P.; Martins, N.; Paserba, J.; Pourbeik, P.; Sanchez-Gasca, J.; Schulz, R.; Stankovic, A.; Taylor, C.; Vittal, V.; Causes of the 2003 major grid blackouts in North America and Europe, and recommended means to improve system dynamic performance Power Systems, IEEE Transactions on Volume 20, Issue 4, Nov. 2005 Page(s):1922 – 1928

[24] P. Kundur, Power System Stability and Control, McGraw-Hill, Inc., 1994.

[25] I.A.Erinmez, D.O.Bickers, G.F.Wood, W.W..Hung, "NGC experience with frequency control in England and Wales-provision of frequency response by generators" Power Engineering Society 1999 Winter Meeting, IEEE Volume 1, 31 Jan. 4 Feb. 1999 Page(s):590 - 596 vol.1

[26] The Great Britain Grid Code, Issue 3 Revision 28, 7th July 2008.

[27] GB Security and Quality of Supply Standard, version 1.0, September 22, 2004.

[28] Seyedi, H.; Sanaye-Pasand, M.,"New centralised adaptive load-shedding algorithms to mitigate power system blackouts", Generation, Transmission & Distribution, IET, vol. 3, Issue 1, pp. 99-114.January 2009.

[29] Wang, P.; Ding, Y.; Goel, L.;" Reliability assessment of restructured power systems using optimal load shedding technique, " Generation, Transmission & Distribution, IET, Vol. 3, Issue 7, pp. 628-640. July 2009.

[30] Morales, J.M.; Conejo, A.J.; Perez-Ruiz, J.;" Economic valuation of reserves in power systems with high penetration of wind power, "IEEE Power & Energy Society General Meeting, 2009, PES '09, pp. 1-1, 26-30 July 2009.

[31] Jaefari-Nokandi, M.; Monsef, H.;"Scheduling of Spinning Reserve Considering Customer Choice on Reliability," IEEE Transactions on Power Systems, vol. 24, Issue 4, pp.1780-1789, Nov.2009.

[32] National Grid, Report of the investigation into the automatic demand disconnection following multiple generation losses and the demand control response that occurred on the 27th May 2008.

[33] P. Kundur, J. Paserba, V. Ajjarapu, G. Andersson, A.Bose, C. Canizares, N. Hatziargyriou, D. Hill, A. Stankovic, C. Taylor, T. Van Cutsem, and V. Vittal," Definition and classification of power system stability IEEE/CIGRE joint task force on stability terms and definitions" IEEE Transactions on Power Systems, vol. 19, Issue 3, pp. 1387-1401, Aug. 2004.

[34] Roos, H.B.; Ning Zhu; Giri, J.; Kindel, B.**,"**An AGC implementation for system islanding and restoration conditions," IEEE Transactions on Power systems, vol. 9, Issue 3, pp. 1399-1410. Aug. 1994.

[35] Fosha, C.E.; Elgerd, O.I.;"The Megawatt-Frequency Control Problem: A New Approach Via Optimal Control Theory**"**, IEEE Transactions on Power Apparatus and Systems, vol. PAS-89, Issue 4, April 1970 pp.563 - 577 , April 1970.

[36] Kothari, M.L.; Nanda, J.; "Application of optimal control strategy to automatic generation control of a hydrothermal system", IEE Proceedings, Control Theory and Application, vol. 135, pp. 268-274, July 1988

[37] Mariano, S.J.P.S.; Pombo, J.A.N.; Calado, M.R.A.; Ferreira, L.A.F.M.; **"**Optimal output control: Load frequency control of a large power system" International Conference on Power Engineering, Energy and Electrical Drives, 2009, POWERENG, pp.369-374, 18-20 March 2009.

[38] Liu, F.; Song, Y.H.; Ma, J.; Mei, S.; Lu, Q.;" Optimal load-frequency control in restructured power systems" IEE Proceedings, Generation. Transmission and Distribution, vol. 150, Issue. 1 pp. 87-95, Jan. 2003

[39] Sadeh, J.; Rakhshani, E.; "Multi-area load frequency control in a deregulated power system using optimal output feedback method", The 5th International Conference on European Electricity Market , 2008, EEM, pp. 1-6, 28-30 May 2008.

[40] Rakhshani, E.; Sadeh, J.; "A reduced-order estimator with prescribed degree of stability for two-area LFC system in a deregulated environment," IEEE/PES, Power Systems Conference and Exposition, 2009, PES'02, pp.1-8, 15-18 March 2009.

[41] Anderson P.M and. Fouad, A. A, Power System Control and Stability, 2nd ed., IEEE, Inc., 2003.

[42] Report I.C.;" Dynamic Models for Steam and Hydro Turbines in Power System Studies", IEEE Transactions on Power Apparatus and Systems Volume PAS-92, Issue 6, Nov. 1973 Page(s):1904 – 1915

[43] K.R. Padiyar , Power System Dynamics: Stability and Control, Anshan Ltd; 2nd edition, Mar 2004.

[44] ANSI/IEEE Standard C37.106-1987, IEEE Guide for Abnormal Frequency Protection for Power Generating Plants.

[45] H.A. Bauman, G.R. Hahn, and C.N. Metcalf, "The Effect of Frequency Reduction on Plant capacity and on System Operation", AIEE Trans., Vol. PAS-73, pp. 1632-1637, February 1955

[46] Olle I. Elgerd , Electric Energy Systems Theory: An Introduction, McGraw-Hill Inc.; 2nd revised edition, Feb 1982.

[47] J. Duncan Glover, Mulukuyla S. Sarma, Thomas J. Overbye , Power System Analysis and Design, Thomson Corporation.; 4th edition, 2008.

[48] D.H. Berry, R.D. Brown, J.J. Redmond, and W. Watson, "Underfrequency Protection of the Ontario Hydro System," CIGRE Paper 32-14, August/September 1970.

[49] IEEE Working Group Report, "Dynamic Models for Fossil Fuelled Steam Units in Power System Studies," IEEE Trans., Vol.PWRS-6, No. 2, pp. 753-761, May 1991.

[50] T.D. Younkins and L.H. Johnson, "Steam Turbine Overspeed Control and Behaviour during System Disturbances," IEEE Trans., Vol. PAS-100, pp. 2504-2511, May 1981.

[51] P. Kundur, D.C. Lee, and J.P. Bayne, "Impact of Turbine Generator Overspeed Controls on Unit Performance under System Disturbance Conditions," IEEE Trans., Vol. PAS-104, pp. 1262-1267, June 1985.

[52] EPRI Report EL-5859, "Technical Limits to Transmission System Operation," Final Report of Project 5005-2, prepared by Power Technologies Inc., June 1988.

[53] P. Lilje, A. Petroianu.," Power Plant Islanding with the Aid of a Controlled Resistor", IEEE AFRICON, 2004 Page(s):775 –781

[54] M.L. Shelton, R.F. Winkleman, W.A. Mittelstadt, and W.L. Bellerby, “Bonneville Power Administration 1400 MW Braking Resistor, “, IEEE Trans., Vol. PAS-94, pp. 602-611, March/ April 1975.

[55] Kai Sun; Da-Zhong Zheng; Qiang Lu;” A simulation study of OBDD-based proper splitting strategies for power systems under consideration of transient stability”, IEEE Transactions on Power Systems, vol. 20, Issue 1, pp.389 – 399, Feb 2005.

[56] Ying Qiao; Chen Shen; Jiayun Wu; Qiang Lu,”The Integrated Simulation Platform for Islanding Control of Large-Scale Power Systems: Theory, Implementation and Test Results, “Power Engineering Society, IEEE General Meeting, 2006, pp.8, 2006.

[57] Sun, K.; Zheng, D.-Z.; Lu, Q.; “Searching for feasible splitting strategies of controlled system islanding”, Generation, Transmission and Distribution, IEE Proceedings-, vol. 153, Issue 1,pp.89-98, 12 Jan. 2006

[58] Bo Yang; Vittal, V.; Heydt, G.T.;”Slow-Coherency-Based Controlled Islanding; A Demonstration of the Approach on the August 14, 2003 Blackout Scenario”., IEEE Transactions on Power Systems, vol. 21, Issue 4, pp.:1840 - 1847, Nov. 2006.

[59] Bo Yang; Vittal, V.; Heydt, G.T.; Sen, A.;”A Novel Slow Coherency Based Graph Theoretic Islanding Strategy” Power Engineering Society, IEEE General Meeting, 2007, pp.1-7, 24-28 June 2007.

[60] Xu, G.; Vittal, V.;”Slow Coherency Based Cutset Determination Algorithm for Large Power Systems”, IEEE Transactions on Power Systems,: Accepted for future publication, Forthcoming, 2009.

[61] National Grid,” 2008 Great Britain Seven Year Statement”, May 2008.

[62] A Report by the Electricity Networks Strategy Group ENSG, Our Electricity Transmission Network: A Vision For 2020, March 2009.

[63] Elders I., Ault G., Galloway S., McDonald J., Kohler J., Leach M. and Lampaditou E., Electricity Network Scenarios for Great Britain in 2050, CWPE 0609 and EPRG 0513, February 2006.

[64] Yu, Y-N., Electric Power System Dynamics, Academic Press Co., New York, 1983.

[65] IEEE Committee, "Computer Representation of Excitation System," IEEE Transactions on Power Apparatus and Systems, Vol. PAS-87, No. 6, June 1968, pp.1460-1464.

[66] Jones, D.I.,” Dynamic system parameters for the National Grid” Generation, Transmission and Distribution, IEE Proceedings-Volume 152, Issue 1, 10 Jan. 2005 Page(s):53 – 60

[67] Pearmine, R., Song, Y.H. and Chebbo, A., “Influence of wind turbine behaviour on the primary frequency control of the british transmission grid”

[68] Inove, T., Tafniguchi H., Ikeguchi Y. et al., " Estimator of power system inertia constant and capacity of spinning-reserve support generators using measured frequency transients", IEEE trans. Power system 1997, 12, pp 136-143

[69] Anderson, P.M. and Mirheydar M. " A low-order system frequency response model" IEEE Trans. Power System 1990, 5 , pp720-729

[70] Weedy B.M., Electric Power system, (Wiley 1987, 3rd ed.)

[71] Concordia C., Kirchmayer, L.K. and Monski Szy, "Effect of speed governor dead band on tie line power and frequency control performance" Trans. AIEE Power Appar. System 1957, 31, pp. 429-434.

[72] Anaya-Lara O., Hughes, M., Jenkins, N., and Strbac. G., "Influence of wind farms on power system dynamic and transient stability" Wind Engineering, Volume 30, No.2, 2006.

[73] Anaya-Lara, O., Jenkins, N., Ekanayake, J., Cartwright, P., Hughes M., Wind Energy Generation: Modelling and Control, John Wiley & Sons, Ltd, 2009.

[74] Hillery R.H. and Holdup E.D.,"Load Rejection Testing of Large Thermal Electric Generating Units," IEEE Trans., Vol. PAS-87, June 1968, pp.1440-1453.

[75] http://www.bmreports.com.

[76] F. Li, M.S.Gabb, C.J.Aldridge, C.H. Cheung, R.L.Walker, T.G.Williams, and M.E. Bradley" Optimal constraint management for system operations under NETA" Power System Management and Control, 2002. Fifth International Conference on (Conf.Publ.No.488), 17-19 April 2002 Page(s):19–24.

[77] Ogata, K., Modern Control Engineering, 3rd Edition, Prentice-Hall Inc., New York, 1997.

[78] Kuo, B. C., Automatic Control Systems, 7th Edition, Prentice-Hall Inc., New York, 1995.

[79] Shanian, B., and Hassul, M., Control System Design Using MATLAB, Prentice-Hall, Englewood Cliffs, New Jersey, 1993.

[80] Doyle, J. C., Glover, G., Khargonekar, P. P. and Francis, B. A., "State-Space Solutions to Standard H2 and H∞ Control Problems," IEEE Transactions on Automatic Control, Vol. 34, No. 8, August 1989, pp. 831-845.

[81] Burl, J. B., Linear Optimal Control: H2 and H∞ Methods, Addison Wesley Longman, Co., Inc., New York, 1999.

[82] Long, Y., Miyagi, H. and Yamashite, k., "Windmill Power Systems Controller Design Using H∞ Theory," IEEE Conference of Systems, Man, and Cybernetics, Vol. 5, 2002, pp. 3490-3495.

[83] Mei, S., Lon-Sen, T., Hu, W. and Lo, Q., "Robust H∞ of Hamilton System and Application to Power Systems," International Conference on Control and Automation, 2002, pp. 84-88.

[84] Connor, B., Lyers, S. Leithead, W. and Grimble, M., "Control of Horizontal Axis Wind Turbine Using H∞ Control," First IEEE Conference on Control Applications, 1992, pp. 117-122.

[85] Pal, B., Chaudhuri, B., Robust Control in power systems, Springer Science & Business Media, Inc., 2005.

A P P E N D I C E S

A p p e n d i x A

Machine Equations

A.1 Synchronous Machines

All conventional generating units discussed in this thesis are represented by synchronous machines. The equations representing the electrical model of the machine are as follows [24]:

$$\mathbf{V_d = R_s\, i_d + \frac{d}{dt}\varphi_d - \omega_R \varphi_q}$$

$$\mathbf{V_q = R_s\, i_q + \frac{d}{dt}\varphi_q + \omega_R \varphi_d}$$

$$\mathbf{V'_{fd} = R'_{fd}\, i'_{fd} + \frac{d}{dt}\varphi'_{fd}}$$

$$\mathbf{V'_{kd} = R'_{kd}\, i'_{kd} + \frac{d}{dt}\varphi'_{kd}}$$

$$\mathbf{V'_{kq1} = R'_{kq1}\, i'_{kq1} + \frac{d}{dt}\varphi'_{kq1}}$$

$$\mathbf{V'_{kq2} = R'_{kq2}\, i'_{kq2} + \frac{d}{dt}\varphi'_{kq2}} \qquad \text{(A.1)}$$

Where

$$\mathbf{\varphi_d = L_d\, i_d + L_{md}(i'_{fd} + i'_{kd})}$$

$$\mathbf{\varphi_q = L_q\, i_q + L_{mq}\, i'_{kq}}$$

$$\mathbf{\varphi'_{fd} = L'_{fd}\, i'_{fd} + L_{md}(i_d + i'_{kd})}$$

$$\mathbf{\varphi'_{kd} = L'_{kd}\, i'_{kd} + L_{md}(i_d + i'_{fd})}$$

$$\mathbf{\varphi'_{kq1} = L'_{kq1}\, i'_{kq1} + L_{mq}\, i_q}$$

$$\mathbf{\varphi'_{kq2} = L'_{kq2}\, i'_{kq2} + L_{mq}\, i_q} \qquad \text{(A.2)}$$

And the Mechanical part of the model is given by:

$$\frac{d}{dt}\omega_m = \frac{1}{2H}(T_e - F\omega_m - T_m)$$
$$\frac{d}{dt}\theta_m = \omega_m . \tag{A.3}$$

A.2 Induction Machines

All FSIG wind farms discussed in this thesis are induction machine based. Hence, the electrical part of the induction machine model is presented by the equations[24]:

$$V_{qs} = R_s\, i_{qs} + \frac{d}{dt}\varphi_{qs} + \omega\,\varphi_{ds}$$

$$V_{ds} = R_s\, i_{ds} + \frac{d}{dt}\varphi_{ds} - \omega\,\varphi_{qs}$$

$$V'_{qr} = R'_r\, i'_{qr} + \frac{d}{dt}\varphi'_{qr} + (\omega - \omega_r)\,\varphi'_{dr}$$

$$V'_{dr} = R'_r\, i'_{dr} + \frac{d}{dt}\varphi'_{dr} - (\omega - \omega_r)\,\varphi'_{qr}$$

$$T_e = 1.5\,p\,(\varphi_{ds}\, i_{qs} - \varphi_{qs}\, i_{ds}) \tag{A.4}$$

Where,

$$\varphi_{qs} = L_s i_{qs} + L_m i'_{qr},$$

$$\varphi_{ds} = L_s i_{ds} + L_m i'_{dr},$$

$$\varphi'_{qr} = L'_r i'_{qr} + L_m i_{qs},$$

$$\varphi'_{dr} = L'_r i'_{dr} + L_m i_{ds},$$

$$L_s = L_{ls} + L_m,$$

$$L'_r = L'_{lr} + L_m . \tag{A.5}$$

And the Mechanical part of the model is similar to (A.3).

A.3 Wind Turbine

The output power of the wind turbine is given by [72]:

$$\mathbf{P_m = C_p(\lambda,\beta)\frac{\rho A}{2} v_{wind}^3}. \tag{A.6}$$

Where P_m is the mechanical output power of the wind turbine, C_p is the performance coefficient of the wind turbine, ρ is the air density, A is the wind turbine swept area, v_{wind} is wind speed, λ is the tip speed ratio of the rotor blade tip to the wind speed, and β is the wind turbine blade pitch angle [72].

$$\mathbf{C_p(\lambda,\beta) = C_1\left(\frac{C_2}{\lambda_i} - C_3\beta - C_4\right)^{\frac{-C_5}{\lambda_i}} + C_6\lambda} \tag{A.7}$$

Where the parameter λ_i is given as:

$$\mathbf{\frac{1}{\lambda_i} = \frac{1}{\lambda + 0.08\beta} - \frac{0.035}{\beta^2 + 1}}, \tag{A.8}$$

And the coefficients C_1 to C_6 are: $C_1 = 0.5176$, $C_2 = 116$, $C_3 = 0.4$, $C_4 = 5$, $C_5 = 21$ and $C_6 = 0.0068$.

A p p e n d i x B

Model Parameters

B.1 All Synchronous Machines parameters (on base of machine rating) are as follows[24]

$\mathbf{V_n}$ = 20000 (VA), $\mathbf{f_n}$ = 50 (Hz),

$\mathbf{x_d}$ = 1.782 (p.u), $\mathbf{x'_d}$ = 0.444 (p.u), $\mathbf{x''_d}$ = 0.283 (p.u),

$\mathbf{x_q}$ = 1.739 (p.u), $\mathbf{x'_q}$ = 1.201 (p.u), $\mathbf{x''_q}$ = 0.2777 (p.u),

$\mathbf{x_l}$ = 0.275 (p.u), $\mathbf{R_S}$ = 0.0041 (p.u),

$\mathbf{T'_{d0}}$ = 6.07 s, $\mathbf{T'_{q0}}$ = 0.055 s, $\mathbf{T''_{d0}}$ = 1.5 s, $\mathbf{T''_{q0}}$ = 0.152 s,

H = 3.98-5 s, **F** = 0.00 (p.u).

B.2 Asynchronous Machine parameters (on base of machine rating [24]

$\mathbf{V_n}$ = 460 (Vrms), $\mathbf{f_n}$ = 50 (Hz),

$\mathbf{L_{ls}}$ = 0.0397 (p.u), $\mathbf{L'_{lr}}$ = 0.0397 (p.u), $\mathbf{L_m}$ = 1.354 (p.u),

$\mathbf{R_S}$ = 0.01965 (p.u), $\mathbf{R'_r}$ = 0.01909 (p.u),

H = 3.00 s, **F** = 0.0548 (p.u).

B.3 Excitation Control System Model [24]

K_A = 200, T_A = 0.01 s, T_E = 0.0 s.

B.4 Fossil Fueled Steam Turbine and Governor Parameters [24]

T_{CH} = 0.3 s, T_{RH} = 7.0 s, T_{CO} = 0.3 s,

F_{HP} =0.3 s, F_{IP} = 0.3 s, F_{LP} = 0.4 s, R_S = 0.04 (p.u).

L_{C1} = 0.1 ─ 1.0 (p.u/s), L_{C2} = -1.0 ─ -0.1 (p.u/s),

L_{I1} = 0.1 ─ 1.0 (p.u/s), L_{I2} =-1.0 ─ -0.1 (p.u/s).

B.5 Nuclear Plant Parameters [24]

T_G = 0.2 s, T_{RH} = 5.0 s, T_{CH} = 0.3 s, T_{CO} = 0.3 s,

F_{HP} =o.3 s, F_{LP} = 0.7 s,

R = 0.04 (p.u), K_G=1/R.

L_{C1} = 0.1 ─ 1.0 (p.u/s), L_{C2} = -1.0 ─ -0.1 (p.u/s),

L_{I1} = 0.1 ─ 1.0 (p.u/s), L_{I2} =-1.0 ─ -0.1 (p.u/s).

B.6 Hydro Plant Parameters [24]

T_G = 0.2 s, T_R = 5.0 s,

T_W = 1.0 s, T_1 = 37.5 s,

R = 0.04 (p.u).

B.7 HVDC Link Parameters [24]:

T_{dc}=0.5 sec, R = 0.04 (p.u).

B.8 Auxiliary Governor Parameters [24]

K_{AX} = 175.

B.9 Case Study Parameters

B.9.1 Case Study 1

Capacity factors:

$k_1 = 0.341$, $k_2 = 0.1705$, $k_3 = 0.1791$, $k_4 = 0.1776$, $k_5 = 0.065127$.

B.9.2 Case Study 2

Capacity factors:

$k_1 = 0.259167$, $k_2 = 0.12958$, $k_3 = 0.1361$, $k_4 = 0.13498$, $k_5 = 0.024746$.

B.9.3 Case Study 2

Capacity factors:

$k_1 = 0.0816159$, $k_2 = 0.07529$, $k_3 = 0.036421$, $k_4 = 0.138237$, $k_5 = 0.07141$, $k_6 = 0.20057$, $k_7 = 0.082126$, $k_8 = 0.11028$, $k_9 = 0.0204$.

B.9.4 Common for all Case Studies

$M_{eq} \approx 4$, $D=0$

Where, M_{eq} is calculated as $M_{eq} = \frac{\sum_{i=1}^{n} M_i P_i}{\sum_{i=1}^{n} P_i}$, k_i is calculated as $k_i = \frac{P_i}{\sum_{i=1}^{n} P_i}$ and P_i is the installed capacity of generator i.

Appendix C

The Linear Quadratic Regulator LQR Problem

C.1 Introduction

Linear Quadratic control (LQ) refers to a body of techniques developed since 1960's for control systems design. The LQ problem is an important part of optimal control. The plant is assumed to be a linear system in state space form, and the objective function is a quadratic functional of the plant states and control inputs. The problem is to minimize the quadratic functional with respect to the control inputs subject to linear system constraints [79].

This thesis considers the steady state case. In this case the control law is a linear time invariant function of the states or outputs of the system. The advantage of LQ formulation of problems is that it leads to linear control laws that are easy to implement and analyze [79].

This section presents introductory information about LQ. Section A.2 defines the linear quadratic regulator problem. Section A.3 discusses the LQR problem solution.

C.2 The linear Quadratic Regulator Problem

Consider the linear system and the quadratic objective function (or cost function)

$$\dot{x} = Ax + Bu$$
$$y = Cx$$

$$J = \frac{1}{2}\int_0^T (x'Qx + u'Ru)dt \tag{C.1}$$

The problem is to minimize J with respect to the control input $u(t)$. This is known as the Linear Quadratic Regulator (LQR) problem.

If the system is scalar (i.e. first order), the cost function becomes

$$J = \frac{1}{2}\int_0^T qx^2 + ru^2 dt \tag{C.2}$$

Where J represents the weighted sum of energy of the state and control. If r is very large relative to q, the control energy is penalized very heavily. This means smaller motors,

actuators, and amplifier gains are needed to implement the control law. Like wise, if q is much larger than r, the state is penalized heavily, resulting in a much damped system [79].

Generally, Q and R represent respective weights on different states and control channels. This makes Q and R the main design parameters. These parameters are chosen, in general, through several design iterations to obtain a stable optimal system with "good" response.

For a meaningful optimization problem, Q must be symmetric positive semi definite (written as $Q \geq 0$) and R must be symmetric definite ($R > 0$) [79, 81].

Another LQR problem is the special case, where the outputs instead of states are weighted, i.e. the cost function is [$y'Qy + u'Ru$].

C.3 LQR Solution

Optimal control problems are solved using the minimum principle. This principle is applied to the Hamiltonian function given by [79]:

$$H(x,\lambda,t) = \frac{1}{2}(x'Qx + u'Ru) + \lambda'(Ax + Bu) \tag{C.3}$$

The minimum principle states that the optimal control and state trajectories must satisfy the following three equations:

State equations $\dot{x} = \dfrac{\partial H}{\partial \lambda}, \qquad x(0) = x_O$

Co-state or adjoint equations $-\dot{\lambda} = \dfrac{\partial H}{\partial x}, \quad \lambda(T) = 0$ (C.4)

and $\dfrac{\partial H}{\partial u} = 0$

Differentiation of equations (A.4) become:

$$\dot{x} = Ax + Bu \qquad x(0) = x_O$$

$$-\dot{\lambda} = Qx + A'\lambda \qquad \lambda(T) = 0 \tag{C.5}$$

$$u^* = -R^{-1}B'\lambda$$

Where u^* is the optimal control.

Substituting the optimal control into the state equation we get:

$$\begin{bmatrix} \dot{x} \\ \dot{\lambda} \end{bmatrix} = \begin{bmatrix} A & -BR^{-1}B' \\ -Q & -A' \end{bmatrix} \begin{bmatrix} x \\ \lambda \end{bmatrix} \triangleq H \begin{bmatrix} x \\ \lambda \end{bmatrix} \tag{C.6}$$

The above matrix, H, is called the Hamiltonian matrix and plays an important role in the LQR theory. Making the following substitution

$$\lambda = Px \tag{C.7}$$

Differentiating both sides with respect to time and substituting for λ we get

$$\frac{d\lambda}{dt} = \frac{dP}{dt}x + P\frac{dx}{dt} = \frac{dP}{dt}x + PAx - PBR^{-1}B'Px = -Qx - A'Px \tag{C.8}$$

The above equation must hold for any x, hence a sufficient condition for optimal control is that P must satisfy

$$-\frac{dP}{dt} = A'P + PA + Q - PBR^{-1}B'P, \;\; P(T) = 0 \tag{C.9}$$

The above is the famous Riccati differential equation. It is a nonlinear first order differential equation that has to be solved backwards in time.

The above formulation and solution of the LQR problem is known as the finite time (or finite horizon) problem. It results in a linear time varying controller of the feedback form [24]:

$$u(t) = -K(t)x(t) \text{ where, } K(t) = R^{-1}B'P(t) \tag{C.10}$$

For the infinite time LQR problem, we let t approach infinity. It turns out that, $P(t)$ approaches a constant matrix P (hence $dP/dt \rightarrow 0$), and hence the positive definite solution of the Algebric Riccati Equation (ARE) results in an asymptotically stable closed loop system.

$$\text{(ARE)} \qquad A'P + PA + Q - PBR^{-1}B'P = 0$$

$$u = -Kx, \qquad K = R^{-1}B'P \tag{C.11}$$

The exact conditions for the above to hold are the following. The pair (A, B) are stabilizable, $R>0$, and Q can be factored as $Q = C'_q C_q$, where C_q is any matrix such that (C_q, A) is detectable. These conditions are necessary and sufficient for existence and uniqueness of an optimal controller that will asymptotically stabilize the system.

A p p e n d i x D

Flow Chart: Design Approach for Linear Quadratic Regulator

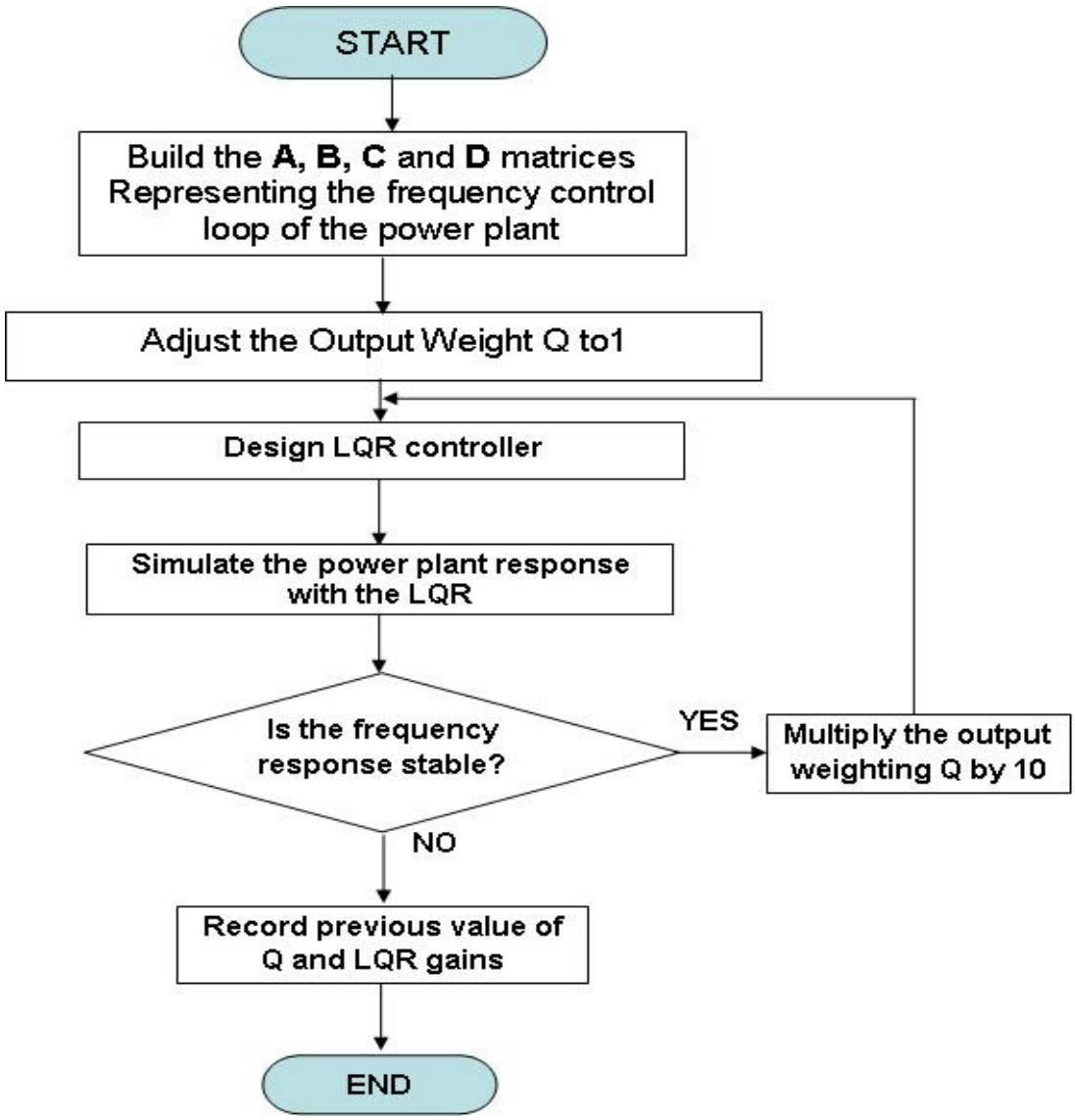

Figure. D.1 Design Approach for LQR Regulator

A p p e n d i x E

LQR Gains for Thesis Case Studies at Different Speed Weightings

Table E.1 LQR Gains versus Speed Weighting for Case Study 1

Q=	1e1	1e2	1e3	1e4	1e5	1e6	1e7	1e8
K_1	0.0010194	0.0092268	0.055035	0.17885	0.41575	0.83438	1.5655	2.8749
K_2	0.0050455	0.046173	0.29173	1.0823	3.0618	**7.8608**	19.459	47.626
K_3	0.039236	0.34489	1.7754	4.5064	8.8896	**17.296**	34.942	73.845
K_4	0.0036905	0.034429	0.23606	0.96759	2.8916	**7.6159**	19.09	47.035
K_5	0.0005097	0.0046134	0.027518	0.089427	0.20788	0.41719	0.78274	1.4375
K_6	0.0025227	0.023087	0.14587	0.54117	1.5309	**3.9304**	9.7297	23.813
K_7	0.019618	0.17245	0.88771	2.2532	4.4448	**8.6479**	17.471	36.922
K_8	0.0018453	0.017215	0.11803	0.4838	1.4458	**3.808**	9.5451	23.518
K_9	0.00060127	0.0054206	0.031769	0.1005	0.22833	0.45107	0.83801	1.5299
K_{10}	0.0030067	0.027401	0.17004	0.61431	1.6991	**4.2917**	10.504	25.512
K_{11}	0.0095703	0.084647	0.45304	1.2664	2.8082	**6.0853**	13.445	30.489
K_{12}	0.00059978	0.0054056	0.031643	0.099934	0.22679	0.44774	0.83156	1.5179
K_{13}	0.0030014	0.027344	0.16947	0.61117	1.6885	**4.2617**	10.427	25.316
K_{14}	0.0094767	0.083815	0.44859	1.2545	2.7829	**6.032**	13.33	30.23
K_{15}	5.1348e-050.0025415	0.00056804	0.0065098	0.035219	0.096896	0.20274	0.3835	0.70481
K_{16}		0.022239	0.10898	0.23364	0.36539	0.55743	0.88161	1.4594
K_{17}	0.0011869	0.010914	0.070166	0.25929	0.70452	1.7272	4.1185	9.8082
K_{18}	**0.22606**	**2.1652**	**16.617**	**81.695**	**300.09**	**992.17**	**3174.3**	**10058**

Table E.2 LQR Gains Versus Speed Weighting for Case Study 2.

Q=	**1e1**	**1e2**	**1e3**	**1e4**	**1e5**	**1e6**	**1e7**	**1e8**
$\mathbf{K_1}$	0.00073335	0.006724	0.041851	0.14194	0.3381	0.68075	1.2519	2.1945
$\mathbf{K_2}$	0.0036486	0.033721	0.2195	0.83397	2.3852	**6.1272**	15.012	35.902
$\mathbf{K_3}$	0.031961	0.28432	1.5108	3.8562	7.444	**14.071**	27.505	55.808
$\mathbf{K_4}$	0.0024877	0.023519	0.16914	0.72845	2.2326	**5.9173**	14.713	35.456
$\mathbf{K_5}$	0.00036668	0.003362	0.020926	0.070972	0.16905	0.34038	0.62596	1.0973
$\mathbf{K_6}$	0.0018243	0.016861	0.10975	0.41699	1.1926	**3.0636**	7.506	17.951
$\mathbf{K_7}$	0.01598	0.14216	0.7554	1.9281	3.722	**7.0354**	13.752	27.904
$\mathbf{K_8}$	0.0012438	0.01176	0.084568	0.36422	1.1163	**2.9587**	7.3564	17.728
$\mathbf{K_9}$	0.00043567	0.00398	0.024356	0.08032	0.18654	0.3689	0.6707	1.1676
$\mathbf{K_{10}}$	0.0021839	0.020111	0.12875	0.47616	1.3292	**3.3535**	8.1131	19.236
$\mathbf{K_{11}}$	0.007574	0.067777	0.37399	1.0511	2.292	**4.864**	10.486	23.015
$\mathbf{K_{12}}$	0.0004349	0.0039718	0.024275	0.079901	0.18532	0.36621	0.66555	1.1584
$\mathbf{K_{13}}$	0.0021812	0.020081	0.12839	0.47391	1.3212	**3.3304**	8.0533	19.088
$\mathbf{K_{14}}$	0.0074947	0.067067	0.37016	1.041	2.2712	**4.8212**	10.396	22.819
$\mathbf{K_{15}}$	-1.5505e-05	-8.6098e-05	0.0012036	0.012286	0.038434	0.082486	0.15354	0.26938
$\mathbf{K_{16}}$	0.0011164	0.0098749	0.049793	0.10677	0.16169	0.23652	0.3561	0.55244
$\mathbf{K_{17}}$	0.00040202	0.0037576	0.02558	0.099816	0.27692	0.6784	1.5952	3.7002
$\mathbf{K_{18}}$	0.20997	2.0227	15.851	79.567	295.39	**981.95**	3151.5	10006

Table E.3 LQR Gains Versus Speed Weighting for Case Study 3.

Q=	1e1	1e2	1e3	1e4	1e5	1e6	1e7	1e8
K_1	0.0001815	0.0016717	0.010315	0.03182	0.063842	0.10193	0.13901	0.16786
K_2	0.00094043	0.0087682	0.05812	0.21517	0.57135	**1.3147**	2.7838	5.5418
K_3	0.005563	0.050213	0.2771	0.70819	1.3116	**2.2846**	3.9582	6.8705
K_4	0.00077069	0.007258	0.050525	0.20011	0.55196	**1.2924**	2.7591	5.5152
K_5	0.00016743	0.0015422	0.0095157	0.029354	0.058894	0.094032	0.12824	0.15485
K_6	0.00086755	0.0080887	0.053616	0.1985	0.52707	**1.2129**	2.5681	5.1123
K_7	0.0051319	0.046322	0.25563	0.6533	1.2099	**2.1075**	3.6515	6.3381
K_8	0.00071096	0.0066955	0.046609	0.1846	0.50918	**1.1923**	2.5453	5.0878
K_9	8.0993e-05	0.00074601	0.0046031	0.0142	0.028489	0.045487	0.062034	0.074906
K_{10}	0.00041967	0.0039128	0.025936	0.096021	0.25497	**0.58671**	1.2423	2.473
K_{11}	0.0024825	0.022408	0.12366	0.31603	0.58528	**1.0195**	1.7664	3.066
K_{12}	0.00034392	0.0032389	0.022547	0.089299	0.24631	**0.57674**	1.2312	2.4612
K_{13}	0.00030741	0.0028315	0.017471	0.053895	0.10813	0.17265	0.23545	0.28431
K_{14}	0.0015929	0.014851	0.098441	0.36445	0.96773	**2.2269**	4.7151	9.3864
K_{15}	0.0094223	0.085049	0.46934	1.1995	2.2215	**3.8695**	6.7043	11.637
K_{16}	0.0013054	0.012293	0.085577	0.33894	0.93488	**2.189**	4.6732	9.3414
K_{17}	0.00015881	0.0014628	0.0090257	0.027843	0.055861	0.089191	0.12164	0.14687
K_{18}	0.00082288	0.0076722	0.050855	0.18828	0.49993	**1.1504**	2.4359	4.8491
K_{19}	0.0048676	0.043937	0.24246	0.61966	1.1476	**1.999**	3.4635	6.0117
K_{20}	0.00067435	0.0063508	0.044209	0.1751	0.48296	**1.1309**	2.4142	4.8258
K_{21}	0.00044603	0.0041083	0.025349	0.078198	0.15689	0.2505	0.34162	0.41251
K_{22}	0.0023111	0.021548	0.14283	0.52879	1.4041	**3.231**	6.8413	13.619
K_{23}	0.013671	0.1234	0.68098	1.7404	3.2232	**5.6143**	9.7274	16.884
K_{24}	0.001894	0.017837	0.12416	0.49177	1.3564	**3.1761**	6.7805	13.554
K_{25}	0.00018263	0.0016822	0.01038	0.032019	0.064241	0.10257	0.13988	0.16891
K_{26}	0.00094631	0.008823	0.058483	0.21652	0.57492	**1.323**	2.8012	5.5764
K_{27}	0.0055978	0.050527	0.27883	0.71261	1.3198	**2.2988**	3.983	6.9135
K_{28}	0.00077551	0.0073034	0.050841	0.20136	0.55541	**1.3005**	2.7763	5.5497
K_{29}	0.00026941	0.0024748	0.015059	0.045332	0.08904	0.14014	0.18947	0.22771
K_{30}	0.001413	0.013136	0.085794	0.30975	0.80482	**1.8236**	3.8216	7.558
K_{31}	0.0036956	0.03358	0.19343	0.55149	1.1672	**2.2976**	4.395	8.2064
K_{32}	0.0030382	0.028282	0.18555	0.66158	1.6598	**3.6287**	7.4002	14.369
K_{33}	**0.20686**	**1.9956**	**15.717**	**79.224**	**294.6**	**979.97**	**3146.2**	**9991.5**

A p p e n d i x F

Case studies equivalent systems SIMULINK models

F.1 Case Study 1 Equivalent System SIMULINK models

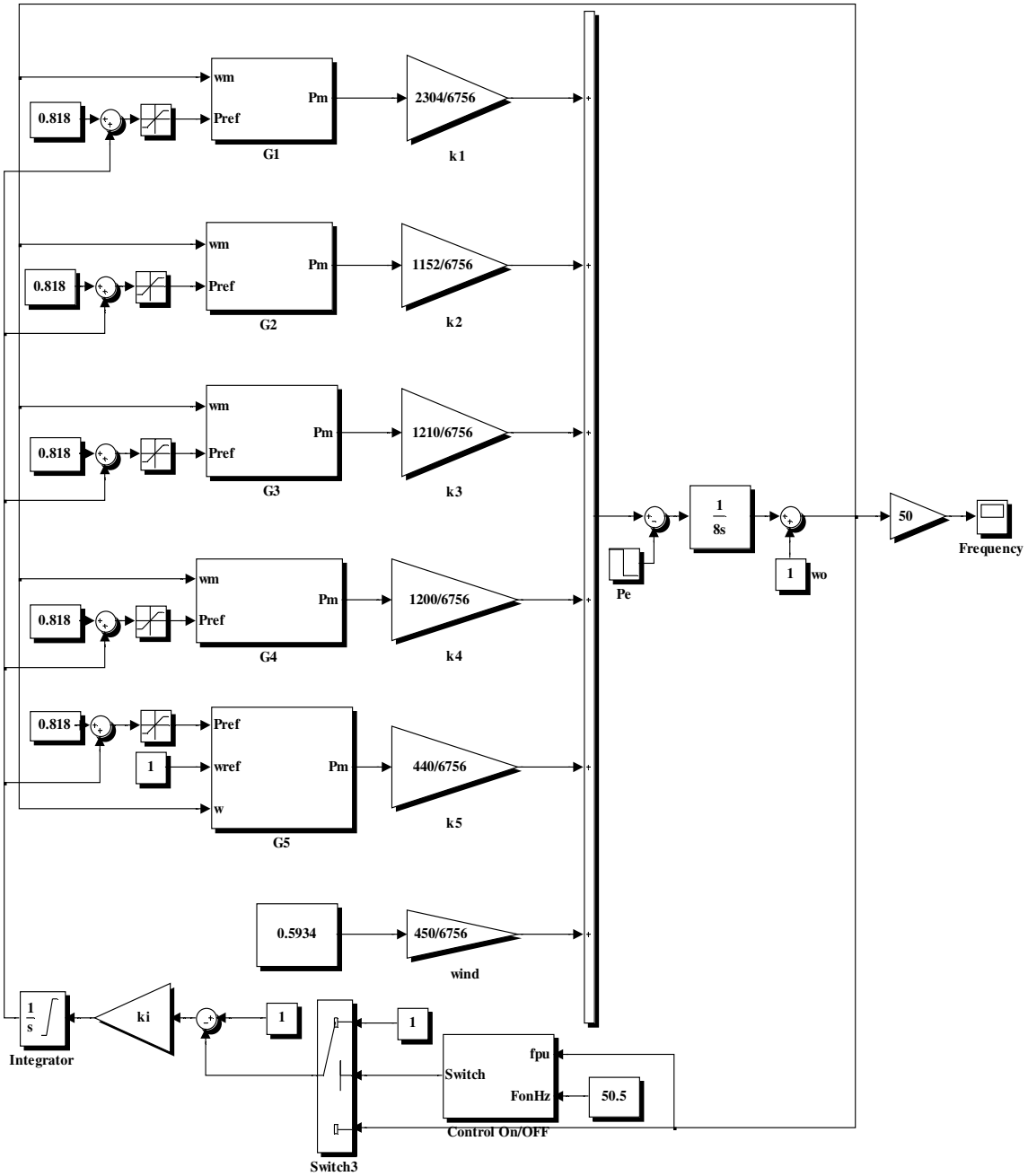

Figure F.1 Equivalent System of Case Study 1

F.2 Case Study 2 Equivalent System SIMULINK model

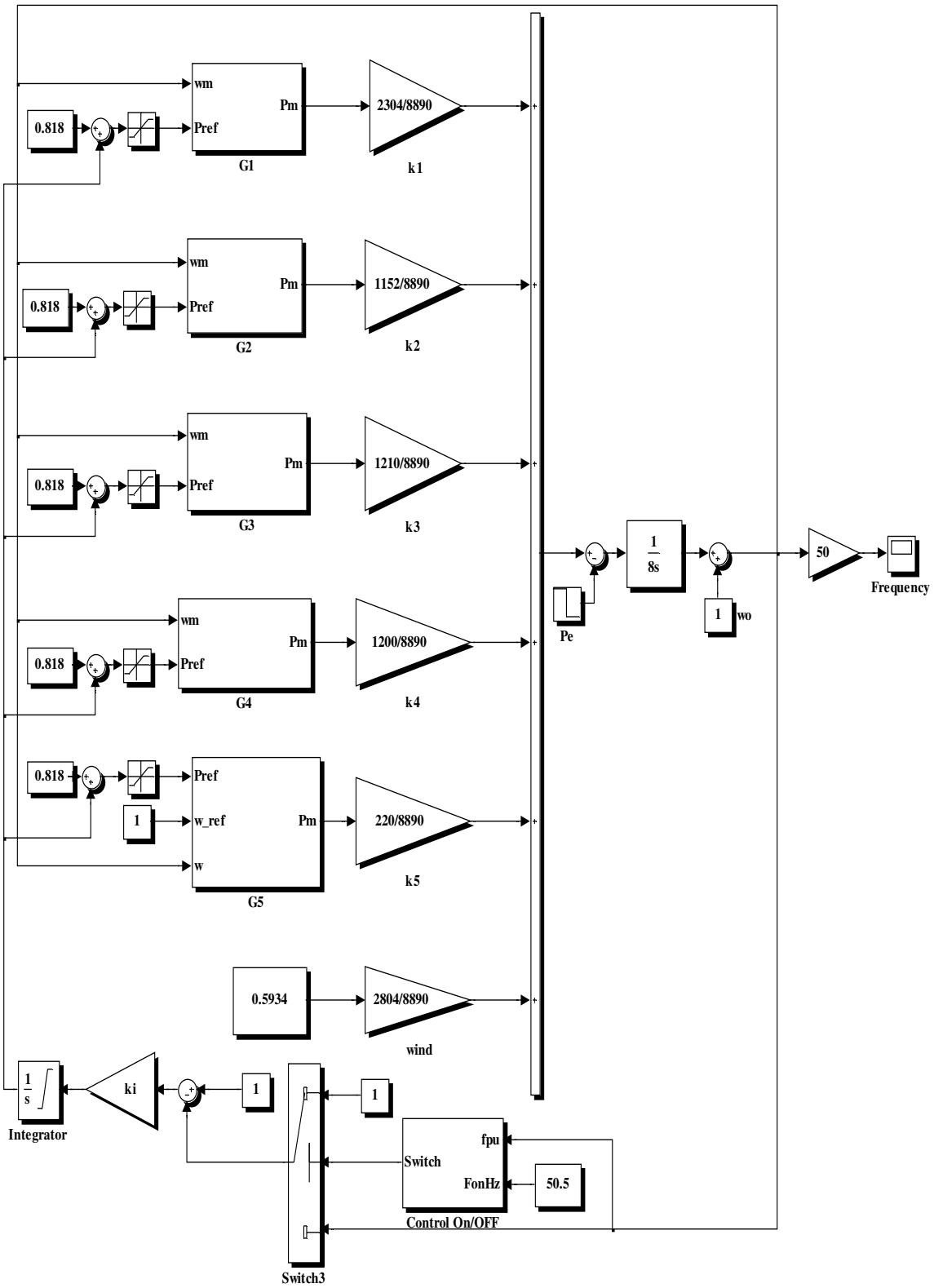

Figure F.2 Equivalent System of Case Study 2

F.3 Case Study 3 Equivalent System SIMULINK model

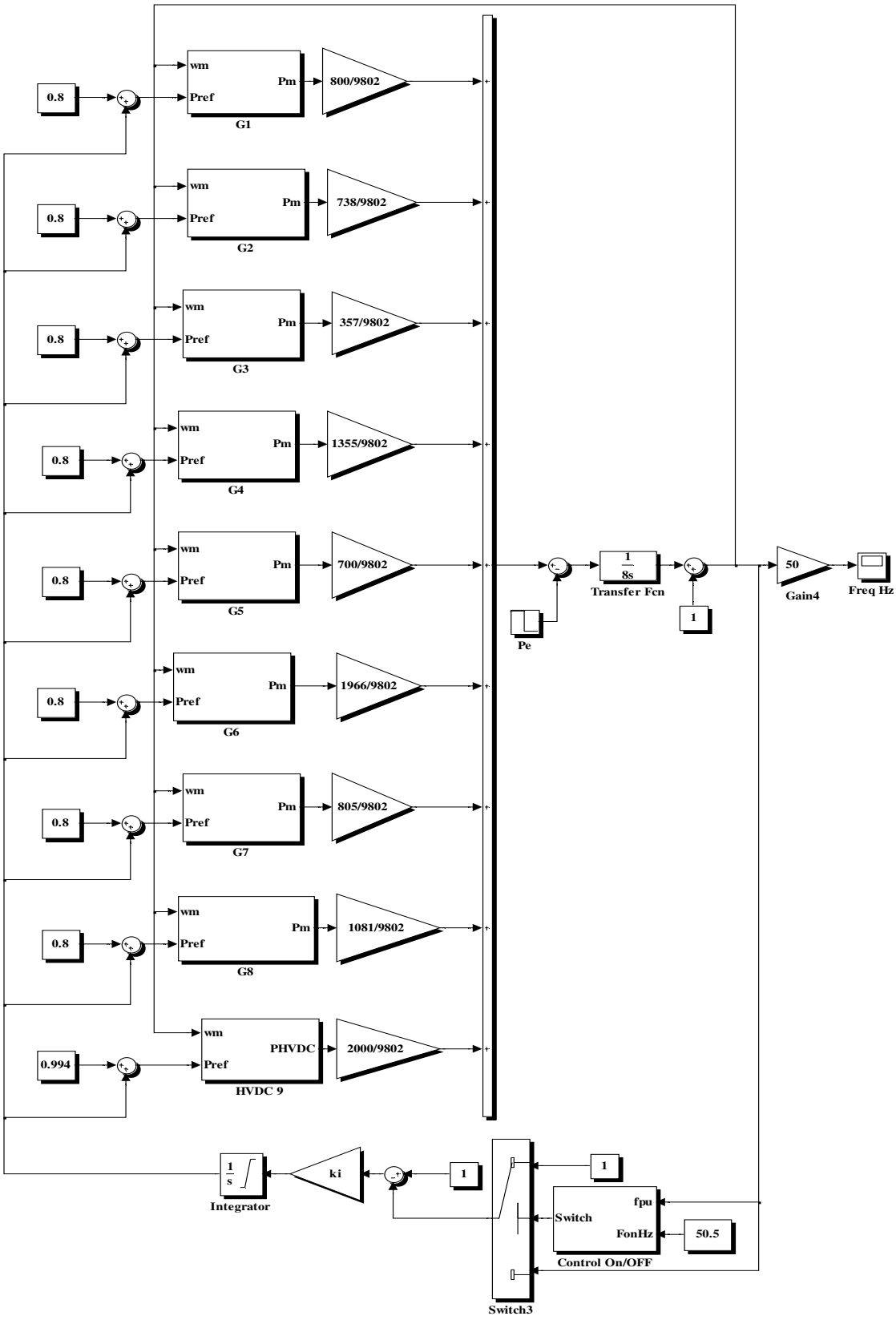

Figure F.3 Equivalent System of Case Study 3

F.3 Case Studies Prime Movers SIMULINK Models

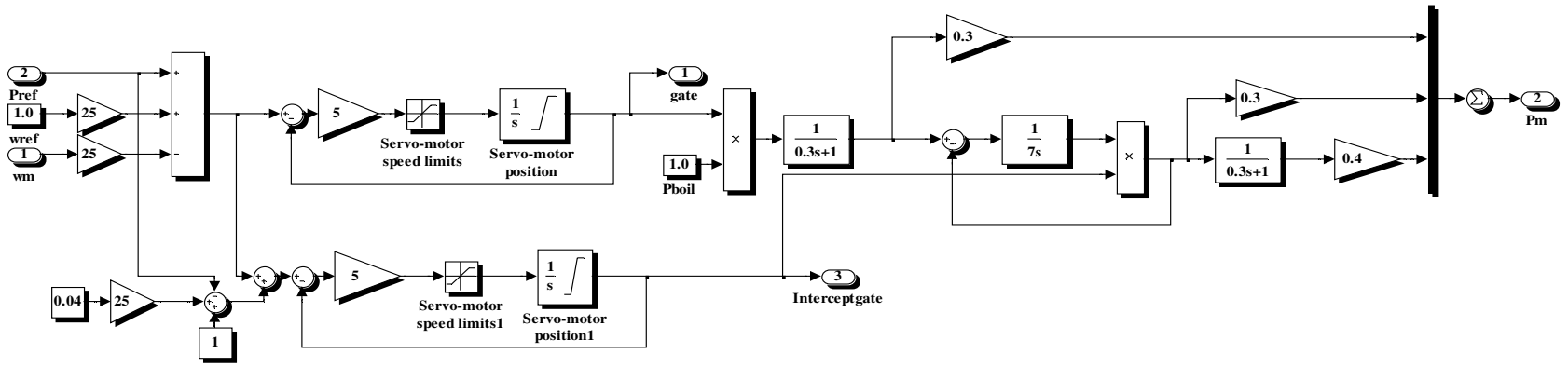

Figure F.4 Fossil Fuel unit prime mover model

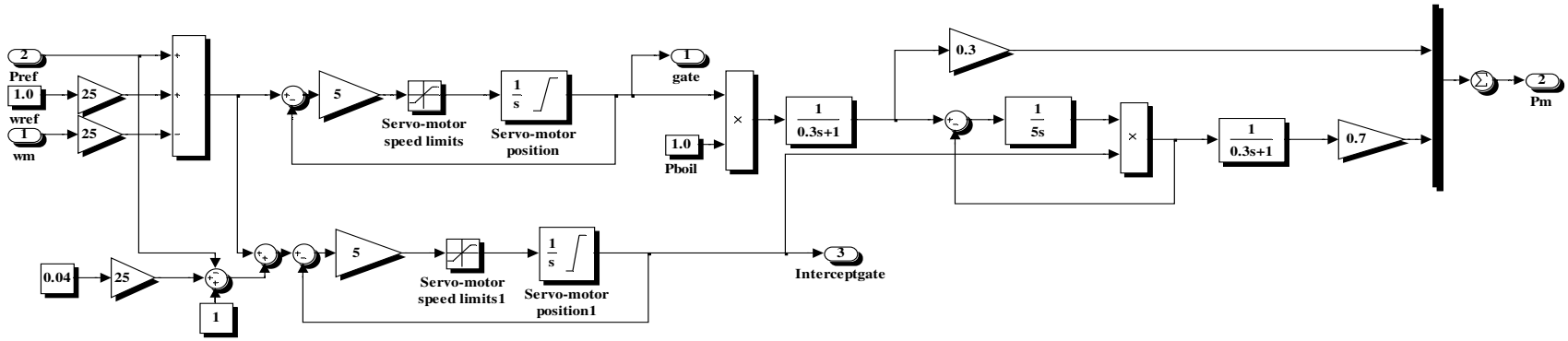

Figure F.5 Nuclear unit prime mover model

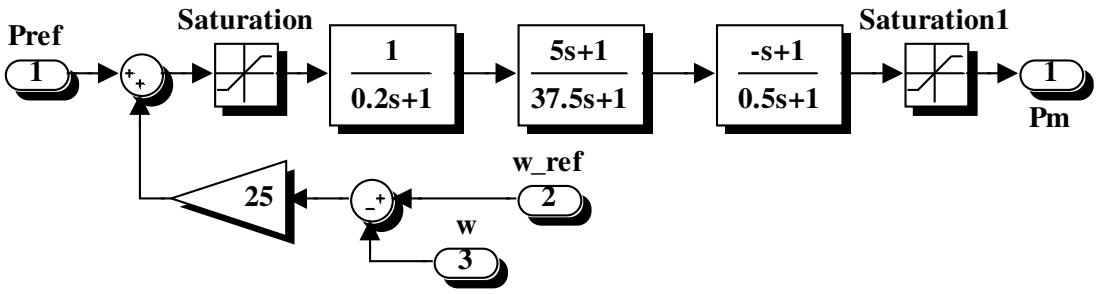

Figure F.6 Hydro unit prime mover model.

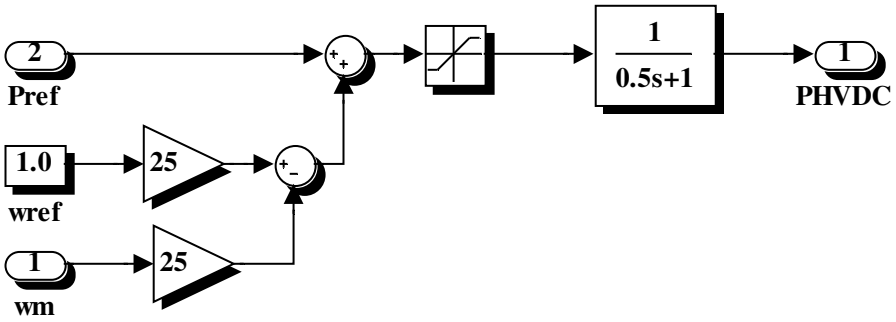

Figure F.6 HVDC model for frequency study.

A p p e n d i x G

Programs in M-FILE/MATLAB code for CASE STUDY 1, 2 and 3

Program 1

```
%Input capacity factors for generators of Case Study 1
k1=0.341;
k2=0.1705;
k3=0.1791;
k4=0.1776;
k5=0.065127;
% Input Fossil fuel Parameters
Tgs=input('Tgs=');
Rs=0.04;
FHs=0.3;
TCHs=0.3;
FIs=0.3;
TRHs=7;
FLs=0.4;
TCOs=0.3;
% Input Nuclear plant Parameters
Tgn=input('Tgn=')
Rn=0.04;
FHn=0.3;
TCHn=0.3;
TRHn=5;
FLn=0.7;
TCOn=0.3;
% Input Hydro plant Parameters
Tg=0.2;
Rh=0.04;
```

```
Tr=5;
rt=0.3;
T2=(rt/Rh)*Tr;
Tw=1;
% Input system parameters
M=8;
D=0;
%Build ABCD matrix for Case Study 1
%G1
Ac(1,1)=-1/Tgs;
Ac(1,18)=-1/(Rs*Tgs);
Ac(2,1)=FHs/TCHs;
Ac(2,2)=-1/TCHs;
Ac(3,2)=FIs/(FHs*TRHs);
Ac(3,3)=-1/TRHs;
Ac(4,3)=(FLs/FIs)/(TCOs);
Ac(4,4)=-1/TCOs;
Ac(18,2)=k1/M;
Ac(18,3)=k1/M;
Ac(18,4)=k1/M;
Bc(1,1)=(1/Tgs);
%G2
Ac(5,5)=-1/Tgs;
Ac(5,18)=-1/(Rs*Tgs);
Ac(6,5)=FHs/TCHs;
Ac(6,6)=-1/TCHs;
Ac(7,6)=FIs/(FHs*TRHs);
Ac(7,7)=-1/TRHs;
Ac(8,7)=(FLs/FIs)/(TCOs);
Ac(8,8)=-1/TCOs;
Ac(18,6)=k2/M;
Ac(18,7)=k2/M;
Ac(18,8)=k2/M;
Bc(5,1)=(1/Tgs);
```

```
%G3 nuclear
Ac(9,9)=-1/Tgn;
Ac(9,18)=-1/(Rn*Tgn);
Ac(10,9)=FHn/TCHn;
Ac(10,10)=-1/TCHn;
Ac(11,10)=FLn/(FHn*(TRHn+TCOn));
Ac(11,11)=-1/(TRHn+TCOn);
Ac(18,9)=0;
Ac(18,10)=k3/M;
Ac(18,11)=k3/M;
Bc(9,1)=(1/Tgn);
%G4 nuclear
Ac(12,12)=-1/Tgn;
Ac(12,18)=-1/(Rn*Tgn);
Ac(13,12)=FHn/TCHn;
Ac(13,13)=-1/TCHn;
Ac(14,13)=FLn/(FHn*(TRHn+TCOn));
Ac(14,14)=-1/(TRHn+TCOn);
Ac(18,12)=0;
Ac(18,13)=k4/M;
Ac(18,14)=k4/M;
Bc(12,1)=(1/Tgn);
%G5 hydro
Ac(15,15)=-1/Tg;
Ac(15,16)=0;
Ac(15,17)=0;
Ac(15,18)=-1/(Rh*Tg);
Ac(16,15)=(1/T2)-(Tr/(T2*Tg));
Ac(16,16)=-1/T2;
Ac(16,17)=0;
Ac(16,18)=-Tr/(T2*Rh*Tg);
Ac(17,15)=-2*((1/T2)-(Tr/(T2*Tg)));
Ac(17,16)=(2/Tw)+(2/T2);
Ac(17,17)=-2/Tw;
```

```
Ac(17,18)=(2*Tr)/(T2*Rh*Tg);
Ac(18,15)=0;
Ac(18,16)=0;
Ac(18,17)=k5/M;
Ac(18,18)=-D/M;
Bc(15,1)=1/Tg;
Bc(16,1)=Tr/(T2*Tg);
Bc(17,1)=(-2*Tr)/(T2*Tg);
Bc(18,2)=-1/M;
Cc(1,18)=1;
Dc(1,2)=0;
%EigenValue Calculation
E=eig(Ac)
% Changing from ABCD format to Transfer function
[num,den]=ss2tf(Ac,Bc,Cc,Dc,1)
% Root Locus to design an Integral Controller
den2=[den 0]
rlocus(num,den2)
v=[-10 10 -10 10]
axis(v)
% Designing LQR controller and calculating eigenvalues after control
q=input('q=')
Qc=[q];
Rc=[1];
[Kc,Sc,Ec]=lqry(Ac,Bc(:,1),Cc,Dc(:,1),Qc,Rc)
%LQR Gains and System Eigen value after controller applied
Kc;
Ec;
```

Program 2

```
%Input capacity factors for generators of Case Study 1
k1=0.259167;
```

```
k2=0.12958;
k3=0.1361;
k4=0.13498;
k5=0.024746;
% Input Fossil fuel Parameters
Tgs=input('Tgs=');
Rs=0.04;
FHs=0.3;
TCHs=0.3;
FIs=0.3;
TRHs=7;
FLs=0.4;
TCOs=0.3;
% Input Nuclear plant Parameters
Tgn=input('Tgn=')
Rn=0.04;
FHn=0.3;
TCHn=0.3;
TRHn=5;
FLn=0.7;
TCOn=0.3;
M=8;
% Input Hydro plant Parameters
Tg=0.2;
Rh=0.04;
Tr=5;
rt=0.3;
T2=(rt/Rh)*Tr;
Tw=1;
% Input system parameters
M=8;
D=0;
%Build ABCD matrix for Case Study 1
%G1
```

```
Ac(1,1)=-1/Tgs;
Ac(1,18)=-1/(Rs*Tgs);
Ac(2,1)=FHs/TCHs;
Ac(2,2)=-1/TCHs;
Ac(3,2)=FIs/(FHs*TRHs);
Ac(3,3)=-1/TRHs;
Ac(4,3)=(FLs/FIs)/(TCOs);
Ac(4,4)=-1/TCOs;
Ac(18,2)=k1/M;
Ac(18,3)=k1/M;
Ac(18,4)=k1/M;
Bc(1,1)=(1/Tgs);
%G2
Ac(5,5)=-1/Tgs;
Ac(5,18)=-1/(Rs*Tgs);
Ac(6,5)=FHs/TCHs;
Ac(6,6)=-1/TCHs;
Ac(7,6)=FIs/(FHs*TRHs);
Ac(7,7)=-1/TRHs;
Ac(8,7)=(FLs/FIs)/(TCOs);
Ac(8,8)=-1/TCOs;
Ac(18,6)=k2/M;
Ac(18,7)=k2/M;
Ac(18,8)=k2/M;
Bc(5,1)=(1/Tgs);
%G3 nuclear
Ac(9,9)=-1/Tgn;
Ac(9,18)=-1/(Rn*Tgn);
Ac(10,9)=FHn/TCHn;
Ac(10,10)=-1/TCHn;
Ac(11,10)=FLn/(FHn*(TRHn+TCOn));
Ac(11,11)=-1/(TRHn+TCOn);
Ac(18,9)=0;
Ac(18,10)=k3/M;
```

```
Ac(18,11)=k3/M;

Bc(9,1)=(1/Tgn);

%G4 nuclear

Ac(12,12)=-1/Tgn;

Ac(12,18)=-1/(Rn*Tgn);

Ac(13,12)=FHn/TCHn;

Ac(13,13)=-1/TCHn;

Ac(14,13)=FLn/(FHn*(TRHn+TCOn));

Ac(14,14)=-1/(TRHn+TCOn);

Ac(18,12)=0;

Ac(18,13)=k4/M;

Ac(18,14)=k4/M;

Bc(12,1)=(1/Tgn);

%G5 hydro

Ac(15,15)=-1/Tg;

Ac(15,16)=0;

Ac(15,17)=0;

Ac(15,18)=-1/(Rh*Tg);

Ac(16,15)=(1/T2)-(Tr/(T2*Tg));

Ac(16,16)=-1/T2;

Ac(16,17)=0;

Ac(16,18)=-Tr/(T2*Rh*Tg);

Ac(17,15)=-2*((1/T2)-(Tr/(T2*Tg)));

Ac(17,16)=(2/Tw)+(2/T2);

Ac(17,17)=-2/Tw;

Ac(17,18)=(2*Tr)/(T2*Rh*Tg);

Ac(18,15)=0;

Ac(18,16)=0;

Ac(18,17)=k5/M;

Ac(18,18)=-D/M;

Bc(15,1)=1/Tg;

Bc(16,1)=Tr/(T2*Tg);

Bc(17,1)=(-2*Tr)/(T2*Tg);

Bc(18,2)=-1/M;
```

```
Cc(1,18)=1;
Dc(1,2)=0;
%EigenValue Calculation
E=eig(Ac)
% Changing from ABCD format to Transfer function
[num,den]=ss2tf(Ac,Bc,Cc,Dc,1)
% Root Locus to design an Integral Controller
den2=[den 0]
rlocus(num,den2)
v=[-10 10 -10 10]
axis(v)
% Designing LQR controller and calculating eigenvalues after control
q=input('q=')
Qc=[q];
Rc=[1];
[Kc,Sc,Ec]=lqry(Ac,Bc(:,1),Cc,Dc(:,1),Qc,Rc)
%LQR Gains and System Eigen value after controller applied
Kc;
Ec;
```

Program 3

```
%Input capacity factors for generators of Case Study 1
k1=0.0816159;
k2=0.07529;
k3=0.0364211;
k4=0.138237;
k5=0.07141;
k6=0.20057;
k7=0.082126;
k8=0.11028;
k9=0.0204;
% Input Fossil fuel Parameters
```

```
Tgs=input('Tgs=');
Rs=0.04;
FHs=0.3;
TCHs=0.3;
FIs=0.3;
TRHs=7;
FLs=0.4;
TCOs=0.3;
% Input Nuclear plant Parameters
Tgn=input('Tgn=')
Rn=0.04;
FHn=0.3;
TCHn=0.3;
TRHn=5;
FLn=0.7;
TCOn=0.3;
%Input HVDC Parameters
R=0.04;
Tdc=input('Tdc=');
% Input system parameters
M=8;
D=0;
%Build ABCD matrix for Case Study 1
%G1
Ac(1,1)=-1/Tgs;
Ac(1,33)=-1/(Rs*Tgs);
Ac(2,1)=FHs/TCHs;
Ac(2,2)=-1/TCHs;
Ac(3,2)=FIs/(FHs*TRHs);
Ac(3,3)=-1/TRHs;
Ac(4,3)=(FLs/FIs)/(TCOs);
Ac(4,4)=-1/TCOs;
Ac(33,2)=k1/M;
Ac(33,3)=k1/M;
```

```
Ac(33,4)=k1/M;
Bc(1,1)=(1/Tgs);
%G2
Ac(5,5)=-1/Tgs;
Ac(5,33)=-1/(Rs*Tgs);
Ac(6,5)=FHs/TCHs;
Ac(6,6)=-1/TCHs;
Ac(7,6)=FIs/(FHs*TRHs);
Ac(7,7)=-1/TRHs;
Ac(8,7)=(FLs/FIs)/(TCOs);
Ac(8,8)=-1/TCOs;
Ac(33,6)=k2/M;
Ac(33,7)=k2/M;
Ac(33,8)=k2/M;
Bc(5,1)=(1/Tgs);
%G3
Ac(9,9)=-1/Tgs;
Ac(9,33)=-1/(Rs*Tgs);
Ac(10,9)=FHs/TCHs;
Ac(10,10)=-1/TCHs;
Ac(11,10)=FIs/(FHs*TRHs);
Ac(11,11)=-1/TRHs;
Ac(12,11)=(FLs/FIs)/(TCOs);
Ac(12,12)=-1/TCOs;
Ac(33,10)=k3/M;
Ac(33,11)=k3/M;
Ac(33,12)=k3/M;
Bc(9,1)=(1/Tgs);
%G4
Ac(13,13)=-1/Tgs;
Ac(13,33)=-1/(Rs*Tgs);
Ac(14,13)=FHs/TCHs;
Ac(14,14)=-1/TCHs;
Ac(15,14)=FIs/(FHs*TRHs);
```

```
Ac(15,15)=-1/TRHs;
Ac(16,15)=(FLs/FIs)/(TCOs);
Ac(16,16)=-1/TCOs;
Ac(33,14)=k4/M;
Ac(33,15)=k4/M;
Ac(33,16)=k4/M;
Bc(13,1)=(1/Tgs);
%G5
Ac(17,17)=-1/Tgs;
Ac(17,33)=-1/(Rs*Tgs);
Ac(18,17)=FHs/TCHs;
Ac(18,18)=-1/TCHs;
Ac(19,18)=FIs/(FHs*TRHs);
Ac(19,19)=-1/TRHs;

Ac(20,19)=(FLs/FIs)/(TCOs);
Ac(20,20)=-1/TCOs;
Ac(33,18)=k5/M;
Ac(33,19)=k5/M;
Ac(33,20)=k5/M;
Bc(17,1)=(1/Tgs);
%G6
Ac(21,21)=-1/Tgs;
Ac(21,33)=-1/(Rs*Tgs);
Ac(22,21)=FHs/TCHs;
Ac(22,22)=-1/TCHs;
Ac(23,22)=FIs/(FHs*TRHs);
Ac(23,23)=-1/TRHs;
Ac(24,23)=(FLs/FIs)/(TCOs);
Ac(24,24)=-1/TCOs;
Ac(33,22)=k6/M;
Ac(33,23)=k6/M;
Ac(33,24)=k6/M;
Bc(21,1)=(1/Tgs);
```

```
%G7
Ac(25,25)=-1/Tgs;
Ac(25,33)=-1/(Rs*Tgs);
Ac(26,25)=FHs/TCHs;
Ac(26,26)=-1/TCHs;
Ac(27,26)=FIs/(FHs*TRHs);
Ac(27,27)=-1/TRHs;
Ac(28,27)=(FLs/FIs)/(TCOs);
Ac(28,28)=-1/TCOs;
Ac(33,26)=k7/M;
Ac(33,27)=k7/M;
Ac(33,28)=k7/M;
Bc(25,1)=(1/Tgs);
%G3 nuclear

Tgn=input('Tgn=');
Rn=0.04;
FHn=0.3;
TCHn=0.3;
TRHn=5;
FLn=0.7;
TCOn=0.3;
M=8;
Ac(29,29)=-1/Tgn;
Ac(29,33)=-1/(Rn*Tgn);
Ac(30,29)=FHn/TCHn;
Ac(30,30)=-1/TCHn;
Ac(31,30)=FLn/(FHn*(TRHn+TCOn));
Ac(31,31)=-1/(TRHn+TCOn);
Ac(33,29)=0;
Ac(33,30)=k8/M;
Ac(33,31)=k8/M;
Bc(29,1)=(1/Tgn);
%HVDC
```

```
Ac(32,32)=-1/Tdc;
Ac(32,33)=-1/(R*Tdc);
Ac(33,32)=k9/M;
Bc(32,1)=1/Tdc;
%speed
Ac(33,33)=-D/M;
Bc(33,2)=-1/M;
Cc(1,33)=1;
Dc(1,2)=0;
%EigenValue Calculation
E=eig(Ac)
% Changing from ABCD format to Transfer function
[num,den]=ss2tf(Ac,Bc,Cc,Dc,1)
% Root Locus to design an Integral Controller

den2=[den 0]
rlocus(num,den2)
v=[-10 10 -10 10]
axis(v)
% Designing LQR controller and calculating eigenvalue after control
q=input('q=')
Qc=[q];
Rc=[1];
[Kc,Sc,Ec]=lqry(Ac,Bc(:,1),Cc,Dc(:,1),Qc,Rc)
%LQR Gains and System Eigen value after controller applied
Kc;
Ec;
```